CRANFIELD UNIVERSITY

Eva Tur García

Development of a flexible biosensor for the monitoring of lactate in human sweat for its medical use in pressure ischemia

School of Engineering

PhD
Academic Year: 2011 - 2014

Supervisor: Professor Séamus P. J. Higson

November 2014

CRANFIELD UNIVERSITY

School of Engineering

PhD

Academic Year 2011 - 2014

Eva Tur García

Development of a flexible biosensor for the monitoring of lactate in human sweat for its medical use in pressure ischemia

Supervisor: Professor Séamus P. J. Higson

November 2014

This thesis is submitted in partial fulfilment of the requirements for the degree of PhD

Abstract

Pressure ischemia is a medical condition characterised by the necrosis of the skin and underlying tissues in body areas exposed to prolonged pressure. This condition leads to the development of bedsores and affects 9% of hospitalised patients, costing the NHS between £1.4 and £2.1 billion per year. The severity of pressure ischemia has been linked to the concentration of sweat lactate, a product of sweat gland metabolism under anaerobic conditions, such as hypoxia. Normal levels of lactate in human sweat are 20±7 mM, but under ischemic conditions these can rise up to approximately 70 mM.

This project presents the development of a novel flexible electrochemical enzyme-based biosensor for the continuous and non-invasive monitoring of sweat lactate with the potential for becoming a body-worn device for the early detection of pressure ischemia onset. The core of the recognition system is a flexible laminate, comprising two highly porous polycarbonate membranes, which provide support for the lactate oxidase enzyme, immobilised via covalent cross-linking. Oxidation of lactate produces H_2O_2, which is subsequently determined electrochemically. The transducer comprises a two-electrode system on a single flexible polycarbonate membrane, sputter-coated with gold (CE/RE) and platinum (WE) to render it conductive. The developed design has been improved through investigation into different factors regarding the immobilisation method of the enzyme in the laminate and the lowering of interferences from oxidising compounds present in sweat.

The sensing system exhibits lactate selectivity at physiologically relevant concentrations in sweat for pressure ischemia (0–70 mM), with good reproducibility (7.2–12.2% RSD) for a hand-manufactured device. The reliability of the sensor's performance and the capability to detect lactate fluctuations on human sweat samples has been demonstrated. The sensing system showed excellent operational and mechanical stability. The application of Nafion® on the WE lowered interferences from ascorbic acid and uric acid by 96.7 and 81.7%

respectively. These results show promise towards the further development of a body-worn monitoring device for determining lactate levels in undiluted human sweat samples in a reproducible, fast and accurate manner.

Keywords: biosensor, lactate, sweat, pressure ischemia

Acknowledgements

I would like to begin by expressing my gratitude to my supervisor, Professor Séamus Higson, for providing me with the opportunity to undertake this research project, for his guidance and encouragement and for allowing me to grow as a research scientist. I would also like to thank my second supervisor, Dr. Frank Davis (who will surely miss reading my "Spanglish") and Dr. Jo Holmes for their help and support and especially to Dr. Stuart Collyer for his patience and guidance from my very first day through the field of Electrochemistry.

I would like to thank the Gloucestershire Hospitals NHS Foundation Trust for sponsoring this project. I wish to give special mention to Professor Hugh Barr for his guidance and encouragement and the enthusiasm he has put into this project.

Life at Cranfield University during these years would not have been the same without the amazing people I have met throughout my studies. I would like to give special mention to my wonderful PhD colleagues, Sinéad and Susana, with whom I have shared all the laughs and stressful moments that come from undertaking a PhD project and together with other fantastic friends, such as Luca and Natalia, for all the good times inside and outside of the university. This experience would not have been the same without you all.

In addition to the wonderful people I have made during my PhD, I have always carried in my heart the greatest friends. Amongst them all, I will always be grateful to Alicia and David, for always being there and believing in me.

A warm thank you to you, Craig, and your family, for your love, support, wonderful times and for being a second family to me. Thank you all for everything.

Last but not least, I would like to give my greatest THANK YOU to my family and especially to the best parents and brother in the world. There are no words in any dictionary that can express how lucky and grateful I feel to have you all in my life. You always believed in me and this would not have been possible without you. This thesis is for you. Finally, I would like to give a last mention to my grandfather, who I'm sure would have been very proud. I love you all.

Declaration

This is a declaration to certify that no portion of the work referred to in this thesis has been submitted in support of an application for another degree or qualification of this or any other university or other institute of learning.

Eva L. Tur García

November 2014

Table of contents

Table of Figures

Table of Tables

List of Abbreviations

Φ_m	Potential of the working electrode
Φ_{REF}	Potential of the reference electrode
Φ_s	Potential of the solution
μA	Microampere
μm	Micrometre
μl	Microlitre
ν	Sweeping rate
ΔE_p	Peak potential difference
A	Ampere
AA	Ascorbic acid
AC	Alternating current
ADP	Adenosine diphosphate
Ag	Silver
AgCl	Silver chloride
ATP	Adenosine triphosphate
Au	Gold
BSA	Bovine serum albumin
C	Coulomb
CE	Counter electrode
CoA	Coenzyme A
COPD	Chronic obstructive pulmonary disease
CV	Cyclic voltammetry
DNA	Deoxyribonucleic acid

E	Potential
E^0	Standard potential
E_p^A	Anodic peak potential
E_p^C	Cathodic peak potential
ESEM	Environmental scanning electron microscopy
F	Faraday constant
FA	Ferrocenecarboxylic acid
GHB	Gamma hydroxybutyrate
GOD	Glucose oxidase
i	Current
I_p^A	Anodic peak current
I_p^C	Cathodic peak current
IPE	Ideal polarised electrode
iR	Inherent resistance of the solution
IHP	Inner helmholtz plane
J	Joule
K_M	Michaelis-Menten constant
L	Litre
ln	Neperian logarithm
LDH	Lactate dehydrogenase
LOD	Lactate oxidase
LSV	Linear sweep voltammetry
ml	Millilitre
mm	Millimetre
mV	Millivolt

nA	Nanoampere
NAD^+	Nicotinamide adenine dinucleotide (oxidised form)
NADH	Nicotinamide adenine dinucleotide (reduced form)
NHS	National Health Service
OHP	Outer Helmholtz plane
PBS	Phosphate buffer saline
P_i	Orthophosphate group
PD	Panic disorder
pK_a	Acid dissociation constant
PO_2	Oxygen partial pressure
PCO_2	Carbon dioxide partial pressure
Pt	Platinum
q^M	Charge in electrode
q^S	Charge in solution
RE	Reference electrode
RSD	Relative Standard Deviation
SEM	Scanning electron microscopy
t	Unit of time
UA	Uric acid
V	Volt
WE	Working electrode

CHAPTER 1

RATIONALE FOR RESEARCH

1 Rationale for research

1.1 Rationale for research

The present research project has been sponsored by the Gloucestershire Hospitals NHS Foundation Trust in order to develop a biosensor for the continuous and non-invasive monitoring of lactate levels in human sweat for its potential use in the early detection of pressure ischemia onset in hospitalised patients.

Pressure ischemia is a medical condition characterised by the necrosis of the skin and underlying tissues in certain areas of the body suffering from the local occlusion of blood supply on exposure to continued pressure. It is estimated that approximately 9% of hospitalised patients develop these pressure sores, which can be related to an increase in mortality rates. It is calculated that the treatment of pressure sores costs the NHS 4% of its budget, amounts to between £1.4 and £2.1 billion per year.

Pressure ischemia is considered to be a preventable condition, which arises mainly because of a lack of warning indicators. Studies have shown that the severity of pressure ischemia is directly related to the levels of lactate in sweat. Lactate is a carboxylic acid produced by the breakdown of glucose during cellular respiration and is also a by-product of anaerobic metabolism in situations such as tissue compression, which causes a lack of oxygen in the affected areas. Sweat lactate is then produced by the sweat glands undergoing anaerobic metabolism. For all of the aforementioned reasons, sweat lactate offers promise as a good biomarker for the early detection of pressure ischemia onset.

Commercialised devices for the monitoring of lactate in blood samples are available, but blood analysis techniques can cause discomfort and be time consuming, expensive and rely on single-point measurements. For this reason, being able to develop a device to selectively monitor sweat lactate in real-time would have significant clinical benefits. Furthermore, the possibility of carrying out these measurements out in a non-invasive way (without breaking the skin and/or producing damage to any organs or tissues) could offer significant

advantages. To date very few biosensors have been developed for the monitoring of lactate in sweat and at the time of writing none of them is capable of its detection in undiluted human sweat samples at physiologically relevant concentrations for pressure ischemia, whilst preserving its stability over a significant period of time.

1.2 Aims and objectives

This research project is aimed towards the development of a novel sensor for the monitoring of sweat lactate *in vitro*. The sensor will be thin and flexible in order to be further developed into a diagnostic device with a sticking-plaster design, that can be applied directly to the skin in order to monitor lactate from undiluted sweat samples *ex vivo*. This non-invasive and continuous lactate biosensor will be potentially applied for the early detection of tissue damage produced by pressure ischemia.

The objectives of this project are as follows:

1. To develop and characterise a sensing platform based on a thin and flexible electrode system.
2. To improve the biosensor technology for the *in vitro* detection and quantification of lactate in human sweat samples at physiologically relevant concentrations (from 10 to 70 mM), with good performance in terms of reproducibility and linearity of the response.
3. To develop a flexible sensor design with good mechanical and operational stability for its future direct application to the skin and the continuous monitoring of sweat lactate *ex vivo*.
4. To provide a proof-of-principle for the monitoring of lactate in diluted and undiluted human sweat samples with the developed sensing device.

5. To evaluate any possible detrimental effects in the electrochemical response produced by the components of sweat samples and explore methods for lowering these interferences, in order to improve the performance of the sensor.

CHAPTER 2

LITERATURE REVIEW

2 Literature review

2.1 Introduction

The objective of the present PhD project is to develop a biosensor for the monitoring of lactate in undiluted human sweat *in vitro*, aiming towards its use as a clinical device for the early diagnosis of the onset of pressure ischemia. Therefore, the present chapter focuses on two main topics: pathophysiology of pressure ischemia and biosensor technology.

The first part of the literature review will give an overview of pressure ischemia and its impact in the economy and patient morbidity and mortality. Then, lactate will be discussed in the context of human anaerobic metabolism, its role within the biochemistry of soft tissues subjected to prolonged pressure and the changes in its composition in sweat during soft tissue breakdown. Finally, the need for the early diagnosis and prevention of pressure ischemia through the development of a continuous and non-invasive monitoring system will be highlighted.

The second part of the literature review will give an introduction about the history and development of biosensors, followed by a general overview of glucose biosensors as the first bio-sensing system recorded in published literature. Lactate biosensors will then be discussed and the chapter will conclude with an overview of electrochemical concepts relevant for the present research project.

2.2 Pressure ulcers

Pressure ischemia is the condition in which skin and underlying tissue necrosis occurs due to either malnutrition of the tissues in body areas exposed to continued pressure, or pressure in combination with shear and/or friction (Bansal *et al.*, 2005).

When the skin undergoes prolonged pressure, the underlying blood vessels become occluded, either partially or totally. As a result of this, oxygen and other nutrients carried in the blood are not delivered in sufficient quantities to satisfy the metabolic demands of the affected tissue. Cells are then obliged to use their own stores of energy through an anaerobic metabolic pathway in order to survive. Consequently, breakdown products from metabolism start to accumulate within both the affected cells and the interstitial spaces. As the levels of energy stores diminish, cellular processes start to fail, the ionic flow across cellular membranes begins to fall and then cell necrosis occurs, with the subsequent formation of a pressure ulcer (pressure sore). Hence, pressure ulcers arise from prolonged tissue ischemia (Polliack *et al.*, 1993) (Figure 2.1).

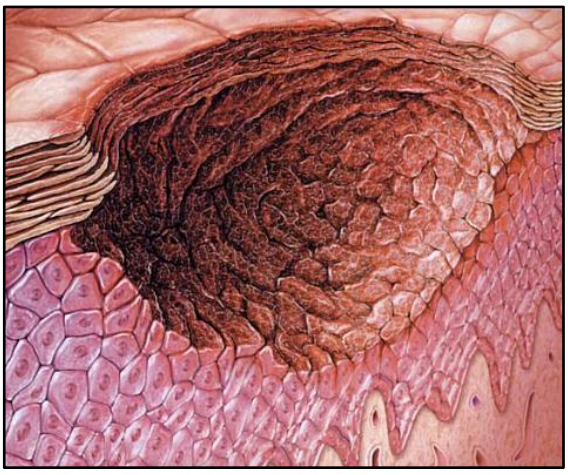

Figure 2.1 Representation of the skin and underlying tissue under the pressure ischemia condition.

(Maklebust and Sieggreen, 2001).

People more susceptible to pressure ulcers include those with mobility problems such as bedridden, wheelchair-bound, debilitated or paralyzed patients. People suffering from cardiovascular and neurological diseases can in many cases also suffer from pressure ischemia, since these diseases lead to an impairment in the state of the patient, impaired blood supply, poor diet, increased likelihood of developing other health conditions and/or poor hygiene (Bansal *et al.*, 2005; NHS Choices, 2014). Other health conditions that increase the risk of developing pressure sores are type 1 and 2 diabetes, since the high levels of sugar in blood associated with the disease can disrupt the normal blood flow; kidney failure, which can cause the accumulation of dangerous toxins in the blood, leading to tissue damage; and chronic obstructive pulmonary disease (COPD), associated with low levels of blood oxygen, which can weaken the skin. Moreover, poor nutrition (anorexia, dehydration, dysphagia) can also increase the risk of developing pressure ulcers, since it impairs the healthy state of the skin. Age also increases the vulnerability of the patient to develop bedsores due to the skin losing elasticity, becoming more vulnerable to damage; the blood flow is reduced; and the amount of fat underneath the skin that protects it, tends to decrease (NHS Choices, 2014).

2.2.1 Classification of pressure ulcers

Pressure sores are complex wounds, which vary significantly in size and severity. At the National Pressure Sore Advisory Panel Consensus Development Conference, held in 1989, it was agreed to classify pressure sores into four different categories or stages (National Pressure Ulcer Advisory Panel & European Pressure Ulcer Advisory Panel, 2009). Such a classification is summarised in Table 1.

Table 2.1. Staging and symptomatology of pressure ulcers according to the National Pressure Ulcer Advisory Panel.

(National Pressure Ulcer Advisory Panel & European Pressure Ulcer Advisory Panel, 2009)

Stage	Symptoms
1	Acute inflammation of all skin layers. The ulcer is present clinically as a nonblanching redness of intact skin, usually above a bony prominence, compared to the surrounding area. This category may be difficult to detect in individuals with dark skin tones.
2	The ulcer presents a partial skin thickness loss involving epidermis, dermis or both. The ulcer is superficial and is present as an abrasion, blister with erythema surrounding the skin break.
3	Full thickness skin loss involving damage to or necrosis of subcutaneous tissue. However, bone, tendon or muscle are not exposed. The depth depends on the anatomic location of the ulcer.
4	Full thickness tissue loss with penetration of pressure ulcer into the deep fascia. Extensive destruction, tissue necrosis, or damage to muscle, bone, joints and surrounding tissues.

The National Pressure Ulcer Advisory Panel (NPUAP) has also described two additional categories: suspected deep tissue injury and unstageable, which together with the previously described stages, are shown in Figure 2.2.

Suspected deep tissue injury may be indicated by a purple or maroon localised area of the skin or a blood-filled blister, caused by initial damage of underlying soft tissue due to applied pressure and/or shear. Prior to this, the affected tissue can be painful, firm, mushy, cooler or warmer than adjacent areas. Evolution of this stage can be rapid even with optimal treatment.

A pressure ulcer is described as unstageable when the actual depth of the ulcer is obscured by slough and/or eschar on the wound area, which are yellow, grey, tan, brown or green tissue. Therefore, until enough slough and/or eschar are

removed to expose the wound, its true depth and stage cannot be determined. However, slough and/or eschar do not form on stages I and II and therefore this stage will always be characterised as III or VI once the tissue is removed (National Pressure Ulcer Advisory Panel & European Pressure Ulcer Advisory Panel, 2009).

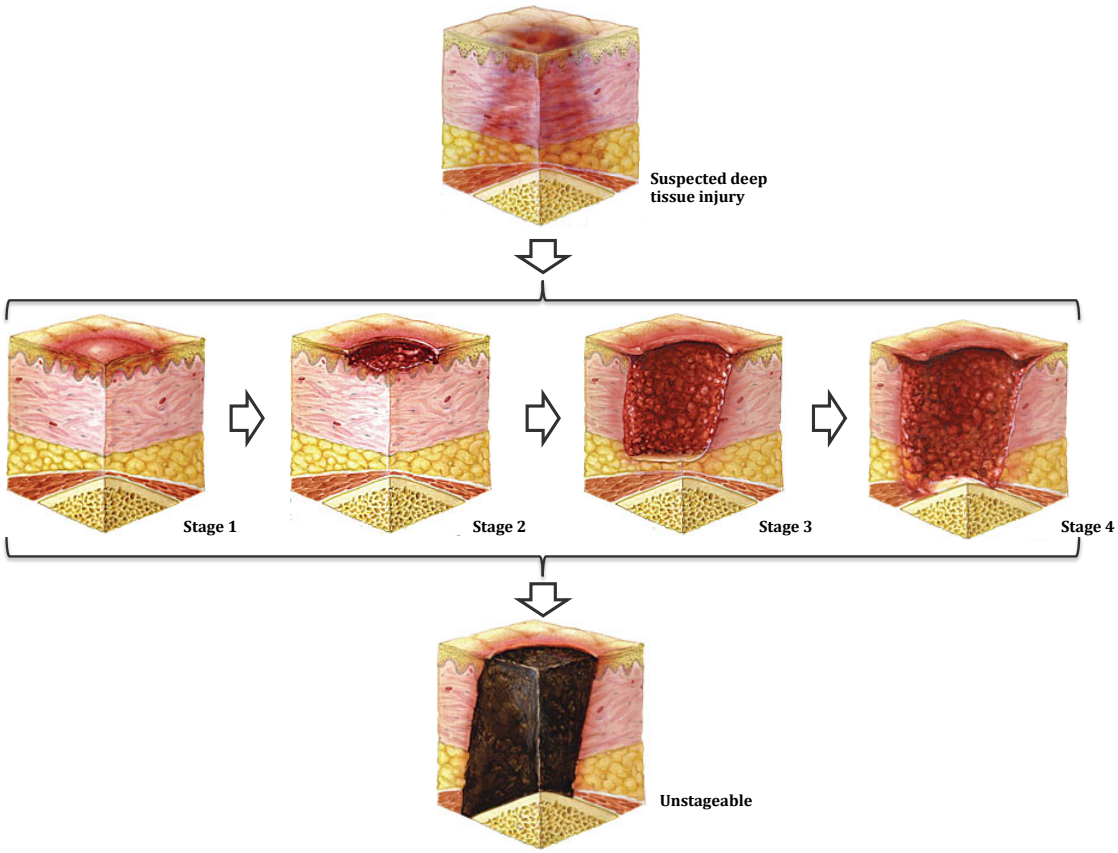

Figure 2.2. Stages of pressure ulcers according to the National Pressure Ulcer Advisory Panel.

(National Pressure Ulcer Advisory Panel, 2007)

2.2.2 Incidence

It is estimated that, in general terms, approximately 9% of hospitalised patients develop pressure sores (Bauer *et al.*, 2006). Moreover, it is well understood that pressure ischemia is related to a notable increase in mortality rates (Lyder and Ayello, 2008).

In acute care hospitals, the prevalence of pressure ulcers varies between 10.2 and 10.3% (Phillips and Buttery, 2009). It was estimated in 2004 that the treatment of pressure ulcers costs the National Health Service (NHS) in the UK 4% of its budget, a cost of between £1.4 and £2.1 billion per year (Bennett *et al.*, 2004). It is for this reason that pressure ischemia has significant implications in cost and quality of service for the health sector (Great Britain. Department of Health, 1995).

2.2.3 Epidemiology

96% of tissue destruction in pressure ischemia occurs in areas below the level of the umbilicus, commonly known as navel. Usually, pressure ulcers in patients appear in either the supine or seated position. In fact, up to 75% of them occur around the pelvic joint (Bauer *et al.*, 2006). Most of them develop in the skin around the waist, sacrum or buttocks. They also occur in certain parts of the body exposed to prolonged pressure such as the heels. Finally, in fewer cases (8%) they can also appear in the cheeks, over the nasal area and the chest (Maslauskas *et al.*, 2009; Bridel, 1993). Some of these unusual pressure ulcers can arise from using a facemask for nasal ventilation or when a patient lies in a prone position – or even with the face resting on the hand (Weng, 2008).

To date, several potential risk factors for the development of pressure ulcers have been reported (Collier and Moore, 2006). Some of these risk factors play a key role in the development of this condition such as a decrease in mobility and sensitivity, age of the patient, dementia, paralysis, poor nutrition, bad skin condition, local pressure to the tissues, friction and perfusion (Bansal *et al.*, 2005; Bours *et al.*, 2001; Thompson, 2005; Lahmarm *et al.*, 2005; Bauer *et al.*, 2006). All these are known as factors related to poor healing outcomes.

2.2.4 Diagnosis, treatment and prevention

One of the most common clinical practices for the early detection of pressure ischemia was based on a periodical inspection of the skin colour of the patient. In

one study, areas of the skin persistently red were often classified as “Stage I” pressure sores; corresponding clinical analyses were then performed. However, this approach had some limitations. It was usually difficult to differentiate between persistent and temporary redness of the skin. Moreover, in advanced stages of pressure ischemia, the area of redness of the skin is reduced as the region starts becoming cyanotic with the increase of the levels of unoxygenated haemoglobin in the arterial blood. Finally, it was difficult to observe colour changes in the skin of non-white patients (Ferguson-Pell and Hagisawa, 1988).

Later diagnosis methods were based on an alternative approach using tissues as the source of information. The first technique consisted of the monitoring of blood flow, which constituted a slight improvement from the observation of skin colour (Ferguson-Pell and Hagisawa, 1988). It was known that even in early stages of pressure ulcer formation, the tissues responded with an accumulation of metabolites, a decrease in pH and oxygen partial pressure (PaO_2, which is the amount of oxygen that will bind to haemoglobin within the red blood cells) and an increase in partial pressure of carbon dioxide ($PaCO_2$) (Matsen *et al.*, 1981). However, the techniques derived from this idea were refused since they implied the use of invasive methods on areas of risk for the collection of samples.

Due to the elevated amount of factors that contribute to the development of pressure ulcers, their treatment usually involves orthopaedic surgery, internal medicine, mental health care or even plastic surgery in the most severe cases (Bauer *et al.*, 2006).

Pressure ischemia is considered a preventable condition that arises from poor clinical management, reduced nursing staff and a lack of warning indicators (Bours *et al.*, 2001). However, in reality it is understood that it is not that easy to prevent because all the previously mentioned factors that cause it.

2.3 Lactate

2.3.1 Introduction

2-hydroxypropanoic acid, commonly known as lactic acid, is a chiral molecule which plays an important role in several biochemical processes. In 1780, the Swedish chemist Carl Wilhelm Scheele isolated the compound for the first time. Lactic acid is a carboxylic acid. Its chemical formula is $C_3H_6O_3$ and it has a pK_a of 3.86. When in solution, the molecule disassociates with its proton, giving rise to its conjugate base, lactate (Figure 2.3). Therefore, lactate is an anion. It has two optical isomers, L-lactate and D-lactate, among which only the first is physiologically relevant. L- lactate is a natural product of anaerobic metabolism, which is one of the pathways for the obtaining of energy in the form of adenosine triphosphate (ATP).

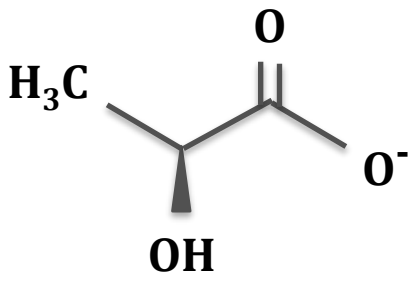

Figure 2.3. Chemical structure of L-lactate.

2.3.2 Adenosine triphosphate (ATP)

ATP is the main energy transfer molecule required in many biological processes within the human body such as motion, active transport or biosynthesis. Most catabolic processes comprise of reactions that extract energy from fuels such as fats and carbohydrates. This energy is converted into ATP through oxidation-reduction reactions (Berg *et al.*, 2006).

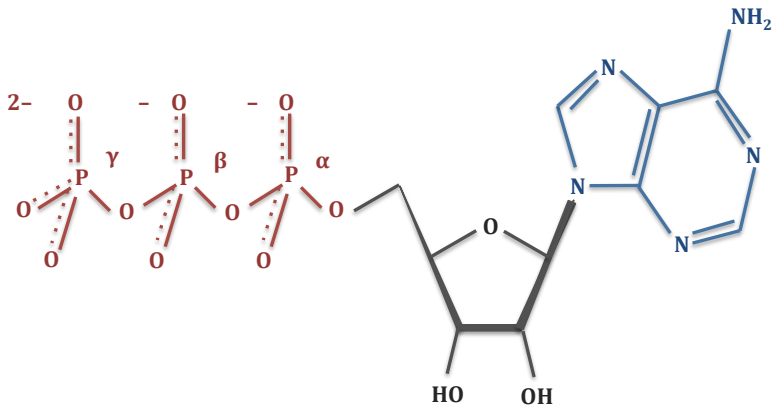

Figure 2.4. Structure of ATP.

ATP is a nucleotide consisting of an adenine, a ribose and a triphosphate unit (Figure 2.4). However, its role as an energy carrier is based on its triphosphate unit with two phosphoanhydride bonds. ATP can be hydrolysed to adenosine diphosphate (ADP), with a release of an orthophosphate group (P_i), or to adenosine monophosphate (AMP) with the release of a pyrophosphate group (PP_i). It is during this hydrolysis that a large amount of free energy is liberated. This energy is then used to drive reactions, which require an input of free energy, such as muscle contraction (Berg *et al.*, 2006). Simultaneously, ATP molecules are formed from ADP and Pi when fuel molecules are oxidised. This cycle from ATP to ADP and vice versa (Figure 2.5) is the fundamental way in which energy is exchanged in biological systems (Berg *et al.*, 2006).

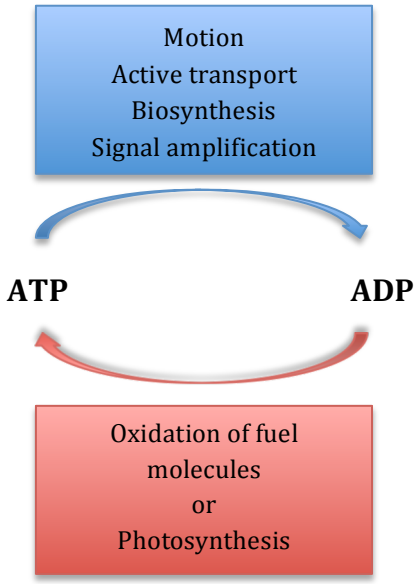

Figure 2.5. ATP-ADP cycle.

(adapted from Berg *et al.*, 2006)

After the enzymatic digestion of the small organic molecules from food, their oxidation begins. As has been previously mentioned, fats and carbohydrates are the main substrates for ATP synthesis in the human skeletal muscle, among others (Van Loon *et al.*, 2001). However, since glucose dominates energy production in most animal cells, in the following sections we will focus on this carbohydrate and the pathway to obtain ATP from its metabolism, in both aerobic and anaerobic conditions – although both of these share an initial pathway: glycolysis.

2.3.3 Glycolysis

Glycolysis is a chain of reactions, which converts each molecule of glucose (among other sugars) into two smaller molecules of pyruvate (Figure 2.5). The conversion from glucose to pyruvate involves ten steps or separate reactions. Each reaction is catalysed by a different enzyme and produces a different intermediate. Along the glycolysis process, two kinds of cofactors are produced: ATP and NADH (the reduced form of nicotinamide dinucleotide) (Alberts *et al.*, 2002).

The net reaction in glycolysis is:

$$\text{Glucose} + 2\ P_i + 2\ \text{ADP} + 2\ NAD^+ \rightarrow 2\ \text{pyruvate} + 2\ \text{ATP} + 2\ \text{NADH} + 2\ H^+ + 2\ H_2O$$

Even though no molecular oxygen is needed for the glycolysis process to take place, oxidation occurs in which NAD^+ removes electrons from some of the carbon atoms within the glucose molecules, hence producing NADH, the reduced form of the cofactor. Some of this energy released from the oxidation process is used to perform the conversion from ADP and Pi to ATP, which is energetically unfavourable (Alberts *et al.*, 2002).

2.3.4 Aerobic pathway for ATP synthesis (oxidative phosphorylation)

After pyruvate is formed in the cytosol, this passes to the mitochondria of the cell. There, each molecule of pyruvate is converted into CO_2 and a two-carbon acetyl group. This group is then attached to coenzyme A (CoA) through a high-energy linkage, thus forming acetyl-CoA. This high requirement of energy makes the acetyl group easily transferable to other molecules. Therefore, after being transferred to the oxaloacetate molecule in the mitochondria, the acetyl group undergoes a chain of reactions known as the citric acid cycle (Figure 2.6). In this new process, the acetyl group is oxidised to CO_2 with the subsequent production of large amounts of NADH. The net reaction of the citric acid cycle is:

$$\text{Acetyl-CoA} + 3\ NAD^+ + \text{FAD} + \text{GDP} + P_i + 2\ H_2O \rightarrow$$

$$2\ CO_2 + 3\ \text{NADH} + FADH_2 + \text{GTP} + 2\ H^+ + \text{CoA}$$

As a last step, the high-energy electrons within the NADH molecule go through an electron-transport chain, located in the inner membrane of the mitochondria

(Figure 2.6). Electrons are transferred by oxidation processes, from NADH to molecular oxygen (O_2), through a respiratory chain formed by three protein complexes (Berg *et al.*, 2006). Most of the energy released from the transfer of electrons in this last stage is used to produce most of the ATP that the cell requires (Alberts *et al.*, 2002). Unlike in glycolysis and the citric acid cycle, the number of ATP molecules generated after the electron transport chain is uncertain due to the stoichiometries of proton pumping. It is estimated, however, that the whole process in which glucose is oxidised into CO_2 generates approximately 30 molecules of ATP. Most of this ATP, 26 or 30 molecules, is generated along the electron transport chain (Berg *et al.*, 2006).

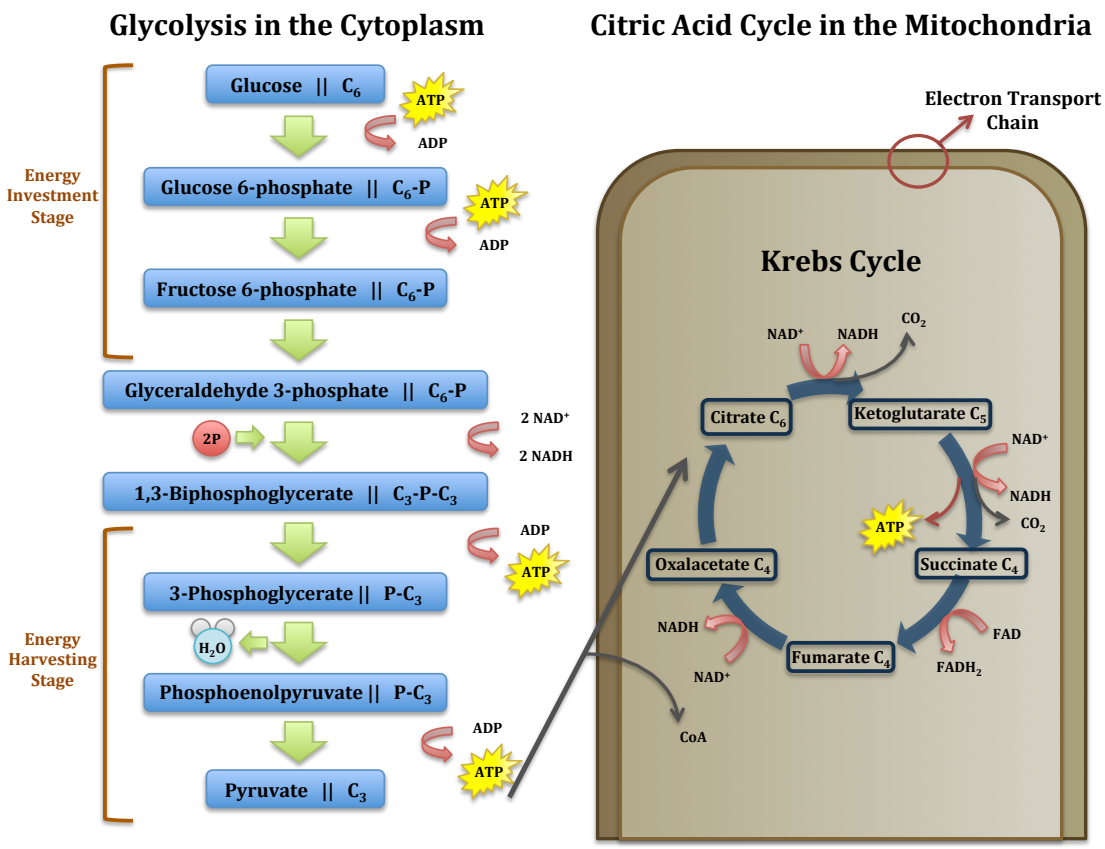

Figure 2.6. Reactions comprising the glycolysis pathway and the subsequent pathway under aerobic conditions.

2.3.5 Anaerobic pathway for ATP synthesis

Through the respiratory chain, the NAD^+ required for performing the glycolysis process again is generated from the oxidation of NADH (Alberts *et al.*, 2002). However, when molecular oxygen is limited, as in when a skeletal muscle is being vigorously contracted or in ischemic tissues, the respiratory chain as a way to reoxidate NADH to NAD^+ becomes insufficient for maintaining glycolysis. In these situations, the required levels of NAD^+ are generated through the conversion from pyruvate to lactate after the glycolysis process. This reduction of pyruvate by NADH is catalysed by the enzyme lactate dehydrogenase. In this way, the skeletal muscle can continue working when molecular oxygen is limited (Hames and Hooper, 2000). Under these anaerobic conditions, the pyruvate and the NADH and its electrons stay in the cytosol instead of passing to the mitochondria (Alberts *et al.*, 2002). The overall reaction for the conversion of glucose into lactate is:

$$\text{Glucose} + 2\ P_i + 2\ \text{ADP} \rightarrow 2\ \text{lactate} + 2\ \text{ATP} + 2\ H_2O$$

In the conversion from glucose to lactate, there is no net oxidation-reduction. This means that all the NADH molecules formed along the glycolysis are consumed to reduce pyruvate to lactate. However, it is the NAD^+ produced along this last process by lactate dehydrogenase that sustains the continued process of glycolysis in the absence of molecular oxygen (Berg *et al.*, 2006). The overall reaction for the conversion of the pyruvate to lactate is:

$$\text{Pyruvate} + \text{NADH} + H^+ \rightarrow \text{lactate} + NAD^+$$

The lactate produced by active skeletal muscle is also a source of energy in other organs of the human body. When the skeletal muscle is contracted with vigorous exercise, the rate at which pyruvate is generated from glycolysis exceeds the rate at which it is oxidised in the citric acid cycle. In these situations, lactate

dehydrogenase compensates the excess of pyruvate by converting it to lactate, thus restoring the redox balance. However, lactate cannot be metabolised per se. For that to happen, it needs to be converted back to pyruvate. Therefore, the lactate and pyruvate produced after glycolysis diffuse from the muscle cells into the bloodstream. This generation and release of lactate in muscle cells allows them to synthesise ATP molecules in the absence of oxygen and facilitates the transport of lactate to other organs, which can perform the metabolism of lactate and shift that burden away from the muscle. Once the lactate diffuses into well-oxygenated cells of other tissues, it is reverted into pyruvate and enters the citric acid cycle and electron transport chain, thus generating ATP. As these cells use lactate instead of glucose, this carbohydrate becomes more available for the active muscle cells. Moreover, lactate is also transported to the liver, where it is converted into pyruvate and then into glucose by a gluconeogenic pathway. Hence, when muscles are contracted, they supply lactate to the liver for it to be synthesised to glucose, restoring the levels that muscle cells need to remain active during exercise performance. These reactions compose the Cori cycle (Berg *et al.*, 2006), illustrated in Figure 2.7.

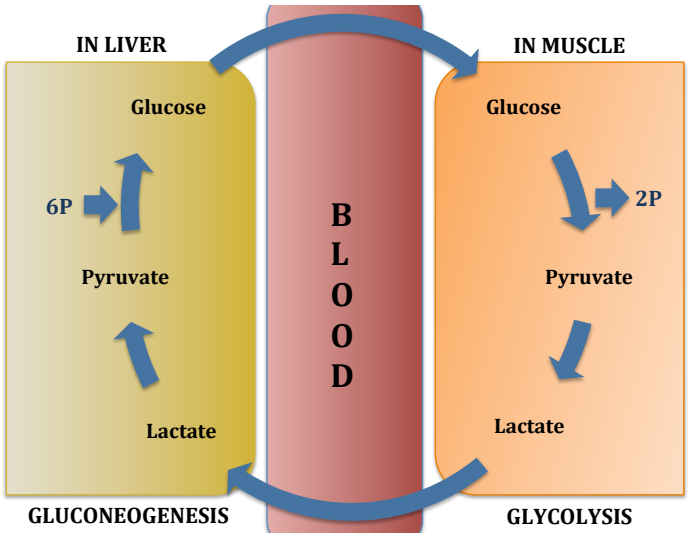

Figure 2.7. The Cori cycle.

(adapted from Berg *et al.*, 2006)

2.3.6 Lactate and pressure ischemia. Importance of wearable sensors for continuous sweat lactate monitoring

L-lactate is a key metabolite produced along the anaerobic metabolism of glucose for the synthesis of ATP under conditions of limited oxygen availability (hypoxia). This production of lactate leads to an increase in proton concentration inside the cells. If the rate of lactate production and clearance is imbalanced, the proton-buffering capacity of a cell under hypoxia may be exceeded, causing lactic acidosis, which leads to cell death.

Lactic acidosis, caused by an excessive lactate production, takes place with any condition that results in anaerobic metabolism, such as cardiogenic or endotoxic shocks (Karlsson *et al.*, 1975; Sayeed and Murthy, 1981), respiratory failure (De Backer *et al.*, 1997), liver disease (Kruse *et al.*, 1987), systemic disorders, renal failure and tissue hypoxia (Bellomo, 2002; Rimachi *et al.*, 2012). For this reason, lactate levels are a useful alarm signal for the diagnosis of patient conditions in general clinical practice and also in hospital intensive care units and operating rooms.

As stated, approximately 9% of hospitalised patients develop pressure sores while being confined to a bed or a wheelchair (Bauer *et al.*, 2006). When a tissue is compressed, underlying vessels collapse and the tissue starts suffering from ischemia. This induced ischemia causes a decrease in oxygen and glucose levels. This state of hypoxia (lack of oxygen) forces the cells within the vascularised tissues to change to anaerobic metabolism. The cells then reduce their glucose reserves in order to produce more lactic acid, which starts accumulating (Stekelenburg *et al.*, 2008). However, the state of hypoxia also leads to a phenomenon called oxygen conformance (Arthur *et al.*, 2000; Boutilier, 2001). Oxygen conformance down-regulates the metabolic demands by delaying glucose depletion and, therefore, acid accumulation, which can lead to apoptosis, causing programmed cell death (also known as necrosis). While the concentrations of lactic acid remain below a toxic threshold, the metabolism is down-regulated. However, if lactate concentration exceeds or glucose levels fall below a certain threshold

level, cell death will occur (Gawlitta *et al.*, 2007; Stekelenburg *et al.*, 2008). This proposed sequence of events during tissue compression was suggested by the same authors, based on previous experiments in a muscle model (Stekelenburg *et al.*, 2006; Stekelenburg *et al.*, 2007; Gawlitta *et al.*, 2007).

As well as the disorders described above, lactate levels also constitute a useful warning indicator for the formation of pressure ulcers, which are considered preventable with appropriate clinical intervention. Normal lactate values in blood and sweat are typically in the range of 1.6±0.5 and 20±7 mM, respectively (Sakharov *et al.*, 2010). Under pressure ischemia conditions, however, these levels in sweat can raise to 73 mM or more (Polliack *et al.*, 1997). It has been reported that, in susceptible patients, pressure ulcers can develop in just one or two hours (Edlich *et al.*, 2004), even though in some cases the damage will only become evident a few days later. Therefore, an immediate and continuous monitoring of lactate is a key factor for in-time intervention by physicians (Smith *et al.*, 2001). This monitoring requires biosensors with direct, simple and highly specific lactate measurements, low response time, inexpensive and with minimal or no sample preparation. Due to the accomplishment of these technical and operational challenges, electrochemical lactate sensors, explained in depth in the next section, dominate the market. To date, these commercially available sensors are based on plasma or blood samples and perform single-point measurements, usually from the earlobe or fingerprint. This procedure becomes extremely inconvenient when performing a continuous lactate monitoring sample by sample, since it requires the extraction and collection of many blood samples, causing the patient additional stress as well as provides incomplete information, since it relies only on periodic measurements or "snapshots" without providing any continuous data on lactate level fluctuations between different measurements. For this reason, devices for the continuous monitoring of lactate are in demand, since they would represent a significant benefit for patients in medical and critical care. Implantable vascular sensors for in-situ monitoring of lactate levels have been developed. However, these entail a high risk of thrombosis and embolism (Spehar-Deleze *et al.*, 2012). This issue and the current trend for non-invasive diagnostic and real-time

monitoring methods have led researchers to search for other body fluids on which to perform lactate measurements, such as interstitial fluid, saliva, tear fluid, exhaled breath or sweat. Among these, sweat shows the most promise, as it is the most accessible specimen to collect with an absorptive pad, its collection is non-invasive and its real-time analysis offers valuable physiological information (Coyle *et al.*, 2010). Also, sweat analysis allows specific body areas to be studied (i.e. pressure points).

In 1934, Kuno reported a decrease in the sweat rate after the arterial occlusion of an arm (Kuno, 1934). Sweat is a hypotonic solution composed of chloride and sodium ions in water, together with other components such as lactate, potassium and urea (Bader and Oomens, 2006). Sweat glands are supplied with abundant capillary blood, which carries biochemical compounds that could be used as potential markers for pressure ischemia (Ferguson-Pell and Hagisawa, 1988). In 1952, a study showed that sweat composition was affected under pressure ischemia, increasing the levels of lactate and urea (Van Heyningen and Weiner, 1952). In this study, van Heyningen and Weiner studied the volume and concentration of chloride, lactate and urea, which had been shown to account for approximately 95% of the osmotically active substance in sweat. It was in this study that the presence of lactate was highlighted, as the significance of its rapid increase and its high concentrations in sweat in an occluded arm was unknown. Unlike blood monitoring techniques, the idea of using sweat as a marker to monitor changes in tissues appeared to be feasible, as only simple and noninvasive techniques are needed (Van Heyningen and Weiner, 1952).

In 1988, a study suggested that sweat composition could be a reliable physiological marker for pressure ischemia if it was collected during the ischemic event (Ferguson-Pell and Hagisawa, 1988). The authors stated that the high levels of lactate found during the ischemic event were caused by changes in the metabolism of the sweat gland, and that these levels of lactate in sweat were generally independent of the levels in capillary blood and therefore they do not correlate. They also demonstrated the feasibility of using electrochemical

techniques for the measurement of lactate and sodium concentration levels from sweat.

Fellman *et al.* finally suggested in 1989 that sweat lactate would be a good marker for evaluating the severity of peripheral occlusive arterial disease which, as well as pressure ischemia, implies a local occlusion of blood supply (Fellmann *et al.*, 1989). Subsequent studies agreed with this fact and stated that sweat lactate could be a sensitive indicator of damage in soft tissues (Polliack *et al.*, 1993; Polliack *et al.*, 1997; Knight *et al.*, 2001).

In order to achieve a continuous monitoring, wearable sensors have attracted increasing interest from the research community and the industry during the last decade (Morris *et al.*, 2009). To date, most of the existing wearable sensors have been developed for the monitoring of physiological parameters of the patient, such as breathing range, hear rate or temperature (Coyle *et al.*, 2007). Wearable chemo-sensors (described in the next section), although being at an early stage, have the potential to measure many more variables related to the wearer's health. Moreover, the potential of these sensors to perform chemical and continuous measurements of body fluids (i.e. sweat) opens a new insight for medical science by providing valuable real-time feedback information about the patient's health status, which is the key for preventative healthcare and early diagnosis of disease (i.e. pressure ischemia). Wearable sensors for the continuous monitoring for sweat lactate will be discussed in section 2.5.4.1.

2.4 Sweat lactate

2.4.1 Lactate in the human body – Overview

In a healthy adult subject, normal metabolism results in the daily turnover of approximately 1,500 to 4,500 mmol of lactic acid (Bellomo and Kellum, 2008), which in aqueous conditions dissociates almost completely in lactate and H^+. The production of lactate as a product of the anaerobic metabolism of glucose takes place primarily in tissues with high rate of glycolysis such as muscle (25%), skin (25%), brain (20%), intestine (10%) and red blood cells (20%)(Okorie and Dellinger, 2011). As a consequence of this, lactate can be found in many body fluids such as interstitial fluid (MacLean *et al.*, 1999)saliva (Nunes and Macedo, 2013) and exhaled breath (Marek *et al.*, 2010), which levels have been reported to correlate with those in blood. Lactate can also be found in sweat, secreted by sweat glands throughout their metabolism (Derbyshire *et al.*, 2012) as well as in urine (Biagi *et al.*, 2012). As mentioned in the previous section, normal lactate levels in human sweat are in the range 20±7 mM (Sakharov *et al.*, 2010).

2.4.2 Sweat production and composition

Sweat is a clear hypotonic solution produced by sweat glands located in the epidermis. The pH of this biofluid has a median of 5.3, ranging in between 4.0 and 6.8 (Mena-Bravo and Luque de Castro, 2014). 90% of the sweat content is constituted by water, which is known to contain a minimum of 61 different chemical constituents at varying concentration (Stefaniak and Harvey, 2006; Harvey *et al.*, 2010). 95% of the osmotically active substances in sweat are electrolytes such as chloride, potassium and sodium; and other constituents such as urea and lactate (Van Heyningen and Weiner, 1952). Other abundant sweat constituents are amino acids, bicarbonate and calcium (Kreyden and Scheidegger, 2004). A variety of xenobiotics can also be found in sweat, such as drugs, cosmetics and ethanol (Sato *et al.*, 1989).

Sweat is secreted by mainly two types of sweat glands, known as eccrine and apocrine glands (Figure 2.8), of different structure and functions. Both glands consist of two parts: a coiled portion located in the dermis of the skin, which secretes a precursor sweat solution; and a duct portion located in the epidermis, which modifies this precursor sweat solution by reabsorbing some of its ionic constituents (mainly chloride and sodium ions) prior to this solution reaching the surface of the skin, where it is secreted as sweat (Stefaniak and Harvey, 2006). Eccrine sweat glands play the main role in body thermoregulation and excretion of electrolytes (Sato and Dobson, 1973; Sato *et al.*, 1989). For this reason, the sweat produced by these glands is mainly composed by water with various salts, mainly sodium and chloride but also potassium, lactate, urea, amino acids, bicarbonate and calcium (Kreyden and Scheidegger, 2004). There are between 1.6 and 4.0 million of eccrine sweat glands distributed over nearly the entire body surface (Sato *et al.*, 1989). The apocrine sweat glands, although bigger than the eccrine, are less numerous. Their main function is the production of chemical signals (pheromones). These, together with other products such as lipids, cholesterol and steroids, and the bacterial decomposition of sweat, give the solution an individual smell that plays an important role in mammalian reproduction (Coyle *et al.*, 2010). For this reason, apocrine sweat is relatively thick and viscous as it contains small concentrations of proteins, peptides, amines, amino acids metal ions, inhibitors, antigens and antibodies (Mena-Bravo and Luque de Castro, 2014).

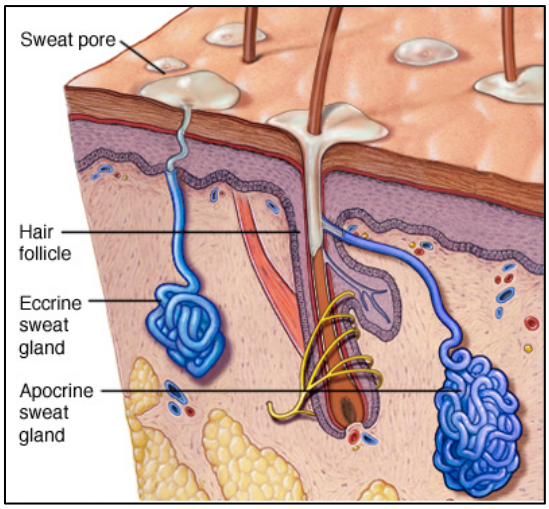

Figure 2.8. Schematic structure of the skin. Eccrine and apocrine sweat glands.

(Mayo Foundation for Medical Education and Research)

It is estimated that human sweat contains at least 61 different chemical constituents, whose concentrations can vary (Stefaniak and Harvey, 2006; Harvey *et al.*, 2010). The composition of sweat is influenced by a number of factors such as body region (in general terms, sweat glands are distributed over the entire body except for the lips, nipples and external genital organs), age, diet, season, degree of acclimation, activity level, emotional state, gender, race, collection/sampling technique (Stefaniak and Harvey, 2006; Coyle *et al.*, 2010), and a variety of hereditary factors, all these influencing mainly the sweat rate and the metabolism of sweat glands. Diseases can also change the composition of sweat by altering the concentration of its components and/or leading to the production of new ones which may act as biomarkers for such disease (Mena-Bravo and Luque de Castro, 2014).

During normal metabolism, in presence of oxygen, oxidative phosphorylation is the main metabolic pathway of the eccrine sweat gland to obtain ATP. However, under conditions of ischemia and/or anaerobic conditions, glycolysis becomes its main metabolic pathway for obtaining ATP, which results in the formation of lactate as an end product from the sweat gland (Sato and Dobson, 1973). This justifies the increase in lactate observed from sweat samples collected from

patients suffering from ischemia in many studies (Van Heyningen and Weiner, 1952; Ferguson-Pell and Hagisawa, 1988; Polliack *et al.*, 1993; Polliack *et al.*, 1997; Knight *et al.*, 2001).

2.4.3 Applications of sweat analysis

Sweat analysis has many different applications depending on the target analyte. It is well known that a sweat test is a golden standard technique for the diagnosis of cystic fibrosis, where concentration levels of sodium and chloride ions in sweat are monitored in newborns, since they are known to increase under this condition(Massie *et al.*, 2000).

Sweat analysis has also been reported to be useful for monitoring illicit drug use or doping control, as a small but sufficient amount of these drugs enter sweat by passive diffusion and accumulate over several days. The most common compounds tested in sweat are opiates, amphetamines, buprenorphine, cocaine, cannabinoids, Gamma hydroxybutyrates (GHB) and prescription drugs such as benzodiazepines and antipsychotics (Gallardo and Queiroz, 2008).

Another application of sweat analysis are the detection of toxic xenometals (cadmium, lead, mercury or arsenic) that are dissolved in sweat as a consequence of individual contamination, either through contaminated food or by absorption through the skin (Sears *et al.*, 2012). Sweat analyses have also been performed for the detection of biomarkers of diabetes (Moyer *et al.*, 2012; Papanas *et al.*, 2013).

Applications of sweat lactate analysis

Up to date, there has been limited research into the applications of sweat lactate. Most of the research has focused on the detection of this metabolite in sweat in the field of sports science, since it has been shown that an increase in the exercise intensity leads to increased product of sweat lactate as a consequence of the anaerobic metabolism of the eccrine sweat gland, as described in the previous

section (Pilardeau *et al.*, 1979; Pilardeau *et al.*, 1988). Sweat lactate has also the interesting application of the early detection of pressure ischemia, previously described in section 2.2. As described in section 2.3.6, several authors have shown in their studies that sweat lactate is a very useful warning indicator for the development of pressure ulcers since the local occlusion of blood supply reduces the oxygen tissue perfusion, which forces eccrine sweat glands to undergo anaerobic metabolism for the production of energy and thereby synthesising lactate as a product of the glycolysis, as described in the previous section.

The analysis of sweat lactate has also a potential application in the diagnosis of cystic fibrosis, as this condition impairs lung function, which could lead to a progressive decrease in oxygen intake and increase the anaerobic metabolism of cells such as those in sweat glands, leading to the production of lactate in sweat (Bijman and Quinton, 1987).

Two other potential applications for the analysis of sweat lactate, although no follow-up work has been performed, are its use as a marker for the diagnosis of panic disorder (PD) (Kukumberg *et al.*, 2009) and Frey's Syndrome (Laccourreye *et al.*, 1993).

2.5 Biosensors

2.5.1 Introduction

A sensor can be defined as a device that registers a physical, chemical or biological change and converts it into a signal that can be measured (Eggins, 2002). A sensor has three main components. First, a recognition element, which provides a selective response to a particular analyte or a group of analytes. This selective response allows the minimisation of any interferences from other components in the sample. Second, a transducer, which is the detector device that produces the measurable signal. Third, a signal processor, which collects, amplifies and displays the signal (Ronkainen *et al.*, 2010).

2.5.2 Classification

Sensors can be divided into three different groups: (1) physical sensors, for measuring distance, pressure, mass, temperature, etc. (2) chemical sensors, for the measurement of chemical substances through chemical or physical responses, and (3) biosensors, which measure chemical substances by using a biological sensing element coupled to or in close proximity to a transducer. Chemical sensors are defined as devices that respond to a certain analyte in a selective way through a chemical reaction. This response can be used for the detection of the analyte in a qualitative or a quantitative way (Eggins, 2002).

Chemical sensors can be classified according to the operating principle of the transducer. Under this classification, we find optical (changes of optical phenomena), electrochemical (electrochemical interaction between an analyte and an electrode), electrical (change of electrical properties by the interaction of the analyte when no electrochemical interactions take place), mass sensitive (mass changes), magnetic (change of paramagnetic properties), thermometric (heat effects of a specific chemical reaction involving the analyte), among others (Hulanicki *et al.*, 1991).

In the present work, we will be focusing on electrochemical biosensors. In the economic sector, electrochemical sensors rank first in commercialisation in many areas such as clinic, industry, environment and agriculture (Korotcenkov, 2010). They compete well with the sensing techniques from other chemical sensors such as optical, electronic, mechanical and thermal, especially when looking for a sensitive, inexpensive and low-powered sensor. This is because usually these other sensors require expensive equipment such as spectrometers or complex electronics. Moreover, electrochemical sensors are, in most cases, able to provide a response at room temperature (Korotcenkov *et al.*, 2009).

Electrochemical sensors are designed for detecting electroactive species, which take part in chemical recognition processes, and that are transferred to an electrode from a solid or liquid sample or vice versa. The sensing technique used by electrochemical sensors only requires a closed electrical circuit that allows the

taking of measurements by enabling the flow of direct or alternating current (Korotcenkov, 2010). As will be explained in section 2.6.2, in order to allow the flow of current, at least two electrodes are needed in the system: a working electrode (WE) where the targeted chemical reaction occurs, a counter or auxiliary electrode (CE) and, in the case of a three-electrode system, a reference electrode (RE), which is used to provide a stable reference potential against which the working electrode may be polarised (Fraden, 2004). Electrochemical sensors can be divided into three main groups according to the method of measurement: current (amperometric sensors), potential or charge accumulation (potentiometric sensors) and impedance (impedimetric sensors) (Ronkainen *et al.*, 2010).

Even though biosensors are a sub-set of chemical sensors, they are treated separately in the classification of sensors. They can be defined as devices which incorporate a biological sensing element, connected to a transducer (Eggins, 2002). The use of biosensors usually eliminates the need of preparing samples before their analysis (Ronkainen *et al.*, 2010). Typically, the performance of a biosensor is evaluated through different parameters such as its sensitivity, limit of detection (LOD), reproducibility, selectivity and so on. Moreover, an ideal biosensor would also be regenerable in order to be able to perform several measurements or analyses before its replacement. However, some disposable, single-use biosensors have been reported to be successful for some applications, such as the glucose sensor for diabetic people (Eggins, 2002). There are two main types of biosensors: biocatalytic and affinity-based biosensors. Biocatalytic sensors mainly use enzymes due to their well-known high biocatalytic activity and their specificity for their substrate. They can also use other biological components such as whole cells or tissue slices. The recognition element interacts with the target analyte, with the subsequent production of electroactive species, which are detected by the transducer. They often comprise fairly simple designs, since they do not require very expensive or complex instrumentation. For this reason, these devices are usually very simple to use (Ronkainen *et al.*, 2010). Affinity biosensors are based on the selective and strong binding of biomolecules such as oligonucleotides (*i.e.* DNA), antibodies or membrane receptors. Such receptors interact with the target

analyte through a complementarity in size and shape between their binding site and that of the target analyte (Wang, 2006). These sensors are known to be highly sensitive and selective, due to the strong affinity and specificity of the receptor for its ligand (Eggins, 2002).

A large majority of biosensors use electrochemical transducers as they are quite inexpensive, easy to use, portable and their construction is fairly simple (Eggins, 2002; Ronkainen *et al.*, 2010). In the present work, we will focus on this kind of electrochemical biosensors.

2.5.3 Glucose biosensors

Diabetes mellitus is the most common endocrine disorder, caused by a disorder in the metabolism of carbohydrates. It is a leading cause of morbidity and mortality worldwide and a major health problem for most developed societies. Due to the importance for diabetic people to maintain normal blood glucose levels, the biosensor technology for glucose detection has developed rapidly, to a point where today's biosensor market is dominated by these glucose biosensors (Yoo and Lee, 2010).

Generally, biosensors for glucose monitoring are based on the enzyme glucose oxidase (GOD).

The first biosensor designed for monitoring glucose levels was developed in 1962 by Clark and Lyons from the Children's Hospital of Cincinnati (Clark Jr. and Lyons, 1962). This biosensor comprised an oxygen electrode, an inner oxygen semipermeable membrane, a thin layer of the enzyme GOD and an outer dialysis membrane. The enzyme was immobilised to an electrochemical detector in order to form an enzyme electrode for the monitoring of oxygen concentration, which was proportional to the concentration of glucose in the sample.

Clark's sensor defined the first generation of glucose sensors, which were based on the use of natural oxygen substrate and on the detection of hydrogen

peroxide (H_2O_2) produced. The measurement of H_2O_2 has the main advantage of being simpler, especially when using miniaturised devices (Wang, 2008).

$$\text{glucose} + O_2 \xrightarrow{\text{GOD}} \text{gluconic acid} + H_2O_2$$

However, the main problem that the first generation glucose biosensors entailed was that this amperometric monitoring of H_2O_2 concentrations required a high operation potential in order to provide a high selectivity to the device. Also, the low solubility of oxygen in biological fluids compromised the correct functioning of the sensors, since it produced fluctuations in the oxygen tension (Liu and Wang, 2001).

These limitations led to the development of second-generation glucose biosensors in the 1980s, which were based on the use of artificial redox mediators instead of physiological ones such as oxygen. These mediators are able to carry electrons from the active site (redox centre) of the enzyme to the surface of the working electrode, which was the limiting factor in the operation of amperometric glucose biosensors (Liu and Wang, 2001). When accepting electrons, the mediator becomes reduced and is then reoxidised at the surface of the electrode, thus providing an amperometric signal proportional to the concentration of glucose (Turner *et al.*, 1999). Such a mediation cycle is shown in Figure 2.9. Some of the most widely employed redox mediators were ferrocene, ferricyanide or quinones. Among these, ferrocenes are considered good mediators, since they do not react with oxygen, their oxidised and reduced forms are stable in any pH, exhibiting reversible electron transfer kinetics, and they react rapidly with the enzyme with a high turnover rate (Chaubey and Malhotra, 2002).

$$GOD_{(red)} + 2M_{(ox)} \rightarrow GOD_{(ox)} + 2M_{(red)} + 2H^+$$

$$2M_{(red)} \rightarrow 2M_{(ox)} + 2e^-$$

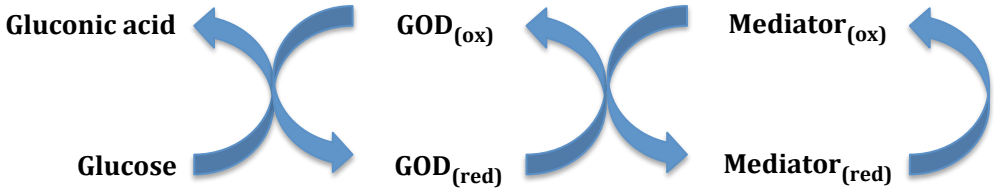

Figure 2.9. Sequence of events taking place in a mediator-based glucose biosensor.

The third-generation glucose biosensors commenced with the need to eliminate the mediator and develop a reagentless glucose biosensor which could operate at a low potential, close to the redox potential of the enzyme. This had the main advantage of being highly selective, due to this low operating potential. In these biosensors, the transfer of electrons takes place between the redox site or the enzyme and the electrode (Wang, 2008). Instead of using mediators that may have a high toxicity, other materials can be used on the electrode such as organic conducting materials, based on charge transfer complexes (Khan *et al.*, 1996). However, only a few enzymes have been proved to perform an optimum electron transfer at normal electrode surfaces (Zhang and Li, 2004).

2.5.4 Lactate biosensors

In 1973, the first lactate sensor was developed by Hoffman la Roche, using an artificial redox mediator, ferricyanide (Mindt *et al.*, 1973). Since then and for almost four decades, a large amount of studies have focused on the development of sensors for lactate detection and quantification. Nikolaus and Strehlitz compiled in a review 214 references from work performed in amperometric lactate biosensors between the years 1974 and 2007 (Nikolaus and Strehlitz, 2008). The review analyses the different aspects within the preparation of amperometric biosensors such as biorecognition elements, methods of immobilisation, mediators and cofactors as well as fields in which these sensors can be applied.

The first aspect to be discussed about the different amperometric biosensors for lactate is the electrode material. The working electrode can be made of different materials, some of them being more favourable than others. The most commonly employed materials for working electrodes are metal or carbon-based (Thevenot *et al.*, 2001), both of these being employed almost equally in the different biosensors reported. Carbon-based electrodes are slightly more common, and they can be found in the form of carbon paste electrodes, glassy carbon electrodes, screen printed electrodes with printing ink based on graphite, and graphite electrodes. It should be noted; metal-based working electrodes are also widely used for lactate sensing. Most of these are composed of platinum (Pt) or gold (Au), the first one being more widely used (Nikolaus and Strehlitz, 2008).

The second aspect discussed in the review is the biorecognition element that amperometric sensors use for lactate sensing. Such biorecognition elements include enzymes, cell fractions and even whole bacteria or yeast cells. Among these, enzymes are the most widely used. Since the present work will be focused on enzyme-based sensors, from now on enzymes will be referred as the recognition element of amperometric biosensors for lactate. Three different lactate-converting enzymes are used in the different lactate amperometric biosensors: lactate oxidase (LOD), lactate dehydrogenase (LDH) and cytochrome-dependant lactate dehydrogenase. In the reactions they catalyse, NAD^+ and NADH are the oxidised and reduced forms, respectively, of nicotinamide dinucleotide (Nikolaus and Strehlitz, 2008). These enzymes can be utilised in mono-enzyme or in multi-enzyme configuration and will be described in different sections.

Lactate oxidase (LOD)

Lactate oxidase (LOD, EC 1.13.12.4) catalyses the reaction:

$$\text{Lactate} + O_2 + H_2O \rightarrow \text{pyruvate} + H_2O_2$$

In this reaction, H_2O_2 is produced and subsequently detected at the electrode. LOD is the most widely used enzyme for amperometric lactate biosensors with both mono and multi-enzyme configuration. The main reason for this is that the enzyme has the advantage of not needing the presence of cofactors for performing the catalysis of the reaction. Only oxygen is required for the reaction to take place. However, the detection of H_2O_2 at noble metal electrodes requires elevated overpotentials, which can cause interferences by species that are easily oxidisable (Nikolaus and Strehlitz, 2008), as it will be explained in further detail in chapters 6 and 7.

The Michaelis-Menten constant (K_M) for lactate oxidase has a value of 0.7 mM. The value of K_M constant is specific for each enzyme and describes the reaction kinetics for a simple enzyme-catalysed process. K_M is described as the concentration of substrate at which the reaction rate is half the value of the maximum rate (Berg *et al.*, 2006). The K_M provides useful information regarding the construction of the system where the enzyme will be incorporated, since the value of this constant can be shifted by restricting the flow rate of substrate through the system so that higher substrate concentrations can be analysed.

Lactate dehydrogenase (LDH)

Lactate dehydrogenase (L-LDH, EC 1.1.1.27/D-LDH, EC 1.1.1.28) catalyses the reaction:

$$\text{Lactate} + NAD^+ \rightarrow \text{pyruvate} + NADH + H^+$$

In this case, the reaction product to be detected at the electrode is NADH. When the LDH enzyme is used as the only enzyme in the system, it requires the presence of a cofactor such as NAD^+. This need for a cofactor is a disadvantage, since it implies an additional immobilisation step, which often makes the process more difficult; otherwise, the cofactor can be added to the solution. Moreover these approaches share the same disadvantage as LOD-based sensors, since the direct oxidation at the electrode of the NADH produced in the reaction requires high applied potentials, which can again cause interferences from other oxidisable species (Nikolaus and Strehlitz, 2008). Also, the reaction takes place through radical intermediates, which lead to contamination of the electrodes and a drop in stability (Cosnier *et al.*, 1997; Lobo-Castañón *et al.*, 1997). LDH-based sensors have also been reported to be less sensitive than those based on LOD for determining the concentration of L-lactate when this is of a micromolar range (Zaydan *et al.*, 2004). However, the use of LDH-based amperometric sensors has the advantage that no oxygen is required, which makes them suitable for monitoring lactate in surroundings where oxygen is lacking or very depleted.

Lactate dehydrogenase (cytochrome)

LDH (cytochrome) (FCb, EC 1.1.2.3) catalyses the reaction:

$$\text{Lactate} + 2\ \text{ferricytochrome c} \rightarrow \text{pyruvate} + 2\ \text{ferrocytochrome c}$$

The enzyme is independent of the presence of external cofactors, only ferricytochrome c, which is an advantage during the immobilisation steps. Also, this approach is independent of oxygen (Williams *et al.*, 1970). However, this enzyme also has some disadvantages. D-lactate is a competitive inhibitor of the oxidation reaction of L-lactate, and pyruvate is also known to be a competitive inhibitor for the oxidised enzyme in low concentrations (Urban and Lederer, 1988). Moreover, lactate easily saturates the enzyme. Hence, since the concentrations of lactate in serum and sweat are quite high, it is necessary to add a dilution step to the preparation process. This is especially important in the determination of lactate in sports or in ischemic tissues, where the concentrations of lactate in these human fluids are much higher (Nikolaus and Strehlitz, 2008).

Lactate amperometric biosensors can also be based on a multi-enzyme system, which has the main advantage that the substrate of the reaction can be recycled, which leads to an amplification of the signal (Nikolaus and Strehlitz, 2008).

One of the most important features in the development of an enzymatic sensor is the immobilisation method of the enzyme at the transducer. In fact, the performance of a sensor strongly depends on the method used to immobilise the enzyme (Sung and Bae, 2006). There are many different ways in which enzymes can be immobilised to a transducer. An enzymatic solution can be entrapped behind a membrane permeable to an analyte. Enzymes can additionaly be entrapped within a polymeric matrix or in self-assembled monolayers or bilayer lipid membranes. Enzymes can also be bonded covalently on membranes or activated surfaces. The electrode material can also be modified. Finally, the enzyme can be entrapped in a polymer matrix (Nikolaus and Strehlitz, 2008) to the material of the working electrode. Regarding this method, most authors have used glutaraldehyde for achieving a covalent bonding, though many other compounds exist, which produced the same effect (Nikolaus and Strehlitz, 2008).

The last important feature when developing amperometric lactate biosensors is the use of artificial cofactors, also known as mediators, since they enhance the

sensitivity and selectivity of the sensing method. Cofactors are non-protein chemical compounds who's presence is required for enzymes to perform their biological activity, since they act as electron carriers. All oxidase enzymes, such as GOD or LOD, use O_2 as their natural cofactor. Due to this, oxidase-based devices, which rely on the use of oxygen, are often subject to errors caused by its limitation in the solution (Wang, 2008). Moreover, since the availability of oxygen in the solution is difficult to control, errors in sensor performance such as electrochemical response and linearity are difficult to avoid. Artificial cofactors, known as mediators, are important since they act as an electron shuttle, thus forming a redox coupling between the electrode of the sensor and the redox centre within the enzyme (Nikolaus and Strehlitz, 2008) when redox enzymes are used, which have very low rates of electron transfer. Moreover, mediators reduce the overpotential needed for the oxidation of NADH or the detection of H_2O_2 at the electrode. However, mediators are usually highly toxic compounds that can compromise the stability of the enzyme (Leonida *et al.*, 2003). Mediators used for amperometric lactate biosensors are divided into three different types: metal compounds, conducting polymers and organic dyes (Nikolaus and Strehlitz, 2008). If the mediator binds tightly to the protein molecule so it becomes part of the enzyme, the complex is called a prosthetic group. Alternatively, if the mediator is free of the enzyme complex and attaches to the active site alongside the substrate, these complexes are called coenzymes (Berg *et al.*, 2006).

2.5.4.1 Wearable sensors for monitoring of sweat lactate

Despite the extensive research focused on the development of lactate sensors, most of these technologies are focused towards the analysis of blood, urine or in industrial processes such as wine fermentation.

As it was discussed in section 2.3.6, in order to achieve a continuous and non-invasive monitoring of lactate for medical applications, alternative biological fluids to blood have to be tested, sweat being a very attractive alternative due to its accessibility and non-invasive collection. Sweat also allows the development of

wearable technologies in order to obtain continuous and real-time information of lactate-level fluctuations in the subject under study. However, although efforts have been made towards the development of non-invasive systems for measuring lactate in sweat (Lamas-Ardisana *et al.*, 2014; Cai *et al.*, 2010; Weber *et al.*, 2006; Mitsubayashi *et al.*, 1994; Faridnia *et al.*, 1993), these technologies are not designed as wearable devices for providing a real-time continuous monitoring of the metabolite. In the last years, however, a few studies have been reported on the development of wearable technologies for the monitoring of sweat lactate.

In 2012, Khodagholy *et al.* demonstrated an organic electrochemical transistor patch with integrated room temperature ionic liquid in a gel-format as an immobilisation matrix for the enzyme LOD and a supporting electrolyte. However, despite performing lactate measurements in PBS in the range 10-100 mM, no studies were performed on real sweat samples (Khodagholy *et al.*, 2012).

In 2013, Jia *et al.* reported the development of an electrochemical tattoo-based wearable sensor based on dispersed carbon fibres, which conferred mechanical stability. The enzyme LOD was immobilised on the electrode surface, previously functionalised with tetrathiafulvalene and multiwalled carbon nanotubes as an electron shuttle and to avoid interferences from compounds present in the sweat sample (Jia *et al.*, 2013). However, despite demonstrating the capability of the sensor to perform continuous and real-time measurements of sweat lactate, the upper detection limit of the system was 20 mM, which barely covers the concentration range in sweat reported for healthy subjects and is not suitable for the measurement of higher sweat lactate levels present in non-healthy subjects (i.e. suffering from pressure ischemia), where lactate levels may raise over 70 mM.

In April 2014, Pribil *et al.* reported in a letter the development of a wearable electrochemical sensor where lactate oxidase enzyme was modified in order to decrease its affinity for its substrate and increase the working concentration range. However, despite of demonstrating the capability of the sensing system to perform real-time and continuous monitoring of sweat lactate, the operational stability of the device decreased after 4 hours of continuous operation (Pribil *et al.*, 2014),

which is not suitable for its use as a medical device for the continuous monitoring of lactate concentrations during a longer period of time prior to its replacement.

For all the aforementioned systems, the development of a wearable sensor capable of performing real-time and continuous measurements of sweat lactate in the physiologically relevant concentration range for hypoxia-related conditions along a relatively long period, relevant for its application, prior to replacement is still needed, which leads to the importance of the research presented in this thesis.

2.6 Electrochemistry

2.6.1 Introduction

Electrochemistry is a branch of chemistry, which studies, in its majority, the chemical changes occurring as a consequence of the flow of electric current and also the production of electrical energy in chemical reactions (Bard and Faulkner, 2001).

In opposition to many chemical measurements, which often occur in homogeneous bulk solutions (Wang, 2006), an electrochemical process often involves the transfer of charge across the interface formed between a metallic electrode, which conducts electricity, and a solution phase (electrolyte), which conducts ions, both contained in an electrochemical cell (Bard and Faulkner, 2001; Fisher, 1996). Most of the charge transfer processes studied by electrochemistry comprise a transfer of electrons during the oxidation and/or reduction of the species within the bulk solution or electrolyte (Brett and Brett, 1998). The interface that forms when the electrode is immersed in the electrolyte is called the double layer and its electrical properties are important, since they significantly affect electrochemical measurements (Stojek, 2002).

It is usually possible to get information about an electrochemical system by applying an electrical perturbation on such system and observing the changes that

occur in the characteristics of the system as a result of this perturbation (Bard and Faulkner, 2001).

There are three main types of electroanalytical measurements that can be performed, which differ in the type of electrical signal used for the quantitation namely; conductometric, potentiometric and voltammetric measurements. In conductimetry, the resistance of a solution is measured to obtain the concentration of charge. Even though this technique is not species-selective, it can be useful in those cases when the total ion concentration has to be determined. Potentiometry uses an impedance voltmeter to measure the equilibrium potential of an electrode against a reference electrode. Voltammetry, which will be further explained in more detail, allows the determination of different species almost simultaneously within the same experiment by analysing the current as a function of applied potential. This potential can be constant or vary during the experiment. Therefore, voltammetry provides more information and also permits lower detection limits - that is, the detection of smaller concentrations of the species. A subclass of voltammetry is amperometry, in which the electrode is set to a fixed potential for a certain length of time, causing the reaction of the species and the flow of current. When the potential of the electrode is chosen appropriately, the magnitude of current is directly proportional to the concentration of such reacting species (faradaic current) (Brett and Brett, 1998).

2.6.2 Electrochemical cells

A typical electrochemical process takes place in an electrochemical cell, a container of variable geometry, in which two independent electrodes are immersed in a conductive solution and connected to each other through the solution and also externally by wires, electrical loads or batteries, thus forming an electrical circuit. Electrochemical reactions such as oxidation and reduction take place at each one of the electrodes. In these reactions, electrons are consumed at one electrode and supplied at the other one in such a way that no electrons are consumed in the global chemical reaction (Brett and Brett, 1998). Electrodes can be made of different materials, the most typical being solid metals (Pt, Au), liquid

metals (Hg, amalgams), carbon (graphite), and semiconductors (indium-tin oxide, Si). In the electrolyte phase, the most typical electrolytes used are liquid solutions, which contain ionic species such as H^+, Na^+ and Cl^- in either water or a non-aqueous solvent (Bard and Faulkner, 2001).

Electrochemical cells in which faradaic currents flow are classified as being either galvanic or electrolytic cells (Figure 2.10). In galvanic cells, reactions take place at the electrode spontaneously once they are connected externally by a conductor. In electrolytic cells, non-spontaneous redox reactions at the electrode take place when applying an external voltage with higher value than the open-circuit potential of the cell. Hence, in electrolytic cells electrons are forced to flow in the opposite direction to how they naturally would in a galvanic cell. For this reason, anode and cathode in galvanic cells have opposite signs to the electrolytic cell, since electrons flow from the anode into the cathode (Brett and Brett, 1998).

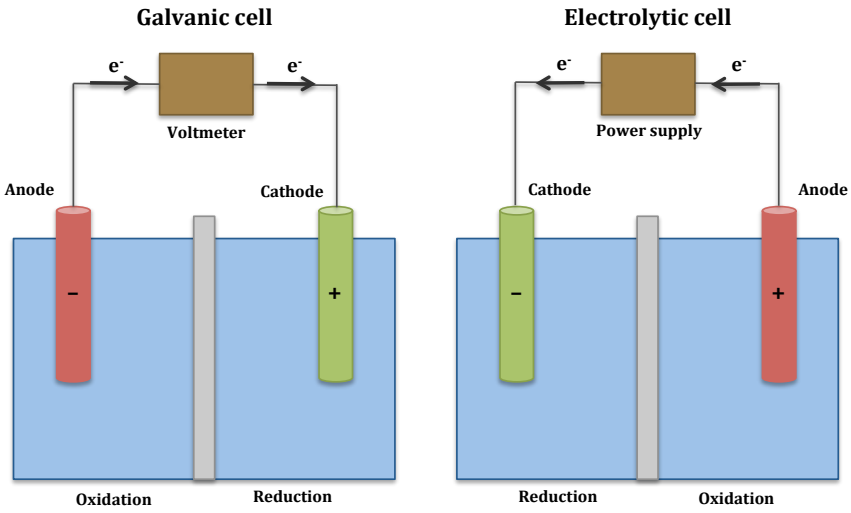

Figure 2.10. Comparison between a galvanic and an electrolytic cell.

In the galvanic cell, the electrode in the anode is spontaneously oxidised and the electrode in the cathode is spontaneously reduced. The potential is recorded with a voltmeter. In an electrolytic cell, an external potential greater than the one for the spontaneous reaction is applied. This forces the electrons to flow from the anode (where reduction is taking place) to the cathode (where reduction occurs). Hence, the anode in an electrolytic cell is positive since electrons are flowing from it, and the cathode is negative because electrons are flowing into it.

In most of the cases, the difference in electric potential is measured between the electrodes within the electrochemical cell by using a high impedance voltmeter. The cell potential is measured in volts (V), being 1 V = 1 joule/coulomb (J/C). This potential is a measure of the available energy to drive charge in the external circuit between the electrodes. As it will be explained later, this transition in electric potential from the electrode surface to the solution occurs almost exclusively at the interface between these two phases. Moreover, the magnitude of the applied potential controls the direction of the charge transfer and the rate at which it occurs.

The global chemical reaction taking place in an electrochemical cell is composed of two independent half-reactions that describe the chemical changes taking place at each one of the electrodes. Usually, only one of these half reactions is of interest and the electrode where it takes place is known as working electrode. In order to study this electrode, it is necessary to standardise the other half of the cell by using a reference electrode, which surface is made of a constant composition and of high impedance and, because of this, its potential is fixed and it does not pass current. Therefore, any changes occurring within the cell can be attributed to the working electrode and its potential can be analysed with respect to the reference electrode (Bard and Faulkner, 2001). The potential at the reference electrode is usually controlled by an instrument called a potentiostat. As it will be further explained, in some cases it is useful to work with a system composed of three electrodes. In a three-electrode system (Figure 2.11), the current of the electrochemical cell flows between the working electrode and a counter or auxiliary electrode, which performs the other half cell reaction, opposite to the one taking place at the WE. In some cases, it is important to ensure that no reaction products from the counter electrode reach the working electrode by dividing the cell into two half-cells by using, for example, a glass frit separator (Brett and Brett, 1998). The counter electrode, typically made of Pt, usually has a larger surface area than that of the WE in order to ensure that the electrochemical reaction taking place at the CE is fast enough so it does not limit the electron transfer and affect the reaction occurring at the WE. The RE is often placed in a

Luggin capillary so its thin tip can be placed in close proximity to the WE in order to minimise the uncompensated electrolyte resistance without preventing the reactants from reaching the surface of the WE (Qi, 2008).

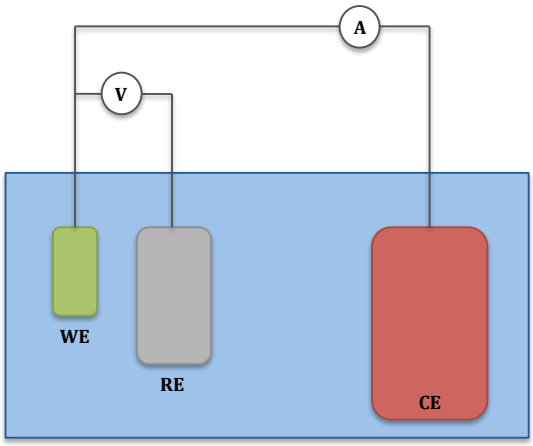

Figure 2.11. Diagram representing a three-electrode system.

The three electrodes are denoted as WE (working electrode), RE (reference electrode) and CE (counter electrode). The reaction of interest takes place at the WE and the functions of a CE/RE in a two-electrode system are divided between the RE and the CE. The potential between the WE and the RE electrodes is controlled by a potentiostat. The current passes between the WE and the CE.

If more cathodic potentials are applied on the electrode, electrons flow from the electrode to the solution, giving rise to a reduction current. In a similar way, if anodic potential values are applied on the electrode, the energy of the electrons is lowered and they may find a more favourable energy on the electrode and will transfer there from the solution, giving rise to an oxidation current. The potentials at which these electron transfers occur are called standard potentials, E^0, and are specific for each chemical substance in the system (Bard and Faulkner, 2001).

2.6.3 Faradaic and Nonfaradaic processes

In electrodes, two different kinds of processes can take place. One kind comprises reactions in which charges such as electrons are transferred across the interface between the metal of the electrode surface and the solution. These electrons allow oxidation and reduction (redox) processes to take place on the surface of the electrode. Since Faraday's law ("one mole of electrons produce 96,487 coulomb of charge") governs such redox processes; these are known as faradaic processes and the electrodes where they take place are in some cases called charge-transfer electrodes. However, some other processes can occur at the electrochemical cell such as adsorption (adhesion of particles to a surface) and desorption (release of a substance from a surface). These can produce the change in the structure of the interface between the electrode surface and the solution if the potential, the electrode area or the solution composition are altered. Such processes are called nonfaradaic processes. In this case, even though charges cannot cross the interface, external currents can flow, thus changing the structure of the interface. Both faradaic and nonfaradaic processes occur when the reactions take place at the surface of the electrode (Bard and Faulkner, 2001). To sum up, given an electron travelling through the external circuit towards the surface of an electrode, once it reaches such surface the electron has two alternative destinations. It can leave the surface of the electrode, thus transferring to a species in the solution and becoming this way a part of a faradaic current. Alternatively, the electron can remain at the surface of the electrode and increase the charge of the double layer, which will be explained shortly, thus becoming part of a non-faradaic current.

i. Nonfaradaic processes

An ideal polarised electrode (IPE) is an electrode at which no charge transfer can take place across the interface between its surface and the solution, in spite of the potential applied by an external power supply. Even though in reality no

electrode can behave like an IPE, some electrode-solution systems can show similar characteristics to this ideal system.

The interface between the electrode surface and the solution in this kind of systems has similar characteristics to a capacitor, which consists of two metal sheets that are separated by a dielectric material. If a given potential is applied, both the electrode and the solution will be charged, with their charges being q^M and q^S respectively. Depending on the potential across the interface and the composition of the solution, q^M and q^S will be positive or negative (Bard and Faulkner, 2001). However, at all times $q^M = -q^S$ in order for the interface to maintain electrical neutrality (Fisher, 1996). q^M is the charge on the metal and represents an excess or deficiency of electrons. This charge is located in a very thin layer (less than 0.1 Å) on the metal surface of the electrode. The charge in solution, q^S, represents an excess of either cations or anions in the vicinity of the electrode surface. The resulting array of charged species and oriented dipoles at the interface between the electrode surface and the solution when a potential is applied is called the electrical double layer (Bard and Faulkner, 2001).

The electrical double layer

The aforementioned model describing the composition of the interface between the electrode surface and the solution or electrolyte was proposed in 1853 by Hermann von Helmholtz (as shown in Figure 2.12a. The charges described for the solution and the metal of the electrode arise from the redistribution of the ions at the interface and/or the reorientation of dipoles in solvent molecules due to an electrostatic driving force. This creates a potential difference across the interface, thus producing an electric field gradient across the charge separation layer. Ions within the solution in proximity to the electrode surface are attracted or repelled electrostatically, thus creating an excess or deficiency of either anions or cations, depending on the case. The attracted ions are able to approach the surface of the electrode up to a certain distance, which is determined by the solvation shell of such ions, since it is assumed that there is a solvation monolayer between the

ion and the electrode. As a result of this, the plane described by the centre of such ions disposed in the proximity of the electrode surface is called the Outer Helmholtz Plane (OHP). For this reason, the electric double layer described by Helmholtz is similar to a capacitor, where two layers of charge are separated by a fixed distance. These ions balance the excess of charge on the metal surface, and the potential drop across the interface is linear and takes place entirely in the region between the electrode surface and the OHP.

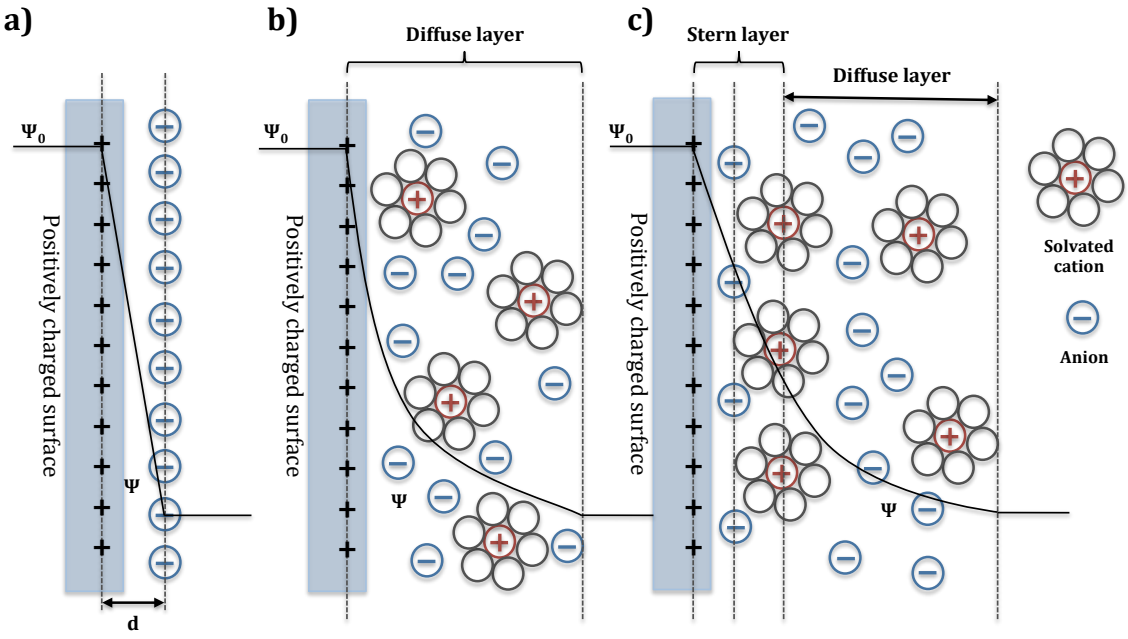

Figure 2.12. Diagram representing the different models for the electrical double layer. A positively charged surface is considered.

a) Helmoltz model, **b)** Gouy-Chapman model, and **c)** Stern model. IHP represents the Inner Helmholtz Plane and OHP, the Outer Helmholtz Plane. *d* is the distance between the plane described by the centre of the ions disposed in the proximity of the surface and such surface.

In 1910, Louis G. Gouy and David Chapman improved Helmholtz's model after postulating that the density of charge in excess within the solution was not situated exclusively at the OHP. This new model is shown in Figure 2.12b and represented the ions as point charges and proposed that the charge density within the solution is contained within a single diffuse layer in the vicinity of the electrode surface. In this diffuse layer, the net charge density decreases with the distance

away from the electrode surface. In this case, the potential drop across the diffuse layer is also mainly concentrated in the region closest to the electrode surface, but this time some of this charge is now situated further away from the electrode surface than the OHP.

In 1924, Otto Stern took Gouy and Chapman's model one step further by accepting the existence of a minimum distance of approach for the ions to the vicinity of the electrode surface (the OHP) and also supporting the existence of a diffuse layer. Therefore, Stern's model (Figure 2.12c) comprised a combination between the two past models. In this third model, the potential drops sharply between the electrode surface and the OHP, after which the potential falls gradually to a value that is characteristic for each bulk electrolyte.

In 1947, David C. Grahame proposed a new model based on the fact that, even though the vicinity of the electrode surface is mainly composed by solvent molecules, ionic or uncharged species may penetrate in this region. This could occur if such ions had no solvation shell around them or if they had lost it while approaching the electrode surface. In this case, ions are directly in contact with the electrode and are said to be specifically adsorbed. With this new model, a new plane of minimum approach was proposed, closer to the electrode surface than the OHP. Hence, this new plane was called Inner Helmholtz Plane (IHP) (Fisher, 1996).

ii. Faradaic processes

Consider a typical electrochemical experiment, in which a working electrode and a reference electrode are immersed in a solution, and the difference in potential between the electrodes can be changed by using an external power supply. This variation in the potential, E, gets reactions to occur in the electrode's surface and electrons to cross the electrode/solution interface. As a consequence of this, current flows in the external circuit. The number of electrons can be determined according to the total charge, Q, flowing through the circuit. This charge is expressed in units of coulombs (C), being 1 C equivalent to 6.24×10^{18}

electrons. If it is considered that the amount of electrons that cross the interface is directly proportional to the concentration of the reactant consumed and the product generated at the electrode, this relationship between current and concentration is given by Faraday's law of electrolysis, which states that the passage of a charge of 96,485.4 C causes the consumption of 1 equivalent of reaction, which is a mole of reactant or the production or 1 mole of product, in a one-electron reaction.

$$Q = \int_0^t i\, dt$$

The current, *i*, is the rate of flow of coulombs (or, as mentioned, electrons), where a current of 1 ampere (A) is equivalent to 1 C passed per unit of time, *t*, in this case a second (C/s). When the current is plotted as a function of the applied potential, a current-potential (*i vs. E*) curve is obtained (Bard and Faulkner, 2001), also called a voltammogram, which represents the current signal in the vertical axis versus the excitation potential in the horizontal axis. The shape and magnitude of a voltammetric response is dependant on the processes involved in the reaction taking place at the electrode. The total current obtained is the combination of the faradaic currents, from the sample and blank solutions analysed, and nonfaradaic charging background currents from the electric double layer effect (Wang, 2006). Therefore, voltammograms give information about the nature of the electrodes and the solution and also about the reactions that take place in the interface between them (Bard and Faulkner, 2001). The main objective of controlled-potential electroanalytical experiments is the obtaining of a current response related to the concentration of the analyte reacting at the electrode. This is achieved by monitoring the transfer of electrons along the redox process of the analyte (Wang, 2006). A general charge transfer reaction would be expressed as:

$$O(aq) + ne^{-}(m) \leftrightarrows R(aq)$$

in which *n* electrons would be transferred (Fisher, 1996). O and R would be the oxidised and reduced forms of the redox couple, respectively. Such reaction would take place at a certain potential range that made the electron transfer in this

reaction kinetically or thermodynamically favourable. For those systems that are controlled by the laws of thermodynamics, the concentration of the electroactive species at the surface of the electrode, [O] and [R], at equilibrium can be determined with an applied potential, according to the Nernst equation:

$$E = E^{O} \pm \frac{2.3RT}{nF} log \frac{[O]}{[R]}$$

where E^0 is the standard potential for the redox reaction, R is the universal gas constant (8.314 J/K·mol), T is the temperature in Kelvin and F is the Faraday constant (96,487 C). Note that the 2.3 multiplier is used when applying log (or log_{10}) on the equation instead of the neperian logarithm (*ln)* (Bushman, 2002). When E^0 is negative, reduction is more favourable and usually the oxidised form tends to get reduced. The current that results from the change in oxidation state of the electroactive species is known as faradaic current because, as it has been aforementioned, it obeys Faraday's law, and it is a direct measure of the rate of the redox reaction (Wang, 2006).

Factors affecting the electrode reaction rate and the current

In general, the charge-transfer reaction taking place at the electrode is quite complex and involves several steps or sequence of processes such as the mass transfer of O to the surface of the electrode, electron transfer at the surface of the electrode, mass transfer of R back to the bulk solution, chemical reactions taking place before or after the electrode transfer, or other reactions taking place at the surface of the electrode such as adsorption, desorption, electrodeposition, etc. A basic summary of the steps involved is shown in Figure 2.13. Each of this processes occur at a different rate that, in some cases, depends on the applied potential. Therefore, the overall reaction rate at the working electrode (electrode reaction rate or current) will be limited by the slowest step such as mass-transport of the electroactive species (O) to the electrode surface, the electron transfer within the reaction across the interface or the mass-transport of the product (R) back to the bulk solution (Bard and Faulkner, 2001; Wang, 2006; Fisher, 1996).

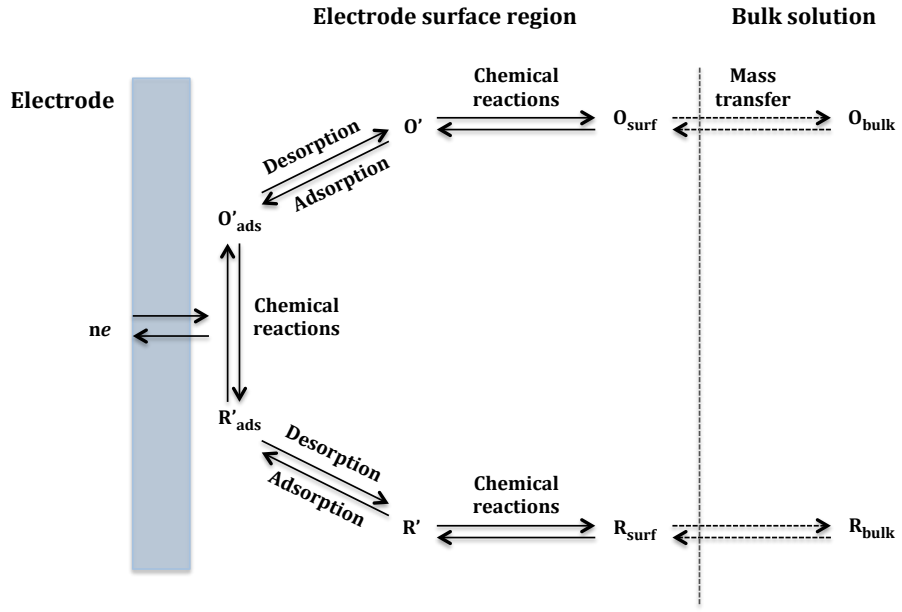

Figure 2.13. Diagram describing the pathway of a general electrode reaction

(adapted from Bard and Faulkner, 2001).

Mass transport

As it has been mentioned earlier, the rate at which some processes involved in the electrolysis of O into R occur can be controlled through the potential applied on the electrode. This is the case of the electron transfer. Therefore, if the electrolytic reaction is forced to work at a higher rate by increasing the potential, mass transport plays an important role (Fisher, 1996).

There are three main processes by which the reactant molecule in the solution is transported to the surface of the electrode: diffusion, convection and migration (Figure 2.14).

Diffusion (Figure 2.14a) is the spontaneous movement due to a concentration gradient, which makes particles travel from more concentrated regions of the solution to less concentrated ones in order to homogenise the concentration in the solution. The rate of diffusion depends on the concentration gradient at the particular location under analysis.

Migration (Figure 2.14b) produces the movement of charged particles along an electrical field caused by the drop in electrical potential at the electrode/solution interphase.

Convection (Figure 2.14c) is the process that makes particles move to the electrode due to physical movement. These are mainly mechanical forces such as stirring the solution or rotating or vibrating the electrode. However, convection can also occur naturally due to density gradients within the solution. In some electrochemical experiments it is common to introduce an element of forced convection, which is higher, and therefore controllable, than natural convection. This enables the establishment of a quantitative description of the flow in solution and the prediction of the pattern of mass transport to the surface of the electrode.

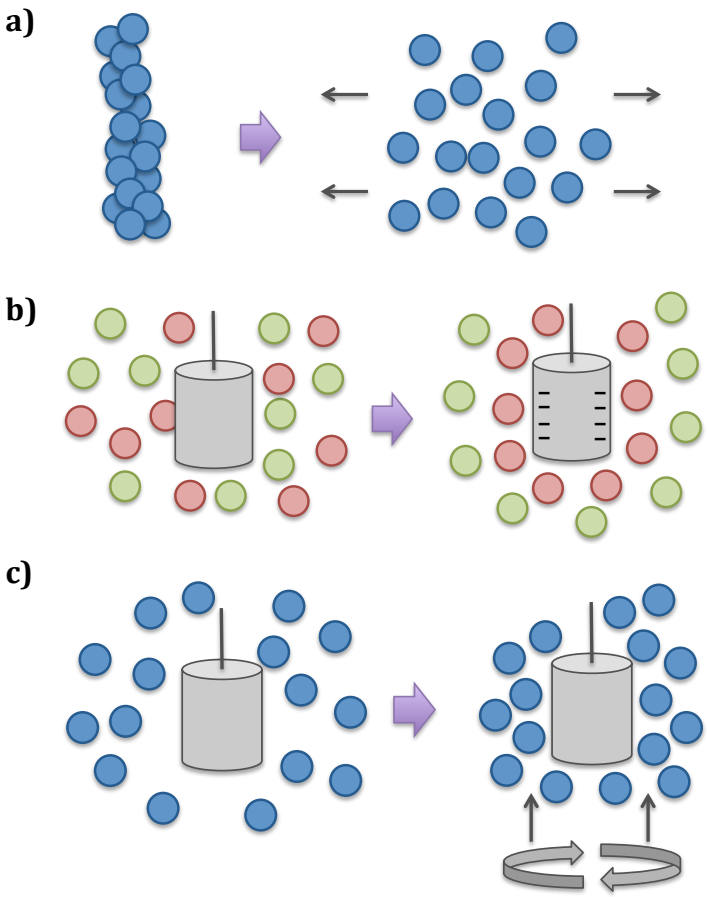

Figure 2.14. Diagrams describing the three modes of mass transport.

a) diffusion, **b)** migration and **c)** convection. In figure b), the red circles represent the positively charged molecules and the green ones, the negatively charged particles.

2.6.4 Voltammetry

Voltammetry is the electrochemical group of techniques involving the study and measurement of the current response at the electrode as a function of the voltage that is applied to the electrolytic cell, or the potential response as a function of an applied current. Voltammetric sensors, therefore, work by registering current-potential profiles (Fisher, 1996; Brett and Brett, 1998). A particular case of voltammetric sensors is amperometric sensors, which work with a fixed potential to register current as a function of time.

2.5.4.1 Experimental measurement of current/voltage characteristics

In voltammetry, the simplest approach for the measurement of current/voltage is using a system composed by two electrodes: a working electrode and a reference electrode. As it has been previously explained, the working electrode is where the reaction of interest takes place. The reference electrode is fixed at a set potential, so when a certain current voltage is applied between both electrodes, the potential between the working electrode (Φ_m) and the solution (Φ_s) can be accurately determined as $\Phi_m - \Phi_s$. This difference in potential is the driving force that makes it possible for electrolysis to take place at the interface between the electrode and the electrolyte, and it depends on the applied current voltage. This two-electrode system (working and reference electrodes) is especially useful when the current that flows is small; this is, for example, when working with microelectrodes. However, when working with larger electrodes, the applied potential is no longer directly affecting the potential between the working electrode and the solution ($\Phi_m - \Phi_s$), since there are more factors in the equation that have to be taken into consideration. Given a voltage or current, *E*, which is applied between a working and a reference electrode, both of large dimensions, and assuming that a finite current flows between them, we can assume that:

$$E = (\phi_m - \phi_s) + iR + (\phi_s - \phi_{REF})$$

E is split into 3 different terms. The first one, ($\Phi_m - \Phi_s$), is the driving force for electrolysis at the interface between the working electrode and the solution. The second term, *iR*, corresponds with the voltage drop in the solution as a consequence of the flow of current between the working ad reference electrodes. In this term, *R* is the electrical resistance of the solution. The third term, ($\Phi_s - \Phi_{REF}$) corresponds to the potential drop at the interface between the reference electrode and the solution. This value is determined in voltammetry by the chemical composition of such reference electrode.

The aim of any voltammetric experiment is to determine *i* as a function of the changes in the value of ($\Phi_m - \Phi_s$). When working with microelectrodes, the term *iR* can be neglected and ($\Phi_s - \Phi_{REF}$) is constant. Therefore, *E* is determined by:

$$E = (\phi_m - \phi_s) + constant$$

This reinforces what was mentioned above, when working with microelectrodes, the applied potential is directly reflected in the potential in the interface between the working electrode and the solution. However, when the electrodes are of larger dimensions, *iR* cannot be neglected and, as a consequence of this, changes in the applied potential E are not directly reflected in changes in the driving force ($\Phi_m - \Phi_s$). Moreover, since this time bigger currents will flow through the reference electrode, its chemical composition may be altered and, therefore, the term ($\Phi_s - \Phi_{REF}$) will no longer be constant. This proves that it would not be possible to work with large currents in a two-electrode system, since the current would not be directly related to the value of the driving force and it would be impossible to interpret this current.

In order to overcome this problem, when performing voltammetric experiments using large currents it is usual to use a three-electrode system in which, in addition to the working and reference electrode, a counter or auxiliary electrode is added. This third electrode is controlled by a potentiostat with the objective of ensuring that current only flows between the working and the counter electrode. This now makes the reference electrode stable, and the potential of the working electrode can now be held relative to it. The potentiostat makes sure that no current flows through the reference arm of the circuit (Fisher, 1996).

In voltammetry, it is possible to observe the behaviour of current, *i*, with time, *t*, after applying a certain potential of magnitude *E* (potential step). Another option is to analyse the change of current as the potential is changed at a sweep rate υ (potential sweep) (Bard and Faulkner, 2001). These two electrochemical techniques will be explained below.

2.5.4.2 Potential sweep methods

In potential sweep techniques, a chosen region of potential is scanned and the current response, which arises from the electron transfer and associated reactions that occur, is measured. These techniques are commonly used for investigating electrode processes, which comprises the first step towards the development of an electroanalytical procedure. Potential sweep techniques can also give quantitative information, since the obtained currents are proportional to the concentration of the species reacting at the electrode. Two main potential sweep methods will be discussed in this section: linear sweep voltammetry and cyclic voltammetry.

Linear sweep voltammetry

The simplest of all potential sweep methods is linear sweep voltammetry (LSV), which consists of sweeping the potential of the electrode between an initial value E_1 to a final one E_2 at a sweeping rate ν (Figure 2.15a) (Pletcher *et al.*, 2001). Once the experiment begins at E_1, when the initial potential reaches the proximity of the value of the standard potential $E^{0'}$, between E_1 and E_2, the reduction of the species starts taking place and a cathodic current flow begins. As the potential continues getting more negative, the concentration of the reactant at the surface of the electrode starts to drop, thus increasing the flux of the compound and, therefore, the current. As the potential of the electrode gets greater than $E^{0'}$, the concentration of the reactant in the surface of the electrode drops nearly to zero. This makes the rate of mass transfer to the electrode surface reach a maximum and finally decline as the depletion effect starts occurring. As a result of this process, the observed response is a peaked current-potential curve (Figure 2.15b) (Bard and Faulkner, 2001).

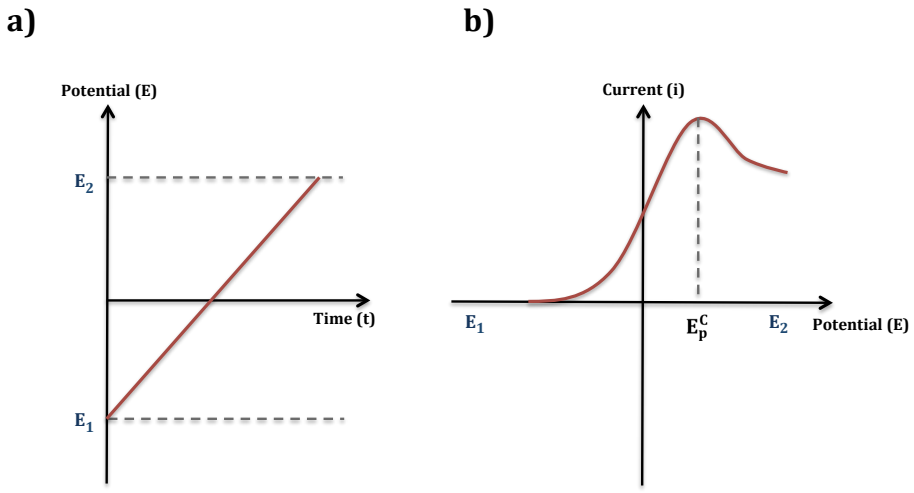

Figure 2.15. General schematic representation of a) a linear potential sweep and b) the resulting voltammogram in a linear voltammetry experiment.

E_1 and E_2 correspond to the potential values between which the experiment is run. $\mathbf{E_p^c}$ corresponds to the cathodic peak current value.

Cyclic voltammetry

A more useful potential sweep technique is cyclic voltammetry (CV), which starts in the same way as LSV but once the potential in the electrode reaches the value E_2 the sweep is reversed (typically at the same rate ν) instead of the experiment being stopped at this point (Figure 2.16a). There are three different options when this potential is reversed from E_2. The potential can either go back to E_1, come to an abrupt stop or continue further to a value E_3 (Pletcher *et al.*, 2001). As the potential approaches and then passes $E^{0'}$ again to more positive values, the concentration of product in the surface of the electrode drops and the concentration of the initial compound starts increasing. As a result of this, the anion species become reoxidised and an anodic current flows. At some point passed $E^{0'}$, the concentration of anion species drops to zero and the mass transport rate reaches its maximum. The obtained response for the reversal current is therefore also a peaked current-potential like the forward peak, but with opposite-sign values (Figure 2.16b) (Bard and Faulkner, 2001). This obtained current response for cyclic voltammetry will be further explained in more detail.

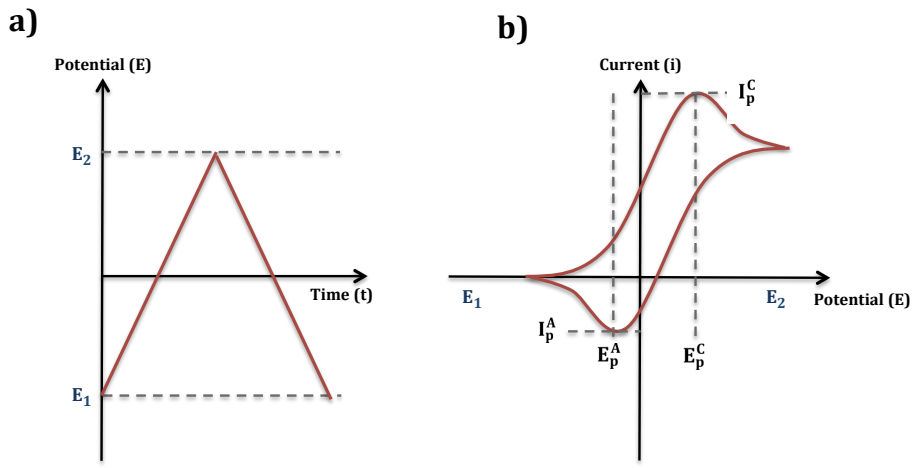

Figure 2.16. General schematic representation of a) a cyclic potential sweep and b) the resulting voltammogram in a cyclic voltammetry experiment.

E_1 and E_2 correspond to the potential values between which the experiment is run. $\mathbf{E_p^A}$ and $\mathbf{E_p^C}$ correspond to the anodic and cathodic peak current values, respectively. $\mathbf{I_p^A}$ and $\mathbf{I_p^C}$ are the anodic and cathodic peak current values, respectively.

As it has been mentioned, in both LSV and CV the current within the cell is recorded as a function of the applied potential. The values for the sweep rate most commonly employed in these experiments oscillate between a few mV/s to a few hundred V/s. If sweep rate values are too high, they may introduce some experimental difficulties. One way for obtaining high quality data with high sweep rate values is using microelectrodes, which minimise the charging currents and the effects produced by an uncompensated resistance (Pletcher *et al.*, 2001).

Data interpretation

The form of the resulting voltammogram can have a different shape depending on whether the reaction that takes place at the electrode is reversible, quasi-reversible or totally irreversible.

a) Reversible systems

In order to understand reversible systems, a simple reversible reaction has to be considered:

$$O + ne^- \rightleftharpoons R$$

Under steady state conditions, concentrations above a certain distance from the surface of the electrode remain uniform by natural convection. However, in the region next to the electrode surface, the concentration gradients are essentially linear. The ratio of the concentrations the species O and R at the electrode surface, $[O]^\sigma/[R]^\sigma$, is, for a reversible reaction, given by the Nernst equation. Therefore, as the applied potential is more negative, the concentration of the reactant at the electrode surface is progressively decreased, thus increasing the concentration gradient at this point and the current. This current in the forward reaction is called cathodic current. Eventually the concentration of the reactant O in the solution approaches zero and the steady state concentration profile cannot change anymore. At this point, the current reaches a plateau value. This current that flows in the external circuit is proportional to the gradient at the electrode surface. If the sweep rate is increased, the diffuse layer does not have time to relax and reach an equilibrium state. Therefore, this layer is not as extensive and the concentration profiles in this area are not linear. Once the concentration of O at the surface of the electrode, $[O]_{x=0}$, reaches zero, the concentration gradient starts to decrease and so does the current. As a result of this behaviour, a current-potential response with the shape of a peak is obtained. This peak occurs at a cathodic peak potential E_p^C and with a cathodic peak current value I_p^C. Moreover, with higher sweep rates, the concentration gradients and the resulting currents will increase as well due to a

shorter timescale of the experiment, since the potential reaches its value E_2 for the experiment in a shorter time.

Once the potential reaches the value E_2, the sweep potential is reversed. If the sweep rate is low, the current should follow the same pathway as in the forward step. However, for high sweep rates this does not occur. In these cases, when the sweep is reversed, there is a significant concentration of R in the vicinity of the electrode surface when the potential is still close to E_2. Once the potential starts to get close to $E^{0'}$, the R present in the vicinity of the electrode surface starts being reoxidised back to O so the surface concentrations are those required by the Nernst equation. As a result of this, a reverse current flows, called an anodic current. Similarly to what occurred in the forward reaction, as the potential reaches a value E_3, the concentration of R at the surface of the electrode, $[R]_{x=0}$, reaches zero and the resulting current response will also be peak shaped, but with opposite sign. This time, the peak occurs at an anodic peak potential E_p^A and with an anodic peak current value I_p^A. It is important to notice that the charge within the anodic process is lower than the one in the forward reduction process. This is due to the fact that during the first step of the experiment, the reduction of O, part of R was driven away from the electrode surface due to a concentration difference. Hence, part of this product R diffused into the bulk solution and in the reverse process it cannot be reoxidised back to O in the timescale of the experiment (Pletcher *et al.*, 2001).

If a charge-transfer process is reversible (Figure 2.16b), there is no surface interaction between the reagents within the solution and the electrode surface, and the redox products O and R are stable (Mallik and Ray, 2011). A test of reversibility is to check if $I_p/v^{1/2}$ is a constant; this is, if a plot of I_p as a function of $v^{1/2}$ is both linear and passes through the origin (Figure 2.17). If this is true, then there are several reversibility conditions to be tested, which are shown in Table 2.

Table 2.2. Diagnostic tests for cyclic voltammograms of reversible processes (at 25°C).

1. $\Delta E_p = E_p^A - E_p^C = 59/n$ mV
2. $\left|E_p - E_{p/2}\right| = 59/n$ mV
3. $\left|I_p^A / I_p^C\right| = 1$
4. $I_p \propto \nu^{1/2}$
5. E_p is independent of ν (Figure 2.17)
6. at potentials beyond E_p, $I^{-2} \propto t$

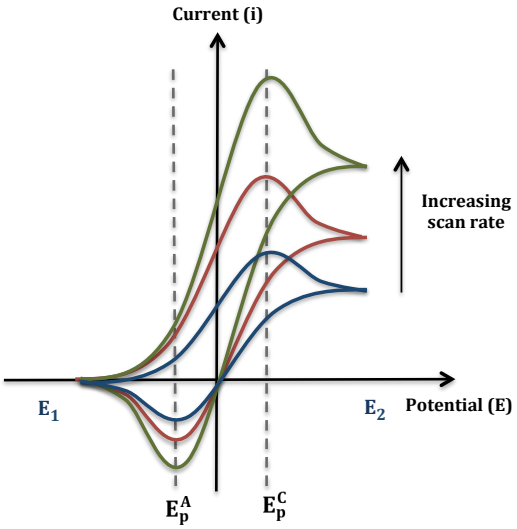

Figure 2.17. Cyclic voltammograms for a reversible process with increasing sweep rates.

The diagram shows how in a reversible system, the anodic and cathodic current peak values are independent of the sweep rate employed. E_1 and E_2 correspond to the potential values between which the experiment is run. $\mathbf{E_p^A}$ and $\mathbf{E_p^C}$ correspond to the anodic and cathodic peak current values, respectively.

b) Irreversible systems

In the case of reversible systems, the rates for electron transfers at all potentials are significantly higher than the mass-transport rates. Hence, the Nernstian equilibrium is maintained at all times at the electrode surface. However, when the rate at which electrons are transferred is insufficient to maintain equilibrium at the surface of the electrode, the shape of the cyclic voltammogram presents slight changes. At low potential sweep rates, the rate of electron transfer is higher than the rate of mass transfer, and the obtained cyclic voltammogram corresponds to the one of a reversible system. However, as the sweep rate increases, the rate at which mass is transported increases as well and it becomes comparable to the rate of electron transfer. The first thing to be noticed when this occurs is that the separation between peaks (for the forward and reverse reactions) increases. The best way to study this effect is to normalise the current values for the change in the diffusion rates, in this case, to replot the data so $I/v^{1/2}$ is a function of E. In the system is reversible, the normalised voltammograms superimpose at all sweep rates, in the case that the effects of the double layer can be disregarded. However, if the system is irreversible, the response obtained is similar to the one shown in Figure 2.18.

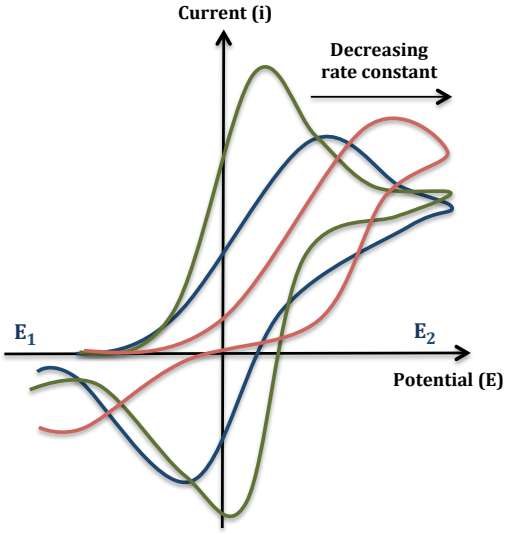

Figure 2.18. Cyclic voltammograms for an irreversible process with increasing sweep rates.

The diagram shows how in an irreversible system, the anodic and cathodic current peak values depend on the sweep rate employed, being $\Delta\mathbf{E_p}$ higher (bigger distance between $\mathbf{E_p^A}$ and $\mathbf{E_p^C}$) for decreasing sweep rates. E_1 and E_2 correspond to the potential values between which the experiment is run. $\mathbf{E_p^A}$ and $\mathbf{E_p^C}$ correspond to the anodic and cathodic peak current values, respectively.

Moreover, it can also be noticed that if the system is irreversible the peak height is slightly reduced from the one in a reversible system. However, the most noticeable fact in a cyclic voltammogram from a totally irreversible system is that the reverse peak is absent, but this feature does not always imply the reversibility of a system. Therefore, several diagnostic tests have to be made. A range of such tests are summarised in Table 3.

Table 2.3. Diagnostic tests for cyclic voltammograms of irreversible processes (at 25°C).

1. No reverse peak
2. $I_p^C \propto \nu^{1/2}$
3. E_p^C shifts $-30/\alpha_C n_\alpha$ mV for each decade increase in ν
4. $\left\|E_p - E_{p/2}\right\| = 48\ \alpha_C n_\alpha$ mV

c) Quasi-reversible systems

As it has been shown, it is quite common for a system that is reversible for low sweep rates to become irreversible at higher sweep rates. In order for these systems to go from a reversible to an irreversible state, they have to pass through a region of intermediate sweep rate values at which the system is quasi-reversible. A system is quasi-reversible when the rate at which electrons are transferred with respect to the mass-transport rate is insufficient to maintain the Nernstian equilibrium at the surface of the electrode. In the quasi-reversible intermediate region, the observed current is a result of the contribution of both forward and reverse reactions. If I_p is plotted as a function of $\nu^{1/2}$, the change from reversible to quasi-reversible and then to irreversible is clearly seen. The diagnostic tests for detecting a quasi-reversible system are shown in Table 4.

Table 2.4. Diagnostic tests for cyclic voltammograms of quasi-reversible processes (at 25°C).

1. I_p increases with $\nu^{1/2}$ but is not proportional to it
2. $\left|I_p^A/I_p^C\right| = 1$ provided $\alpha_C = \alpha_A = 0.5$
3. ΔE_p is greater than $59/n$ mV and increases with increasing ν
4. E_p^C shifts negatively with increasing ν

2.5.4.3 Potential step methods

Potential step methods are also known as controlled-potential techniques, which basis is the measurement of the current response to an applied potential. In the potential step measurement, the applied potential is instantaneously jumped from one value E_1 to another E_2 (Figure 2.19a). There are several potential step techniques, such as chronoamperometry, polarography, pulse voltammetry and alternating current (AC) voltammetry. Chronoamperometry measures the current when the potential at the working electrode is stepped. Polarography uses a dropping mercury working electrode. Pulse voltammetry is a group of techniques, which employs a potential step (or pulse) to analyse the rate of the decay of the charging and the resulting faradaic currents. AC voltammetry involves the superimposition of an alternate current voltage of small amplitude on a linear ramp. Due to its importance in the present work, chronoamperometry will be explained in more detail below.

Chronoamperometry

Chronoamperometry is an amperometric technique, which consists of stepping the potential of the working electrode from a value at which no faradaic reaction takes place to a second potential at which the concentration of the electroactive species at the surface of the electrode is effectively zero. In this kind of process, the working electrode is immersed in an unstirred solution. As its name indicates, chronoamperometry allows the monitoring of the current along time. Since in this case mass is only transported to the vicinity of the electrode surface by diffusion, this current-time curve (Figure 2.19b) represents the change in the concentration gradient in this area. Because of this, the diffuse layer within the electric double layer expands gradually with the depletion of the reactant, thus decreasing the slope of the concentration profile with time. Simultaneously, the current decreases with time. This is given by the Cottrell equation:

$$i(t) = \frac{nFACD^{1/2}}{\pi^{1/2}t^{1/2}} = kt^{-1/2}$$

where n is the number of electrons, F is Faraday's constant, A is the surface area of the electrode, C is the concentration, D is the diffusion coefficient and t is the time. At prolonged times, the behaviour of the system deviates from the Cottrell equation due to natural convection processes caused by coupled chemical reactions and when using non-planar electrodes or microelectrodes of high surface area.

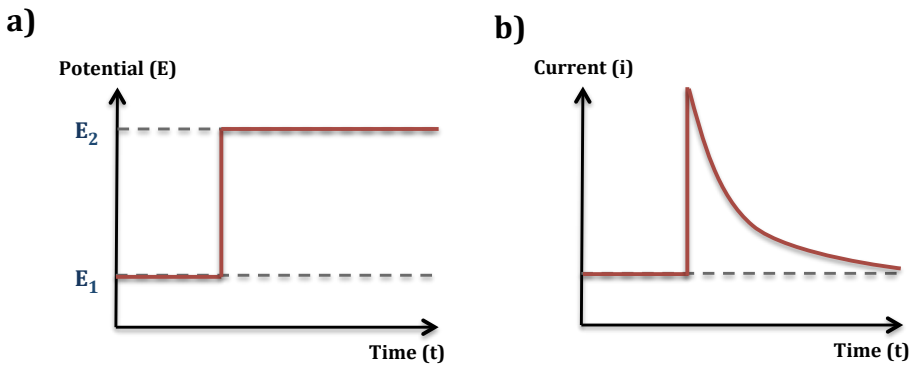

Figure 2.19. General schematic representation of a) a potential-time waveform and b) the resulting current-time response.

Chronoamperometry is commonly used for the measurement of the diffusion coefficient of electroactive species or also the surface area of the working electrode. Chronoamperometry can also be applied to study processes occurring at the electrode surface (Wang, 2006).

CHAPTER 3

MATERIALS AND METHODS

3 Materials and Methods

3.1 Materials and reagents

3.1.1 Reagents

Potassium hexacyanoferrate (III) ($K_3Fe(CN)_6$, ≥99.0% purity), ferrocenecarboxylic acid ($C_{11}H_{10}FeO_2$, purum, ≥97%), sodium acetate anhydrous ($C_2H_3NaO_2$/NaOAc, ≥99.5%), glucose oxidase enzyme (from *Aspergillus niger,* type VII, lyophilised powder, ≥100,000 units/g solid), lactate oxidase (from *Pediococcus sp*., lyophilised powder, ≥20 units/mg solid), D(+)-Glucose ($C_6H_{12}O_6$, ~98% purity), sodium L-lactate ($C_3H_5NaO_3$, ~98% purity), urea (CH_4N_2O, 99.0–100.5%), Nafion perfluorinated resin solution (5% in lower aliphatic alcohols and water), hydrogen peroxide solution (H_2O_2, 30% wt. in water) and albumin for bovine serum (BSA, lyophilised powder, essentially fatty acid free, ≥98 purity) were purchased from Sigma-Aldrich (Dorset, U.K.).

Sodium dihydrogen orthophosphate 1-hydrate ($NaH_2PO_4{\cdot}H_2O$), disodium hydrogen orthophosphate 12-hydrate ($Na_2HPO_4{\cdot}12H_2O$), sodium chloride (NaCl), L-ascorbic acid ($C_6H_8O_6$, ≥98%), acetic acid glacial (CH_3COOH/HAc ≈100%), hydrochloric acid (HCl) and glutaraldehyde solution ($CH_2(CH_2CHO)_2$, ≈50%) were purchased from VWR BDH (Poole, U.K.).

Uric acid ($C_5H_4N_4O_3$, 99+% purity) was purchased from Acros Organics (Loughborough, U.K.).

All reagents were used as received unless otherwise stated.

3.1.2 Materials

Polycarbonate membrane disks of different pore sizes from 0.1 to 10 μm diameter and a thickness of 10 μm were purchased from both Whatman (Maidstone, U.K.) and Millipore (Consett, U.K.).

Glass microscope slides (ground edges, twin frosted glass 76mm x 26 mm, 0.8 mm to 1.0 mm thick) were purchased from Fisher Scientific (Loughborough, U.K.).

Araldite® epoxy resin (Rapid setting), multicore wires and silver conductive paint were purchased from RS Components (Corby, UK).

Platinum and gold disc targets of 57 mm diameter and 0.1 mm thickness were purchased from Agar Scientific (Essex, UK).

3.2 Solutions

3.2.1 Phosphate buffered saline solution (pH 7.4)

A phosphate buffered saline (PBS) solution was prepared at pH 7.4 constituting 5.28×10^{-2} M $Na_2HPO_4 \cdot 12H_2O$, 1.3×10^{-2} M $NaH_2PO_4 \cdot H_2O$ and 5.1×10^{-3} M NaCl using distilled deionised water (>18 MΩ cm^{-1}).

3.2.2 Sodium acetate buffer solution (50 mM, pH 5.1)

A sodium acetate buffer solution was prepared at pH 5.1 at a concentration of 50 mM constituting 1.5×10^{-2} M HAc and 3.5×10^{-2} M NaOAc using distilled deionised water (>18 MΩ cm^{-1}).

3.2.3 Ferrocenecarboxylic acid solution

Ferrocenecarboxylic acid solutions were prepared to a range of concentrations, from 1 to 5 mM, in pH 7.4 PBS.

3.2.4 Glutaraldehyde solution

A glutaraldehyde solution was prepared at concentrations of 5 and 10% v/v from a ≈50% v/v glutaraldehyde solution in pH 5.1 sodium acetate buffer or pH 7.4 PBS, depending on the type of enzymatic system being investigated.

3.2.5 Bovine serum albumin (BSA) solution

A BSA solution was prepared at concentrations of 0.1 and 0.2 g ml^{-1} in pH 5.1 sodium acetate buffer or pH 7.4 PBS, depending on the type of enzymatic system being investigated.

3.2.6 Glucose oxidase (GOD) in BSA

A glucose oxidase/BSA solution was prepared using 500 U ml^{-1} GOD dissolved in 0.1 g ml^{-1} BSA solution in pH 5.1 sodium acetate buffer for use within an enzyme laminate. The enzyme/BSA solution was stored in Eppendorf tubes at -20°C until use.

3.2.7 Lactate oxidase (LOD) in BSA

A lactate oxidase/BSA solution was prepared dissolving LOD in 0.1 g ml^{-1} of BSA solution in pH 7.4 PBS to concentrations of 830 and 1,667 U ml^{-1} for use within an enzyme laminate. The enzyme/BSA solution was stored in Eppendorf tubes at -20°C until use.

3.2.8 Glucose solution

Glucose solutions were prepared in a range of concentrations, from 0.1 to 20 mM, in pH 5.1 sodium acetate buffer solution.

3.2.9 Lactate solution

Lactate solutions were prepared in a range of concentrations, from 0.1 to 70 mM, in pH 7.4 PBS.

3.2.10 Hydrogen peroxide solution

Hydrogen peroxide solutions were prepared in a range of concentrations, from 0.02 to 151 mM, in pH 7.4 PBS.

3.2.11 Synthetic sweat solution

Synthetic sweat solutions were prepared in pH 7.4 PBS constituting 1.55 g L^{-1} sodium chloride, 0.6 g L^{-1} urea, $7.81x10^{-3}$ g L^{-1} acetic acid, $9.92x10^{-3}$ g L^{-1} uric acid and $1.76x10^{-3}$ g L^{-1} ascorbic acid. Lactate was dissolved in this solution to a range of concentrations, from 0 to 60 mM.

3.2.12 Diluted human sweat solution

Diluted human sweat solutions were prepared in a 1:8 dilution in pH 7.4 PBS.

3.2.13 Ascorbic acid solution

Ascorbic acid solutions were prepared in a range of concentrations, from 0.01 to 4.5 mM, in pH 7.4 PBS.

3.2.14 Uric acid solution

Uric acid solutions were prepared in a range of concentrations, from 0.059 to 15.1 mM, in pH 7.4 PBS.

3.3 Equipment

3.3.1 Water purification system

Distilled deionised water used in for all solutions preparation was obtained using Purelab® UHQ from ELGA (Marlow, U.K.). The distilled deionised water had a resistivity of >18 MΩ cm^{-1}.

3.3.2 Potentiostat

A Uniscan (Derbyshire, U.K.) PG580 with dedicated PC-driven software was used for electrochemical studies such as linear and cyclic voltammetry as well as chronoamperometry experiments.

3.3.3 Rank Oxygen Electrode

Initial experiments were performed with a Perspex Oxygen Electrode (Figure 3.1), designed by Rank Brothers Ltd. (Cambridge, U.K.). The electrode is designed for following the production or consumption of oxygen by cell suspensions,

subcellular particles or enzyme systems. However, it is also suitable for monitoring the production of other molecules, such as hydrogen peroxide (H_2O_2).

The Oxygen Electrode is divided into two main components that are connected together for use. The lower section houses the electrode system, which comprises a 2 mm-diameter platinum disk working electrode (cathode) surrounded by a silver/silver chloride counter/reference electrode (anode), approximately ten times larger in surface area than the platinum electrode. The upper section comprises an incubation or monitoring chamber which is designed to ensure the maintaining of a constant temperature for the different experiments if required, which is important for obtaining reproducible results. It is in the central part of the incubation chamber where the test solution is placed to be analysed. The upper section is mounted on top of the base, placing the enzyme laminate in contact with the test chamber, and a silicone rubber 'O' ring holding the membrane in place over the electrode area.

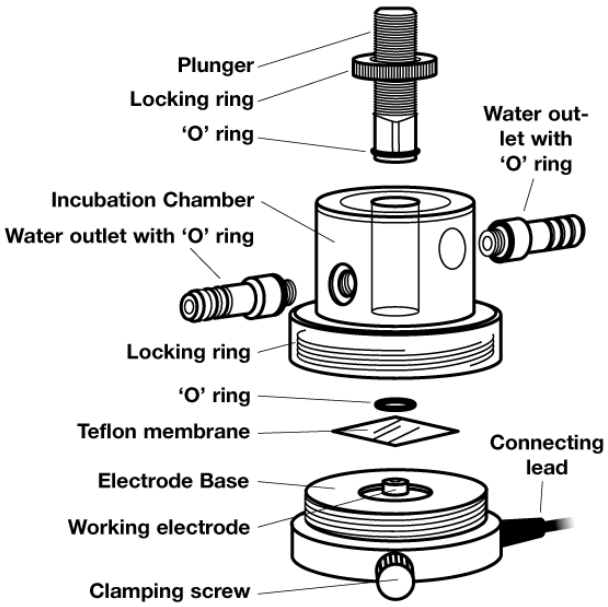

Figure 3.1. Diagram view of the Perspex Oxygen Electrode.

3.3.4 Sputter coater

Sputter coating gold and/or platinum onto the polycarbonate membranes to render them conductive was performed by using an AGAR B7341 Automatic Sputter Coater from Agar Scientific Ltd. (Essex, U.K.) in conjunction with an external Pfeiffer Rotary Vane Pump from Pfeiffer Vacuum Ltd. (Newport Pagnell, U.K.). In this device, the sequence of flush, leak, coat and vent is controlled automatically. However, if desired, the coating step duration can be operated manually. The device supports sputtering currents up to 40 mA, which allows working with a wide range of target materials. The user can define a coating time, which can be altered accordingly depending on required gold-layer thickness or target material strength.

3.3.5 Digital multimeter

A digital TRMS multimeter Asyc II MX54C, obtained from Metrix Electronics (Bramley, Hampshire, U.K.), was employed in order to test the resistance in Ω of the conductive gold and platinum electrodes. This resistance measure was taken as a mean value taken from various points. In the first design (Figure 3.2), measurements were made at the circumference edges of the diameter of the disks. In the second design, the points where measurements were made on each electrode are indicated in Figures 3.3 and 3.4.

3.3.6 Scanning electron microscope (SEM)

A Philips XL30 Scanning Electron Microscope equipped with a Field Emission Gun filament (SEM-SFEG), obtained from Philips Analytical (Guilford, UK), was employed in order to characterise the surface of the Pt working electrode of the developed sensing system. In this device, a focused electron beam scans over the previously dried sample. The resulting interaction between the specimen and the

beam excites secondary electrons and the resulting radiation is detected and analysed in order to obtain useful information about the topography and composition of the specimen under analysis (i.e. the Pt electrode surface of the sensing system).

3.4 Common procedures

3.4.1 Cyclic voltammetry analysis

The principle behind the cyclic voltammetry analysis has been extensively explained in section 2.5.4.

The electrode system was connected to the potentiostat as described in section 3.3.2, connecting the three electrodes to their corresponding inputs on the potentiostat, described in section 3.3.2.

The parameters for each experiment were selected in the company PC-driven software. The electrodes were characterised in ferrocenecarboxylic acid solutions (described in section 3.2.3) between potentials of -0.4 and +0.8 V (vs. Ag/AgCl) at a sweep rate of 20 mV s^{-1}.

3.4.2 Chronoamperometric analysis

As well as cyclic voltammetry, the principle behind chronoamperometry is described in section 2.5.4.

The electrode system was connected to the potentiostat as described in section 3.3.2. When the sensor comprised three electrodes, each one of them was connected to the corresponding input on the potentiostat. However, when the sensor consisted of two electrodes, the inputs for the counter and reference electrode were merged and then both electrodes (working and counter/reference) were connected to their corresponding inputs in the potentiostat.

The potentiostat was set to polarise the working electrode at +650 mV vs. Ag/Au depending on the system under investigation and the resulting current was monitored for a range of times from between 1 to 36 hours, using the software described in section 3.3.2. This potential of +650 mV was chosen since it is known to be the optimum value for the oxidation of hydrogen peroxide (De Michelli *et al.* 2011).

At the beginning of the experiment, a high current followed by a dramatic decay in the response is observed. This is due to the formation and relaxation of the electrical double layer in the system under analysis, also called polarisation. Once the polarisation was complete, the current reached a constant baseline in terms of steady state current (constant current against time). The time for the polarisation to conclude varied depending on the nature of the experiment (i.e. the hydration status of the enzyme laminate).

Once the polarisation step concluded with a stable baseline being obtained, the system was ready to use for analysing different samples. After the experiment, the current/time profile was analysed for each substrate concentration. In order to calculate normalised current responses, the baseline current was subtracted.

3.4.3 Enzyme cross-linking

The enzyme cross-linking into a protein matrix between two polycarbonate membranes was achieved as follows. The enzyme was prepared from lyophilised powder at the desired concentration in a BSA solution in PBS. The enzyme/BSA solution was stored in Eppendorf tubes and kept at -20°C until use. When preparing the enzyme laminate, the enzyme/BSA solution was rapidly mixed with a dilution from 50% glutaraldehyde in a 2:1 ratio. The mixture was then pipetted on the surface of a polycarbonate membrane, placing another membrane on top. Both membranes were pressed together with light-finger pressure between two microscope glass slides for a certain time, separating them carefully afterwards,

leaving a robust enzyme laminate, which ensured the entrapment of the enzyme within the cross-linked matrix, avoiding its leakage while in solution.

3.4.4 Rank oxygen electrode preparation

When preparing an experiment for the oxygen electrode, described in section 3.3.3, the following steps were followed. The enzyme laminate was prepared with two 1-cm^2 polycarbonate membranes and the enzyme-crosslinking mix, as described in section 3.4.3. Once the robust enzyme laminate was obtained, it was placed on top of the working electrode within the base section of the sensor. On top of the membrane, the 'O' ring was placed, checking that it was in contact with the retaining indent completely and that the membrane fully covered the working electrode surface.

Once the 'O' ring was in place, the top of the sensor was screwed to the base, the inputs for the counter and reference electrodes were connected together and then this input and the output for the working electrode were connected to the potentiostat appropriately.

Finally, the incubation chamber of the cell was filled with the desired test solution at the volume to ensure complete coverage of the membrane area and the WE was then polarised at the relevant potential.

3.4.5 Sputter coating gold and/or platinum

The gold and platinum-sputter coating of the membranes was performed as described in section 3.3.4. The membrane was fixed to a glass plate by using adhesive and placed on the table of the device, closing the top plate afterwards. The pressure of the argon gas supply was then set at 0.3 bar. The chamber was then flushed for 5 seconds, then leaked. When the pressure of the chamber was approximately 0.08 mb, an automatic coating mode was selected and, in the cycle

option, the sample was coated for 120 (gold) or 150 seconds (platinum). After that, the experiment was stopped and the sputtered membrane removed. The stage height and deposition time were kept consistent in order to minimise any coating thickness variability from membrane to membrane.

3.4.6 Construction of the mechanical support for the enzyme laminate

In order to test the ability of the enzyme laminate to measure different concentrations of lactate, it was required to design a sensing platform, which provided mechanical support for the enzyme laminate and allowed for measurement of any resultant current following polarisation.

Two main designs for a sensing platform have been developed in this work, which are described below.

3.4.6.1 Mechanical support based on two separated gold-coated membranes as electrodes

A polycarbonate disk was sputter-coated with gold following the process and using the parameters described in section 3.4.5.

Once the gold-sputtered membranes were obtained, they were cut into two strips of 10x30 mm (working electrode) and 14x35 mm (counter/reference electrode). Also, a non-coated membrane of the same material was cut into a strip of 16x18 mm and constituted the inner membrane used to separate the working and counter/reference electrodes.

Two lengths of wire of 10-15 cm were cut and stripped of the insulating plastic coat 3 mm on each end. The copper wires at one of the ends of the wires were spread and attached to the gold coated side of both working and counter/reference electrodes using silver conductive paint in order to make electrical connection

between the wire and the membrane. The silver conductive paint was allowed to set for one hour.

A microscope glass slide was used to cut two pieces of the same width as the slide and 6 mm long. Another glass slide was used to place both gold-coated membranes, one at each side, in such a way that 16 mm of the larger strip (i.e. CE/RE) and 10 mm of the smaller strip (i.e. the WE) hung from the end of the slide. This was done by applying epoxy resin to one side of the 6 mm glass pieces and pressing them against the gold-coated membranes, ensuring contact to the central glass slide on both sides. Both electrodes were orientated so the gold-coated side was facing the central glass slide. In between the membranes, a non-coated membrane was also placed, which would form part of the enzyme laminate together with the conductive face of the working electrode. Moreover, this uncoated membrane was placed in such a position to avoid any short circuit between the two gold-coated membranes. Epoxy resin was also applied on the wires at the top of the glass slide in order to provide additional mechanical strength and avoid wire movement. The epoxy resin was allowed to set until completely dry. A schematic of this construct is shown in Figure 3.2.

6 μl of the enzyme/BSA solution was rapidly mixed with 3 μl of 5% glutaraldehyde. The enzyme solution was pipetted onto the gold surface of the working electrode and was pressed strongly against the uncoated membrane and the other electrode between two glass microscope slides for at least five minutes.

The results obtained with this design led to the variation of the number of the internal membranes and will be further discussed in the relevant results section.

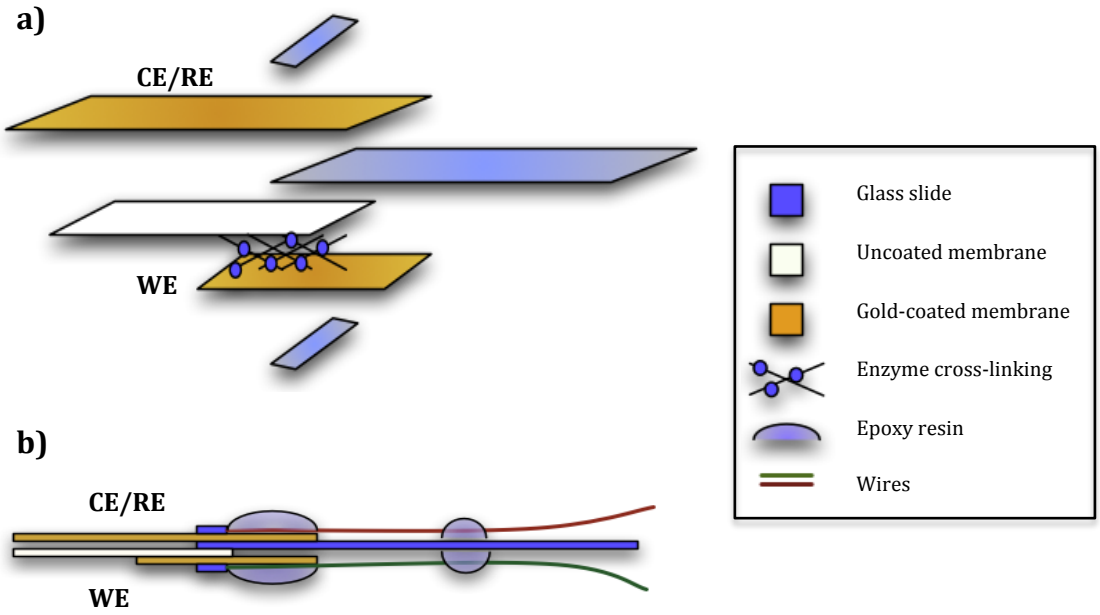

Figure 3.2. Schematic view of the mechanical support based on two separated gold-coated membranes as electrodes.

a) Schematic view of the different layers that comprise the sensor**. b)** Lateral view of the assembled mechanical support.

3.4.6.2 Mechanical support based on two electrodes on a single sputter-coated membrane

i. Electrode system based on gold-coated CE/RE and WE.

A polycarbonate disk of 25 mm was defined in shape with electrical tape of approximately 1 mm width, following the pattern shown in Figure 3.3a and Figure 3.4. Then, the disk was sputter-coated with gold following the process and using the parameters described in section 3.4.5.

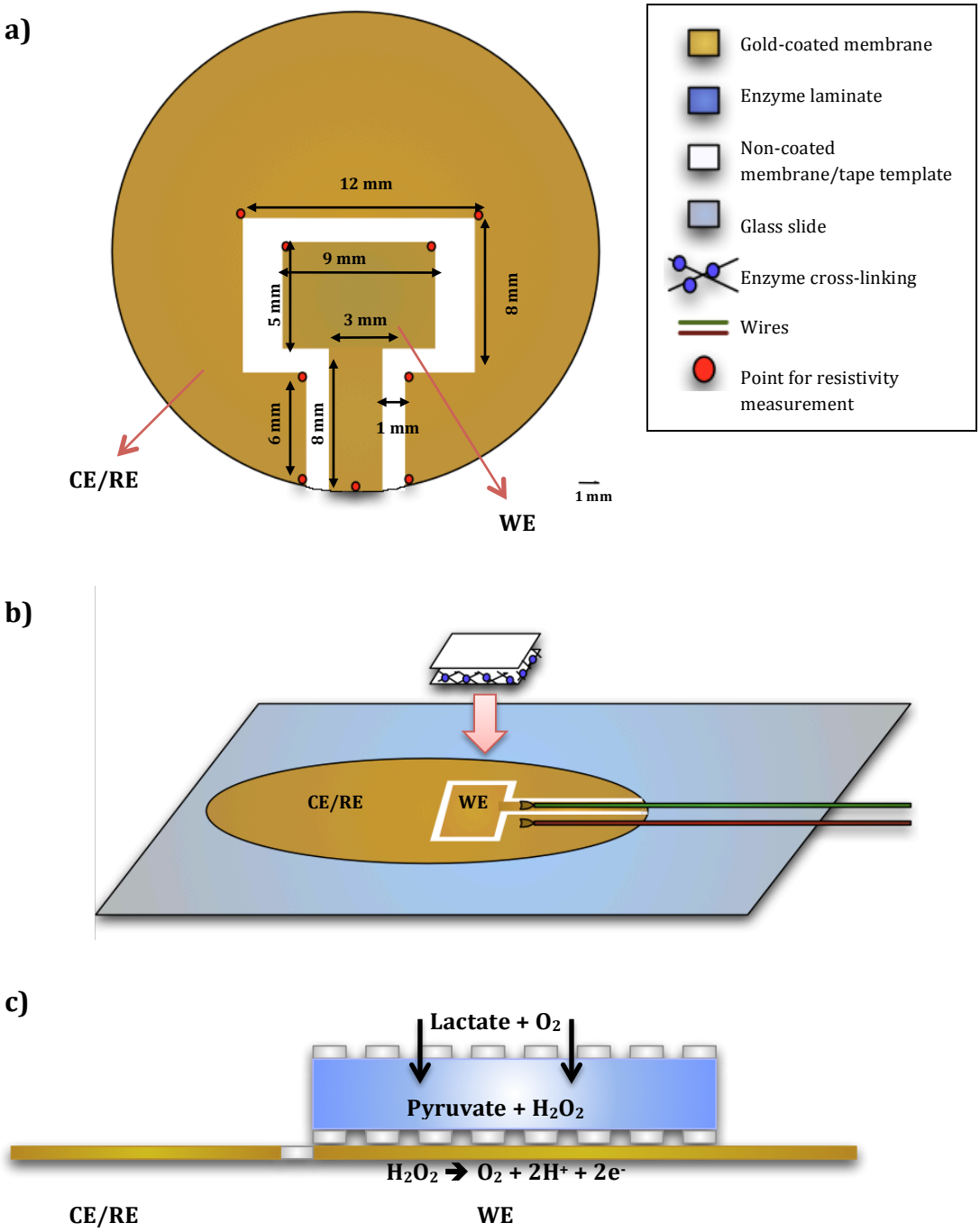

Figure 3.3. Schematic view of the mechanical support based on two electrodes on a single gold-coated membrane.

a) Schematic view of the working and counter/reference electrodes on the gold-coated polycarbonate membrane. **b)** Representation of the sensor on top of a glass slide and position of the enzyme laminate. **c)** Schematic lateral view of the electrode system with the membrane on top and the electrochemical process behind the experiment.

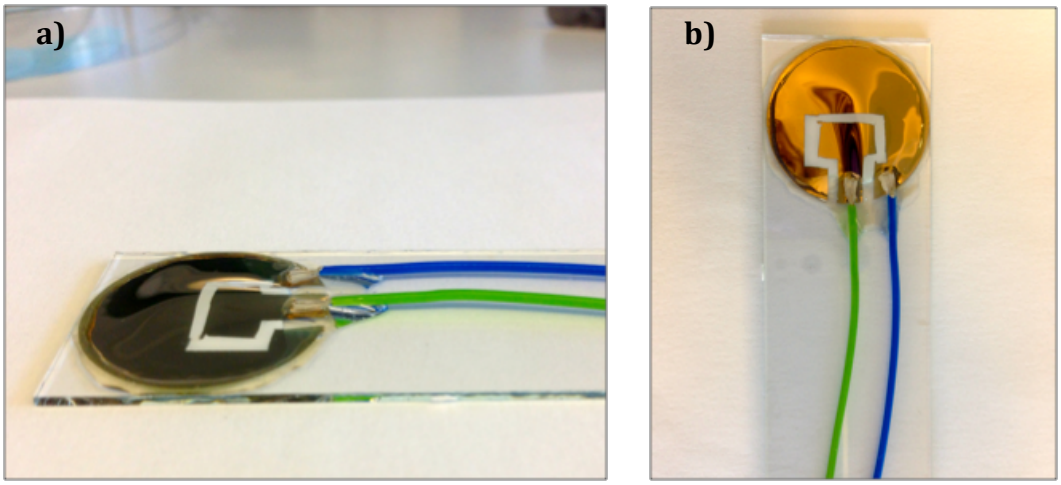

Figure 3.4. Photographs showing the mechanical support based on two electrodes on a single gold-coated membrane.

Once the gold-sputtered membrane was obtained, the insulating tape strips were carefully peeled off, leaving a structure comprised of two electrodes (inner one WE, outer one CE/RE) on a single membrane separated and isolated from each other by a region of non-coated membrane, as shown in Figure 3.3a and Figure 3.4.

The gold-coated membrane was then fixed on a microscope glass slide using insulating tape and the borders were sealed with epoxy resin to avoid solution creep to the back of the membrane through the edges of the disk. The epoxy resin was allowed to set until totally dry.

Once the epoxy resin was dry, two lengths of wire of 10-15 cm were cut and stripped of the insulating plastic coat 3 mm on each end. The 'copper' wires at one of the ends of the wires were spread and attached to the golden area of both working and counter/reference electrodes (as shown in Figure 3.3b. and Figure 3.4) using silver conductive paint. This was done in order to make insulating connection between the wire and the membrane. The silver conductive paint was allowed to set for one hour. Finally, the wires were fixed to the membrane surface by applying epoxy resin, allowing it so set until dry, to ensure they were insulated from solution and to add structural integrity.

The enzyme laminate was prepared with two 5x9 mm polycarbonate membranes and the enzyme-crosslinking mix as described in section 3.4.3. Once the robust enzyme laminate was obtained, it was placed on top of the working electrode (Figure 3.3b, c). The membranes of the enzyme laminate were cut appropriately so they would mimic the shape of the working electrode without making contact with the counter/reference electrode area. Finally, the enzyme laminate was attached to the electrode by placing thin strips of insulating tape along the edges without encroaching on the CE/RE area.

ii. Electrode system based on gold (CE/RE) and platinum (WE) sputter-coated membrane.

A polycarbonate disk of 25 mm was defined in shape with electrical tape, covering the area for the working electrode and the non-coated region between electrodes, following the pattern shown in Figure 3.5a and Figure 3.6. The disk was then sputter-coated with gold following the process and using the parameters described in section 3.4.5.

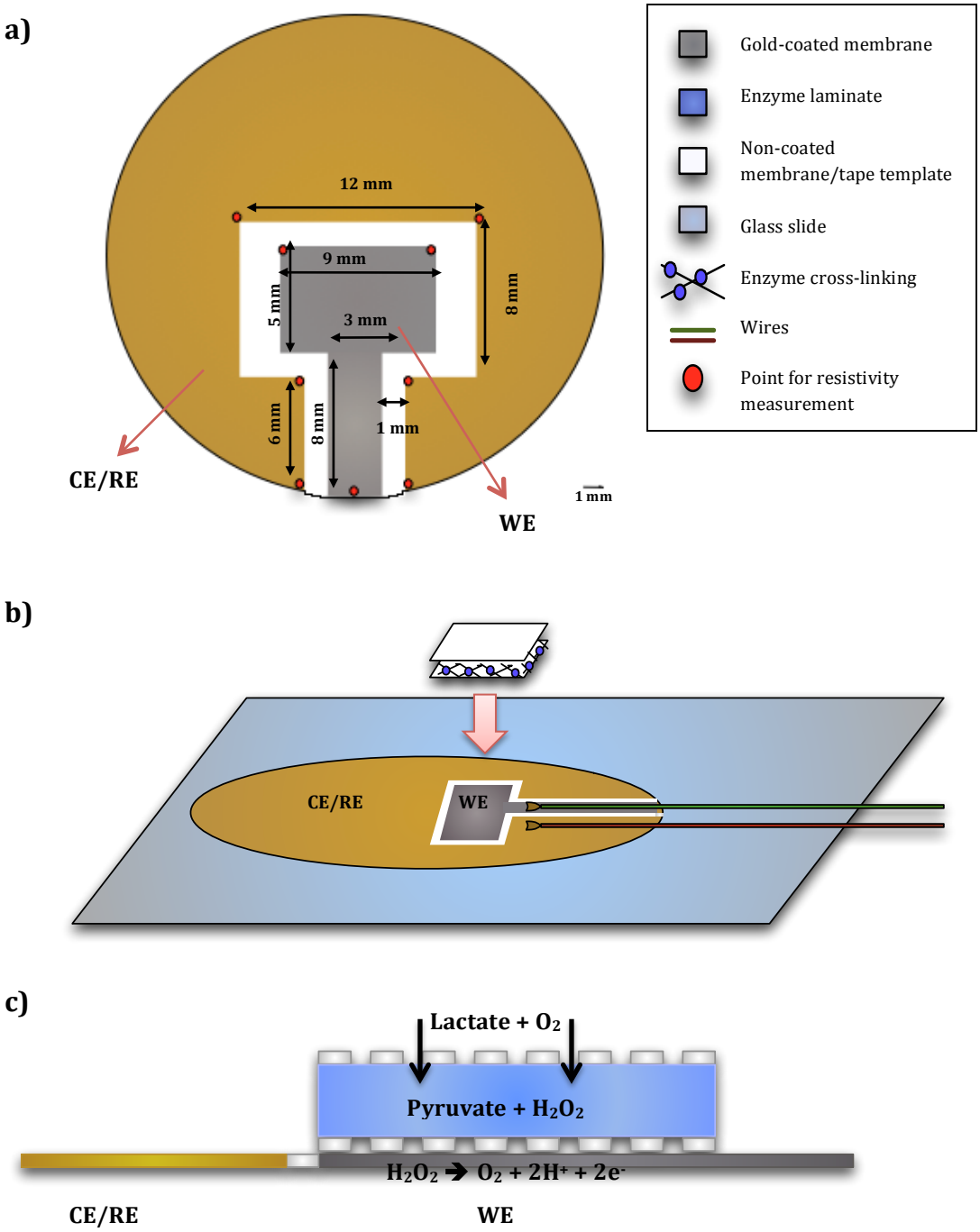

Figure 3.5. Schematic view of the mechanical support based on two electrodes on a single gold (CE/RE) and platinum (WE) sputter-coated membrane.

a) Schematic view of the working and counter/reference electrodes on the sputter-coated polycarbonate membrane. **b)** Representation of the sensor on top of a glass slide and position of the enzyme laminate. **c)** Schematic lateral view of the electrode system with the membrane on top and the electrochemical process behind the experiment.

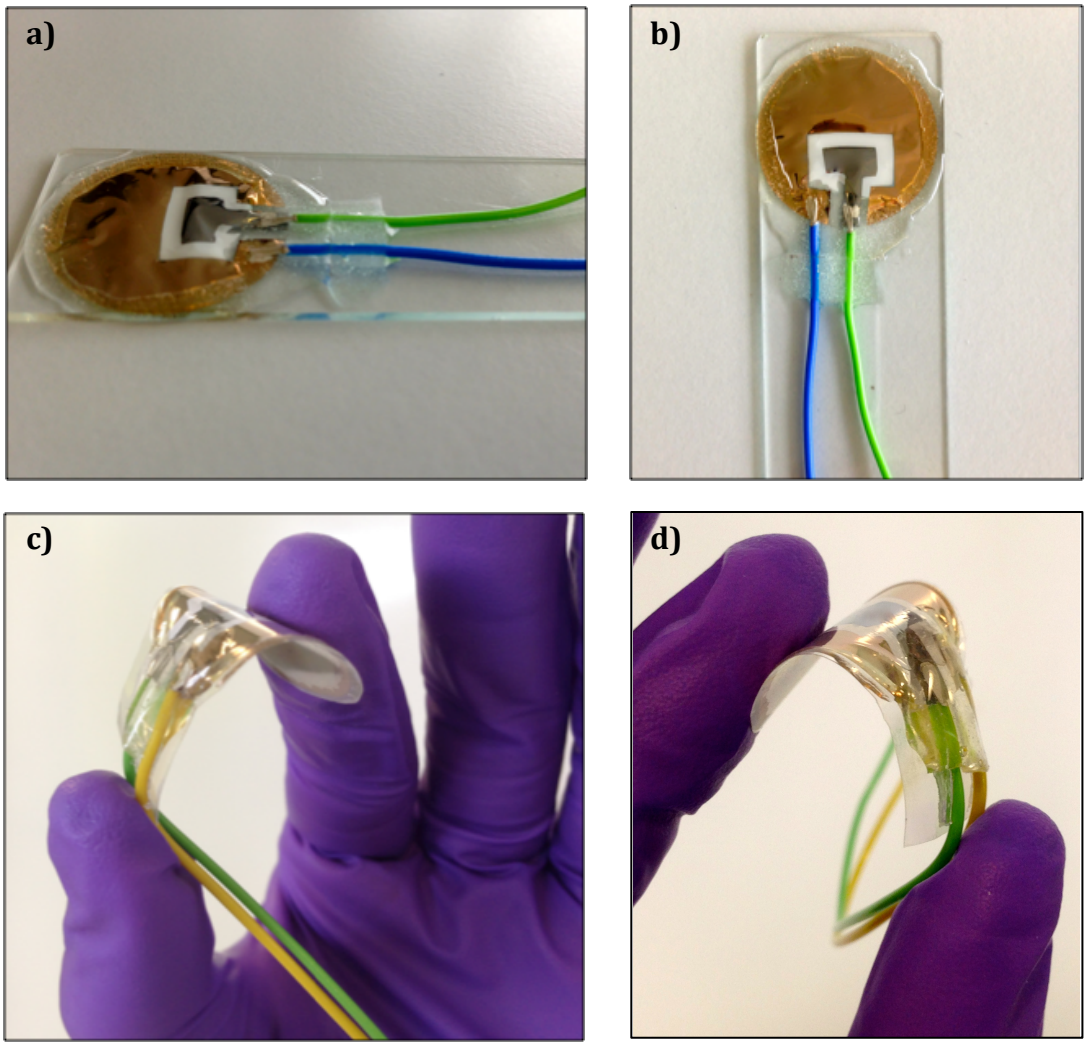

Figure 3.6. Photographs showing the mechanical support based on two electrodes on a single gold (CE/RE) and platinum (WE) sputter-coated membrane fixed on (a,b) a microscope glass slide and (c,d) a flexible plastic surface.

Once the membrane had been gold-sputtered, the electrical tape template was carefully peeled off. The resulting sputter-coated membrane was subsequently 'templated' by manufacturing a plastic film carefully cut to cover the polycarbonate disk but leaving the working electrode area exposed. The template with the membrane beneath was fixed to the glass plate of the sputter-coater with electrical tape. The disk was then sputter-coated with platinum following the process and using the parameters described in section 3.4.5. Then, the plastic template was removed, leaving a structure comprised of two electrodes (inner one platinum-coated WE, outer one gold-coated CE/RE) on a single membrane separated and

isolated from each other by a region of non-coated membrane, as shown in Figure 3.5a and Figure 3.6.

The resulting gold and platinum-coated membrane was fixed to a microscope slide (Figure 3.6a, b) or, alternatively, to a flexible plastic surface (Figure 3.6b, c). The manufacturing process of the mechanical support following this step and preparation of the laminate were carried out as described in section 3.4.6.2.i. In this case, however,

3.4.7 Electrode-surface characterisation through Scanning Electron Microscopy

The characterisation of the topography and composition of the Pt working electrode of the developed AuPt sensing system was performed using a scanning electron microscope (SEM) as described in section 3.3.6. The electrode area (previously dried) was cut around the edges with a sharp scalpel and mounted with adhesive carbon tape on aluminium stubs in order to maximise conductivity. Following this, samples were introduced into the electron microscope for their analysis. The magnifications employed were in the range 1,000–50,000x.

3.4.8 Collection and handling of human sweat samples

The procedure for the collection and handling of human sweat samples involved a subject performing moderate-intense physical exercise on a treadmill for up to one hour and collecting sweat periodically from different body areas. Sweat collection was achieved by attaching a large piece of impermeable plastic (Parafilm) to different body areas (chest, mid back and upper back or neck) with a large adhesive wound dressing such as Smith & Nephew ALLEVYN™. This modified collector was peeled off the subject and replaced by a new one depending on the length and requirements of the experiment. Alternatively, sweat was directly

collected by using new autoclaved plastic collection tubes of different capacities, such as Eppendorf or Millipore microcentrifuge tubes, and applying them in direct contact with the skin of the subject under study.

The obtained sweat patches were kept in separate 50-ml centrifuge tubes with a filter unit, where sweat was collected by centrifugation at 3000 rpm for 10 minutes and collection of the precipitate samples. The collected samples were preferably used immediately after their collection or otherwise divided into 1–ml aliquots and stored at -20°C until use.

3.4.9 Electrode-surface modification with Nafion

Nafion was employed in order to add a protective layer on the surface of the working area of the electrode system. The sensor employed for the Nafion coating was the developed AuPt sensing system, described in section 3.4.6.2.ii. Each polymer layer was created by physical deposition through pipetting of 10 μl of 5% w/w Nafion over the catalytic Pt layer of the WE. The Nafion sample was spread over the electrode surface area until fully covered with a pipette tip, avoiding its contact with the surface of the electrode. Once Nafion was cast, it was allowed to dry for 24 hours at room temperature prior to its analysis or the application of the next polymer layer. Up to two Nafion coats were applied to the electrode surface. Prior to the analysis of the resulting Nafion-modified electrode system, an enzyme laminate was prepared according to the protocol outlined in section 3.4.3 with or without LOD enzyme. The resulting laminate was attached to the electrode surface area as outlined in section 3.4.6.2.ii.

CHAPTER 4

DEVELOPMENT OF A MECHANICAL SUPPORT FOR THE LACTATE BIOSENSOR

4 Development and optimisation of a mechanical support for the lactate biosensor

4.1 Introduction

This chapter presents the progress and the steps followed in the development of a mechanical support for a lactate biosensor based on a laminate design with the aim of developing a sensing platform for the monitoring of lactate in sweat *in vitro*, which in the future could be utilised as an *ex vivo* diagnostic device. In order to achieve this, the sensor design had to be thin, flexible, easy and reproducible to fabricate with the capability to perform reproducible lactate measurements.

Preliminary studies were performed on a Rank electrode cell as a base system for the measurement of hydrogen peroxide to which results obtained with subsequent sensing designs could be compared. A number of different sensing platforms constructed will be described and compared, leading to the development of a new sensing design for the measurement of lactate, based on preliminary studies and the electrode configuration of a Rank cell.

4.2 Lactate biosensor based on a Rank electrode cell

4.2.1 Introduction

This section describes the preliminary work that was performed on a Rank electrode cell (described in section 3.3.3.) as an introduction towards the production of biosensors based on a membrane design. Alongside this, the use of the Rank cell is also used as a technique to perform reproducible measurement of hydrogen peroxide in solution and since the final lactate sensor will utilise this as a detection method, it can therefore be used as the base system to which subsequent results can be compared.

Initial electrochemical experiments with this electrode cell were performed with glucose oxidase (GOD), due to this enzyme being used in many commercial biosensors due to its stability and robustness. This allowed for the standardisation of the protocols for the analysis of samples using an enzyme laminate in a Rank electrode cell, to be obtained and taken forward to future experiments.

The protocol for the experiments is outlined in section 3.4.4, with the laminates being constructed as described in section 3.4.3. Here, 6 μl of (GOD/LOD)/BSA solution and 3 μl of glutaraldehyde 5% v/v were crosslinked between the two 1-mm^2 polycarbonate membranes. LOD was prepared in BSA at a concentration of ~830 U ml^{-1}. The resulting system was then interrogated using the chronoamperometry protocol, described in section 3.4.2. As a first step of each experiment, the incubation chamber of the cell was filled with 5 ml of PBS and was set to polarise at +650 mV vs. Ag/AgCl. This potential was chosen since it is known to be the optimum value for the oxidation of H_2O_2 produced in the enzymatic reaction (De Micheli *et al.*, 2011). The enzyme laminate was allowed to equilibrate for a certain amount of time until the current reached a steady-state value and thus the baseline current was obtained (usually, this took approximately one hour). After this, the sensor was then used to analyse a range of concentrations of glucose or lactate solutions, depending on the enzyme system used.

The main study in this chapter involves the measurement of the normalised current response for various concentrations of glucose and lactate.

4.2.2 Glucose biosensor based on a Rank electrode

As previously stated, preliminary studies were performed with the enzyme GOD. These experiments sought to analyse the current response against different concentrations of glucose, develop a consistent protocol to be used in the future determination of lactate system and define the reproducibility of the experimental procedure. GOD was therefore used in this initial development step because it is highly specific for its analyte (i.e. glucose), highly stable and has a high turnover rate.

A range of solutions of glucose in sodium acetate buffer, from 0 to 1 mM, were analysed in triplicate by adding 5 ml of the test solution at a time to the incubation chamber. Prior to each new concentration, fresh sodium acetate buffer was added in order to bring the current response back to a baseline state. The current outcome for each concentration was normalised by subtracting the background signal, obtained when the sodium acetate buffer was added; the mean values are represented in a calibration plot with the corresponding standard deviation (Figure 4.1).

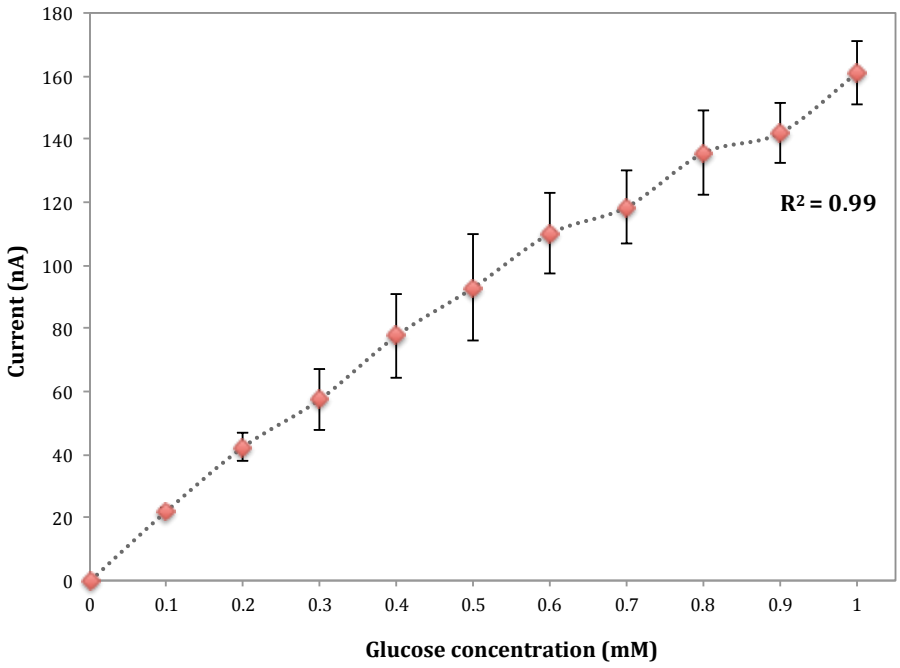

Figure 4.1. Calibration curve for GOD on the Rank electrode system for a range of glucose concentrations from 0 to 1 mM.

As the results show, in the range of concentrations tested, from 0 to 1 mM, the linearity of the response is relatively good (R^2 = 0.99), which is to be expected for low concentrations. Moreover, the standard error for each mean current value is relatively small, since all values are less than one standard deviation away from the mean. This low variation indicates that the results have a high reproducibility, at least for the glucose concentrations tested herein. Therefore, the protocol for the development of the enzyme laminate was adequate for the monitoring of glucose at low concentrations with a high reproducibility, the enzyme GOD was well immobilised and stable in the developed laminate together with this performance shows promise for the measurement of glucose at higher concentrations.

4.2.3 Lactate biosensor based on a Rank electrode

Once the assay protocol was successfully developed using the enzyme GOD and measuring glucose solutions, the Rank electrode cell method was then employed for testing lactate concentrations in PBS using an enzyme laminate with lactate oxidase (LOD) with the same parameters utilised in section 4.2.2. This interrogation was performed in order to gain an insight into the measurement of lactate in solution at different concentrations, optimise the protocol for a lactate sensor based in a laminate design (i.e. using a more labile enzyme) and evaluate the reproducibility of the results for the lactate system.

During the different experiments it was observed that the enzymatic activity of LOD deteriorated over a shorter time than GOD, since for a certain lactate concentration analysed repeatedly over several days with the enzyme LOD, the current response obtained started to decrease at a faster rate than the corresponding glucose concentration with the enzyme GOD. Therefore, this time six different concentrations of lactate in PBS were analysed in this experiment, from 0 to 0.5 mM, by adding 5 ml of the test solution to the incubation chamber at a time. As described in section 4.2.2, previous to the analysis of each lactate concentration, PBS was added in order to reach a baseline current response. The current outcome for each concentration was normalised by subtracting the background signal obtained with PBS only and the values are represented in the calibration profile of Figure 4.2.

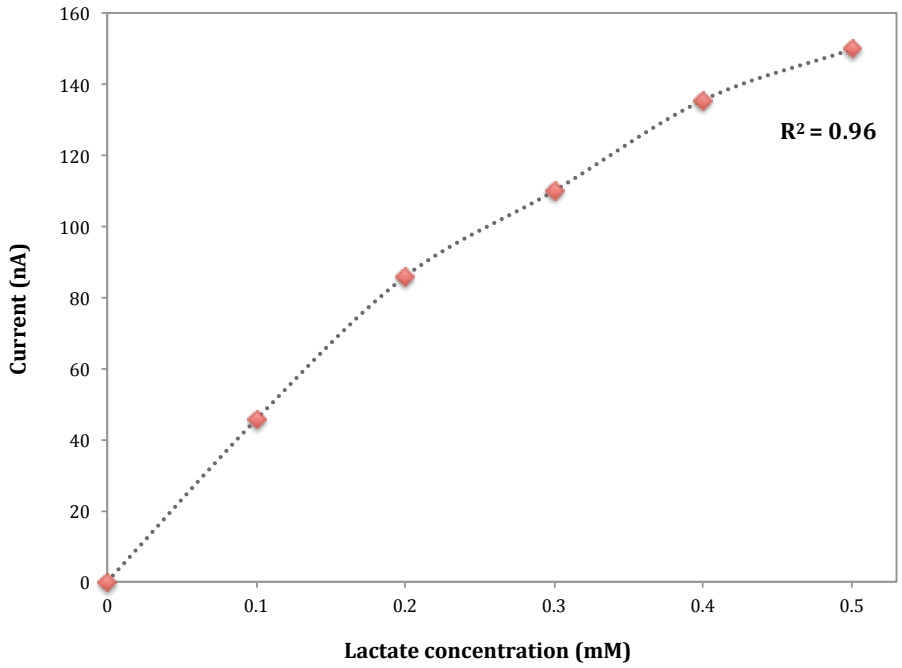

Figure 4.2. Response curve for LOD on the Rank electrode system for a range of lactate concentrations from 0 to 0.5 mM.

As the results show, the current response, produced as a consequence of the enzyme LOD specific binding to lactate and its transformation into pyruvate and H_2O_2, increased with raising concentrations of lactate. This proved that again the enzyme was well immobilised and stable in the developed laminate design. Moreover, the linearity of the response, although slightly lower than that of the glucose oxidase system described above, was relatively high, with current values for each concentration increasing accordingly with concentration. The linearity of the response and the reproducibility of the results will be some of the parameters to be optimised within the enzyme sensor to be developed. However, this served as a base protocol method for further development of an electrode system for lactate sensing.

4.3 Development of a mechanical support for a novel lactate sensing platform

4.3.1 Introduction

The present project is aimed towards the development of a lactate sensor with a flexible format in order to develop it into a diagnostic device that can be directly applied on the skin with a sticking plaster-type design. This section describes the process involved in the development of a mechanical support for an enzyme laminate-based sensor aimed towards a future 'flexibilisation' of the design.

Initial experiments involved the construction of an optimised version of a mounted enzyme laminate sensor previously designed (Derbyshire, 2011) for its further use in the analysis of lactate solutions. The results obtained during these experiments and described herein have led to a continuous optimisation of the design for enhanced lactate sensing, leading to the development of a mechanical support where both electrodes are on a single membrane (section 4.3.3).

4.3.2 Mechanical support based on two separated gold-coated membranes as electrodes

The initial design of the sensor described in this section originated from that developed by Derbyshire in 2011 (Derbyshire, 2011). This design involved the construction of a mechanical support based on two separate gold-coated membranes as electrodes (one as the WE, the other as CE/RE combined) with a non-coated membrane between them. The gold-coated membranes were positioned in such a way that the coated side of the working electrode was facing the non-coated membrane and the coated side of the counter/reference electrode was facing away.

Through investigations of this preliminary design, it was considered that the position and orientation of the coated surface of the electrodes increased the inter-

electrode spacing between them, hindering current flow. This was due to a potential drop between the WE and the CE/RE, caused by the inherent resistance (i_R) of the solution, thus increasing the overall resistance of the system and therefore severely lowering the current response observed for different lactate concentrations analysed. For this reason, a new design for this mechanical support was suggested, incorporating a modification in the position of the electrodes, which were now oriented with both coated sides facing the middle non-coated membrane. This new arrangement of the electrodes (Figure 3.2) aimed to improve the quality of the response signal recorded in terms of magnitude and reproducibility by minimising the distance between the electrodes, or more specifically, their electro-active surfaces.

The laminate sensors of this new design were interrogated as described in section 3.4.2. A range of concentrations of lactate in PBS, from 0 to 1 mM, were analysed. The sensor was placed in a 25-ml beaker, where 20 ml of each lactate concentration sample were placed, sequentially, for their analysis. Prior to the analysis of each concentration, the beaker was quickly rinsed with PBS. As described previously, the inputs for the counter and reference electrode in the potentiostat were merged and connected. The results for the current response at each lactate concentration are represented in Figure 4.3, where the values were normalised by subtracting the baseline current at lactate 0 mM (i.e. PBS only).

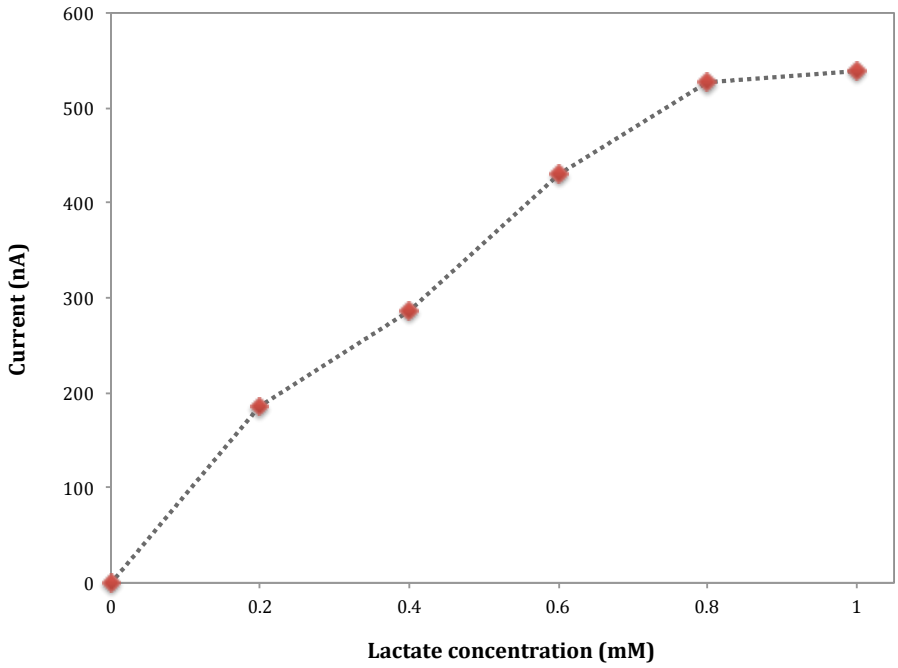

Figure 4.3. Response curve for LOD at a range of lactate concentrations from 0 to 1 mM for the laminate with two gold-coated electrodes with the coated surface facing the middle membrane.

As the results show, there was a higher current response with increasing concentrations of lactate in PBS. This indicated that the enzyme was well immobilised and stable in this new laminate design. The current response as a function of the concentration exhibited a good linearity from 0 to 0.8 mM lactate (R^2 = 0.99), however enzyme saturation was reached at 1 mM. Moreover, the current response for each concentration of lactate was greater than the corresponding ones obtained using the Rank electrode cell (Figure 4.2). A larger surface electrode area is associated with a higher capacitance and lower impedance, giving as a result a bigger current response. Therefore, this increase in the current response with the new design was expected, since the surface area of the WE electrode in the Rank cell (3.14 mm^2) is smaller than the one in this new laminate design (100 mm^2). Also, the obtained current response was higher than the one obtained for the corresponding concentrations with the previous design (Derbyshire, 2011) (e.g. the current response for lactate 1 mM obtained with the previous design was of ≈500 nA, and with the new design this current was of 575 nA). This indicated that this new design, with both gold-coated sides of the

electrode membranes facing inwards, enhanced the monitoring of lactate in PBS, with a higher current response difference between concentrations. However, there was still an issue in the sensor fabrication, since in some constructed sensors the current response obtained for each concentration was very low and hardly varied for increasing concentrations. It was thought that this occurred due to the flow of solution through both sides of the porous electrode membranes, thus competing with the lactate molecules, and therefore a concentration gradient forms in the proximity of the working electrode, affecting the obtained current response signal.

In order to avoid this situation, a new modification was applied to the enzyme laminate design. This modification consisted of placing a glass slide be the full length of the CE/RE strip, and securing the CE/RE to this slide, thus preventing solution ingress from the 'back'. The pore size of the CE/RE membrane was also reduced from the one employed originally (from 1 μm to 0.15 μm) and the edges were sealed by applying insulating tape in order to 'fix' the electrode to the glass slide piece. This aimed to block the diffusional mass transfer (i.e. traversing) through the CE/RE, and instead allow flow only through the WE to the enzyme laminate, and from here to the surface of the CE/RE. This design is shown in Figure 4.4.

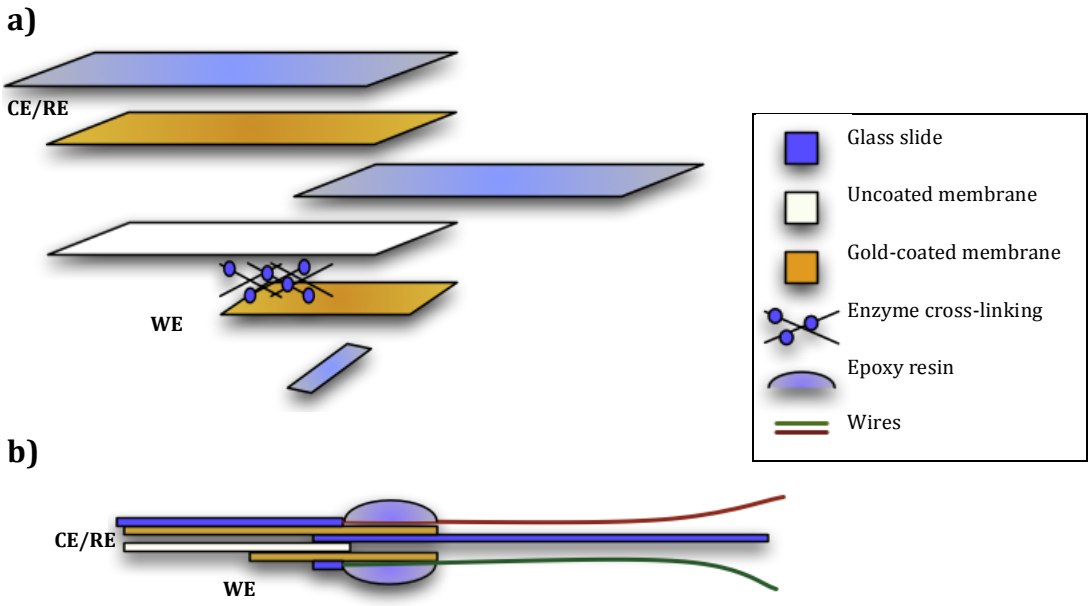

Figure 4.4. Schematic view of the mechanical support based on two separated gold-coated membranes as electrodes. The design blocks the CE/RE against a microscope glass slide piece.

a) Schematic view of the different layers that comprise the sensor**. b)** Lateral view of the assembled mechanical support.

The laminate sensor was again interrogated as described in section 3.4.2. As with the previous design, the sensor was placed in a 25-ml beaker where 20 ml of lactate samples of the relevant concentrations in PBS were analysed. Again, before each addition of a new concentration, the beaker was rinsed with PBS to avoid the obtaining of current responses not proportional to the lactate concentration analysed. However again in some instances the observed current response was still very low, even for higher concentrations of lactate (Figure 4.5). It was then thought that this was caused by applying too much pressure between the WE and the non-coated membrane whilst preparing the enzyme laminate, thus causing seepage of the enzyme mixture out of the membrane laminate, causing a diminution of the amount of available enzyme for the catalytic oxidation of substrate. Moreover, some other problems were encountered with the fabrication of the membranes; resulting in a signal output that indicated the presence of a short circuit between the gold membranes despite the presence of the non-coated

membrane in the middle. Alongside this was also thought that the glutaraldehyde/BSA conjugate was being adsorbed on the WE surface when preparing the enzyme laminate between this WE and the non-coated membrane (as shown in Figure 4.4), thus insulating the WE surface. This prevented the solution to ingress through the pores and also reduced the free gold-coated surface area of the electrode for the oxidation of the H_2O_2 produced by LOD, thus severely affecting any observed signal response (Figure 4.5).

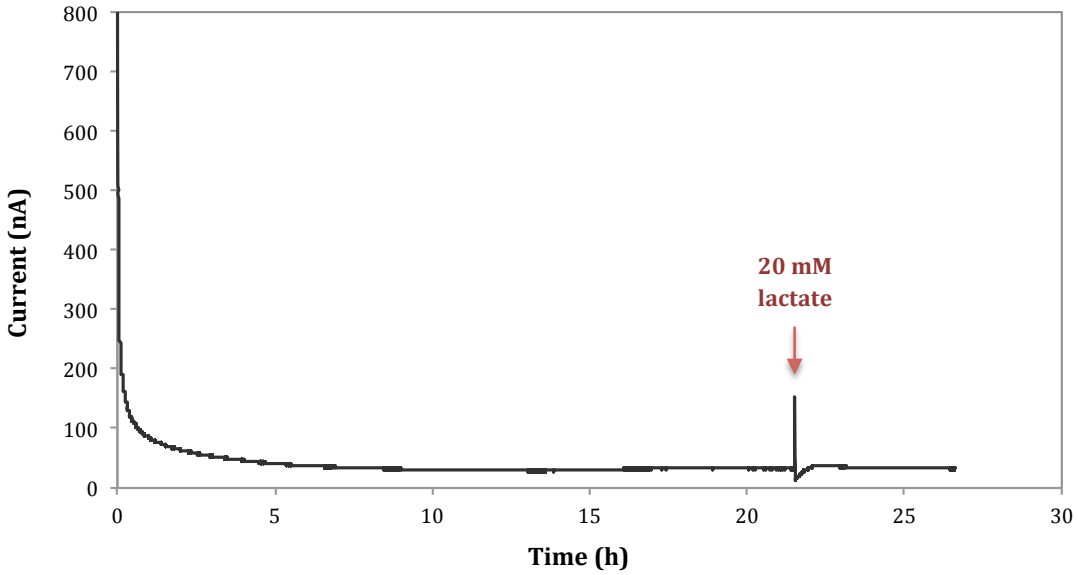

Figure 4.5. Example of the obtained current response along the time of the experiment using a laminate design sensor based on two separated gold-coated membranes as electrodes, where design blocks the CE/RE against a microscope glass slide piece. A dilution of lactate in PBS at a concentration of 20 mM was analysed.

The arrow indicates the moment at which the PBS solution was extracted from the beaker and the lactate test solution was introduced.

In order to avoid this situation, it was decided to introduce an extra non-coated membrane in the middle of both gold-coated membranes. This membrane aimed to overcome both problems encountered with the previous design and, in essence, it would mimic the laminate structure placed upon the WE electrode in a Rank cell. It was suggested that, since in this instance the enzyme laminate would be prepared between both non-coated membranes, of an area larger than the WE,

the surface area for the enzyme cross-linking would be increased, thus reducing the seepage of the enzyme mixture out through the edges of the membranes on to the WE. Furthermore, by preparing the enzyme laminate between the two non-coated membranes, the 'passivation' of the WE, caused by the poisoning and blocking of the electrode with the accumulation of glutaraldehyde/BSA conjugate at its surface, could be avoided.

In this case, the enzyme laminate was prepared prior to the assembling of the sensor. After this, the construction of the mechanical support was performed as described previously. This time the experiments were carried out not only by sensors with an immobilised CE/RE (Figure 4.6), but also sensors with the WE immobilised (Figure 4.7). The membrane to be blocked against the microscope glass slide piece had a reduced pore size from the one used in the first design (from 1 μm to 0.15 μm). This was undertaken since it was suggested that by immobilising the CE/RE, the solution would flow through the WE, thus hindering the approximation of H_2O_2 to its surface, compromising the functioning of the sensor and the obtained current response. With the WE immobilised, the solution would flow through the CE/RE to the enzyme laminate, and from here to the surface of the WE instead, where the H_2O_2 produced by the lactate oxidase enzyme would be oxidised. Based on this and coupled to the fact that in a Rank cell the solution contacts the WE once passed through the membrane, it was thought that this configuration of the laminate design could produce better results. Both configurations (immobilising the CE/RE and the WE) were investigated to ascertain the optimum design for a better sensing of lactate.

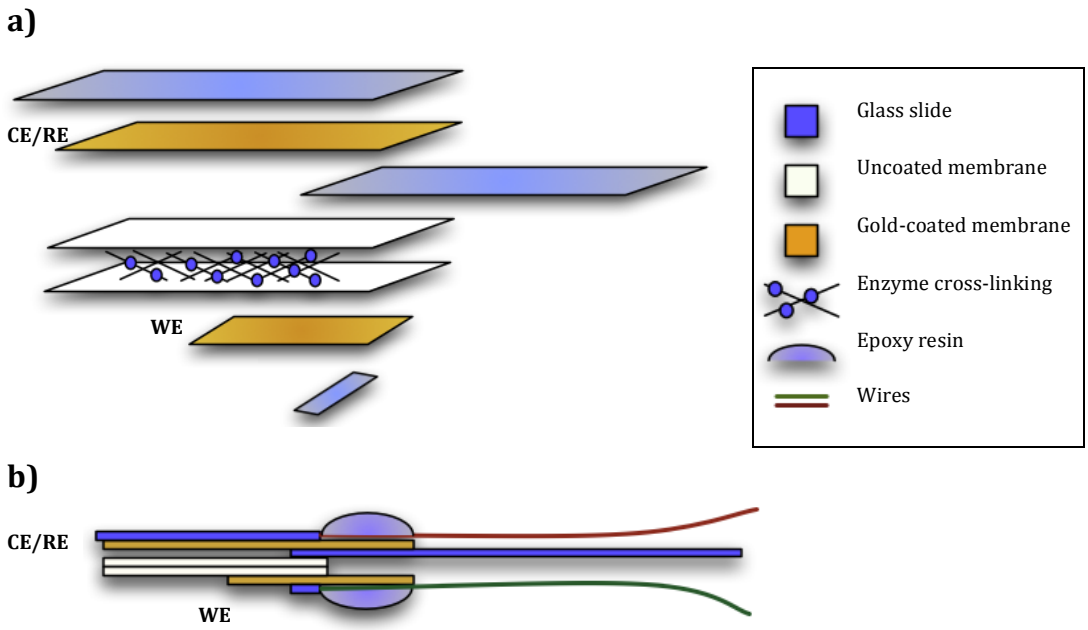

Figure 4.6. Schematic view of the mechanical support based on two separated gold-coated membranes as electrodes and two non-coated membranes in the middle. The design blocks the CE/RE against a microscope glass slide piece.

a) Schematic view of the different layers that comprise the sensor**. b)** Lateral view of the assembled mechanical support.

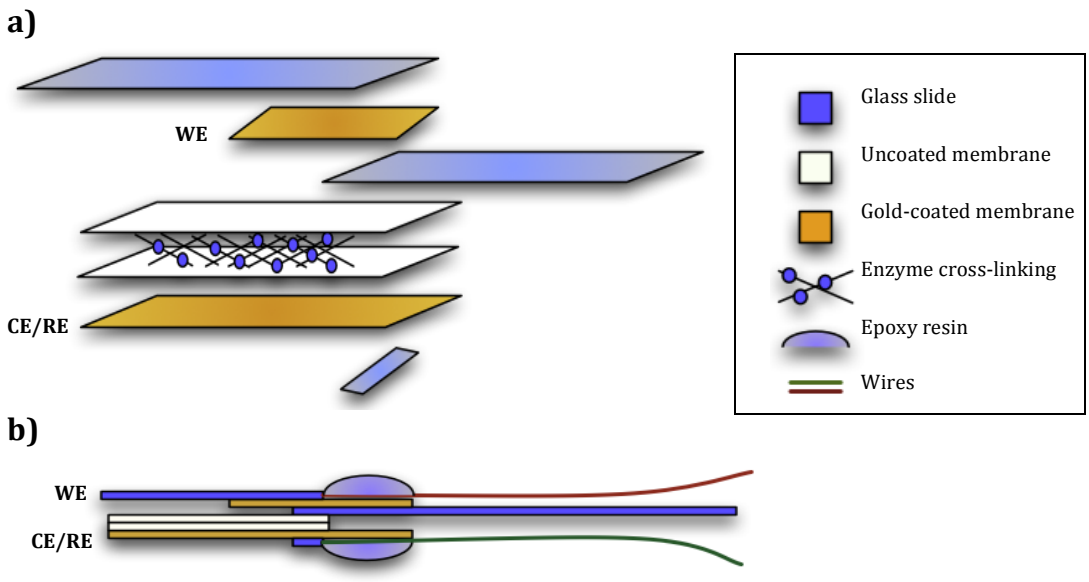

Figure 4.7. Schematic view of the mechanical support based on two separated gold-coated membranes as electrodes and two non-coated membranes in the middle. The design blocks the WE against a microscope glass slide piece.

a) Schematic view of the different layers that comprise the sensor**. b)** Lateral view of the assembled mechanical support.

Several sensors of each one of these two configurations were constructed and different dilutions of lactate analysed. With this new design the problem with the connection shorting was overcome (i.e. contact between WE and CE/RE when not in solution), since all sensors assembled with this configuration polarised as expected. However, the current responses obtained for different lactate concentrations analysed when either immobilising the CE/RE (Figure 4.8a.) or the WE (Figure 4.8b.) were again very low even for relatively high concentrations of lactate, such as 20 mM, and to this extent unmeasurable. The same experiments were therefore carried out on both configurations of the sensor using the enzyme GOD to discard the possibility of the enzyme LOD in some manner affecting the response. The current transients obtained for glucose measurement are shown in Figure 4.9.

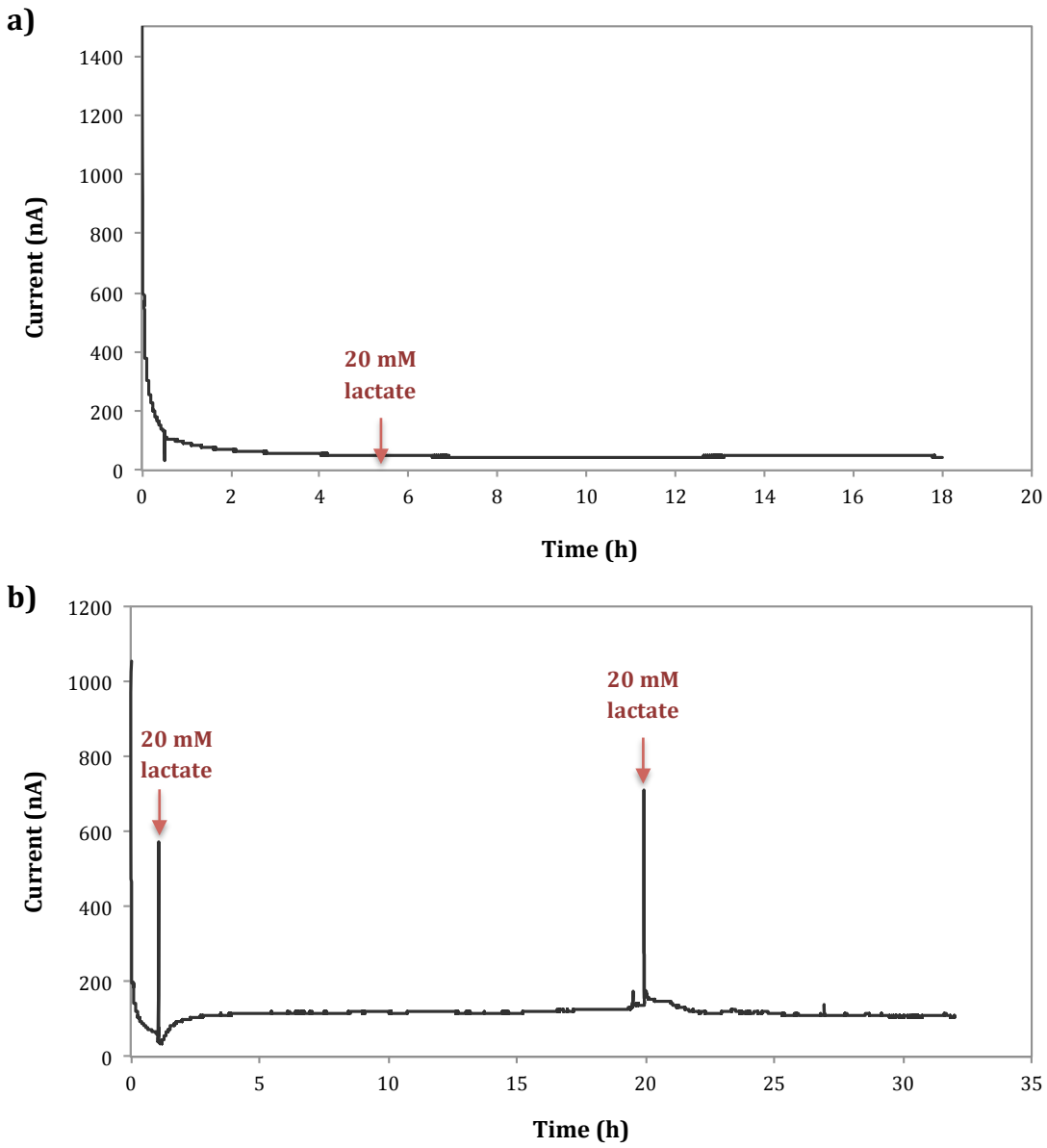

Figure 4.8. Example of the obtained current response along the time of the experiment using a laminate design sensor with one of the electrodes (a) CE/RE, b) WE) immobilised against a microscope glass slide piece. A dilution of lactate in PBS at a concentration of 20 mM was analysed.

The arrows indicate the moment at which the PBS solution was extracted from the beaker and the lactate test solution was introduced.

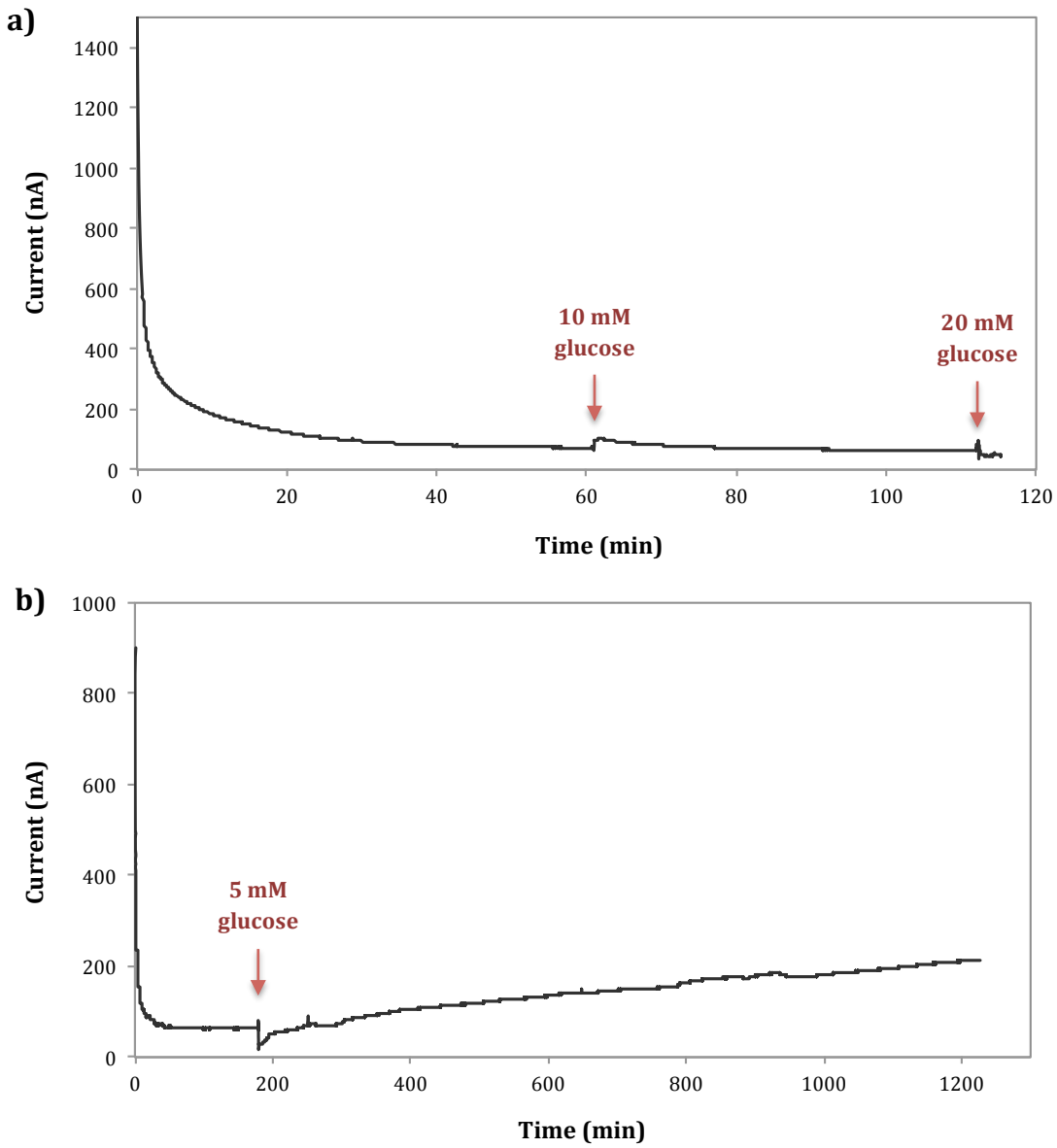

Figure 4.9. Example of the obtained current response along the time of the experiment using a laminate design sensor with one of the electrodes (a) CE/RE, b) WE) immobilised against a microscope glass slide piece. Dilutions of glucose in sodium acetate buffer at a range of concentrations between 5 and 20 mM were analysed.

The arrows indicate the moment at which the sodium acetate buffer solution was extracted from the beaker and the glucose test solutions were introduced.

As the results indicate, the current response for different concentrations of glucose was very low when the CE/RE was immobilised (Figure 4.9a). However, there was a higher current response for a lower concentration of glucose when the

WE was immobilised (Figure 4.9b), although such response in terms of reaching a steady-state value was relatively slow. It was thought that this could be caused by the extent of the diffusional barrier offered by membrane layers in the system that the solution had to flow through. Therefore, a completely new design of the system was suggested, and this is described in section 4.3.3.

4.3.3 Mechanical support based on two electrodes on a single sputter-coated membrane

The development of the sensor described in this section was carried out following the analysis of the results obtained for the preceding designs described in the previous section. These previous results showed that the construction of a mechanical support where the gold-coated membranes as electrodes were facing each other brought many issues (connection shorting, electrode blocking, solution flow blocking), which compromised the obtaining of an optimum and reproducible current response. Therefore, it was decided to develop a laminate sensor with a new design based on the one in the Rank electrode cell, since it was thought that by mimicking the design of a Rank cell these problems could be, in some extent, avoided, due to the properties of its design.

Following the configuration of a Rank cell, in this new configuration both the WE and the CE/RE would be in the same plane, that is, on the same polycarbonate membrane disk. Both electrodes would be separated from each other by a non-coated region. The electrode regions and the separation between them would be defined by using a template made of insulating tape, which would be placed on the membrane and removed once sputter-coated.

This new design aimed to standardise the design of the electrodes, with a constant size and distance between them, to favour the obtaining of more reproducible results. The enzyme laminate would be placed directly on the WE, avoiding the flow of solution through the CE/RE. Also, with this design, any hindrance caused by the number of membrane layers that the solution had to flow

through would be minimised. Moreover, both electrodes were immobilised against a glass slide, thus blocking the flow of solution from both sides of the membrane, since this has been shown previously to have a detrimental effect on signal response depending on the orientation of the immobilised electrode system (Figure 4.8, 4.9). This way, it was expected that the approach of H_2O_2 to the surface of the WE would not be hindered, giving as a result an increased current response and extending the concentration range.

Two sensor configurations were developed within this design. Preliminary studies were performed with an electrode system where both CE/RE and WE were sputter-coated with gold, following the configuration of preceding designs. This laminate sensor design would be subsequently compared with a second configuration where the WE had been sputter-coated with platinum.

The laminates for both electrode configurations were constructed as described in section 3.4.6.2.i, using 6 μl of LOD (~830 U ml^{-1}) in 0.1 g ml^{-1} BSA and 3 μl of 5% v/v glutaraldehyde, allowing to crosslink between two 5x9-mm polycarbonate membranes by pressing them together between two microscope glass slides, and applying light-finger pressure for approximately 5 minutes. The enzyme laminate was then placed above the WE area of the sensor and the edges were sealed with insulating tape, holding it in place. This would avoid the separation of the enzyme laminate from the electrode surface once in contact with the lactate sample, which would result in the flow of solution directly to the WE surface, compromising the signal response.

4.3.3.1 Electrode system based on gold-coated CE/RE and WE

As previously stated, preliminary studies on this new sensor configuration were performed on an electrode system where both CE/RE and WE were sputter-coated with gold. These experiments sought to analyse the current response obtained with this sensor design and to allow its direct comparison with previous designs, where both CE/RE and WE were also gold-sputtered. The sensing system

based on both CE/RE and WE on a single gold-coated membrane was constructed as described in section 3.4.6.2.i as shown in Figure 3.3 and Figure 3.4.

Initial experiments with the new sensor design consisted of introducing the sensor in a 25-ml beaker and placing sequentially 15 ml of the different samples to be analysed. The first experiment consisted of the analysis of a range of lactate concentrations, from 0 to 0.8 mM (Figure 4.10). Prior to this, PBS only would be added in order to obtain a baseline current response.

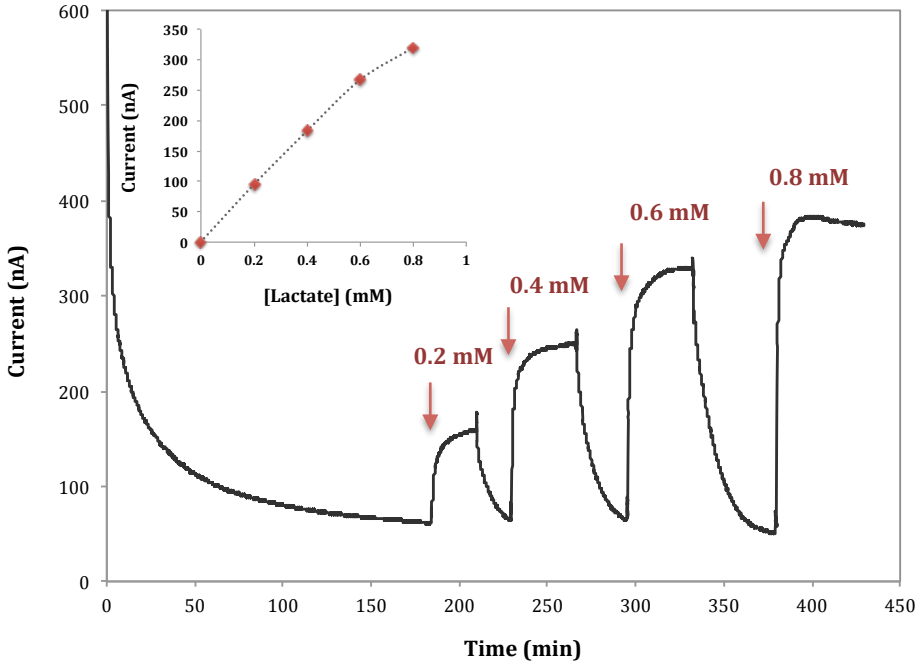

Figure 4.10. Example of steady-state current response and corresponding calibration curve obtained using LOD on the electrode system based on a gold-coated CE/RE and WE over a range of lactate concentrations, from 0 to 0.8 mM.

The arrows indicate the moment at which the PBS solution was extracted from the beaker and the lactate test solutions were introduced.

As the results show, there was a measurable current response when the lactate samples were put in contact with the enzyme laminate, which indicated that the enzyme was well immobilised and stable in this new laminate design. Moreover, the sensor polarised with the current tending towards a low stable baseline with

time, indicating that there was no connection shorting between the two electrodes. The current response obtained was significantly lower than these obtained for the corresponding concentrations with previous designs (Figure 4.3). This could be due to the size of the WE in the new design, which is smaller in area than the one in the first design using gold electrodes (Figure 3.2) (45 mm^2 in this new design compared to 100 mm^2 in the first design) and, as previously mentioned, this can affect the current response. This lower current response in the new design could be also due to a smaller surface area of the laminate membranes, which can cause the seepage of more enzyme mixture than if larger membranes (like those used previously) were used. However, the current density for the first design using gold electrodes (Figure 3.2) and the present design were measured. This current density, defined as the current per unit area of the electrode, is commonly used as a measurement of the rate of an electrochemical reaction and can be expressed according to the equation:

$$j = \frac{i}{A}$$

where j is the current density of a certain electrode, i is the current (A), and A its area (m^2). According to the equation, the larger the electrode area of contact with the solution, the more product will be formed per unit time, with the current density remaining constant. The current density for both sensor designs was calculated, using as an arbitrary value the current response obtained for lactate 0.4 mM. Results showed that the current density for the first design using gold electrodes was of $2.86x10^{-3}$ A m^{-2}, while the one calculated for the present design was of $5.4x10^{-3}$ A m^{-2}. This meant that the current density for this new design was approximately 2 times (1.9 times) higher than the one obtained with the initial design. These preliminary results suggested that this new enzyme-laminate sensor design exhibited promise for a reproducible, fast and accurate sensing of lactate in PBS.

4.3.3.2 Electrode system based on gold (CE/RE) and platinum (WE) sputter-coated membrane.

The development of the sensor configuration described in the present section builds upon the encouraging results obtained with the previous design, based on a two-electrode system on a single gold-coated membrane. These results showed the improvement in the obtaining of a current response and current density that the new developed electrode system, based on the structure of the Rank oxygen electrode, led to, with respect to the initial electrode design using gold electrodes (Figure 3.2) and the following electrode configurations developed.

It has been reported that platinum is a well-known electrocatalyst for the oxidation of H_2O_2(Sánchez *et al.*, 1990; Nyamsi Hendji *et al.*, 1993; Hall *et al.*, 2000) as the potential at which it oxidises falls in the potential region for platinum oxide film formation. Platinum electrodes have been widely used in the construction of amperometric sensors, including the Rank oxygen electrode, which incorporates a platinum-coated WE in its structure. For this reason, a new design for the recently developed electrode system of the sensor was suggested, incorporating a WE sputter-coated with platinum (Figure 3.5 and Figure 3.6) as an alternative to the gold-coated WE used in previous designs. Therefore, the aim of this study was to compare the current response obtained using the recent electrode-system configuration with the previous one, based on a gold-coated WE, and assess the best composition of the electrode system for the obtaining of an improved design for enhanced lactate sensing.

Prior to the development of the sensor, a study was performed in order to assess the optimum platinum sputter-coating procedure on polycarbonate membranes. The aim of this study was to maximise the conductivity of the electrode whilst keeping the platinum deposition times as low as possible. In order to perform this study, polycarbonate membranes of 25 mm diameter and 0.1 pore radii were sputter-coated with platinum using different coating times, between 30 to 180 seconds, in steps of 30 seconds. The protocol followed for coating the membranes is outlined in section 3.4.5. Then, the resistivity of the

platinum-coated membranes was measured between both extremes of the diameter using a digital multimeter as described in section 3.3.5. Each coating time was tested on three different polycarbonate membranes and the average resistivity across the diameter was calculated and represented in a chart (Figure 4.11).

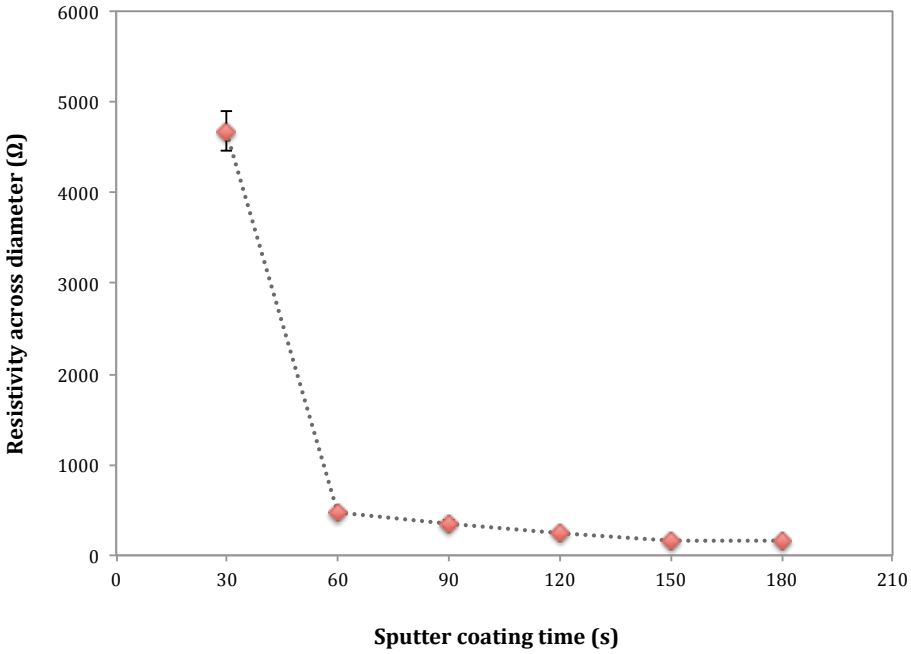

Figure 4.11. Average resistance measured across the diameter of platinum sputter-coated polycarbonate membranes for different platinum deposition times.

As the results show, longer platinum deposition times increased the conductivity of the coated membrane. This would be expected, as longer deposition times increase the thickness of the platinum layer on top of the membrane. Resistance can be expressed according to the equation:

$$R = \frac{l\rho}{A}$$

where R is the resistance of a certain surface (Ω), l is the length of the conductor (m), ρ is the resistivity of the conductor (Ω m) and A its cross-sectional area (m^2).

According to the equation it can be stated that given a material with an intrinsic fixed resistivity, the resistance is only affected by the length and cross-sectional area of the conductor. Here, as it was mentioned above, the resistivity was measured across the same diameter length in all membranes, which makes the length of the conductor constant in the equation. Therefore, in this case the resistivity of the conductor is inversely proportional to its cross-sectional area (thickness).

The resistivity of the platinum-coated membrane surface exhibited a dramatic decrease (from 4676.67 to 470 Ω) as the platinum deposition time increased from 30 to 60 seconds. The resistivity decreased to a smaller degree as the time was increased to 150 seconds, and the difference in resistivity between 150 seconds and 180 seconds was only 2 Ω. As previously mentioned, the platinum deposition time was to be kept as low as possible. Therefore, 150 seconds was chosen as the optimum time for the platinum sputter-coating procedure to be followed in all subsequent work.

The surface of the bare Pt WE was characterised using Scanning Electron Microscopy, described in section 3.4.7, which provided a control to which subsequent surface characterisations (detailed in chapters 6 and 7) would be compared. This type of microscope uses a beam of electrons to create an image of the specimen under study (i.e. the electrode surface) and, for this reason, they usually image conductive or semi-conductive materials. Those materials that are non-conductive can be imaged either by Environmental Scanning Electron Microscopy (ESEM) or, as a more common alternative, coating them with a layer of conductive metal. A very common preparation method is to coat the non-conductive sample with a layer of conductive material through sputter-coating. Since for the construction of the developed electrode system, a polycarbonate membrane (non-conductive) was sputter-coated with platinum and gold, so allowing for the observation of the electrode surface. The AuPt electrode system employed in this part of the study was constructed according to the protocol outlined in section 3.4.6.2.ii. The surface of the working electrode from the AuPt systems was explored through SEM according to the protocol outlined in section

3.4.7. Two magnifications were employed in this study: 5000x and 50,000x. The scanning electron photographs are shown in Figure 4.12.

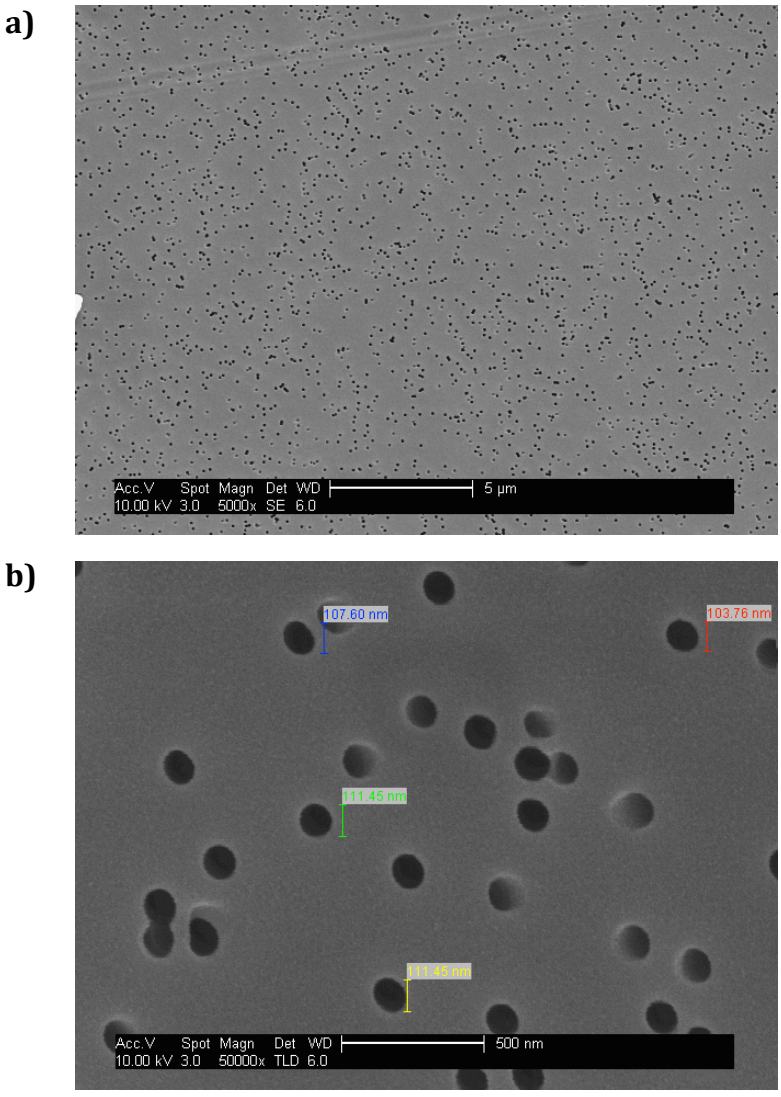

Figure 4.12. Electron microphotographs of the surface of the bare Pt working electrode at magnifications of a) 5,000x and b) 50,000x.

As Figure 4.12 shows, the Pt electrode surface exhibited a homogeneously porous surface (Figure 4.12a) with pore-size radii of approximately 0.1 µm, which corresponds to the pore size of the polycarbonate membranes employed for the sputter-coating of the AuPt electrode system.

The capability of the developed sensing system for providing increasing current response values for consecutive additions of hydrogen peroxide was evaluated. The electrode system was constructed as described in section 3.4.6.2.ii and interrogated over successive additions of H_2O_2 in the range 0.02-0.24 mM. The AuPt electrode system, interrogated following the chronoamperometric protocol outlined in section 3.4.2, was placed in a 25-ml beaker and polarised at +650 mV with 15 ml of PBS only. When a baseline was reached, successive additions of 100 µl from a 3.02 mM H_2O_2 stock solution were successively added. The chronoamperometric response was recorded and the current values corresponding to each H_2O_2 concentration were normalised by subtracting the baseline current response obtained with PBS only and represented in a chart (Figure 4.13).

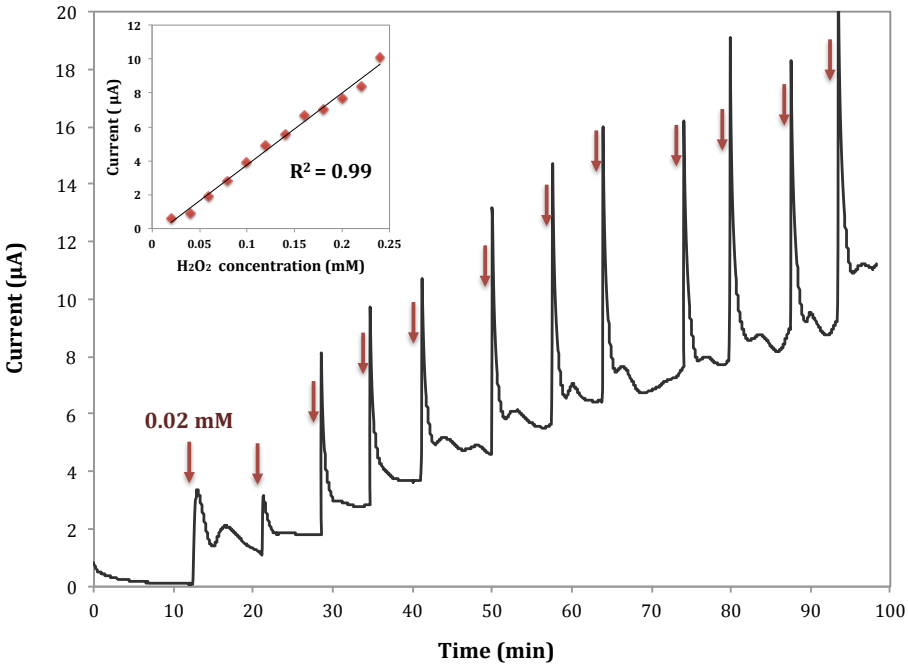

Figure 4.13. Chronoamperometric response for successive additions of 0.02 mM H_2O_2. Inset with normalised current values for each H_2O_2 concentration.

The arrows indicate the moment at which additions of the H_2O_2 stock solution were performed.

Results showed an increase in current response over successive additions of H_2O_2, indicating that its oxidation at the surface of the Pt electrode was taking place and proving the capability of the sensor to detect variations in its concentration in the solution.

Following these results, the present laminate sensor design was constructed as described in section 3.4.6.2.ii and interrogated over a range of lactate concentrations in PBS, with the aim to analyse the current response obtained with this sensor design and to allow its direct comparison with the previous design, based on a gold-coated WE (Figure 3.3 and Figure 3.4). The present laminate sensor design was constructed as described in section 3.4.6.2.ii and it is shown in Figure 3.5 and Figure 3.6.

As with the previous design, initial experiments consisted of introducing the sensor in a 25-ml beaker and placing sequentially 15 mL of a range of lactate concentrations, from 0 to 0.8 mM, for their analysis. Prior to this, PBS only would be added in order to obtain a baseline current response. The obtained response from the first experiment performed on the developed laminate sensor design is shown in Figure 4.14.

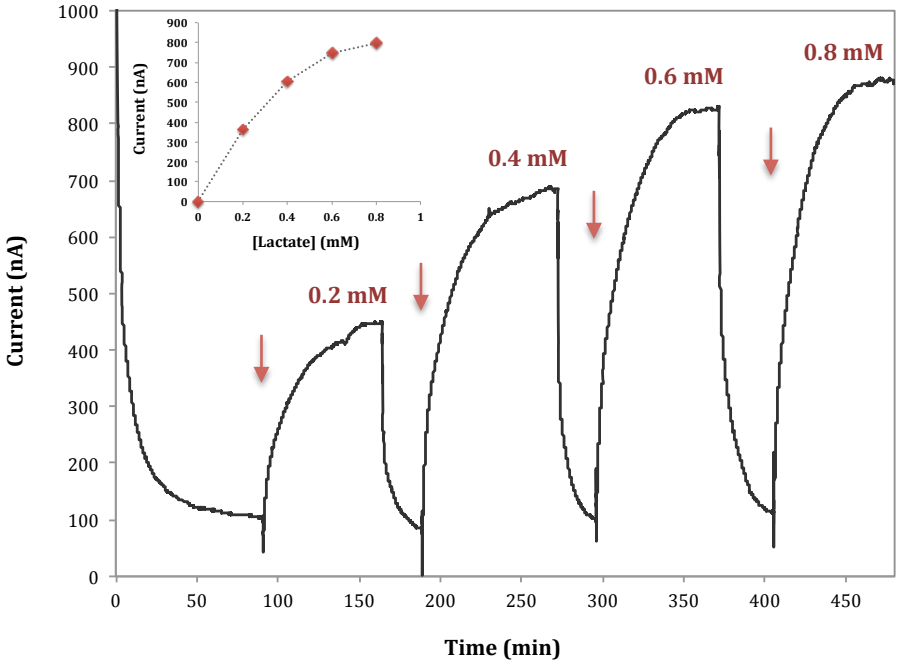

Figure 4.14. Example of steady-state current response and corresponding calibration curve obtained using LOD on the electrode system based on a gold-coated CE/RE and a platinum-coated WE over a range of lactate concentrations, from 0 to 0.8 mM.

The arrows indicate the moment at which the PBS solution was extracted from the beaker and the lactate test solutions were introduced.

Results obtained with the new sensor design based on a platinum-coated WE showed that, as with the previous design, an increasing current response was obtained when the laminate sensor design was put in contact with raising lactate concentrations in PBS, which again indicated that the enzyme was well immobilised in the laminate structure and remained stable over time.

The current density for the present sensor design, calculated for the current response value obtained for 0.4 mM lactate, gave a value of 1.52×10^{-2} A m^{-2}. This indicated that the current density for the platinum-coated WE within this new sensor design was approximately 3 times (2.8 times) higher than the one calculated for the gold-coated WE from the previous design, despite of both electrodes having the same area. These results confirmed the excellent catalytic properties of platinum with respect to gold and constituted a key factor in

choosing this design as the optimum electrode system to be used in all subsequent work.

Subsequent studies performed on the developed sensing device focused on assessing the reproducibility of the electrode-system response. The aim of this study was to assess the quality of the hand-manufactured electrode system in terms of providing a reproducible electrochemical response between different sensing devices. The experiments in this study were performed using cyclic voltammetry as described in section 3.4.1. For this experiment, ferrocenecarboxylic acid (FA) was prepared in pH 7.4 PBS at three different concentrations (1, 3 and 5 mM). FA was chosen in this study as it is a water-soluble redox couple, which undergo a facile one-electron oxidation at most electrodes and it is commonly used to study the electrochemical properties of electrode systems.

The electrode system characterised in FA/PBS pH 7.4 was interrogated as described in section 3.4.6.2.ii. The electrodes were recorded between -0.4 and +0.8 (vs. Ag/AgCl) at a sweep rate of 20 mV s^{-1}, based on the parameters used for the analysis of FA in carbon electrodes by Gornall *et al.*, 2009, which will be described in Chapter 7. Each solution was tested on five different sensors in order to obtain an average current response. The voltammograms obtained from the analysis of each sensor for the range of FA concentrations are shown in Figure 4.15a-d, and the representation of the positive (anodic) and negative (cathodic) average peak current for each concentration is shown in Figure 4.15e with each corresponding standard deviation.

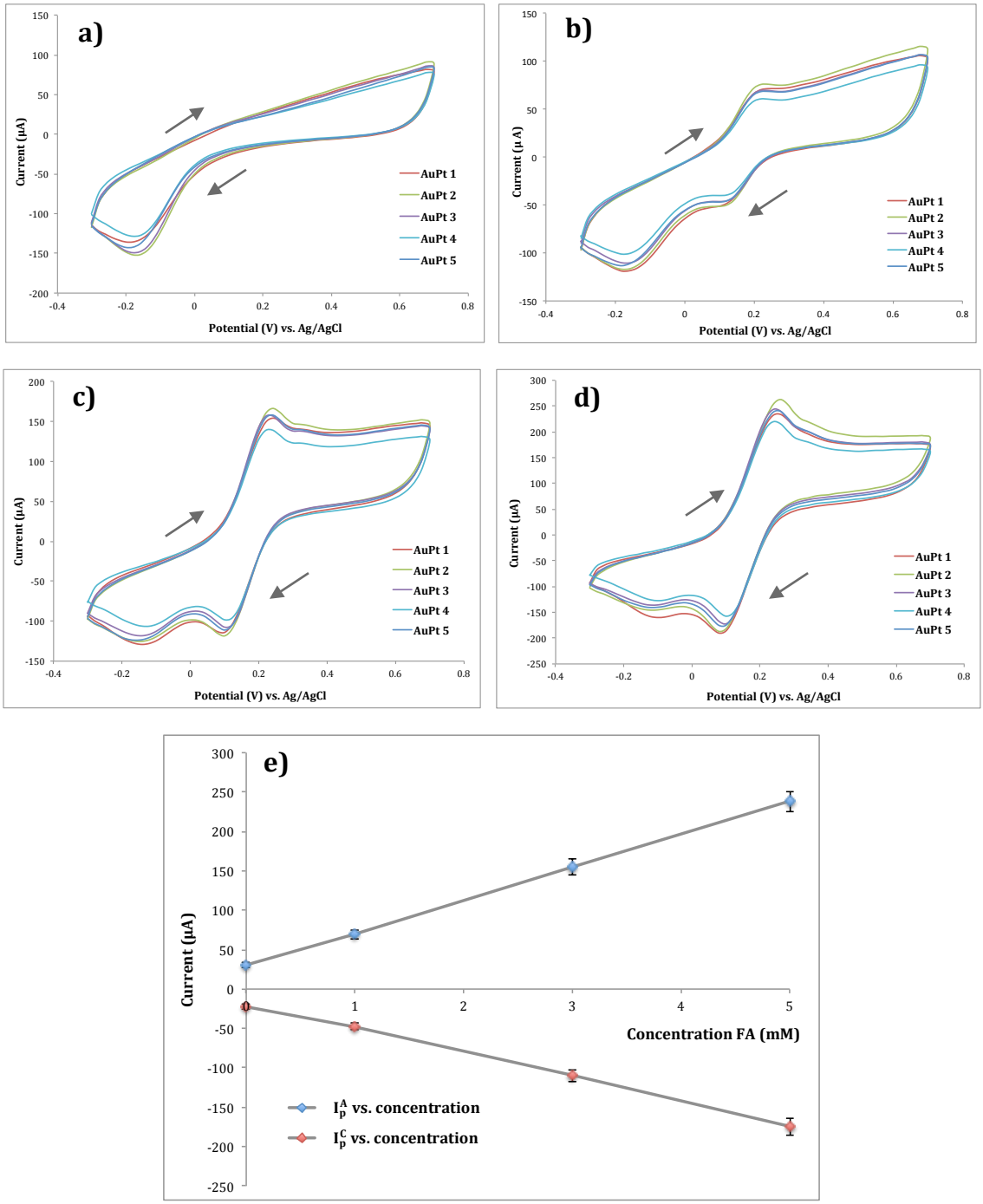

Figure 4.15. a)-d) Cyclic voltammograms for ferrocenecarboxylic acid (FA) at 0 (PBS only), 1, 3 and 5 mM. Scan rate: 20 mV s^{-1}. e) Representation of the anodic (I_p^A) and cathodic (I_p^C) peak current versus the concentrations, for each of the dilutions.

As the results show, the reproducibility of the cyclic voltammetry test for the range of FA concentrations on the developed gold-platinum electrode systems was relatively high, with standard deviations in the range of 5.6-12.8 μA, which corresponded to a range of Relative Standard Deviation (RSD) values of 5.4-9.8%. These results indicated that the variation in electrochemical properties between different hand-manufactured electrode systems was relatively small and, therefore, would take a minimum part in the overall variability within the current response of the system.

The final study performed on the developed AuPt electrode system consisted in evaluating the effect of mechanical bending on its sensing performance. The AuPt systems analysed in this study were constructed following the protocol outlined in section 3.4.6.2.ii. However, for this study the electrode system sputter-coated on a single polycarbonate membrane was fixed to a flexible plastic surface following the same method as for a glass slide, described in the mentioned protocol, allowing for the flexibilisation and mechanical deformation of the electrode system for the performance of the present study. The resulting sensors were interrogated, using the chronoamperometry protocol described in section 3.4.2. The AuPt electrode systems were introduced in a 25-ml beaker and polarised with 15 ml PBS only at +650 mV. Once a baseline was reached, repeated additions of 0.1 and 1 mM H_2O_2 solutions in PBS were repeatedly added. Prior to each sample addition, the electrode systems were bent to an angle of approximately 90° for 2 seconds followed by another 2 seconds of relaxation. The bending/relaxing process was iterated 5 times prior to the interrogation of the AuPt system with a new H_2O_2 solution. The chronoamperometric response for both AuPt sensing systems with both H_2O_2 solutions were recorded and the current value corresponding to each sample addition was normalised by subtracting the baseline current response and represented in a chart (Figure 4.16).

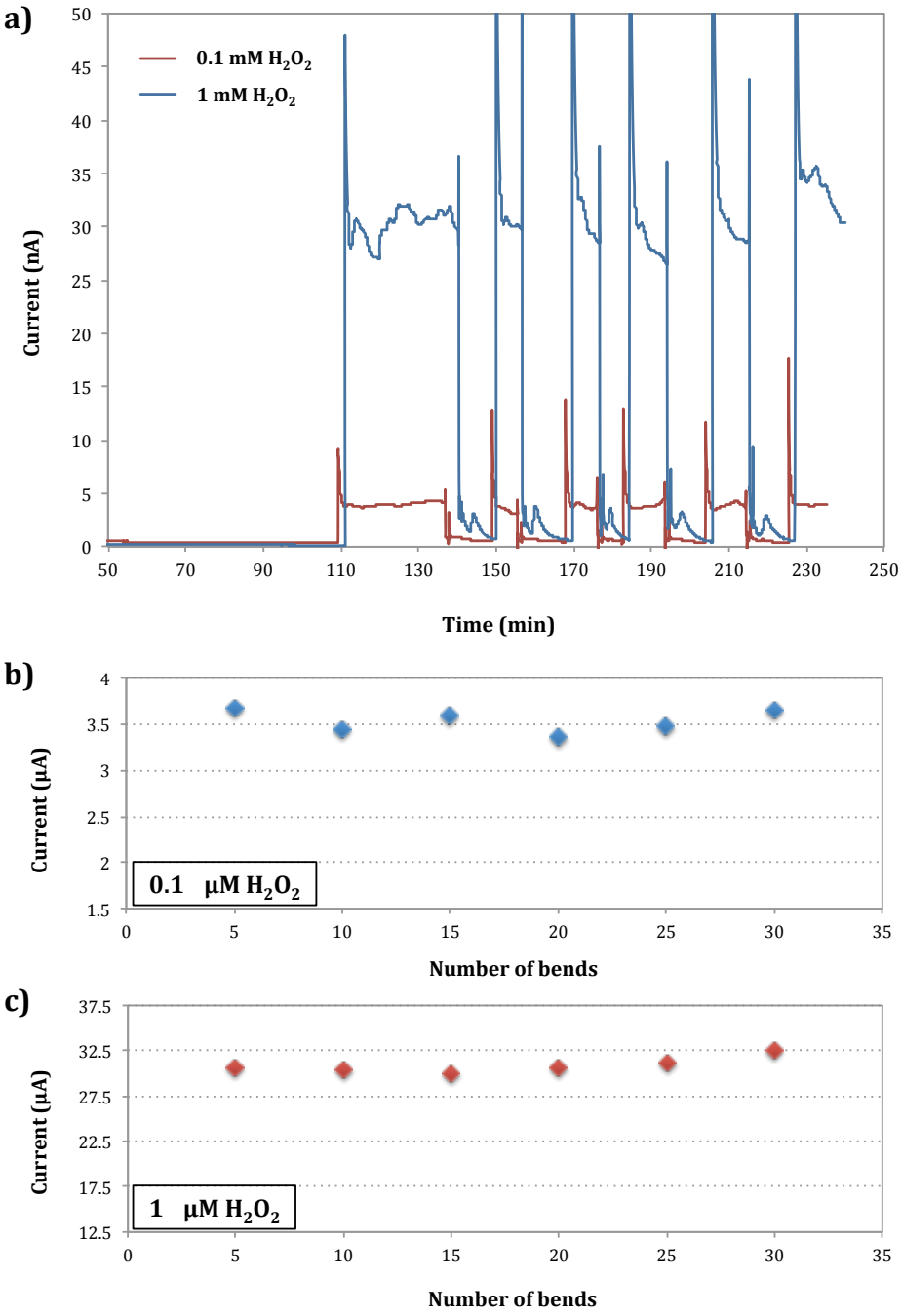

Figure 4.16. Bending test performed on the AuPt electrode system. (a) Chronoamperometric responses for 0.1 and 1 mM H_2O_2 and (b,c) normalised current response values for both concentrations and each number of bends.

The results represented in Figure 4.16 showed that the response of the electrode system was relatively stable over the performance of 30 bends with an RSD of 3.5% and 2.8% between 0.1 and 1 mM H_2O_2 additions, respectively. These

results not only confirmed the low intra-variability for the hand-manufactured AuPt sensing system developed in this project but also the mechanical stability of the system over 30 bending-relaxation iterations, making it suitable for its potential application on to the skin for continuous monitoring of lactate (H_2O_2) in sweat.

The present study shows that a new electrode system for lactate monitoring was developed, based on the configuration of a Rank cell, where both the WE and the CE/RE are in the same plane. This change in the electrode-system configuration allowed the standardisation of the design by assuring a constant size of the electrodes and distance between them. Hindrance problems with previous designs caused by the number of membrane layers between the solution and the WE surface were also minimised.

Subsequent studies on the developed electrode configuration demonstrated that incorporating a platinum-coated WE in the structure, in contrast to previous designs where all electrodes were sputter-coated with gold, led to an improvement of the electrochemical properties of the electrode system. This change in the WE material led to an increase not only in the current response obtained for different lactate concentrations in PBS but also in the current density of the platinum WE, which would be expected as it is known as a good electrocatalyst for the oxidation of H_2O_2.

The hand-manufactured electrode systems based on this latter design showed a good intra- and inter-sensor reproducibility. Moreover, the developed electrode system exhibits good mechanical stability after 30 bending-relaxation iterations. These results indicate the potential for the AuPt system for being applied on to the skin in order to perform continuous lactate monitoring. For all these reasons, the developed electrode system based on a gold-coated CE/RE and a platinum-coated WE on the same polycarbonate membrane was chosen as the optimum electrode system for lactate monitoring to be used in all subsequent work.

4.4 Conclusions

The work presented in this chapter has been focused on the development of a novel sensing platform for the monitoring of lactate in solution.

Preliminary studies were performed on a Rank electrode cell as a base system for obtaining of reproducible lactate measurements of H_2O_2. Alongside this, it allowed a direct comparison of the results obtained with the final developed design (AuPt system), as this was based on the electrode design of the Rank cell system.

Initial constructed sensing designs originated from that developed by Derbyshire in 2011 (Derbyshire, 2011), based on two separated gold-coated membranes as WE and CE/RE with a non-coated membrane between them in order to avoid connection shorting caused by direct contact between both electrodes. The sensing system was optimised by modifying the orientation of the electrodes in order to reduce inter-electrode spacing, fixing one of the electrodes (CE/RE or WE) to a glass slide to block the flow of solution through both sides of the enzyme laminate and introducing a second uncoated membrane between the electrodes to avoid the blocking of the WE surface. However, there was still an issue with the current response obtained for different concentrations of substrate, which was very low.

A completely new design of the system was suggested, following the configuration of a Rank cell, based on two electrodes on a single sputter coated membrane with the aim to enhance the quality of the response signal recorded in terms of reproducibility and magnitude. Two designs were developed, with a common gold-coated CE/RE and a gold or platinum-coated WE and its electrochemical properties were compared.

A platinum sputter-coating procedure on polycarbonate membranes was also investigated in order to maximise the conductivity of the WE.

The use of a platinum-coated WE exhibited an increase in both current response and current density of the electrode. This design also ensured a constant

distance between electrodes and hindrance problems encountered with previous designs were avoided. The electrode system showed good intra and inter-sensor reproducibility and mechanical stability after 30 bending-relaxation iterations, which shows its potential for being applied as a body-worn device. Moreover, the developed design is very thin (~30 μm) and could be placed on a flexible support, allowing its easy contact with the skin surface for the monitoring of sweat lactate.

CHAPTER 5

ENZYME LAMINATE. CONSTRUCTION, ELECTROCHEMICAL CHARACTERISATION AND OPTIMISATION

5 Enzyme laminate. Construction, electrochemical characterisation and optimisation

5.1 Introduction

This chapter describes the steps towards obtaining a working sensing system and the optimisation of its performance, in terms of reproducibility and linearity of the response, over the physiologically relevant lactate concentration range of 0-70 mM for the early detection of pressure ischemia. The need for this study results from the realisation that, along with the experiments performed with the different mechanical support configurations up to the latest design (AuPt) and also the Rank oxygen electrode (Chapter 4), there was a lack of reproducibility for current response. The AuPt system design was tested to determine its electrical and electrochemical properties, as described in the previous section, in terms of conductivity/resistivity and reproducibility. As the electrode system exhibited good electrical properties and intra and inter-electrode surface reproducibility, it was concluded that the problem possibly lay in the construction of the recognition system (i.e. the enzyme laminate construct).

In enzyme-based biosensors, the enzyme used plays an critical role in the obtaining of a working system, as its successful catalysis of the substrate gives rise to a measurable current proportional to the concentration of the catalysed substrate. The main condition for the success of the reaction is that the enzyme's native structure remains stable while catalysis is taking place. In other words, the enzyme has to preserve its catalytic activity. Therefore, in order to accomplish the fabrication of a stable sensing device in terms of operational stability and shelf life, that is also reliable and sensitive over the range of relevant concentrations for the study, the stability of the enzyme within the sensing system is crucial.

It has been reported that the stability of an enzyme is often improved by its immobilisation, compared to the corresponding enzyme solution (Migneault *et al.*, 2004; Chen *et al.*, 1998). This is due to the rigidification (loss of flexibility) caused

by the coupling of the enzyme to a solid support, which hinders the movement of the protein domains that can lead to its denaturation. Among the different methods by which the immobilisation of an enzyme can be achieved, the chemical cross-linking via glutaraldehyde, using BSA as a protein feeder, was chosen in this study as it produces the formation of intra and intermolecular bonds that lead to a more rigid molecule incapable of undergoing conformational changes.

The immobilisation of the enzyme within the laminate system is, therefore, the key issue in the development of a working sensing system and the most suitable conditions have to be carefully selected. An incomplete immobilisation with a concurrent loss in molecular conformation and the dynamics involved in the immobilisation process will have an influence in the performance of the laminate system as the sensing component.

5.2 Membrane porosity

After the development of the latest electrode-system design (AuPt), the first study performed on the laminate system within the sensing device was the effect of the membrane pore size on the lactate response. The main aim of this study was to facilitate the lactate-monitoring concentration range up to physiologically relevant concentrations for pressure ischemic conditions (up to 60-70 mM), with a current response profile that is as linear as possible.

Up to this point of the research, it was observed that the calibration curve obtained with LOD for any of the developed sensing designs plateaued towards 0.7-0.8 mM lactate, which corresponds to the K_M of the enzyme. These experiments were always performed by constructing enzyme laminates with pore sizes of 1 μm radii in both upper and lower membranes. It was thought that this plateau of the response was due to the saturation of LOD, which often occurs for enzymes with a low turnover rate. After this saturation, the signal plateaus and the current response is no longer dependent on the substrate concentration. It has been reported that the creation of a diffusion barrier between the sample under analysis and the enzyme layer can reduce the flux of substrate towards the enzyme, thus preventing its saturation and, with this, increase the linear range of the sensing device (Bilitewski and Turner, 2000; Bridge *et al.*, 2007; P.J. Higson *et al.*, 1993).

For this reason it was suggested that a decrease in pore size of the membranes employed in the laminate construction would create a first diffusional barrier between the lactate solution and LOD, leading to an increase in the working concentration range of the sensor and subsequently an improved linearity of the response.

Three different sets of laminates were constructed according to the protocol outlined in section 3.4.3, using polycarbonate membranes of 1 μm radii for the lower membrane and varying the upper-membrane porosity using 1, 0.1 and 0.015 μm pore radii. The objective behind this was to generate lactate-flow limitations towards the enzyme layer avoiding, however, any diffusional resistance for the transfer of H_2O_2 produced by LOD, through the lower membrane and towards the

electrode surface. Here, 6 μl of LOD solution (~830 U ml^{-1}) in 0.1 g ml^{-1} BSA and 3 μl of 5% v/v glutaraldehyde were cross-linked between two polycarbonate membranes. The constructed laminates were electrochemically interrogated following the chronoamperometry protocol, outlined in section 3.4.2, using the AuPt and Rank oxygen electrode systems as described in sections 3.4.6.2.ii and 3.4.4, respectively. A range of relatively lower lactate concentrations (0-0.8 mM) in PBS were analysed for a better appreciation of the effect of membrane porosity on substrate-flow restriction. The current outcome for each concentration was normalised by subtracting the background signal, obtained when PBS (lactate 0 mM) was initially added to allow the enzyme laminate to equilibrate.

The first part of the study was performed on the AuPt electrode system. The sensor was assessed with a range of increasing lactate solutions, from 0 to 0.8 mM. The calibration curves with normalised mean current values over the range of lactate concentrations for employed upper-membranes with different pore radii are shown in Figure 5.1. As expected, the results exhibited a decrease in current response for smaller pore sizes in the upper membrane of the laminate. Current values obtained using higher upper-membrane porosity (1 μm) were on average around 3 times higher than the ones obtained with 0.1 and 0.015 μm. With higher lactate levels, this difference in current profiles became smaller as they plateaued. This plateau in current response and lower linearity, due to enzyme saturation, was more evident for higher upper-membrane porosities (1 μm, R^2 = 0.89). However, as smaller pore sizes were employed, enzyme saturation for higher lactate concentrations diminished, reaching the current response profile almost total linearity when a membrane with 0.015 μm pore size was employed (R^2 = 0.98).

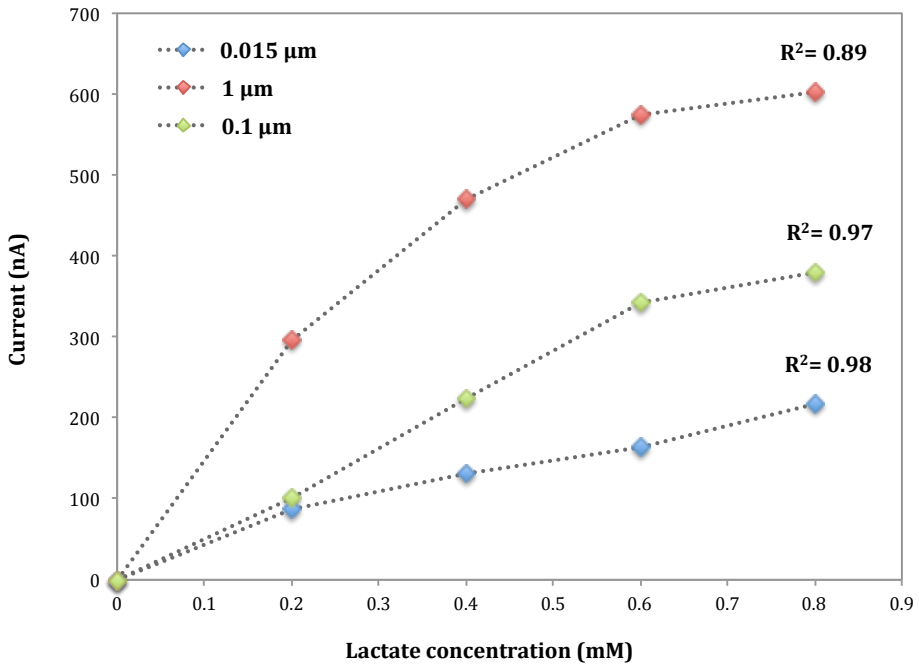

Figure 5.1. Calibration curves for LOD on the AuPt system with laminates constructed with upper-membrane porosities of 1, 0.1 and 0.015 µm at different lactate concentrations, from 0 to 0.8 mM.

Following this, current response profiles for laminates constructed with upper membranes for both the largest and smallest pore radii (1 and 0.015 µm) using the AuPt sensing system were compared with the ones using the Rank electrode cell. Here, the system was electrochemically interrogated by analysing a range of lactate solutions in PBS, from 0 to 0.8 mM, adding 5 ml of each test solution at a time to the incubation chamber. As with the previous study on the AuPt system, the current outcome for each concentration was normalised by subtracting the background signal, obtained with the initial analysis of 0 mM lactate, and represented in a chart. Results from this study showed higher current response profiles for both 1 µm (Figure 5.2a) and 0.015 µm (Figure 5.2b) on AuPt with respect to the ones obtained with the corresponding laminates in the Rank electrode cell. This response was up to 3.69 times (1 µm pore radii) and 7.17 times (0.015 µm pore radii) higher than the values obtained with the Rank electrode system for the corresponding lactate concentrations.

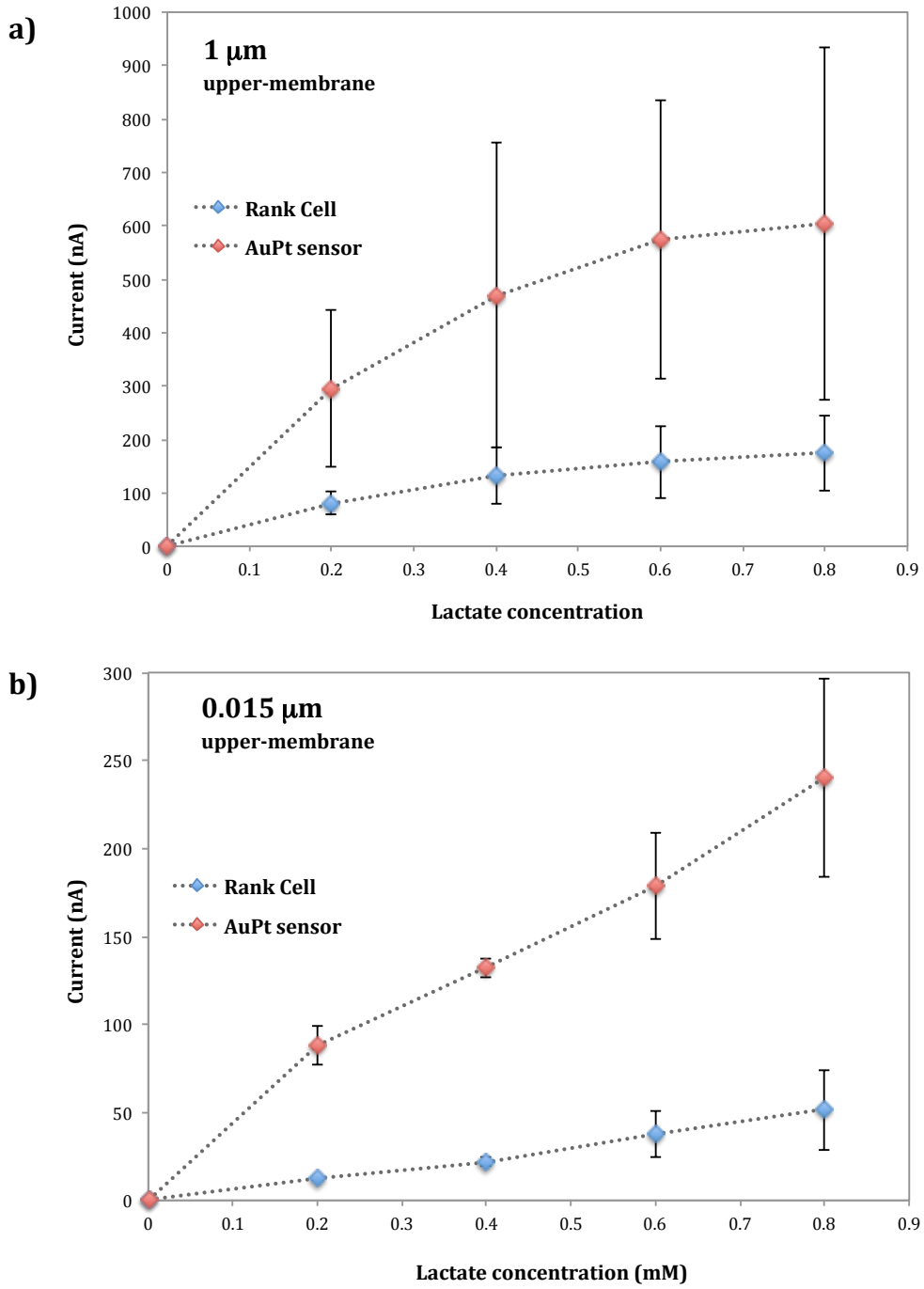

Figure 5.2. Calibration curves for LOD on AuPt and Rank electrode systems with a) 1 and b) 0.015 µm upper-membrane porosities for a range of lactate concentrations, from 0 to 0.8 mM.

Results above show a fall in current response profiles, in the range of 0-0.8 mM lactate, for the 0.015 μm upper-membrane pore radii. This is as expected, as the decrease in pore size leads to the generation of diffusional resistance to the flow of lactate towards the enzyme layer. However, this decrease in current response for smaller upper-membrane pore sizes was compensated with increased linearity, as the R^2 coefficients for each calibration curve suggest (Figure 5.1). For higher porosities, this decrease in linearity was due to the response plateauing towards 0.7-0.8 mM lactate, which corresponds with the K_M of LOD. Results obtained for the linearity of 0.1 and 0.015 μm pore radii are shown to be very similar, however using the smaller of the two, the plateauing of the response towards 0.7-0-8 mM lactate was avoided. This is due to the fact that in an enzyme system with kinetic control a linear dependence is only expected for substrate concentrations below the K_M of the enzyme. However, when diffusion control occurs, lower flow rate of substrate causes a decrease in substrate concentration in the enzyme layer, which avoids enzyme saturation and extends the linear range of the sensor. This deviation from the theoretical linear measuring range for a given enzyme system depends on the extent of the diffusion limitation (Göpel *et al.*, 2008).

In all tests, the use of an upper-membrane 0.015 μm pore radii, despite resulting in a lower current response in the calibration curve, showed an increased linearity, as the saturation of the enzyme for 0-0.8 mM lactate was avoided. Even though this range of concentrations is lower than the physiologically relevant for pressure ischemia (up to 60-70mM), results showed the potential that restricting substrate diffusion by reducing the porosity of the upper membrane could have on the obtaining of a linear response profile for higher concentrations, once other variables in the system had been optimised.

When compared to the Rank electrode system, current values for the obtained profiles using the AuPt system were up to 3.69 and 7.17 times higher for 1 μm and 0.015 μm pore radii, respectively. This increase in current response is mainly due to a higher electrode surface area in the AuPt system. However, as higher current response leads to better sensitivity, these results showed the potential that an

improved version of the new AuPt sensing system could have for the monitoring of lactate concentrations in a more sensitive manner than the standard Rank electrode system.

Despite the encouraging results obtained it was observed that, as happened with previously developed electrode systems described in Chapter 4, the experiments performed with AuPt had a lack of consistency in obtaining a working system. In a large portion of the experiments performed, exposure to lactate solutions did not generate measurable current changes with respect to the baseline. In some other experiments, despite a relatively low current response being obtained, this remained unchanged or was seen to fall for higher substrate concentrations. It was thought that the reason behind the lack of measurable response observed was a loss of enzyme over time, caused by low robustness in the cross-linking matrix, whose main function is to hold LOD in place within the laminate structure.

For this reason, it was decided that, prior to optimising the performance of the sensing system, the optimisation of the laminate construction for the obtaining of a working system in a consistent manner was a study of first importance.

The first aspect to be improved towards the obtaining of the working system was the strength of cross-linking. This depends on different operative parameters such as reaction time, cross-linker concentration, pH and temperature. According to the literature, the pH conditions employed for the cross-linking with glutaraldehyde fell in the optimum range, pH 7.0 to 9.0 (Okuda *et al.*, 1991). It has been reported that the strength of the cross-linking increases with longer incubation times (Chen *et al.*, 2013; Majumder *et al.*, 2008). Therefore, it was decided to focus the next study on the analysis of the influence of the incubation time on the strength of the cross-linking and the stability of LOD.

5.3 Cross-linking time

The first variable to be tested towards improving the consistency in the obtaining of a working system was the time allowed for the cross-linking to occur. This cross-linking time extends from the moment when the LOD/BSA solution was mixed with the glutaraldehyde dilution, to the time at which the constructed enzyme laminate, mounted on the sensor's working electrode, came into contact with the PBS solution. As mentioned in the previous section, the reason behind this study was to assess the optimum incubation time that could increase the strength of the cross-linking and robustness of the matrix, thus reducing enzyme leaching and enhancing the consistency in the obtaining of a working system. It has been previously reported that the degree of cross-linking increases with the incubation time, during which the reaction from glutaraldehyde with amino groups (mainly from lysine, Lys, residues) from LOD and BSA continues to take place (House *et al.*, 2007). Cross-linking time, like many other parameters, passes through an optimum value. However, this incubation time varies depending on many factors, such as the chosen immobilisation method, materials or substrates employed and their concentration, physical characteristics and the concentration of the enzyme to be immobilised and other experiment conditions such as pH or temperature.

Experiments performed in this study were carried out on the AuPt electrode system following the protocol outlined in section 3.4.6.2.ii. The parameters employed for the construction of the laminate were the same as the ones utilised in section 5.2. However, in this study incubation times were varied between 8 and 30 minutes and both upper and lower membranes in the laminate were of 1 μm pore radii. This pore size was chosen for this study in order to avoid any lactate diffusion restrictions due to the membrane employed and to make the results from the electrochemical characterisation of the laminate depend exclusively on the cross-linked matrix and its physical properties. The resulting system was then interrogated over a range of lactate solutions, from 0 to 0.8 mM, using the chronoamperometry protocol described in section 3.4.2.

Up to this point, enzyme laminates have been constructed with an incubation time of 8 minutes, of which 5 minutes were spent in the preparation of the laminate by applying light pressure between the membranes. The remaining 3 minutes were intended for adjusting the laminate to the right size and placing it on top of the working electrode, before finally putting the system into contact with the solution. During these last 3 minutes, the membrane was allowed to dry as the cross-linking continued to take place. The results for the current response at each lactate concentration are represented in Figure 5.3, where the values were normalised by subtracting the baseline current at lactate 0 mM and represented in a chart with the corresponding standard deviation.

With this incubation time, however, a working system was obtained only in ~16.5% of the constructed sensors, where an input of substrate generated a measurable current change with respect to the baseline and increasing for higher lactate concentrations. This indicated a low consistency in obtaining a working system with this incubation time, probably due to a weak cross-linking that led, in most of the cases, to the leaching of part of the enzyme out of the laminate. In addition to this, the current profiles obtained with each of the working systems had a very high variability (Relative Standard Error coefficient, RSD, was obtained in the range 50-60%).

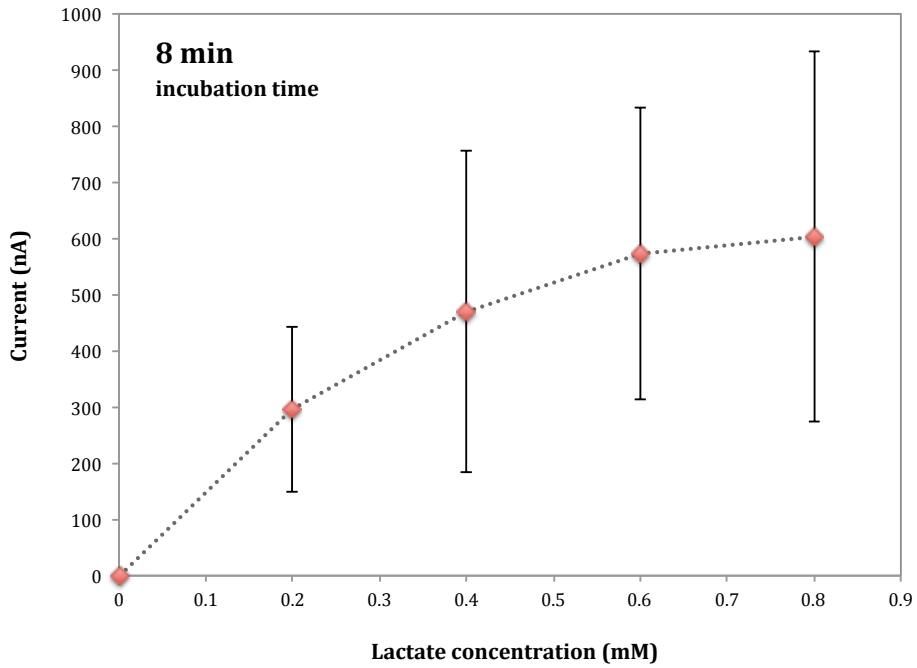

Figure 5.3. Calibration curve for LOD on the AuPt electrode system with an incubation time of 8 minutes for a range of lactate concentrations, from 0 to 0.8 mM.

Given these results, it was considered that a stronger cross-linking was needed to obtain a more robust enzyme laminate where LOD could be held in place and prevent its leaching over time. As a proof of concept of the influence that incubation time had on obtaining a more robust enzyme laminate, a new set of experiments were designed with an incubation time of 30 minutes before placing the system in contact with the solution. With the new incubation time, membranes polarised with a baseline current of a higher value than the usual range for the employed electrode system (~7000 nA, compared to ~100 nA) (Figure 5.4). Moreover, when the sensor came into contact with the first lactate solution, no current change with respect to the baseline current value was observed. This occurred with all sensors where the laminate was prepared under these conditions. This was an indication of the excessive robustness of the membrane that, despite probably hindering the leaching of LOD, was blocking the flow of lactate molecules into the enzyme layer due to a reduced number of cavities in the matrix. Another possible explanation for this lack of current response change was that the cross-linking time had exceeded the optimum value required to recover

the maximum activity of the enzyme. When this optimum cross-linking time is exceeded, the flexibility of the enzyme can become too restricted, compromising its activity. Due to this excessive rigidification of the enzyme, steric hindrance can also occur, which prevents the substrate from reaching the active site of the enzyme (Reshmi and Sugunan, 2013) and therefore no substrate catalysis takes place. These results suggested that the optimum incubation time could involve a compromise between the obtaining of an efficient cross-linking and the need to preserve the enzymatic activity and stability.

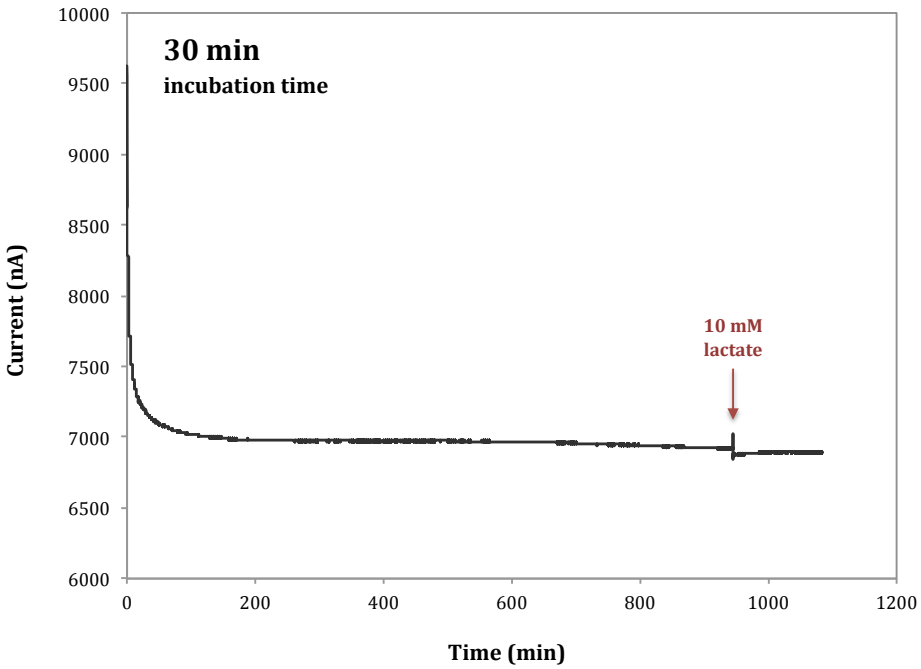

Figure 5.4. Example of steady-state current response obtained using LOD on the AuPt electrode system and an incubation time of 30 minutes. A dilution of lactate in PBS at a concentration of 10 mM was analysed.

The arrow indicates the moment at which the PBS solution was extracted from the beaker and the lactate test solution was introduced.

Due to the fact that a 30-minute incubation showed to exceed, by far, the optimum cross-linking time value, it was decided to reduce this by half, to 15 minutes. A new set of membranes were thus constructed with this new incubation time and analysed to assess its effects in obtaining a robust cross-linking, yet still

able to preserve the enzyme activity and allow the flow of substrate across the laminate. With the new incubation time, the membranes polarised with a baseline current of ~100 nA, which corresponds to the usual value for the present electrode system. However, only one out of five sensors with membranes constructed with this incubation time exhibited a change in current response for higher concentrations of lactate. The current outcome for each lactate concentration was normalised by subtracting the background signal obtained with PBS only and the values were represented in a chart (Figure 5.5). However, this time it was observed that in three of the remaining sensors, despite not showing a current response change for low lactate concentrations (0-0.8 mM), a change in this was seen at higher (5 mM) lactate concentrations. This suggested that the incubation time was still too high, therefore hindering the flow of substrate when this was present at low concentrations.

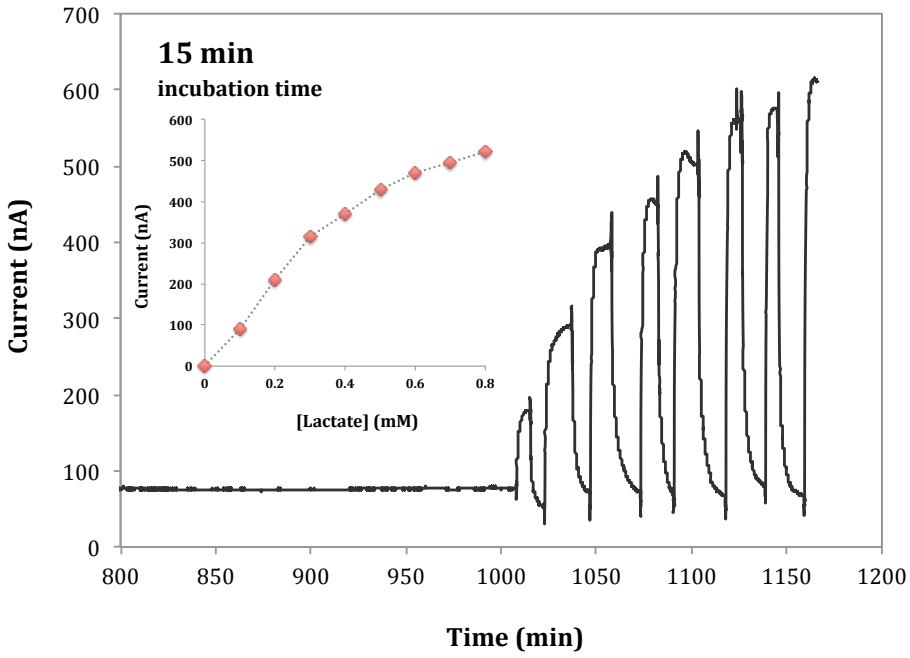

Figure 5.5. Example of steady-state current response and calibration curve obtained using LOD on the AuPt electrode system and an incubation time of 15 minutes for a range of lactate concentrations, from 0 to 0.8 mM.

After these results it was decided that the incubation time still had to be reduced again in order to obtain a sufficient cross-linking to hold the enzyme in the laminate structure, while ensuring a maximum number of cavities within the cross-linked structure to allow the flow of substrate across the laminate into the enzyme layer. It was therefore decided to reduce the cross-linking time by 3 minutes from that previously analysed and let the membranes incubate for 12 minutes. The results for the current response at each lactate concentration are represented in Figure 5.6, where the values were normalised by subtracting the baseline current at lactate 0 mM and represented in a chart with the corresponding standard deviation. With this new incubation time, >60% of the analysed sensors show a measurable current response, which increased with higher lactate concentrations up to 0.8 mM, where the response profile plateaued as the K_M of LOD was reached. These results indicated that a better consistency was reached in the obtaining of a working system with respect to other incubation times previously tested. The reproducibility between experiments was also shown to be higher than when other incubation times were employed, as the RSD this time varied in the range of 3-19%.

The results obtained in this part of the study show that the cross-linking time employed in the construction of the enzyme laminate plays an important role in the consistency of obtaining a working system. Very short incubation times resulted in inadequate cross-linking, allowing the leaching of the enzyme into the solution and/or its inactivation due to a poor rigidification. However, prolonged cross-linking times led to an excessive restriction of the enzyme flexibility, causing its inactivation and also hindering the flow of solution through the laminate system. Therefore, an optimum incubation time, which involved a compromise situation between the robustness of the cross-linking and the stability of the enzyme, had to be determined. Laminates prepared with an incubation time of 12 minutes showed the best results and a consistency in the obtaining of a working system was increased by up to ~60%. However, other variables would need to be

tested and optimised in order to increase the quality of the laminate preparation method.

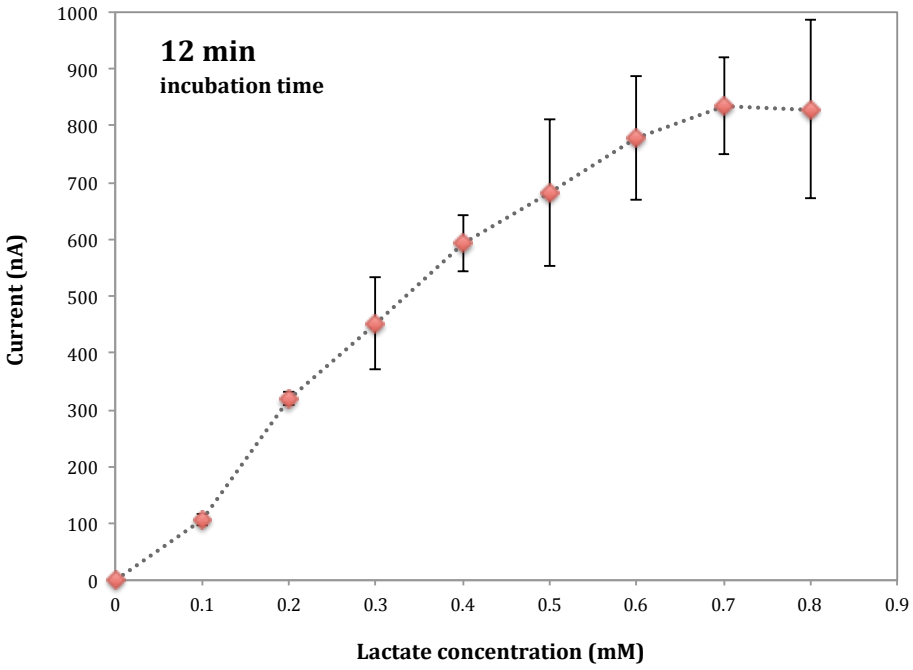

Figure 5.6. Calibration curve for LOD on the AuPt electrode system with an incubation time of 12 minutes for a range of lactate concentrations, from 0 to 0.8 mM.

In the different experiments performed in this section to assess the optimum cross-linking time, it was observed that in most of the sensors where a current response difference for higher concentrations of lactate was obtained, fresh dilutions of glutaraldehyde had been prepared. Therefore, it was thought that a possible deterioration of diluted glutaraldehyde over time could be having an important effect in optimising cross-linking and, hence, a consistent laminate preparation method. It was therefore decided to analyse the effect of fresh dilutions of glutaraldehyde in obtaining a better cross-linking.

5.4 Glutaraldehyde

Glutaraldehyde was assessed as one of the variables for obtaining an optimum and consistent laminate preparation method. Two parameters were studied in this part of the study: the effect of using fresh glutaraldehyde dilutions and the concentration of glutaraldehyde in obtaining a consistently robust laminate. The reason for studying the effect of fresh glutaraldehyde dilutions on the quality of the cross-linking comes from the results obtained from the experiments described in the previous section, which showed that the majority of working systems obtained had been prepared with fresh glutaraldehyde dilutions. Therefore, it was thought that this could be a key aspect in obtaining a working laminate system.

The main reason for the study of the influence of glutaraldehyde concentration came from the results obtained from the analysis of the influence of fresh glutaraldehyde dilutions, which suggested that a higher glutaraldehyde content could increase the robustness of the cross-linking, thus improving the quality of the laminate construction and its electrochemical properties.

The experiments conducted for this part of the study were performed on the AuPt electrode system according to the protocol outlined in section 3.4.6.1.ii. Enzyme laminates were prepared for both LOD and GOD as described in section 3.4.3. Here, the mix was allowed to cross-link for 12 minutes as this incubation time showed the best results in terms of consistency in obtaining a working system. The resulting systems were electrochemically interrogated following the chronoamperometry protocol, outlined in section 3.4.2. The baseline current obtained after the polarisation step was subtracted to the current responses in order to normalise their values.

5.4.1 Fresh dilutions

A new set of enzyme laminates were constructed as described in section 3.4.3. Here, 6 μl of LOD solution (~830 U ml^{-1}) in 0.1 g ml^{-1} BSA and 3 μl of 5% v/v glutaraldehyde, freshly prepared for each experiment, were cross-linked between two polycarbonate membranes with an incubation time of 12 minutes.

Results obtained with this new variation in the preparation of the laminates showed that a working system was obtained in >90% of the experiments. This improvement in consistency concluded that the preparation of fresh dilutions of glutaraldehyde on the construction of every laminate was a key factor in obtaining a more robust cross-linking procedure. This indicated the possibility that the past 5% v/v glutaraldehyde dilutions prepared in PBS and kept in the fridge over 4-5 days of experiments could have deteriorated over time, affecting its ability to cross-link efficiently and, thus, having a negative effect on the robustness of the laminates.

Throughout the experiments performed up to this point, it was observed that when preparing the cross-linking mixture of glutaraldehyde, BSA and LOD, this was still too fluid when placing it on top of the lower (inner) membrane during the laminate preparation and this could be due to the fact that the cross-linking was at a very early stage in its timeline. This fluidity allowed the seepage of part of the mixture out of the laminate when both membranes were pressed together after placing the upper (outer) one. It is also believed that when mixing the glutaraldehyde, BSA and LOD together by agitating the solution prior to placing the mixture on the lower membrane, even though this mixing was done carefully, could generate microscopic bubbles. These bubbles could be hindering the obtaining of a robust cross-link and also possibly generating big cavities in the structure that allowed the leaching of enzyme into the solution. For these two reasons it was thought that an alternative method for the construction of the laminate, to avoid the formation of microscopic bubbles and the seepage of the mixture out of the system, needed to be developed.

5.4.1.1 Use of fresh glutaraldehyde dilutions in the introduction of a new laminate preparation method.

The reason for the study described in this section lies in the need of a better method for the preparation of the enzyme laminate. As previously mentioned, it was thought that part of the reason why a consistent working system was not being achieved was the fact that the cross-linking mixture was still too 'fluid' when both membranes were pressed together, causing seepage out of the laminate; and because of the possibility that microscopic bubbles were hindering a proper cross-linking. For these two reasons, it was thought that a new laminate preparation method was required. In this new approach, the mixture had to be mixed before being placed on top of the lower membrane in such way that the formation of microscopic bubbles would be avoided. Since it was assumed that these were formed from up and down pipetting, it was thought that this situation could be avoided by slowly stirring the mix before placing it on top of the membrane. Also, in this new preparation method the mixture needed to be allowed to cross-link for a certain period of time before placing the upper membrane on top of it. This would ensure a certain viscosity due to a higher cross-linking, avoiding a high spreading and seepage of the mixture out of the laminate when compressed between both membranes.

Several tests were performed to determine the best times to transfer the glutaraldehyde/BSA/LOD mixture on top of the lower membrane and the placing of the upper membrane. These times had to ensure, firstly, a proper mixing of the components involved in the cross-linking reaction and their transfer on top of the lower membrane before the mixture was too viscous due to an advanced cross-linking, hindering its transfer by pipetting. Secondly, an adequate time had to be studied for the cross-linking of the mixture to take place to an extent where its seepage when compressed between both membranes was avoided. The times chosen for each step of this new method added up to a total of 12 minutes, since this showed to be the most adequate time for obtaining a working laminate system (section 5.3.).

The enzyme laminates were prepared with the same parameters as those utilised in section 5.4.1. Here, the times chosen for each step of the new laminate preparation method were the following: 1 minute for stirring the mix, 1 minute 40 seconds left to cross-link on top of the lower membrane, 5 minutes compressed between both membranes and then allowed to dry for 4 minutes without applying any pressure. As previously stated, the resulting laminates were electrochemically interrogated on the AuPt electrode system. Different concentrations of lactate in PBS were analysed in this experiment, from 0 to 60 mM, by adding 15 ml of the test solution to the 25-ml beaker where the sensor had been placed. The results for the current response obtained for each of these lactate concentrations were normalised by subtracting the baseline current at lactate 0 mM, represented in a chart with the corresponding standard deviation and the RSD coefficient (Figure 5.7).

Results obtained from the new set of laminates prepared using this new method showed that a change in current response was obtained for increasing amounts of lactate concentrations in all of the constructed laminates. This achievement allowed the research to move one step forward towards the study of the optimisation of other characteristics related to the performance of the working system, such as reproducibility, concentration range and linearity of the response.

At this stage, the working concentration range of the sensor had been increased, through changes in the incubation time, decreasing the membrane pore-size and the introduction of a new way of mixing and preparing the laminate, from the K_M for LOD (0.8 mM) up to 30-40 mM (Figure 5.7a). However, this range still had to be extended up to physiologically relevant concentrations for pressure ischemic conditions (up to 60-70 mM). Also, the reproducibility of the sensor still had to be improved, since the current responses obtained with different sensors still had variability, calculated with the RSD, of up to 43% (Figure 5.7b, c.). Results also showed that the linearity of the current response profile for the range of lactate concentrations also had to be increased in order to improve the sensitivity of the sensor. In order to achieve all of these, other variables would have to be considered and analysed.

a)

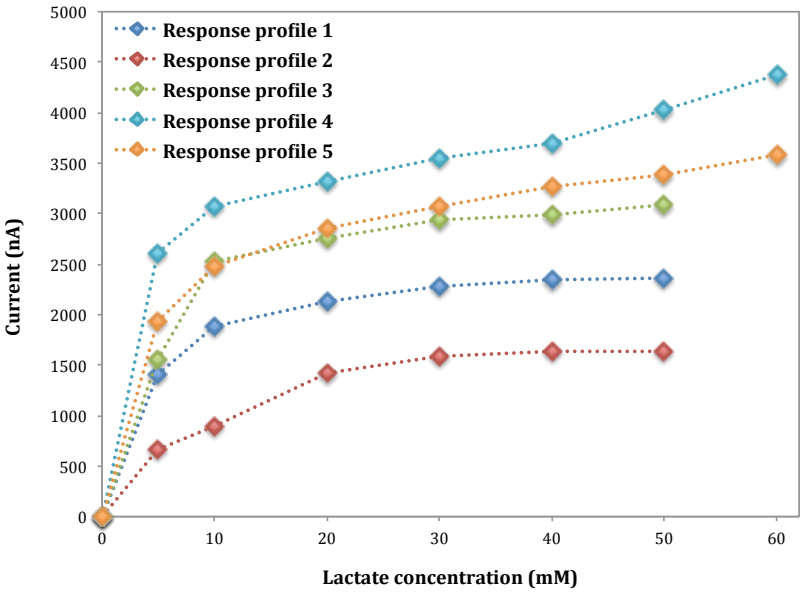

b)

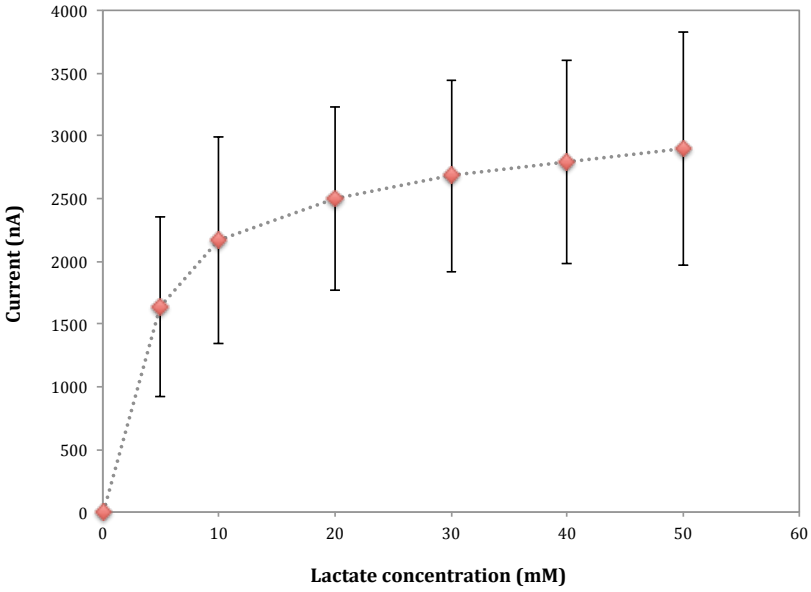

c)

	Current response (nA)		
[Lactate] (mM)	**Mean**	**S. Dev.**	**RSD (%)**
0	0.00	0.00	0.00
5	1636.08	714.40	43.67
10	2170.48	827.00	38.10
20	2496.48	730.74	29.27
30	2682.48	766.44	28.57
40	2788.48	811.13	29.09
50	2896.48	927.45	32.02
60	3985.70	559.60	14.04

Figure 5.7. Response curves and calibration curve for LOD on the AuPt electrode system with the use of fresh glutaraldehyde dilutions and a new laminate preparation method (1' stirring, 1'40'' left to cross-link on top of the lower membrane, 5' compressed between membranes and left to dry for 4'). A range of lactate concentrations, from 0 to 50 mM were analysed.

During the performance of the experiments using the new mixing and preparation method for the enzyme laminate, results showed that two of the experiments (Figure 5.7a, Response profiles 4 and 5) exhibited a more extended concentration range than the others (up to 70 mM). Current values obtained for these two sensing systems were also higher than those obtained with other experiments. It was observed during the preparation of these two enzyme laminates, which took place the same day, that the cross-linking reaction occurred much faster than in the other experiments. As the only component that was different from the rest of the experiments/days was the glutaraldehyde dilution, which was freshly prepared every day, it was thought that this could be the cause of the variation observed. It has been reported that higher cross-linker (i.e. glutaraldehyde) concentrations result in more efficient and robust cross-linking, in shorter incubation times (Migneault *et al.*, 2004; Reshmi and Sugunan, 2013). Therefore, the effect of a higher concentration of cross-linker on the obtaining of a sensing system with an improved linearity, reproducibility and extended concentration range was studied.

5.4.1.2 Use of GOD system with fresh glutaraldehyde dilutions and new laminate preparation method.

When analysing the obtained results (Figure 5.7c), it was thought that one possible cause for the low reproducibility in the current response between different sensing systems was the enzyme activity. Lactate oxidase is known as an unstable enzyme in contrast with other more robust oxidases, such as GOD, which has been reported as being very stable under a range of operating conditions (Wei *et al.*, 2003; Lillis *et al.*, 2000; Minagawa *et al.*, 1998). Therefore, although an optimum cross-linking can increase the stability of an enzyme with respect to when in solution, enzymes can be very sensitive proteins and easily lose their activity to small pH or temperature changes, or even to small variations in the cross-linking microenvironment such as the concentrations of its components such as glutaraldehyde. For this reason, it was decided to test the developed laminate

preparation method with a more robust oxidase enzyme (i.e. GOD) to assess whether the lack of reproducibility in the sensing system was due exclusively to the laminate preparation method or if the enzyme used (LOD) and its catalytic properties and stability also played an important role in the performance of the sensor.

Enzyme laminates were therefore constructed with enzyme GOD as described in section 3.4.3. Here, 6 μl of GOD solution (~500 U ml^{-1}) in 0.1 g ml^{-1} BSA and 3 μl of 5% v/v glutaraldehyde, freshly prepared for each experiment, were cross-linked between two polycarbonate membranes with the same incubation times as described in section 5.4.1.1. A range of glucose dilutions from 0 to 20 mM in sodium acetate buffer were analysed as described in the previous section. The current response for each concentration was normalised by subtracting the baseline current value and represented in a chart with the corresponding standard deviation and the RSD was calculated (Figure 5.8).

Results obtained with the recently optimised laminate construction method based on GOD enzyme showed a much better reproducibility for the concentrations tested (0-20 mM glucose) than when LOD was employed (Figure 5.7b,c.). The variability, given by the RSD, was tightened from 43.7 to 9.4% for 5 mM substrate dilutions, from 38.1 to 10.8% for 10 mM and from 29.3 to 18.2% for 20 mM (Figure 5.7c and Figure 5.8c). Moreover, the current response values obtained for different glucose concentrations were 2-2.5 times higher than the corresponding ones for lactate when the LOD system was under analysis. The current profile obtained with GOD for the different concentrations of glucose (0-20 mM) exhibited a more linear behaviour than that with LOD for the corresponding lactate dilutions (Figure 5.7b).

In the analysis of the results it was also observed that the current values within the profiles obtained with the experiments Exp 1 and 2, performed on the same day, were more similar to each other than to the values in Exp 3 and 4, which also took place on the same day, and vice versa (Figure 5.8a).

a)

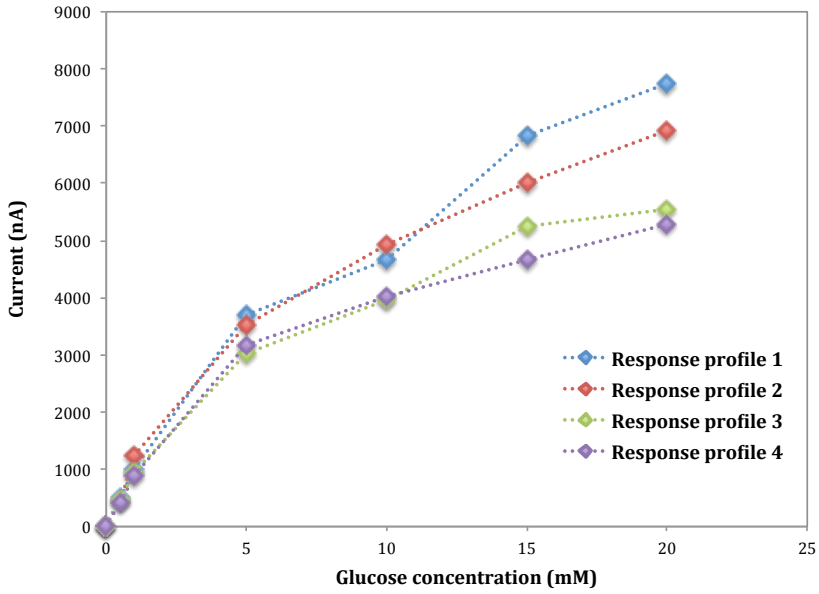

b)

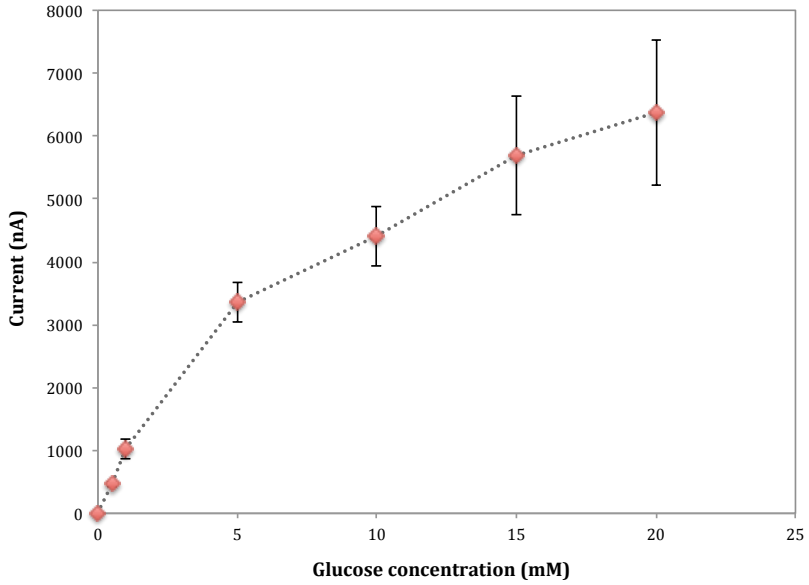

c)

	Current response (nA)		
[Glucose] (mM)	**Mean**	**S. Dev.**	**RSD (%)**
0	0	0.00	0.00
0.5	463.5	38.69	8.35
1	1019.25	150.74	14.79
5	3359.25	317.23	9.44
10	4401.75	478.97	10.88
15	5691.75	941.43	16.54
20	6374.25	1163.16	18.25

Figure 5.8. Response curves and calibration curve for GOD on the AuPt electrode system with the use of fresh glutaraldehyde dilutions and a new laminate preparation method (1' stirring, 1'40'' left to cross-link on top of the lower membrane, 5' compressed between membranes and left to dry for 4'). A range of glucose concentrations, from 0 to 20 mM were analysed.

The results obtained in this study with the enzyme GOD and the new laminate preparation method led to two conclusions. Firstly, a better reproducibility and linear response with higher current values and thus better sensitivity were observed with respect to the LOD system under the same preparation method (Figure 5.9). This would be partially due to GOD being a more stable and robust enzyme with a higher K_M for the catalysis of glucose than that of LOD for its substrate (i.e. lactate). This indicated that, in effect, the variability in the response obtained with the sensing system was not due solely to the preparation method of the laminate, but the enzyme system used (i.e. LOD) also played a very important part in the reproducibility of the sensing system. Therefore, the enzyme employed and its catalytic properties (activity, stability, etc.) while immobilised in a cross-linked matrix also play an important role in the sensitivity of the detection.

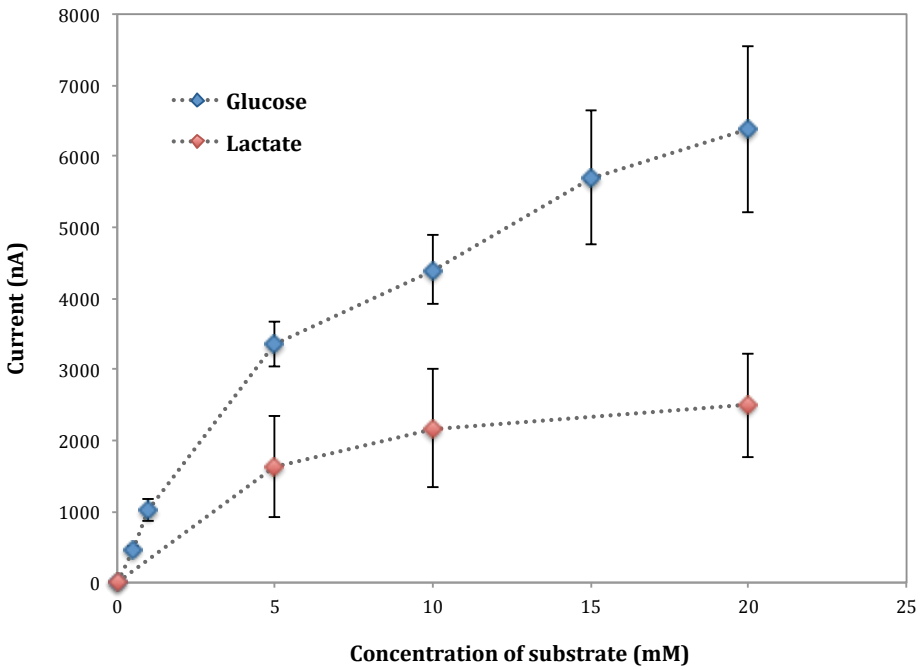

Figure 5.9. Comparison of calibration curves for LOD and GOD on the AuPt electrode system, for a range of lactate and glucose concentrations, from 0 to 20 mM, with the use of fresh glutaraldehyde dilutions and a new laminate preparation method (1' stirring, 1'40'' left to cross-link on top of the lower membrane, 5' compressed between membranes and left to dry for 4').

As had been observed in previous results with two of the sensors using LOD as the enzyme system (Figure 5.7a, Response profiles 4 and 5), in this case it was also shown that experiments performed with GOD on the same day had more similar current response profiles to each other than to experiments undertaken on different days (Figure 5.8a). Furthermore, experiments performed on the first day (Response profiles 1 and 2) exhibited a response profile with higher linearity and current values than experiments performed on the second day (Response profiles 3 and 4). It was again hypothesised that the main reason for this to happen was a slight variation in the concentration between glutaraldehyde dilutions, freshly prepared each day, which could be having an important effect in the robustness of the cross-link and/or the stability of the enzyme. Therefore, the second interesting hypothesis that the described experiments with GOD, together with the ones with LOD, led to was the observation that higher concentrations of glutaraldehyde in the cross-linking mixture were improving the quality of the cross-link and the electrochemical properties of the constructed laminate, rather than being detrimental for the immobilised enzyme.

For all aforementioned reasons, it was decided that two new studies should be performed towards the optimisation of the laminate properties: the influence of glutaraldehyde concentration and the improvement of the stability and activity of LOD in the laminate.

5.4.2 Concentration of glutaraldehyde as a cross-linking agent

The next part of the study considered the effect of the glutaraldehyde content in the mixture, on the physical and electrochemical properties of the enzyme laminate. As it was previously mentioned, experiments showed that an increase in glutaraldehyde concentration increased the working concentration range, the linearity of the response and its reproducibility. This indicated the possibility that an increase in glutaraldehyde content could lead to higher robustness of the cross-

linked matrix, retaining the enzyme in the laminate structure while preserving its activity.

The amount of cross-linker (i.e. glutaraldehyde) is a key parameter in the construction of a working enzyme-based sensing system, since it has an important influence on the enzyme activity and operational stability in a similar way to the incubation time (Sheldon, 2011), described in section 5.3. As for the cross-linking time, the glutaraldehyde to LOD/BSA ratio also has an optimum point. The activity and stability of the enzyme can increase for higher concentrations of cross-linker up to a maximum value, after which higher levels can be detrimental to the enzyme. Low concentrations of glutaraldehyde produce an insufficient cross-linking and a weak matrix, which results in enzyme leaching and loss of current response over time. On the contrary, high amounts of glutaraldehyde produce an excessive cross-linking and rigidification of the enzyme, which loses its flexibility and, thus, its activity (Matijošytė *et al.*, 2010). In addition to higher incubation times, high cross-linker concentrations can create steric hindrance, preventing the substrate from reaching the active site of the enzyme (Majumder *et al.*, 2008). Therefore, the optimum amount of cross-linker is reached when a sufficiently robust matrix is created with enough cavities to avoid excessive mass transfer limitations, while the enzyme preserves its activity and stability. However, this optimum value of cross-linker will depend on the enzyme employed, as the number of free amino groups (mainly from Lys residues) on their surface available to interact with the cross-linker varies from enzyme to enzyme (Sheldon, 2011). In addition to this, in the present work the concentration of BSA in the mixture would also have an important effect on the optimum glutaraldehyde concentration, since BSA is used as a protein matrix to improve the immobilisation and enzyme entrapment, due to its high content of Lys residues.

For all the aforementioned reasons, it was decided to study the effect of a higher concentration of glutaraldehyde on the physical, catalytic and electrochemical properties of the enzyme laminate system. With this, it was intended to improve the reproducibility and the linearity of the response, with an increased concentration working range. For this study, enzyme laminates were

prepared as described in section 3.4.3. As a proof of principle, the amount of glutaraldehyde was increased from 5 to 10% v/v, while keeping constant the concentrations of LOD (~830 U ml^{-1}) and BSA (0.1 g ml^{-1}). Due to the mixture cross-linking faster than in previous experiments with the addition of higher glutaraldehyde content, the preparation method for the enzyme laminate was minimally changed by shortening the stirring time from 1 minute to 30 seconds and extending the time for the mix to cross-link on top of the lower membrane from 1 minute 40 seconds to 2 minutes 30 seconds. These precise times ensured a proper transfer of the cross-linking components after their mixing before the mixture was too viscous and allowed keeping the times for which the mixture was compressed constant between both membranes and subsequently allowed to dry.

A range of lactate concentrations in PBS, from 0 to 60 mM, were analysed on the AuPt electrode system using the chronoamperometry protocol described in section 3.4.2. The obtained current values for each concentration were normalised as explained in previous sections and are shown with their corresponding standard deviation and their RSD coefficient was calculated (Figure 5.10).

Results obtained in this study indicated that the current response profile plateaued at lactate concentrations between 50-60 mM (Figure 5.10a). This implied an increase in the sensor's working concentration range with respect to previous laminates constructed with 5% v/v glutaraldehyde, where the response plateaued between 30-40 mM (Figure 5.7). However, the current values in the obtained calibration curve with 10% v/v glutaraldehyde were much lower (up to an 86% decrease in average current value for each concentration) than those with 5% v/v glutaraldehyde for the corresponding lactate concentrations (Figure 5.10b).

a)

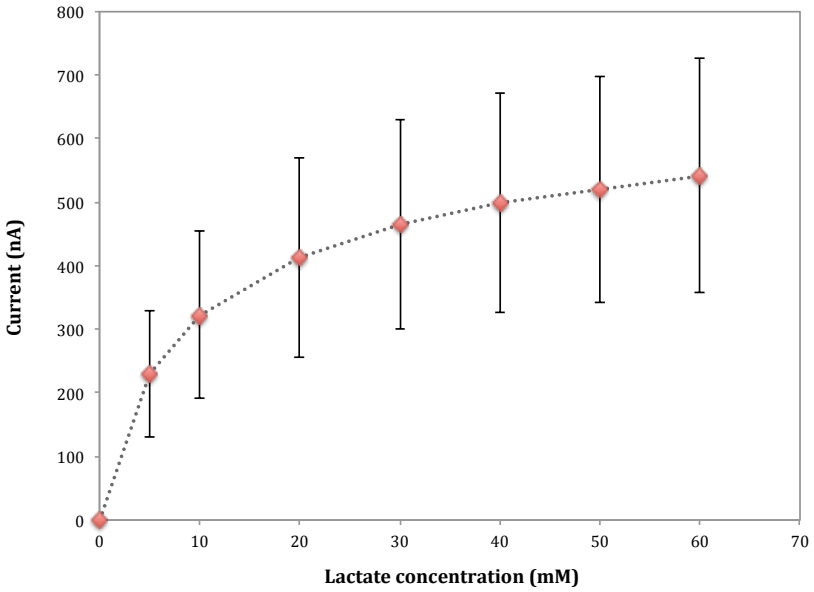

b)

	Current response (nA)		
[Lactate] (mM)	**Mean**	**S. Dev.**	**RSD (%)**
0	0	0.00	0.00
5	229.8	99.88	43.47
10	322.8	131.08	40.61
20	412.2	156.44	37.95
30	465.2	164.49	35.36
40	498.8	172.90	34.66
50	520.6	178.24	34.24
60	542	183.87	33.92

Figure 5.10. Calibration curve for LOD on the AuPt electrode system with the use of 10% v/v glutaraldehyde for a range of lactate concentrations from 0 to 60 mM.

The extended working concentration range of the sensor achieved with the constructed laminates using 10% v/v glutaraldehyde indicated that, in accordance with published literature, higher glutaraldehyde content led to an increased degree of cross-linking and robustness of the laminate, obtaining a better immobilisation of the enzyme in the matrix. However, the decrease in current response was an important aspect to be considered, since it could have a negative effect in the sensor's sensitivity of detection. This obtaining of a lower current response when using a higher glutaraldehyde content led to two possible explanations. The first hypothesis suggested that the new amount of glutaraldehyde could have increased, in excess, the robustness of the cross-linking matrix, containing low amounts of

cavities in its structure, which would produce excessive internal mass transfer limitations and, thus, reduce the available substrate to be oxidised by LOD.

The second possible explanation for the lower current response obtained was that higher amounts of glutaraldehyde were decreasing the relative concentration of LOD (and BSA) to the cross-linker, leading to an increase in the amount of reactions taking place between glutaraldehyde and more Lys amino groups, not only from BSA molecules but also from LOD. This would enhance the probability of glutaraldehyde reacting with Lys residues crucial for the activity of LOD, partially inactivating the enzyme.

Since 10% v/v glutaraldehyde led to an increase in the linearity of the response with respect to when lower concentrations were employed, it was decided to leave this factor constant and consider other variables that could increase the current response values and the reproducibility of the sensing system. For these reasons, it was decided to test the influence of the concentration of LOD in obtaining an improved working system with higher reproducibility and current response values.

5.5 Lactate oxidase

The next part of the study focused on the study of LOD and its optimum relative concentration to glutaraldehyde and BSA in the preparation of the enzyme laminate. The aim of the study was to obtain higher current response values than when 10% v/v glutaraldehyde was employed, thus increasing the reproducibility/sensitivity of the sensor.

The main reason for considering LOD as one of the variables to analyse in the system was because this enzyme is the core of the recognition system and plays the main role in obtaining a working sensing device, determining its shelf life and operational stability. It was expected that higher enzyme content would increase the current response signal for the range of concentrations analysed, with respect to when only 10% v/v glutaraldehyde was employed (section 5.4.2). The second

part of the study focused on the research of an alternative way of preparing the LOD/BSA mix to improve the homogenisation of the enzyme in the solution, thus increasing the reproducibility of the system.

5.5.1 Concentration of lactate oxidase

The first part in the study of LOD as a variable focused on the concentration of the enzyme in the cross-linking mixture and its influence in the obtaining of a working system with higher current response values. In the previous study (section 5.4.2) it was concluded that, while higher glutaraldehyde content led to a more robust matrix that kept the enzyme in-situ, this could also be partially inactivating the enzyme. It has been reported that the nature of an enzyme, particularly its content in Lys residues, has an effect on its water-insolubilisation via cross-linking with glutaraldehyde (Reshmi and Sugunan, 2013; Migneault *et al.*, 2004). In order to achieve this insolubilisation, the ratio between enzyme and glutaraldehyde (and in this study, also BSA) must be carefully studied, as the content in accessible Lys residues varies from enzyme to enzyme (Sheldon, 2011). If the concentration of enzyme in the mixture is low, this will increase the probability of glutaraldehyde reacting with several Lys residues from the same molecule. This, in turn, will enhance the probability of intra-molecular cross-linking in the enzyme and also the reaction between glutaraldehyde and Lys residues from the active site, crucial for its activity (Barbosa *et al.*, 2013; Sheldon, 2007). In both cases, this would lead to a partial or complete inactivation of the enzyme. However, due to the fact that the optimum immobilisation of a certain enzyme is not only dependent on its relative concentration to the cross-linker but also on a delicate balance of factors, the appropriate conditions are often determined by trial and error experiments.

It has also been reported that an increase in the amount of immobilised enzyme also improves the signal height and the stability of the sensor (Gorton, 2005). This is due to the fact that for relatively high substrate concentrations, the

enzyme turnover rate (enzyme kinetics) is the limiting factor of the signal produced. The turnover rate of an enzyme depends on its particular turnover number, which is defined as the maximum number of reactions that the active site of an enzyme can catalyse per unit of time under optimum conditions (saturated enzyme). However, when a sufficient enzyme loading is achieved, substrate molecules reaching the enzyme layer within the laminate will be almost instantaneously converted and, then, the signal produced by the sensor is limited only by the diffusion rate of the substrate to the enzyme layer. At this level of high enzyme loading, the enzyme activity is not a limiting factor for the signal recorded and, thus, this activity can decrease through denaturation or blocking of the active site without it affecting the signal height, thus keeping a high apparent stability (Gorton, 2005). Therefore, it is a key factor to have a good immobilisation method that allows for increasing the amount of enzyme in the laminate, as this will improve the sensitivity and the stability of the sensor.

For these reasons, it was decided to study the effect of higher LOD content in the laminate on the obtaining an optimised working system, whilst preserving the robustness of the cross-linking matrix obtained with 10% v/v glutaraldehyde (section 5.4.2). It was expected that, on one hand, a higher concentration of LOD, and thus, higher content of total protein in the mixture, would increase the amount of free Lys residues available for cross-linking, reducing the probability of residues in the active site of LOD molecules reacting with glutaraldehyde. This would increase the amount of active immobilised enzyme in the laminate. Conversely, it was expected that an increase in LOD loading would increase the lactate turnover rate and the signal response.

As a proof of principle to study the effect of a higher amount of enzyme on the enhancement of the current response signal, a new set of enzyme laminates were prepared, according to the protocol outlined in section 3.4.3., increasing the enzyme content from ~830 (5 U per laminate) to ~1,667 U ml^{-1} LOD (10 U per laminate), doubling with this the concentration of enzyme previously employed. The rest of parameters used in the preparation of the membrane were kept constant with respect to the ones described in section 5.4.2. The concentration of

glutaraldehyde was also maintained at 10% v/v as it led to an improved immobilisation, as results in the previous section showed (section 5.4.2.).

A range of lactate concentrations, from 0 to 70 mM, were analysed on the AuPt electrode system using the chronoamperometry protocol outlined in section 3.4.2. The normalised current response for each concentration was represented in a chart with the corresponding standard deviations and the RSD coefficients were calculated (Figure 5.11).

The main aspect observed from the results was a prominent increase in the current values from the response profile obtained for the lactate concentrations analysed (0-70 mM), being from 7.7 to 9.6 times higher with respect to the ones obtained in the last study (where ~830 U ml^{-1} LOD and 10% v/v glutaraldehyde were employed in the preparation of the enzyme laminate). Moreover, the obtained current values in the response profile were the largest obtained this far. The results also showed a decrease in the variability (26.5-32.5% RSD), with respect to when a concentration of 5 U LOD/laminate was employed (33.9-43.5% RSD), entailing an increase in reproducibility in the range of 16.3-26.2%. The linearity of the response was maintained with respect to the one obtained with 5 U LOD/laminate and 10% v/v glutaraldehyde, where the current response profile plateaued between lactate concentrations of 50-60 mM.

a)

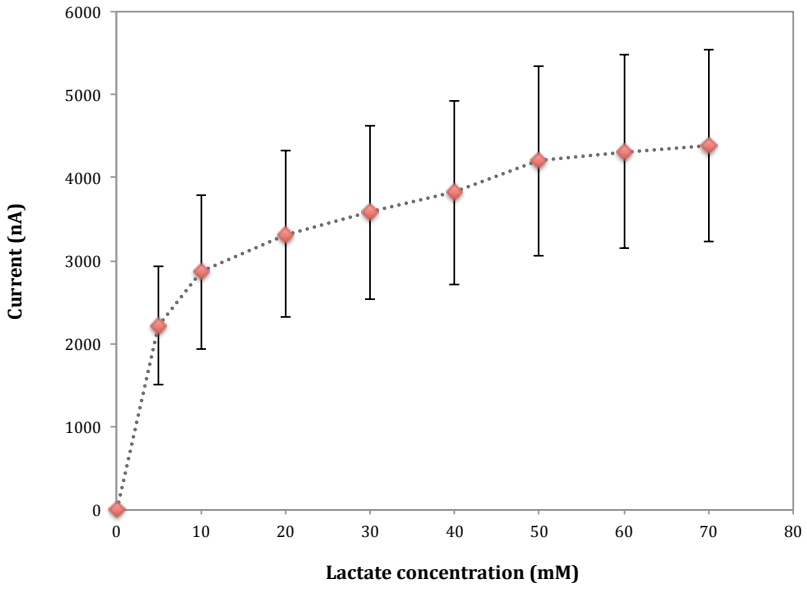

b)

	Current response (nA)		
[Lactate] (mM)	**Mean**	**S. Dev.**	**RSD (%)**
0	0.00	0.00	0.00
5	2220.93	712.52	32.08
10	2865.93	931.64	32.51
20	3320.93	997.89	30.05
30	3584.27	1046.97	29.21
40	3819.27	1107.91	29.01
50	4197.84	1137.32	27.09
60	4309.84	1164.28	27.01
70	4383.84	1161.29	26.49

Figure 5.11. Calibration curve for LOD on the AuPt electrode system with the use of 1,667 U ml^{-1} LOD for a range of lactate concentrations from 0 to 70 mM.

As expected, the use of a higher LOD concentration of 10 U/laminate brought about an increase in current values from the response profile with respect to when 5 U LOD were used (Figure 5.12). This indicated that the increase in glutaraldehyde content from 5 to 10% v/v with 5 U LOD (section 5.4.2.) was, in fact, partially inactivating the enzyme due to a decrease in total protein:glutaraldehyde ratio, thus increasing the probability of the cross-linker reacting with amino groups from Lys residues in the active site of the enzyme molecules. However, when a higher content of enzyme (protein) was added to the mixture, the amount of Lys residues from the active site of the enzyme reacting with glutaraldehyde decreased, probably due to the fact that these Lys residues,

essential for the enzyme's activity, were less accessible than the ones on the surface. This decrease in the amount of Lys residues from the active site of the enzyme reacting with glutaraldehyde improved the activity and stability of LOD in the cross-linking matrix, which in turn led to an improvement in the reproducibility of the sensing device. However, even though the reproducibility of the response was increased, this and the linearity of the response still had to be improved.

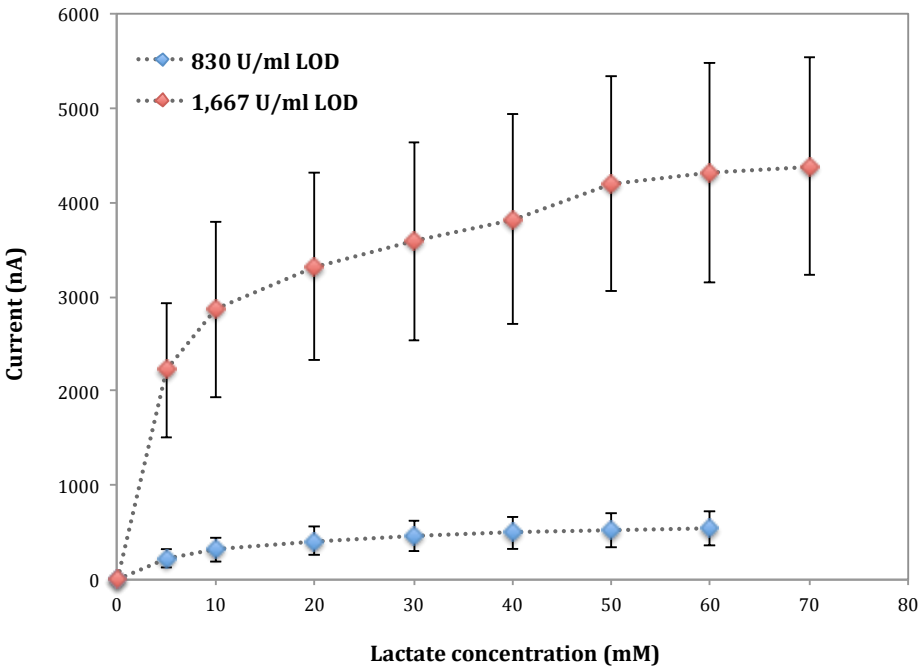

Figure 5.12. Comparison between calibration response curves for LOD on the AuPt electrode system with the use of 830 and 1,667 U ml-1 LOD for a range of lactate concentrations between 0–70 mM.

Throughout the different experiments performed in the study towards the obtaining of an enzyme laminate with improved characteristics, the preparation of LOD/BSA aliquots from a single vial of lyophilised enzyme powder was always a major issue. This problem became more evident during the preparation of laminates with a higher content of enzyme, as lower volumes of BSA buffer were employed. It was considered that the formation of bubbles in the vial during the

preparation of the mix could be hindering the recovery of the initial volume when preparing the aliquots and the proper homogenisation of the enzyme in the BSA buffer. It was therefore decided to study a new method for the preparation of LOD/BSA aliquots to overcome this issue and determine whether this had a positive effect on the reproducibility of the system.

5.5.2 Use of higher enzyme concentration in the introduction of a new preparation method for LOD/BSA aliquots.

The second part of the study with regard to the enzyme LOD focused on the study of an alternative procedure for the preparation of LOD/BSA aliquots and its effect on a better reproducibility of the sensing system. As previously mentioned, the reason behind this study was the fact that the method employed for the preparation of LOD/BSA solutions in the vial could be affecting the reproducibility of the system. The addition of such small volumes of BSA buffer at a relatively high concentration (0.1 g ml^{-1} in PBS) to the enzyme vial caused the formation of bubbles when mixing the buffer with the enzyme and while dissolving, the enzyme attached to the walls of the vial, which required forced pipetting. This issue became more evident during previous experiments (section 5.5.1) where higher concentrations of LOD were employed and smaller volumes of BSA buffer were added. It was thought that this could hinder the inclusion of the total lyophilisate in the LOD/BSA solution, since some enzyme could still remain on the walls of the vial. Finally, on some occasions it was not possible to collect the whole volume added initially to the vial in order to prepare the different aliquots, again probably due to part of the mix remaining on the walls of the vial. For these reasons, it was thought that any of these situations could cause a variation in the concentration of enzyme, either between different aliquots of the same batch (vial) or aliquots from different batches, thus becoming a major cause of variation between laminates prepared from each aliquot.

Since the formation of bubbles could be caused by dissolving the enzyme lyophilisate in a buffer with a relatively high concentration of BSA (0.1 g ml^{-1} in PBS), it was decided to include a new preparation method to minimise the formation of bubbles in the vial. Therefore, the enzyme lyophilisate was dissolved with PBS only, which then allowed forced pipetting with a minimum generation of bubbles. Once this dissolution was achieved, a more concentrated BSA buffer (0.2 g ml^{-1} in PBS) was added to the same final concentration and volume as in previous experiments. Since this last step did not require forced pipetting but just carefully stirring the solution, the formation of bubbles was kept at a minimum. In this study, enzyme laminates were constructed following the same procedure as described in section 5.5.1 but this time, using aliquots prepared with the new method described. Moreover, as it was observed that with this new preparation method, the cross-linking occurred at a higher rate than previously, the preparation method for the enzyme laminate was again changed, with respect to the one described in section 5.4.2, by shortening the stirring time from 30 to 15 seconds and extending 15 seconds the time for the mix to cross-link on top of the lower membrane. A range of lactate concentrations, from 0 to 70 mM, were analysed on the AuPt electrode system using the chronoamperometry protocol described in section 3.4.2. The current outcome for each concentration was normalised and represented in a chart with the corresponding standard deviation and the RSD coefficients were calculated (Figure 5.13).

During the preparation of the aliquots following this new method, it was observed that the formation of bubbles took place in the same way as with the previous preparation method and that this was in reality due to handling small volumes of liquid (30-60 μL) to dissolve the enzyme lyophilisate, rather than to the BSA itself.

a)

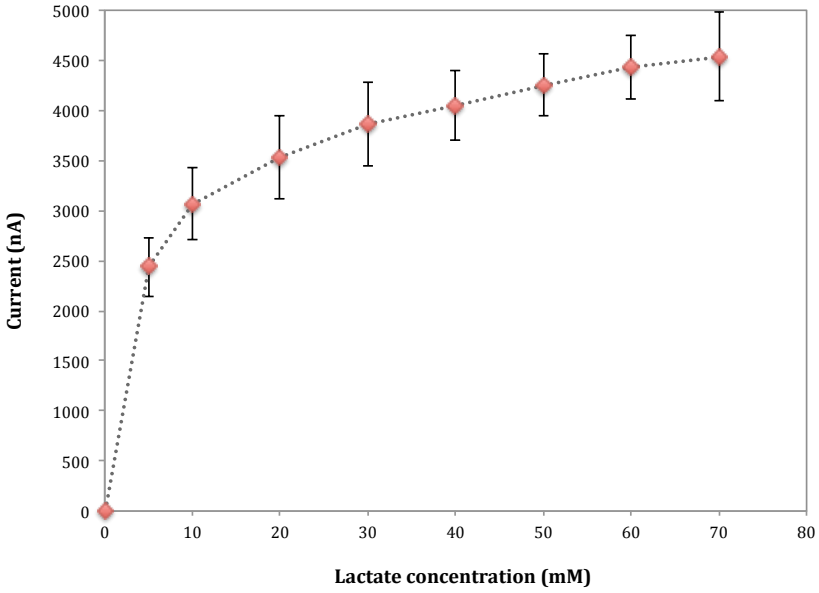

b)

	Current response (nA)		
[Lactate] (mM)	**Mean**	**S. Dev.**	**RSD (%)**
0	0.00	0.00	0.00
5	2436.25	296.99	12.19
10	3066.25	360.23	11.75
20	3533.75	415.58	11.76
30	3861.25	414.50	10.73
40	4050.00	346.15	8.55
50	4250.00	308.87	7.27
60	4430.00	319.61	7.21
70	4540.00	446.89	9.84

c)

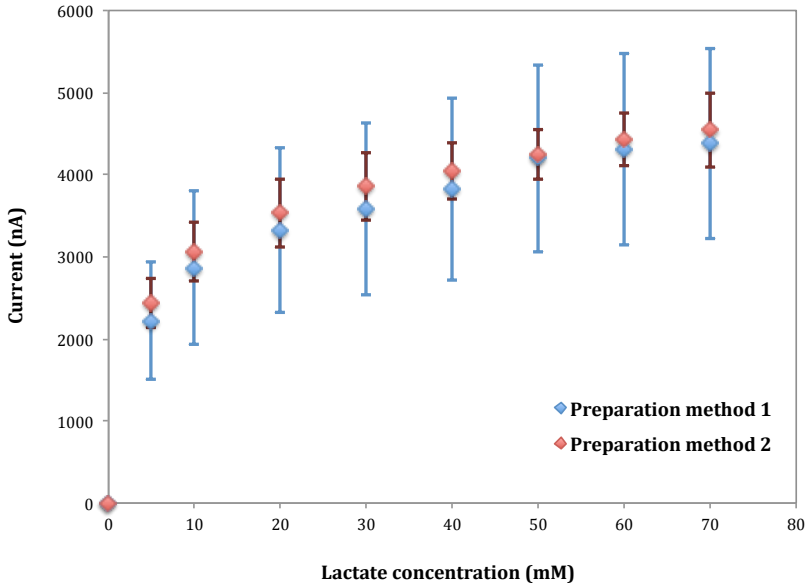

Figure 5.13. Calibration curve for LOD on the AuPt electrode system, for a range of lactate concentrations from 0 to 70 mM, with the use of 1,667 U ml^{-1} LOD and a new aliquot preparation method (subsequent addition of PBS only and 0.2 g ml^{-1} BSA in PBS to a final concentration of 0.1 g ml^{-1}). Comparison with the calibration curve obtained with the previous aliquot preparation method (section 5.5.1).

Results showed a high consistency in the average current values for 0-70mM lactate (Figure 5.13c, Preparation 2) with respect to the ones obtained from the analyses of laminates constructed with the aliquots prepared using the previous method (Figure 5.13c, Preparation 1). The RSD between both sets of average current values was in the range 0.9-6.5%. Within these results, a slight increment in the average current values for the second preparation method was observed, with an RSD in the range 1.2-8.8%, with respect to the ones obtained using the previous method. However, the most interesting fact showed in the results was a notably higher reproducibility in the current values obtained with the new preparation method. The RSD for these values was in the range 7.2-12.2%, meaning a reduction in the standard error of 60.9-73.3% (Figure 5.13b,c).

Results obtained in this part of the study led to two main conclusions. The new method employed with the aim to avoid the formation of bubbles when mixing the BSA solution with the enzyme lyophilisate did not solve the issue as well as expected, as the bubbles appeared when adding the first solution of PBS. This fact indicated that the formation of bubbles was due to forced pipetting of small volumes of liquid, rather than to the BSA as previously thought. Therefore, other methods will have to be tested in the future in order to resolve this issue.

The second interesting fact observed from the results was that the new method for preparing the LOD/BSA solution led to a decrease in variability in current values between different laminates of up to 73.3% for the range of lactate concentrations of 0-70 mM and a slight increase in linearity. It should also be noted that the consistency in average current values between both methods was relatively high, being the maximum RSD recorded between them of 6.5%, which reinforced the quality of the developed laminate preparation method. Moreover, the LOD/BSA solution prepared cross-linked with glutaraldehyde at a rate twice as high as previously. The only aspect of the LOD/BSA preparation that was changed in this new method was the concentration of the initial BSA solution prepared in PBS (0.2 g ml^{-1} instead of 0.1) and its subsequent dilution in PBS. Therefore, it was concluded that the cause for the reproducibility of the system to double with respect to the previous laminate preparation method was that the final

concentration of BSA used to dissolve the enzyme lyophilisate had changed. This fact represented an important point of the research, since it provided new insights into the understanding of the laminate construction, cross-linking matrix formation and enzyme stability; and opened a new path towards the study of BSA as a variable of the system.

Subsequently, it was decided to direct the next part of the research towards the study of the influence of BSA concentration on the physical and electrochemical properties of the cross-linked matrix, as well as the stability of LOD within it.

5.6 BSA concentration

The next part of the study focused on BSA as one of the variables in the system. The analysis focused specifically on the influence of BSA concentration in the stability of LOD in the cross-linking matrix. The aim of this study was to increase the stability and activity of the enzyme and, with this, the performance of the sensing system with respect to when 0.1 g ml^{-1} BSA was used.

The reason behind this study came from the previous test performed on the enzyme laminate system, where a new method for dissolving the enzyme lyophilisate in a BSA buffer was studied, for which a higher concentration (0.2 g ml^{-1}) of BSA was prepared. The resulting improvement in the sensor's reproducibility suggested BSA as the cause of the enhancement of the sensor's performance. It was thought that the preparation of a more concentrated initial BSA solution and its subsequent dilution in PBS only, had altered the final concentration of BSA in the vial, this being higher or lower than that desired (0.1 g ml^{-1}).

It was suggested that the reason why the reproducibility had been increased during the performance of the previous analysis (section 5.5.2) was due to higher retained activity and stability of LOD within the laminate matrix. Previous studies (section 5.5.1) showed an enhancement in the reproducibility of the system when the concentration of LOD, and thus the total protein, was increased. Therefore, it

was thought that a further increase in the total protein, this time through the increase in BSA concentration, had occurred. This increase in total protein would have reduced the number of Lys residues from the active site of LOD reacting with glutaraldehyde, thus enhancing the activity of the enzyme in a higher degree than the one achieved with 10 units of LOD.

For this reason, it was decided to assess the influence of a higher concentration of BSA with respect to LOD and glutaraldehyde in the cross-linking mix. To prove this concept, the concentration of total BSA in the LOD/BSA solution was raised from 0.1 to 0.2 g ml^{-1} in PBS. For this study, enzyme laminates were constructed as described in section 3.4.3, using the same LOD and glutaraldehyde concentrations as in section 5.5.1, as these had led to better results in the performance of the sensing system. The resulting laminates were electrochemically interrogated on the AuPt electrode system using the chronoamperometry protocol outlined in section 3.4.2. A range of lactate concentrations, from 0 to 40 mM, were analysed. The current response for each concentration was normalised and represented in a plot with the corresponding standard deviation and RSD coefficients (Figure 13).

Results show an increase in current response with respect to previous laminate preparation methods. Interestingly, however, a plateau in the current response towards 20-30 mM lactate was observed in all constructed laminates (Figure 5.14a). The reproducibility of the sensing system also showed a decrease for lactate concentrations of 5-20 mM in the range of 43.9-60.6% with respect to the previous preparation method (Figure 5.14b).

a)

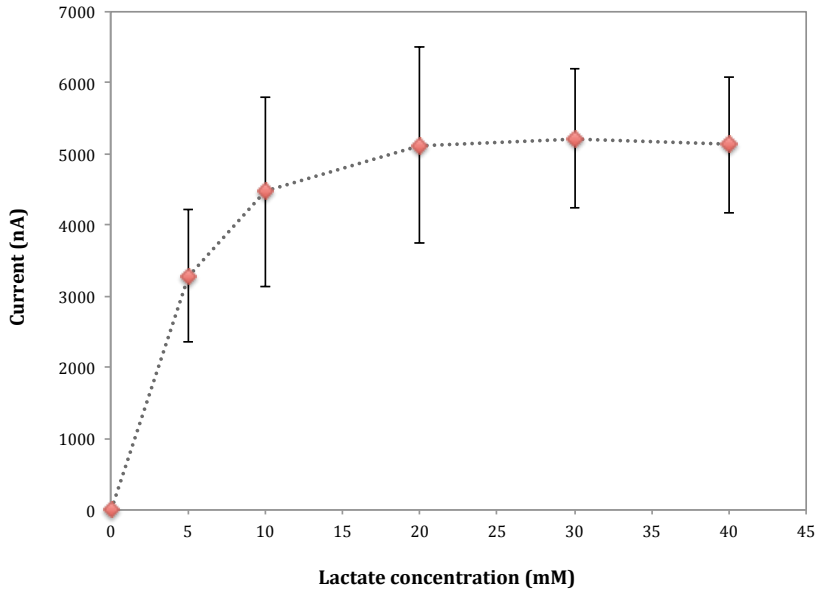

b)

	Current response (nA)		
[Lactate] (mM)	**Mean**	**S. Dev.**	**RSD (%)**
0	0.00	0.00	0.00
5	3285.17	927.13	28.22
10	4469.33	1332.30	29.81
20	5127.67	1382.41	26.96
30	5219.90	984.56	18.86
40	5129.90	961.09	18.74

Figure 5.14. Calibration curve for LOD on the AuPt electrode system with the use of 0.2 g ml^{-1} BSA for a range of lactate concentrations from 0 to 40 mM.

From the analysis of the results obtained from this study with 0.2 g ml^{-1} BSA, two interesting observations were made. On one hand, higher current values were observed with respect to any of the previous laminate preparation methods studied. This indicated that the activity of LOD within the laminate had been increased, thus enhancing the enzymatic conversion of substrate. The reason behind this improvement in enzyme activity could be explained by the fact that higher protein content (BSA) in the mixture was increasing the amount of Lys residues available to react with glutaraldehyde. Therefore, with a higher BSA:LOD ratio, the probabilities of the cross-linker reacting with these Lys residues from BSA molecules rather than those from LOD, increased. Due to this, a lower degree of cross-linking between glutaraldehyde and LOD was taking place, probably

through Lys residues mostly from the surface of the enzyme molecule, leaving its active site intact.

Conversely, however, the plateau of the response observed around 20-30 mM lactate and slight decrease in response towards 40 mM indicated either a loss of enzyme (or its activity) over the timeframe during which the different lactate solutions were being analysed. Given the fact that the activity of the enzyme seemed to have improved, indicated by the increase of current response with respect to previous studies, it was thought that this plateau and further decrease of the response was due to a leaching of enzyme out of the laminate over time. The reason behind this phenomenon could be the fact that an excessive BSA concentration with respect to LOD could be favouring the cross-linking reaction to occur between glutaraldehyde and Lys groups from BSA rather than the enzyme. Thus, a weak or non-existing cross-linking between glutaraldehyde and LOD could produce the leaching of the enzyme out of the cross-linking matrix. This loss of enzyme over time could also explain the loss of reproducibility observed in the results.

Conclusions obtained from the results described above indicated the important effect the variation in BSA concentration had on both enzyme activity and properties of the cross-linked matrix for keeping the enzyme within the laminate structure. However, in order to make use of the potential of BSA for enhancing the performance of the sensing device, other concentrations would have to be studied. On one hand, construction of laminates with lower BSA content than 0.2 g ml^{-1} but higher than the previously employed, 0.1 g ml^{-1}, would be of great interest. On the other hand, at lower concentrations of BSA (total protein) in the mixture, the cross-linking reaction would have occurred between glutaraldehyde and a higher content of Lys residues from LOD. This would have increased the probability of glutaraldehyde reacting with Lys residues from the active site of the enzyme, this being detrimental to its activity. However, in the previous study (section 5.5.2.), both current response values and reproducibility of the system were enhanced, which indicated a higher enzyme activity. Therefore, the study of

lower concentrations of BSA than the previously used 0.1 g ml^{-1} would not be considered.

5.7 Repeatability. Operational and mechanical stability of the enzyme laminate system

The last part of the study performed on the enzyme laminate consisted of carrying out an electrochemical characterisation in terms of repeatability, operational stability and mechanical stability of the sensing system. These parameters are crucial when developing a biosensor for clinical analysis. In the case of the developed AuPt sensing system and its potential application as a wearable sensor for real-time monitoring of sweat lactate for the early detection of the onset of pressure ischemia, the device will have to provide a reliable measurement while being applied on to the skin for a certain period of time and subjected to mechanical deformation – relevant to the daily activity of the wearer – due to bodily movements while being worn by the patient.

While the repeatability is related to the intra-membrane reproducibility of the sensing device, the operational stability depends on the capability of the enzyme to retain its activity in the immobilised matrix when the device is in use. Previous sections within this chapter have focused on the study and optimisation of different parameters involved in the construction of the enzyme laminate in order to improve the immobilisation of the enzyme and its activity and stability. So far, these results have shown the stability and activity of the enzyme in the analysis of the sensing system over a range of lactate concentrations. The aim of the present study is to assess whether these parameters also enhance the repeatability, operational and mechanical stability of the sensing system.

Experiments performed in this study were carried out on an AuPt electrode system following the protocol outlined in section 3.4.6.2.ii. However, for this study the electrode system sputter-coated on a single polycarbonate membrane was fixed to a flexible plastic surface following the same method as for a glass slide,

described in the mentioned protocol. This surface allowed the flexibilisation and mechanical deformation of the electrode system for the performance of the present study. The parameters employed for the construction of the laminate were the same as the ones utilised in section 5.5.2. The resulting sensing system was interrogated using the chronoamperometry protocol outlined in section 3.4.4.

The parameters under study in the present section were evaluated by performing 12 consecutive additions of a 10 mM lactate solution in PBS after the sensor was polarised in 15 ml PBS only at +650 mV and a baseline was reached. This concentration was chosen so the enzyme would not become saturated with substrate, which could lead to its loss of activity. This way, any changes in current response would be associated with the operational stability, given by the stability of the enzyme in the cross-linked matrix, and/or the mechanical stability of the laminate sensor and not with any potential loss of activity of enzyme due to its saturation by high amounts of substrate. The repeated additions of 10 mM lactate were performed over a total time frame of 27.4 hours. After each addition, 15 ml of PBS only would be added to the beaker where the AuPt sensor was placed in order to rinse the membrane and repolarise the sensor. In order to evaluate the effect of mechanical bending on the sensing performance of the AuPt system, prior to each lactate addition the sensor was bent to an angle of approximately 120° for 2 seconds followed by another 2 seconds of relaxation. The bending/relaxing process was iterated 2 times prior to the interrogation of the AuPt system with a new 10 mM lactate solution.

The chronoamperometric response of the AuPt laminate system under study was recorded (Figure 5.15a). The results for the current response values obtained for each lactate addition were normalised by subtracting the baseline current obtained with PBS only and represented in Figure 5.15b.

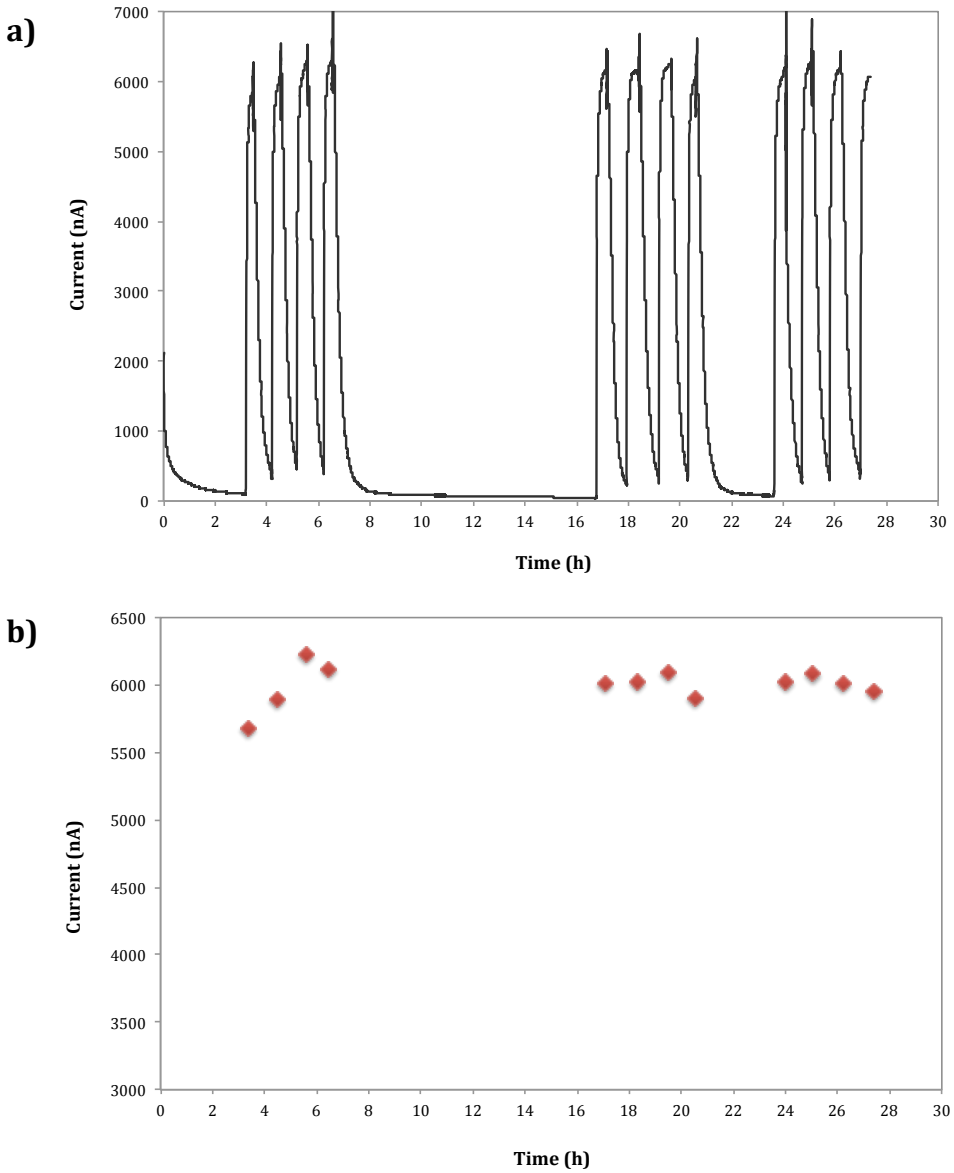

Figure 5.15. Repeatability, operational and mechanical stability of the laminate sensor. (a) Chronoamperometric response and (b) normalised current response values, obtained for 12 additions of 10 mM lactate in PBS, with the AuPt system analysed. The enzyme laminate was constructed with the optimised parameter values reported in section 5.5.2.

The data reported in Figure 5.15 showed that the response of the sensor was relatively stable over a timeframe of 27.4 hours with an RSD of 2.3% for all 12 additions of the 10 mM lactate solution, with no clear sensitivity loss observed during the test period.

These results indicated that the optimisation of the parameters for the construction of the enzyme laminate, described in the previous sections of this chapter, led to an improved performance in the AuPt sensing system. The results demonstrated the capability of the developed sensing system to provide a reliable lactate monitoring for over 27 hours without any significant loss in current response and subject to relevant mechanical stress for the potential application of the sensor as a wearable device. These results also indicate that the laminate sensor did not exhibit any clear and/or significant change and/or loss in the amperometric signal of the electrodes due to mechanical deformation. Therefore, the developed laminate sensor exhibits excellent repeatability (intra-laminate sensor reproducibility) and operational and mechanical stability over the relevant timeframe of analysis. This demonstrates its potential for its application on to the patients skin and provide continuous lactate monitoring for a significant period of time prior to its replacement.

5.8 Conclusions

The present chapter described the steps followed for the successful construction of a working laminate system and the optimisation of the reproducibility and linearity of the response.

A study was performed on the effect of membrane porosity on the linearity of the sensor's response. Results showed an increase in the linearity of the response when using an upper-membrane 0.015 μm pore radii due to a diminution of enzyme saturation, although accompanied by a lower current response. The AuPt electrode system exhibited increased sensitivity when compared to the Rank cell.

The effect of the cross-linking time on improving the consistency in the obtaining of a working system was studied. An incubation time of 12 minutes exhibited an efficient cross-linking whilst preserving the activity and the stability of LOD within the laminate construct.

Studies on glutaraldehyde showed that fresh solutions and an alternative method for the construction of the laminate, where the mixture was allowed to cross-link before pressing it between both membranes, led to an improved construction and performance of the enzyme laminate. Results obtained for the enzyme GOD showed a much better reproducibility than when using LOD, which pointed at the enzyme employed as important factor for the obtaining of a sensitive detection. An increase in glutaraldehyde concentration from 5 to 10% led to a better immobilisation of the enzyme and an extended working concentration range. However, a lower current response was obtained, suggesting a partial inactivation of the enzyme with higher glutaraldehyde concentrations.

The effect of a higher enzyme loading on the sensor's performance was also studied. When LOD concentration was increased from 5 to 10 units per laminate (corresponding with ~830 and 1,667 U ml^{-1} LOD, respectively), a prominent increase in reproducibility and current response values obtained with the developed laminate system was observed due to an increase in protein content in the mixture and, thus, a diminution of Lys residues from the active site of the enzyme reacting with glutaraldehyde, which preserved the activity of LOD.

The study of the influence of BSA concentration in the stability of LOD revealed that a higher concentration of BSA (0.2 g ml^{-1}) led to an initial increase in current response with respect to previous laminate preparation methods, indicating an increase in enzyme stability. However, a decrease in current response over time was observed, suggesting a weak cross-linking between LOD and glutaraldehyde, leading to the leaching of the enzyme out of the laminate.

The repeatability, operational and mechanical stability of the optimised laminate sensor over a timeframe of 27.4 hours and 24 bends was demonstrated, showing the potential of the developed sensing system for being applied on to the patient's skin and provide continuous and reliable lactate measurement for a relatively long period of time prior to its replacement.

CHAPTER 6

DEVELOPMENT TOWARDS THE MEASUREMENT OF LACTATE IN HUMAN SWEAT *IN VITRO*

6 Development towards the measurement of lactate in human sweat *in vitro*

6.1 Introduction

This chapter presents the steps taken for the performance characterisation of the developed AuPt sensing system, as described in section 3.4.6.2.ii, as well as the establishment of a proof-of-principle for the monitoring of lactate in undiluted human sweat. The chapter also describes the limitations encountered at the present stage of development that will drive future work towards improving the performance of the sensor for the analysis of undiluted sweat.

As was mentioned in section 2.4.2, human sweat is a complex solution, which is known to contain a minimum of 61 different chemical constituents at varying concentrations (Stefaniak and Harvey, 2006; Harvey *et al.*, 2010). It has been reported that the potential of +650 mV at which the developed electrode system (AuPt) is polarised, allows the oxidation of H_2O_2 produced in the course of the enzymatic reaction. However, at this potential other metabolites present in sweat such as uric acid and ascorbic acid are also oxidised when they reach the WE, thus interfering with the electrochemical signal and its reliability (Chaubey and Malhotra, 2002).

Preliminary studies focused towards the electrochemical behaviour of the sensor were performed in synthetic sweat dilutions containing different lactate concentrations in the presence of uric acid, ascorbic acid and three of the most abundant compounds in human sweat: sodium chloride, urea and acetic acid. Promising results obtained from the analysis of lactate in synthetic sweat solutions led to the interrogation of the developed sensing system using diluted and, ultimately, undiluted sweat samples. A number of different tests performed on human sweat will be described and the results discussed.

The protocol for the construction of the electrode system and the enzyme laminates are outlined in sections 3.4.6.2.ii and 3.4.3., respectively. Here, 6 μl of LOD solution (~1,667 U ml^{-1} LOD) in 0.1 g ml^{-1} BSA and 3 μl of 10% v/v glutaraldehyde were cross-linked between two polycarbonate membranes. The resulting system was then interrogated using the chronoamperometry protocol as described in section 3.4.2. The sensor was placed in a 25-ml beaker and 15 ml of PBS were initially added. The sensor was then set to polarise at +650 mV until a baseline was reached. After this, 15 ml of each test solution were sequentially added for analysis.

6.2 Interference of lactate monitoring in presence of synthetic sweat components

As previously stated, preliminary studies focused on studying the performance of the developed sensing system on synthetic sweat solutions. The main aim of such a study was to assess possible electrochemical interference effects from compounds present in sweat, affecting the selectivity of the sensor's current response to lactate. Sweat components such as ascorbic acid and uric acid have been reported to undergo oxidation at an electrode potential of +650 mV, employed for H_2O_2 measurement. Therefore, an increase in signal response with respect to that normally obtained for lactate in PBS only was expected, due to interference by electron transfer from these and/or other co-existent compounds present in the prepared synthetic sweat solution. The sensing system was also interrogated for a range of lactate concentrations, from 0 to 50 mM, in the synthetic sweat stock solution, in order to assess its capability for measuring lactate in the physiological concentration range for pressure ischemia in a more complex solution.

The synthetic sweat solution employed in this part of the study was prepared by dissolving some of the most common constituents of sweat in PBS pH 7.4, as described in the literature (Stefaniak and Harvey, 2006). Following this, the solution contained acetic acid, urea, sodium chloride and lactic acid. Ascorbic acid and uric acid were also added to the composition of the solution since they are considered one of the main electroactive interfering compounds at the polarising potential used in the present study. The concentration of each compound was chosen so as to correspond with their reported median values, described in a suggested chemical formulation of a comprehensive artificial human sweat (Stefaniak and Harvey, 2006; Harvey *et al.*, 2010). The concentration of each component in the synthetic sweat stock solution is summarised in Table 6.1. In this solution, a range of lactate concentrations, from 0 to 50 mM, were prepared and analysed with the AuPt electrode system.

Table 6.1. Composition of the synthetic sweat stock solution.

Compound	Concentration (g L^{-1})
Sodium chloride	1.55
Urea	$6.01x10^{-1}$
Acetic acid	$7.81x10^{-3}$
Ascorbic acid	$1.76x10^{-3}$
Uric acid	$9.92\ x10^{-3}$

AuPt laminate sensors were constructed and interrogated as described in section 6.1. The first experiment performed within the present study consisted of exposing and interrogating an AuPt electrode system for 10 mM lactate both in the absence (PBS only) and presence of the synthetic sweat solution. The sensor was placed in a 25-ml beaker and polarised by adding 15 ml of PBS until a baseline was reached. After this, 15 ml of both lactate solutions were alternately added for their analysis (Figure 6.1). The 10 mM lactate solution in PBS only was added first in order to avoid any possible initial alteration of the enzyme activity and/or electrode response produced by any of the components of the synthetic sweat solution and, in this way, to obtain a control current response to which subsequent responses could be compared. Since previous experiments performed on the laminate sensing system had shown that the sensor exhibited good intra-membrane reproducibility (RSD in the range of 0.85-2.19%, obtained from repeated tests on the same laminate for a number of different laminates), possible significant changes in current response observed in the results would be mainly attributed to interference effects produced by the synthetic sweat solution.

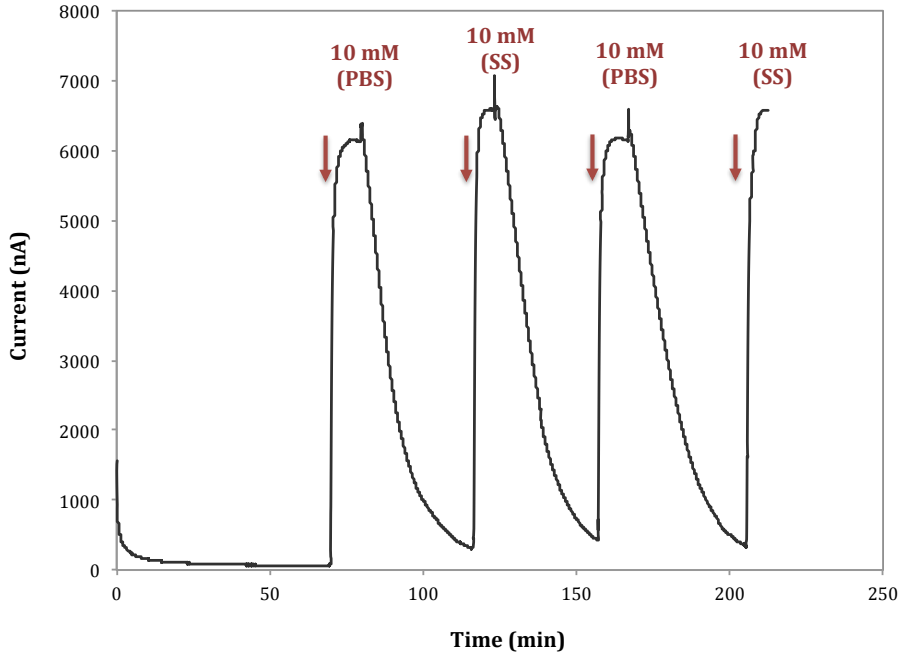

Figure 6.1. LOD steady-state current response over alternating lactate dilutions at 10 mM in PBS only (PBS) and synthetic sweat (S.S.).

The arrows indicate the moment at which the PBS solution was extracted from the beaker and the lactate test solutions were introduced.

Results showed a high reproducibility between the different measurements of lactate in PBS and in the synthetic sweat solution, with the calculated RSD between the different peak current values being 5.29%. This indicated that the interference in the response of the AuPt laminate sensor produced by compounds present in the prepared solution at their median physiological concentration values in human sweat perspiration was relatively low. Nevertheless the next chapter will describe preliminary studies on electrode surface modification in order to lower interferences produced by ascorbic acid and uric acid in the event that these were found at a concentration above their median value in human sweat.

Results observed in Figure 6.1 together with preliminary studies performed at a range of lactate concentrations, from 0 to 50 mM, in a synthetic sweat solution (Figure 6.2) demonstrate the capabilities of the developed sensing system for monitoring lactate at physiologically relevant concentrations in the presence of

reported interfering components at their median concentration in human perspiration.

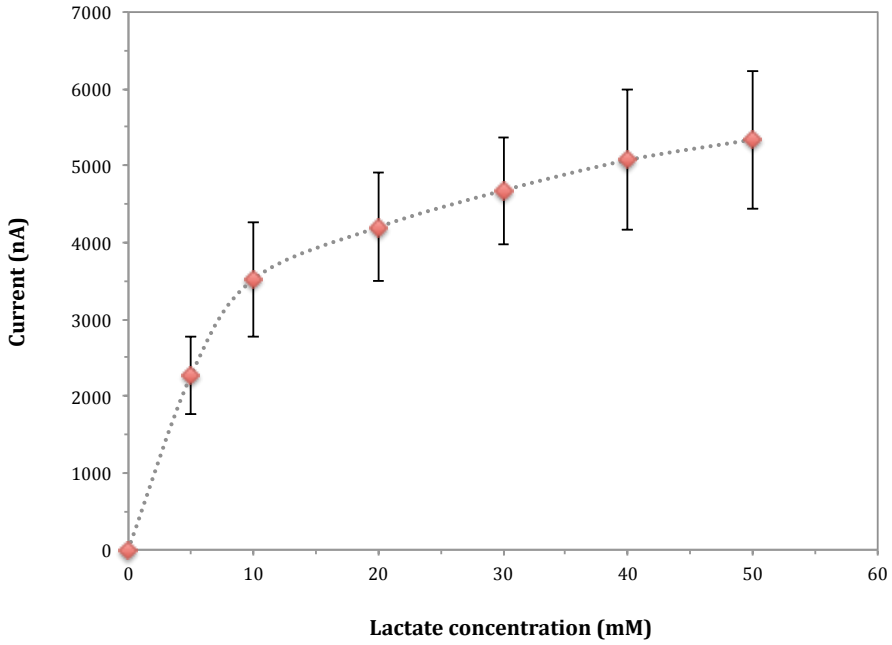

Figure 6.2. Calibration curve for LOD on the AuPt electrode system for a range of lactate concentrations, from 0 to 50 mM, in a synthetic sweat solution composed of sodium chloride, urea, acetic acid, uric acid and ascorbic acid in PBS at their reported median physiological levels in human perspiration.

The promising results of Figure 6.2 allowed the research to take one step forward, towards the interrogation of the developed sensing device with human sweat samples, and this will be described in the next section.

6.3 *In vitro* analysis of human sweat samples

After the encouraging results obtained with the analysis of lactate in synthetic sweat solutions, the work took a step forward to allow for the first time in this study the analysis of human sweat samples. The main aim of this study was to assess the sensor's capability to satisfy its main medical purpose, that being the detection of lactate level fluctuations within sweat and the limitations of the sensing device in this regard.

Due to the lack of sweat samples collected from hospitalised patients suffering from pressure ischemia, the hypoxia conditions that ischemia would lead to in these patients were mimicked by subjecting healthy volunteers to the performance of intense physical exercise for a period of time between 30 minutes and one hour. Eccrine sweat glands rely primarily on aerobic metabolism in order to carry out their secretory function. Moreover, sweat glands depend on the glucose carried in blood and the glycogen stored in eccrine glands as metabolic substrates. However, since the glycogen stores in eccrine glands are insufficient to carry out the secretion of large volumes of sweat, the delivery of blood-glucose becomes essential. Under the performance of intense physical exercise, a decrease in oxygen content in blood occurs, leading to a decrement in the glucose supply, which hinders the aerobic metabolism of sweat glands. Under these conditions, eccrine sweat glands are forced to satisfy their metabolic demands through the performance of anaerobic metabolism, which progressively increases the production of lactate and its content in the secreted sweat (Green *et al.*, 2001).

The ethics approval for the collection, handling and in vitro analysis of human sweat samples obtained from healthy volunteers performing intense physical exercise for a certain period of time was obtained by application to the Cranfield University Health Research Ethics Committee. The letter of approval is shown in Appendix A.

The collection and handling of human sweat samples for their *in vitro* analysis were carried out as outlined in section 3.4.8. Due to the limited amount of sample collected from each subject (in the range of 10-15 ml per subject for a 30-minute

exercise performance with the application of 3 collection patches), the analysis of sweat samples was carried out by placing the sensor horizontally with the electrodes facing up and the sample was deposited on top, covering the entire surface of the electrode system, as showed in Figure 6.3. This new system for sample analysis allowed the reduction of the required sample volume from 15 to 0.8 ml, mimicking in a more approximate way the external conditions and sensor behaviour when applied onto the surface of the skin in future studies.

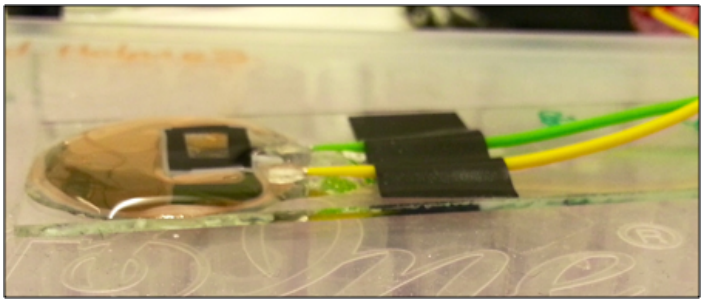

Figure 6.3. Photograph showing the horizontal disposition of the AuPt sensing system for the analysis of sweat samples.

Initial tests on the performance of the sensor on human sweat were carried out on diluted samples in order to avoid large variations in ionic strength (concentration of ions) in the solution, which could compromise the stability and activity of the enzyme. Moreover, the dilution of sweat samples would decrease the concentration of low molecular weight substances and electrochemically active molecules that could be detrimental to the sensor's performance(Koschwanez and Reichert, 2007). As previously mentioned, oxidising species present in the sweat sample (i.e. ascorbic acid and uric acid) at an unknown concentration can oxidise at the electrode surface at the potential set by the experiment, affecting the electrochemical response of the sensor and the selectivity of the measurement (Chaubey and Malhotra, 2002). On the other hand, low molecular weight substances present in complex biological samples can increase the sensor fouling by adsorbing to the surface of the electrode, affecting the sensor's sensitivity and the baseline current(Koschwanez and Reichert, 2007).

The dilution of sweat samples also allowed working at a range of lactate concentrations at which the current response profile for the sensing system is almost linear (1- 5 mM), which allowed a better estimation of the real lactate levels in the undiluted sample by extrapolation of the data from the response curve created as the sensor is calibrated. This accuracy in the estimation of lactate levels allowed the characterisation of the different sweat samples analysed and the detection of fluctuations in lactate levels to which the analysis of undiluted sweat samples would subsequently be compared.

AuPt laminate sensors were constructed as outlined in section 6.1 and chronoamperometrically interrogated as described in section 3.4.2. Here, the sensor was placed in a 25-ml beaker and set to polarise with 15 ml of PBS at +650 mV until a baseline was reached. For the calibration of the sensor, 15 ml of each lactate solution in PBS in the range of 1-5 mM were sequentially added for their analysis. After the calibration step, the sensor was set to polarise again in PBS. For the analysis of sweat samples, the sensor was placed horizontally on a flat surface and 0.8 ml of sample were added on top of the electrode system until fully covered. The epoxy resin applied around the circumference of the sputter-coated membrane (in order to keep it fixed to the glass surface) acted as a physical barrier that avoided the spillage of sample solution out of the electrode-system surface area (Figure 6.3). The current response corresponding to the concentration of lactate in the sample was recorded once it had stabilised. Unless otherwise stated, after each lactate measurement from sweat samples, the biosensor was transferred back to a 25-ml beaker where 15 ml of PBS was added in order to rinse the laminate and polarise the electrode system prior to the next measurement.

The preparation of diluted sweat samples was carried out immediately before their analysis by mixing 0.1 ml of the original undiluted sweat sample with 0.7 ml of PBS to a total concentration of 1/8. After the current produced from the analysis of the sweat samples was recorded, lactate concentration was determined by using the calibration curve constructed with the sequential additions of lactate solutions in PBS. As previously mentioned, the study used a part of the linear range of the

calibration curve up to 5 mM lactate in the model solution, which corresponds to 40 mM lactate in undiluted samples.

The first experiment performed on human sweat samples consisted of interrogating two separate AuPt electrode systems with human sweat samples collected from two different subjects after performing intense physical exercise for 30 minutes. Since the literature suggests that normal lactate levels in sweat are around 20±7 mM (Polliack *et al.*, 1997; Sakharov *et al.*, 2010) and half an hour of intense physical exercise was not expected to raise lactate levels above the normal range, the calibration of the sensor was performed by adding lactate solutions in the range of 1-3 mM, which corresponds to 8-24 mM lactate in undiluted samples. After the sequential addition of the lactate solutions in PBS, the sensor was set to polarise again with PBS. After this, sweat solutions at an 8-fold dilution from two different subjects were added as described previously, polarising the sensor with PBS between both measurements. After the analysis of the second sample the sensor was set to polarise again in PBS and a 2 mM solution of lactate in PBS was analysed for the second time. The chronoamperometric response profiles for both interrogated AuPt systems are shown in Figure 6.4. The current outcome for each sample analysed was normalised by subtracting the background signal, obtained when PBS was added to allow the enzyme laminate to equilibrate. The concentration of lactate in the 8-fold diluted samples 1 and 2 was calculated using the calibration curve constructed with the current response recorded for the different solutions of lactate in PBS. The concentration of the corresponding undiluted samples was subsequently calculated by multiplying the measured (predicted) concentration of lactate in the diluted sample by a factor of 8. The comparison between lactate levels estimated in the diluted sample and predicted in the undiluted sample for both subjects in each sensing system along with their corresponding RSD coefficients are shown in Figure 6.5.

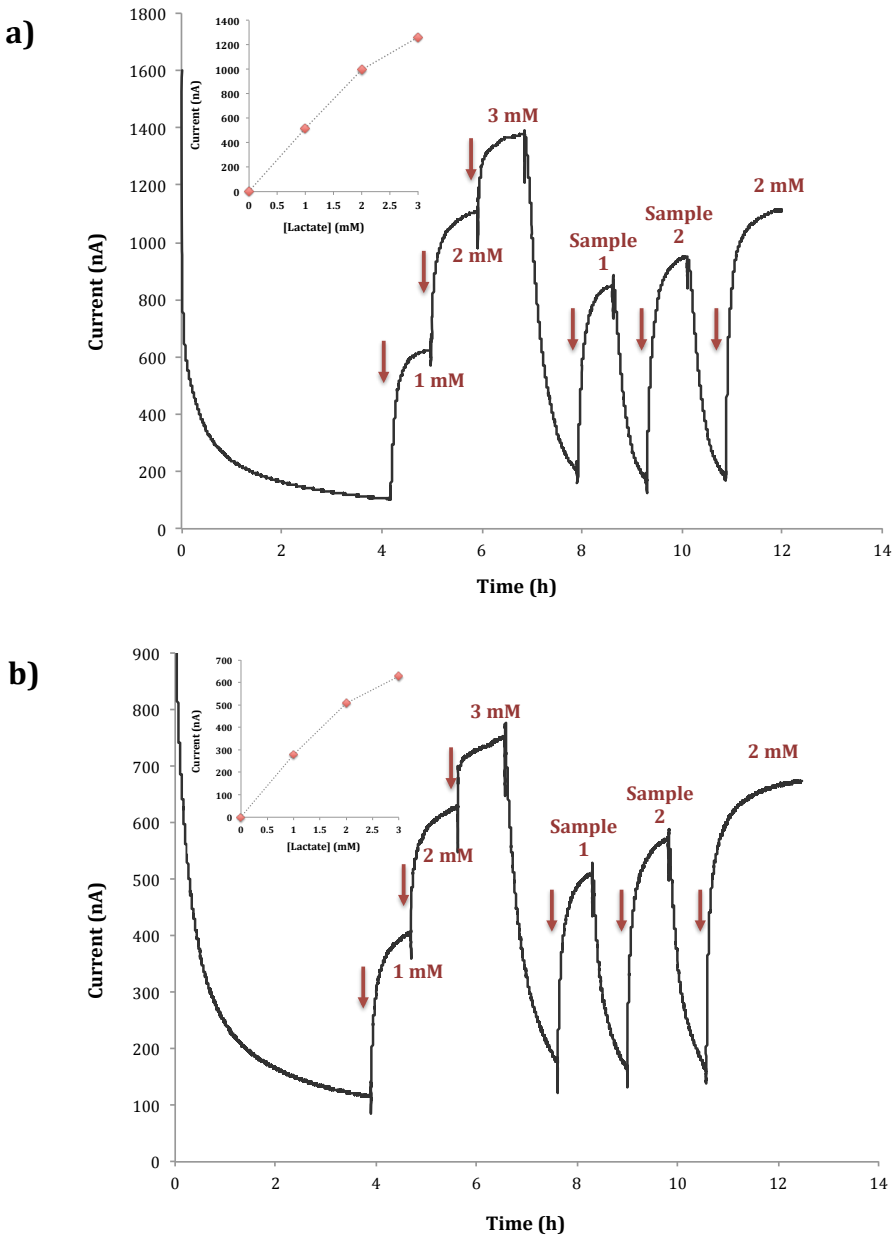

Figure 6.4. Chronoamperometric response for two electrodes (a, b) over additions of lactate solutions in PBS only followed by two separate measurements of diluted human sweat samples (1/8 in PBS) from two different subjects. Samples were collected after a 30-minute exercise. The insets represent the calibration curve of each sensor performed with the initial additions of lactate in PBS.

The arrows indicate the moment at which each solution (lactate in PBS or sweat samples) was put into contact with the sensing system for their analysis.

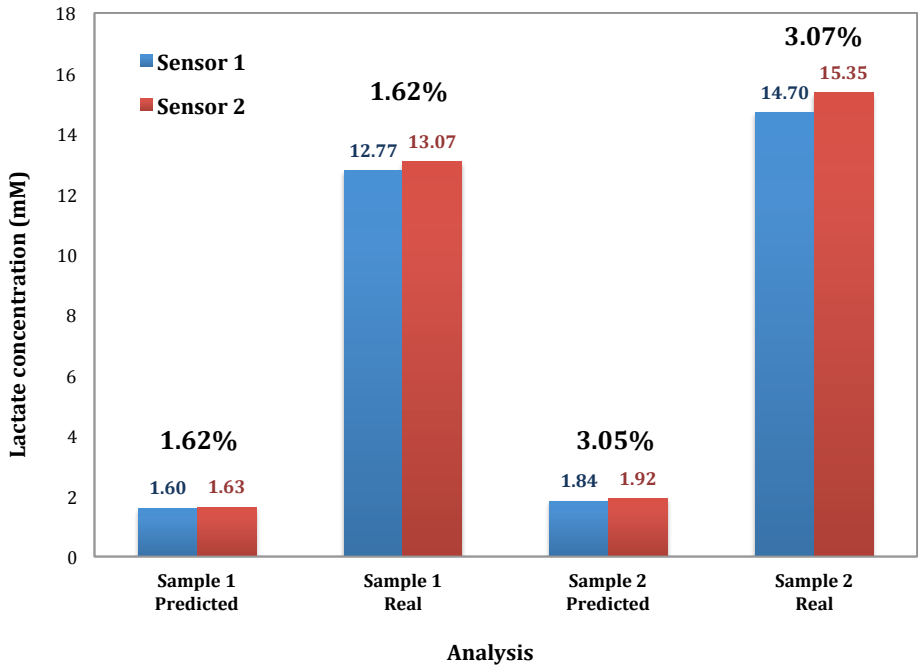

Figure 6.5. Bar diagram representing the samples analysed from two different subjects in two different sensing systems (Sensor 1 and Sensor 2) plotted against the lactate concentration estimated in the diluted (Predicted) and undiluted (Real) sweat samples.

The percentages indicate the RSD coefficients between each pair of measurements.

Results show that, despite both electrode systems giving differing chronoamperometric responses due to them being hand-manufactured, their profiles were internally consistent and the corresponding lactate concentration calculated for both diluted – and undiluted – samples from the corresponding calibration curve for each sensor differed from each other by an RSD of 1.62% for Sample 1 and 3.05% for Sample 2 (Figure 6.5). These results demonstrated the good inter-sensor reproducibility and hence reliability of the developed sensing device for the measurement of lactate levels from diluted sweat samples after calibration with lactate solutions in PBS. In addition to this, the calculated lactate concentration in the undiluted samples for both subjects falls into the normal sweat lactate levels reported by the literature. This again shows the capability of the sensor to perform reliable lactate measurements in diluted sweat samples. Finally, the RSD coefficient between current responses obtained for 2 mM lactate in PBS between the measurement at the beginning and end of the experiment was

0.47% for the first sensor and 6% for the second – the current response in the last one being higher with the second addition of 2 mM lactate. This consistent current response shows that the activity and stability of the enzyme was not compromised by exposing the laminate to diluted sweat solutions.

The reliability of the sensor lactate measurement and capability for sensing its level fluctuations was also assessed by performing a second experiment where two separate AuPt electrode systems were interrogated with sweat samples collected from a third subject, after performing intense physical exercise for 30 minutes, from three different body areas: chest, mid-back and upper back (neck). Previous studies have reported that sweat lactate levels vary depending on the body region where the sweat is collected from the subject under study(Patterson *et al.*, 2000; Derbyshire *et al.*, 2012). The sensor was first calibrated by adding lactate solutions in the range of 1-3 mM, corresponding to 8-24 mM lactate in undiluted samples. After the sequential addition of lactate solutions in PBS, the sensor was set to polarise again with PBS only and sweat solutions from three different body areas corresponding to the same subject were then added as described previously, polarising the sensor with PBS between measurements. Chronoamperometric response profiles for both AuPt systems interrogated are shown in Figure 6.6. As with the previous experiment, the current outcome obtained from the interrogation of the sensors with each sample was normalised by subtracting the baseline current at lactate 0 mM. The concentration of lactate in the 8-fold diluted samples was calculated using the calibration curve constructed with the current response obtained for the sequential additions of lactate in PBS in each sensor. The concentration of the corresponding undiluted samples was subsequently calculated by multiplying the measured (predicted) concentration of lactate in the diluted sample by a factor of 8. The comparison and RSD coefficients calculated between lactate levels estimated in the diluted sample and predicted in the undiluted sample are shown in Figure 6.7, for the three different body areas where sweat samples were collected, using both sensing systems.

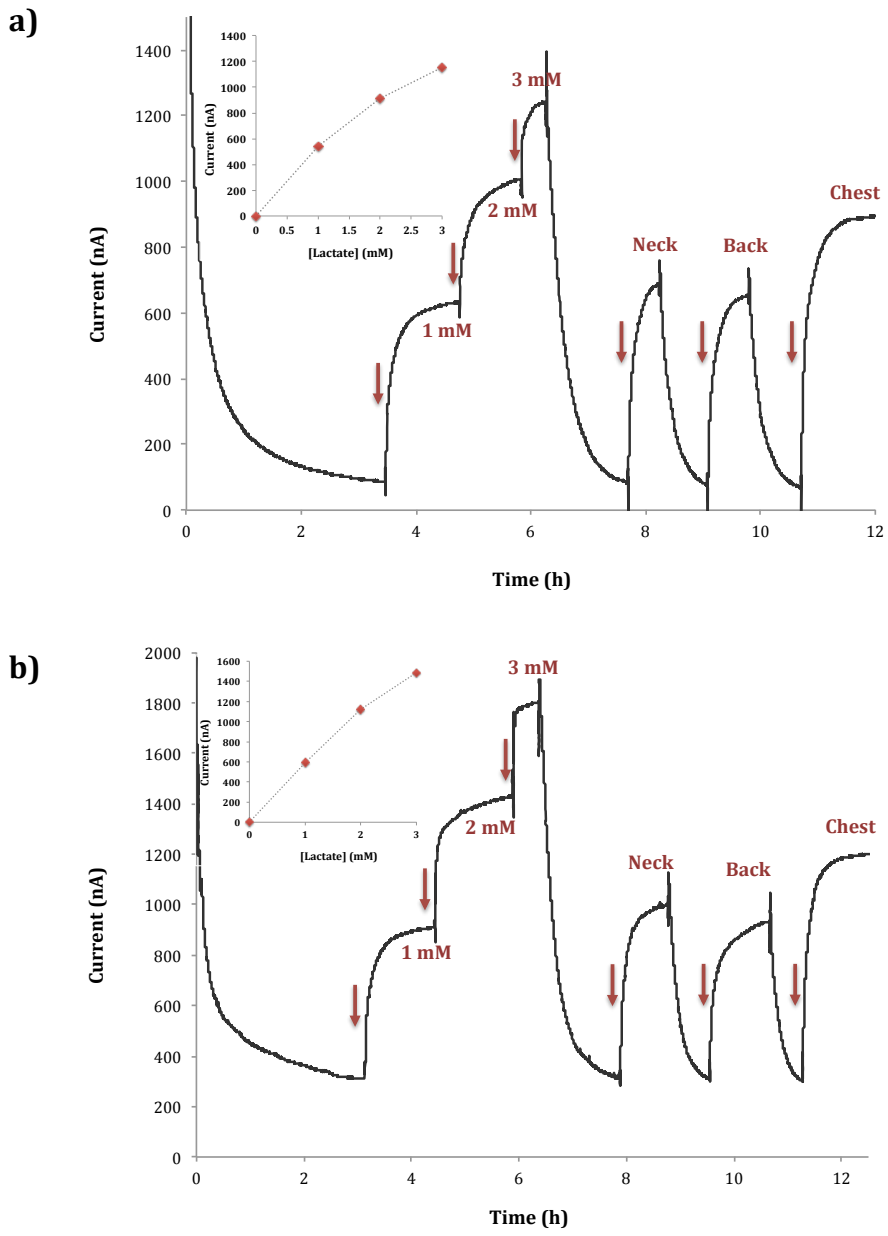

Figure 6.6. Chronoamperometric response for two electrodes (a, b) over additions of lactate solutions in PBS only followed by measurements of diluted human sweat samples (1/8 in PBS) collected from different areas of the body: neck, back and chest. Samples were collected after a 30-minute exercise. The insets represent the calibration curve of each sensor performed with the initial additions of lactate in PBS.

The arrows indicate the moment at which each solution (lactate in PBS or sweat samples) was put into contact with the sensing system for their analysis.

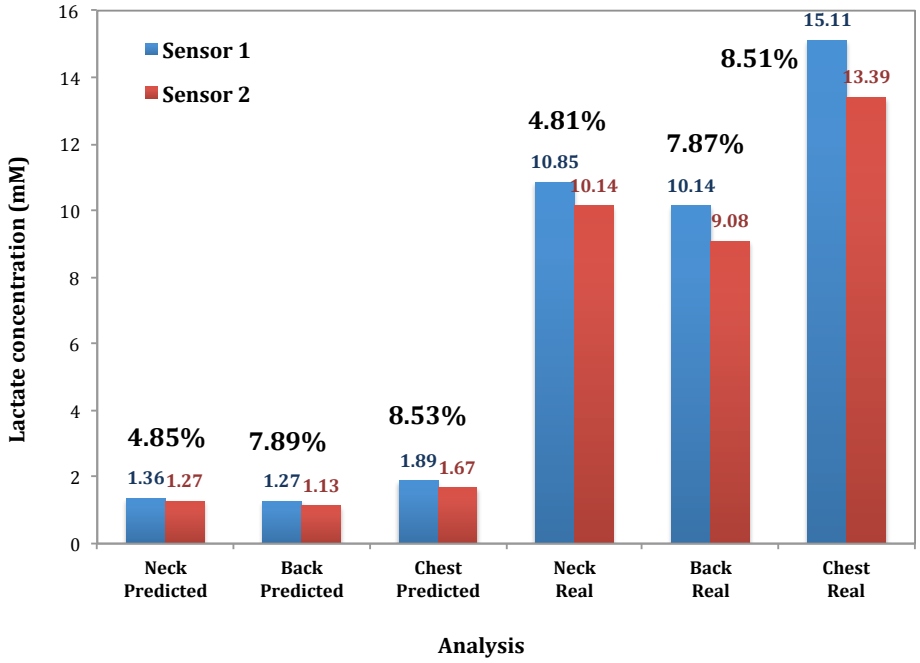

Figure 6.7. Bar diagram representing the analysis of sweat samples collected in three different body areas (neck, back and chest) with two different sensing systems (Sensor 1 and Sensor 2) plotted against the lactate concentration estimated in the diluted (Predicted) and undiluted (Real) sweat samples.

As the results show, despite the differences between both current response profiles (Figure 6.6a, b) due to the sensors (electrode system and enzyme laminate) being hand-manufactured and also due to them having different current background noise, their profiles were internally consistent. The lactate concentrations estimated for the three diluted samples for each sensor differed from each other by an RSD of 4.85% for the neck sample, 7.89% for the back and 8.53% for the chest, with expected similar values for the corresponding undiluted samples (Figure 6.7). This again proved the capability of the sensing system to provide reliable measurements after calibration. The observed differences in current response between the different body areas indicate that lactate levels varied between them, in agreement with the literature. This showed the capability of the sensor to provide a sensitive detection of lactate level differences in diluted human sweat samples.

The last study performed on diluted samples consisted of assessing the capability of the sensor to detect lactate level fluctuations between sweat samples collected at different stages of physical exercise performance. Sweat samples for this study were collected from a fourth subject after performing physical exercise for one hour, increasing the intensity of the exercise after the first half and hour, from 11 to 13 km h^{-1}. Two AuPt systems were interrogated in this study. 1/8 dilution of the original sweat samples were analysed with the first sensing system. The obtained response profile was then compared with the one obtained from the interrogation of the second AuPt system with the corresponding undiluted sweat samples. Samples were collected after the first 30 minutes (11 km h^{-1}) and after the last 30 minutes (13 km h^{-1}) of the exercise program. The protocol for the collection of sweat samples for this part of the study is outlined in section 3.4.8. Given the fact that samples analysed in this experiment were collected after performing intense physical exercise for a longer time than in previous studies, it was expected that the lactate levels in sweat would rise from the levels observed in previous studies and potentially over the normal average of 20 mM, as the state of hypoxia was prolonged. For this reason, the AuPt system interrogated with diluted sweat samples was first calibrated by adding lactate solutions in the range of 1-5 mM, which correspond to 8-40 mM lactate in undiluted samples. The AuPt system interrogated with the corresponding undiluted samples was first calibrated with lactate solutions in the range of 10-20 mM in order to assess the capability of the sensing system to detect fluctuations in lactate levels between these samples. After the sequential additions of the lactate solutions in PBS, the sensors were set to polarise again with PBS and after this, sweat solutions collected from the same subject after exercising for 30 minutes and 1 hour were added as described previously. The current outcome obtained from the analysis of each sample was normalised by subtracting the baseline current obtained with PBS only. The concentration of lactate in the 8-fold diluted samples in Figure 6.8a and in the undiluted samples in Figure 6.8b was calculated using the calibration curve constructed for each sensor. The concentration of the corresponding undiluted samples in Figure 6.8a was subsequently calculated by multiplying the predicted concentration of lactate in the diluted sample by a factor of 8. The

chronoamperometric response profiles from both analyses are shown in Figure 6.8. The comparison and RSD coefficients calculated between lactate levels in undiluted samples, predicted from the corresponding dilutions in the first sensor and estimated from the calibration curve in the second sensor, for both collection times are shown in Figure 6.9.

As the results show, the response profile obtained from the analysis of the diluted sweat sample (Figure 6.8a) exhibited a 2.17-fold increase in lactate levels between 30 minutes and 1 hour after the start of the exercise. Such an observed increase in lactate levels agrees with results reported by previous studies, which have shown that the performance of intense physical activity obliges muscles to work without a sufficient oxygen supply, creating a temporary state of hypoxia under which the anaerobic path becomes the predominant energy-providing metabolic pathway in which glycogen and glucose are progressively split into the degradation product lactic acid, the levels of which in sweat increase over time. Given this, results showed the capability of the developed sensing device to detect these lactate level fluctuations in diluted sweat samples.

This increase in lactate levels in sweat caused by the performance of prolonged physical exercise at different intensities was also observed when analysing the corresponding undiluted samples from the same subject with a second AuPt sensing system (Figure 6.8b). The comparison between lactate levels predicted from the diluted sample and the ones obtained from the analysis of the undiluted sample are shown in Figure 6.9. As the results show, the calculated lactate concentrations in the sample obtained from the analysis of diluted sweat and the real concentration obtained from the analysis of the undiluted samples are very similar for the sample obtained after 30 minutes of exercise. The RSD between these values was 3.62%. However, the difference between these values for samples collected after 1 hour was greater, since the analysis of the diluted sample calculated a real concentration of 27.9 mM and the analysis of the undiluted sample indicated a lactate concentration of approximately 19 mM, the RSD between these values being 26.94%. This preliminary study indicated a

significant decrease in current response over a relatively short period of time with the analysis of undiluted sweat samples.

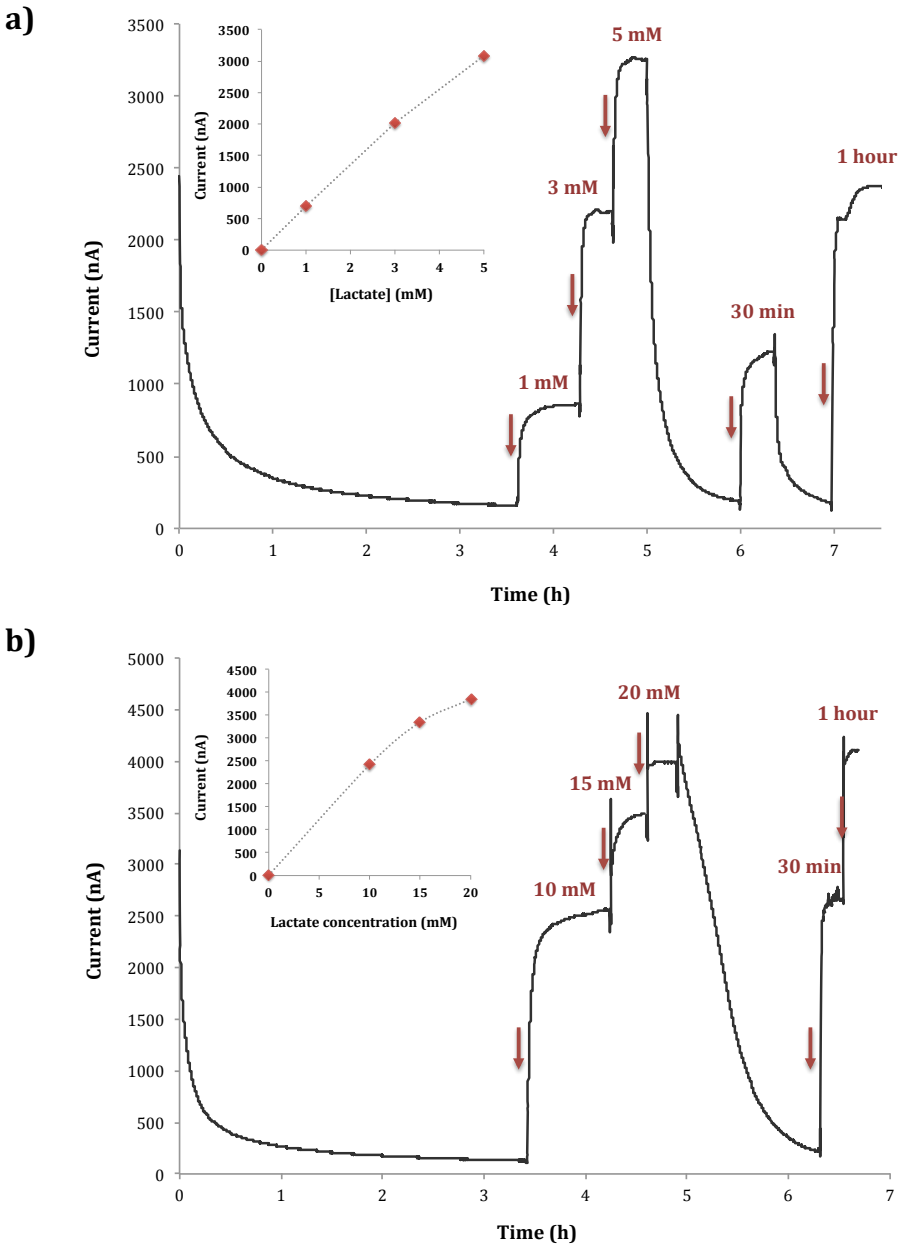

Figure 6.8. Chronoamperometric response over additions of lactate solutions in PBS only followed by measurements of (a) diluted human sweat samples (1/8 in PBS) and (b) the corresponding undiluted samples collected after the first 30 minutes (11 km h^{-1}) and the last 30 minutes (13 km h^{-1}) of intense physical exercise. The insets represent the calibration curve of each sensor performed with the initial additions of lactate in PBS.

The arrows indicate the moment at which each solution (lactate in PBS or sweat samples) was put into contact with the sensing system for their analysis.

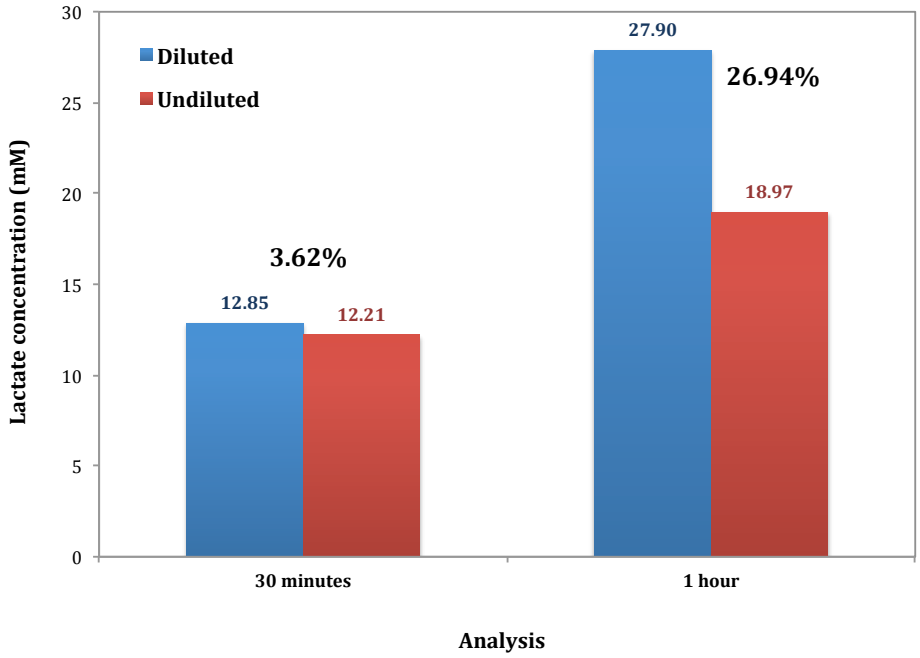

Figure 6.9. Bar diagram representing the analysis of diluted (1/8 in PBS) and undiluted human sweat samples collected after the first 30 minutes (11 km h^{-1}) and last 30 minutes (13 km h^{-1}) of intense physical exercise, plotted against the lactate concentration estimated in the diluted and undiluted sweat samples.

The first hypothesis for this decrease in current response when analysing the second undiluted sample, collected after 1 hour of exercise, was that a progressive adsorption of low molecular weight substances present in the sweat solution to the surface of the electrode over time had occurred. This adsorption would have compromised the electrochemical properties of the electrodes by reducing their active surface area, thus hindering the oxidation of H_2O_2 produced by the enzymatic reaction with this leading to a lower current response for the lactate concentration in the sample.

A second hypothesis was based on the fact that higher molecular weight substances present in the sweat sample flowing through the enzyme laminate could have progressively blocked the pores of the membranes over time, leading to an increasing diffusional hindrance of the flow of solution, thus limiting the amount of lactate reaching the active site of the enzyme.

The third hypothesis suggested was that the activity of the enzyme LOD had been compromised when being exposed to the undiluted sweat samples. This could have occurred, in first place, due to a significant change in the ionic strength of the solution, with a much higher concentration of ions than that of PBS. The ionic strength of a solution (I) is given by half of the total sum of the concentration (c_i) of every ionic species (i) present in the solution times the square of its charge (z_i). This is summarised by the following equation:

$$I = 0.5 \sum (c_i \cdot z_i^2)$$

It has been reported that changes in the ionic strength of a solution can affect the isoelectric point of an enzyme and thus, its catalytic properties, structure and activity due to denaturation(Cao, 2006). Secondly, the enzyme's activity could have been compromised due to the presence of toxic or harmful compounds in the sweat solution. Finally, it was thought that a significant pH change had occurred, inactivating the enzyme through changes in its isoelectric point in a similar manner to the ionic strength of the sweat solution.

In order to discard this third hypothesis, an AuPt sensing system with enzyme laminate containing LOD was interrogated with consecutive additions of the same undiluted sweat sample from the previous subject studied for a time length of 4 hours. The aim of this test was to assess the stability of the current response, and thus the catalytic properties of the enzyme and/or electrochemical properties of the electrode system, over repeated additions of undiluted human sweat. In this test, the sensing system was exposed repeatedly to 0.8 ml of the same sweat sample following the method previously described. Between different measurements, the sensor was transferred back to a 25-ml beaker with PBS. This was done firstly to bring the current response back to the baseline. Secondly, it was thought that the exposure of the sensor to PBS would also rinse the membrane, solving or at least delaying the effect that adsorption of small molecules to the surface of the electrode or the blocking of the membrane pores would have on the response of the sensor. However, if the exposure to undiluted sweat samples was compromising the stability and activity of the enzyme due to its

denaturalisation, this in many cases is an irreversible process and therefore the rinsing steps would not fix this problem. Therefore, in this case a significant decrease in current response would be observed with different additions/concentrations of the sweat solution. The chronoamperometric response obtained from the described analysis with the relative percentage of decay in current response at each measurement is shown in Figure 6.10.

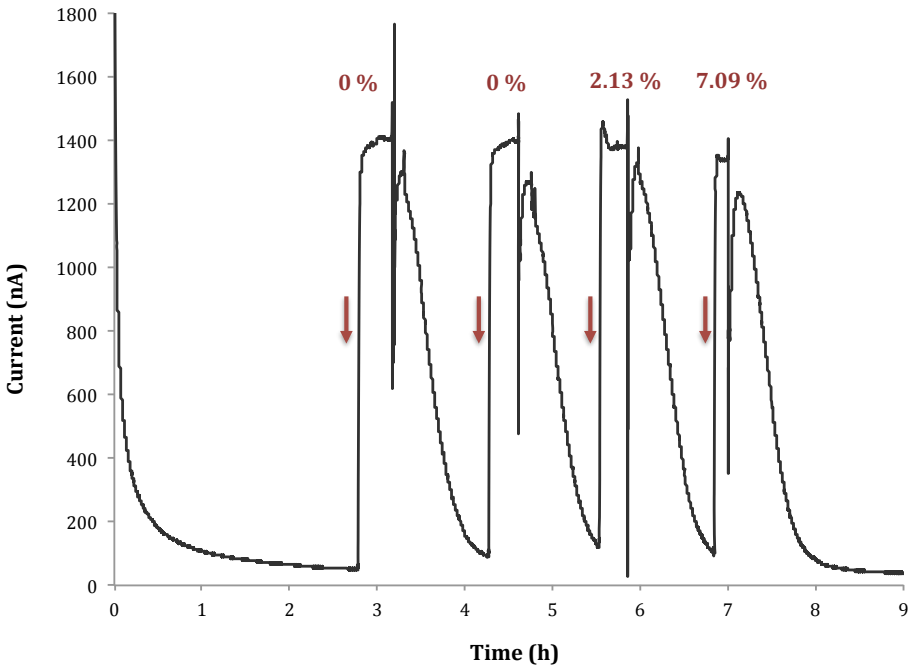

Figure 6.10. LOD steady-state current response over consecutive additions of undiluted human sweat sample.

The arrows indicate the moment at which the PBS solution was extracted from the beaker and the undiluted sweat solutions were added to the surface of the sensing system.

Results showed a relatively high stability of the sensor response over repetitive additions of undiluted human sweat. The RSD between measurements was 3.42% due to a gradual decrease of response after the second sample measurement. This decrease from the current response obtained for the two first measurements was 2.13% for the third measurement and 7.09% for the fourth one.

As results indicate, consecutive additions of undiluted sweat samples over four hours led to a decrease in current response of up to 7.09%. This would indicate that the activity of the enzyme was not compromised in the presence of undiluted sweat or, in the event that it was, this decrease in activity was occurring at a relatively slow rate. However, it was observed that when the sensor was transferred back to PBS after each measurement (indicated with arrows in Figure 6.10), the polarisation of the sensing system took longer than usual. After the addition of PBS, the current response experienced a slight increase after which it decreased at a very slow rate until a baseline current was reached. This indicated that the most probable cause for the observed decrease in response was the progressive decay of the electrochemical properties of the electrode system due to the adsorption of small molecules to its surface or the progressive blockage of the pores of the laminate membranes. However, further research will need to be carried out in this area in order to investigate the effect of different undiluted sweat samples on the electrochemical response of the sensing system over time, to identify with certainty the cause for this decrease in current response and explore means to overcome this limitation on the sensor performance when analysing undiluted sweat samples.

6.3.1 Physical characterisation of AuPt electrode surface through SEM

The reason for the study described in this section lies in the need for investigating the cause(s) for the decrease in the current response observed in the analysis of undiluted human sweat samples with the developed sensing system, as described in the previous section. It was considered that a possible way to achieve this would be through the physical characterisation of the surface of the electrode, specifically the working electrode, before and after the analysis of undiluted human sweat samples as well as determining the presence or absence of molecules that could be producing electrode fouling. The presence of these molecules on the biosensor can be confirmed by scanning electron microscopy (SEM), following the protocol outlined in section 3.4.7., which allowed for the observation of the

electrode surface and differentiation from the non-conductive adsorbed compounds present on its surface originating from the biological sample. This was done in order to explore possible effects of electrode fouling produced by the adsorption of low-weight molecules present in the sample. Since the enzyme laminate is immobilised to the surface of the working electrode, only solutes that will have diffused through this enzyme laminate into the space between the laminate and the electrode surface will be observed.

Two AuPt electrode systems were investigated in this experiment. Both laminates for these sensors were constructed according to the protocol outlined in section 3.4.3 and with the optimised conditions obtained studied in Chapter 5. The constructed sensors were electrochemically interrogated following the chronoamperometry protocol, outlined in section 3.4.2, using the AuPt electrode system as described in section 3.4.6.2.ii. Both sensors were placed in two separate 25-ml beakers and set to polarise with 15 ml of PBS at +650 mV until a baseline was reached. After the polarisation step, both sensors were placed horizontally on a flat surface and 0.8 ml of the same undiluted sweat sample were placed on top of the electrode system, until fully covered, for three hours. After this, the sweat sample was removed from one of the sensors and the enzyme laminate was removed with the sensor being placed horizontally until dry. The second sensor was transferred back to a 25-ml beaker with 15 ml of PBS for 30 minutes, after which the enzyme laminate was removed with the sensor again being placed horizontally until dry.

After drying, the surface of the working electrodes from both AuPt systems was explored through SEM according to the protocol outlined in section 3.4.7. Two magnifications were employed in this study: 1000x and 5000x. Figure 6.11 provides a comparison between scanning electrode photographs from both electrode surfaces after their exposure to the biological sample (with and without rinsing) at different magnifications and the surface of a bare AuPt electrode system prior to its analysis, which was shown in Figure 4.12 from Chapter 4, as a comparative control.

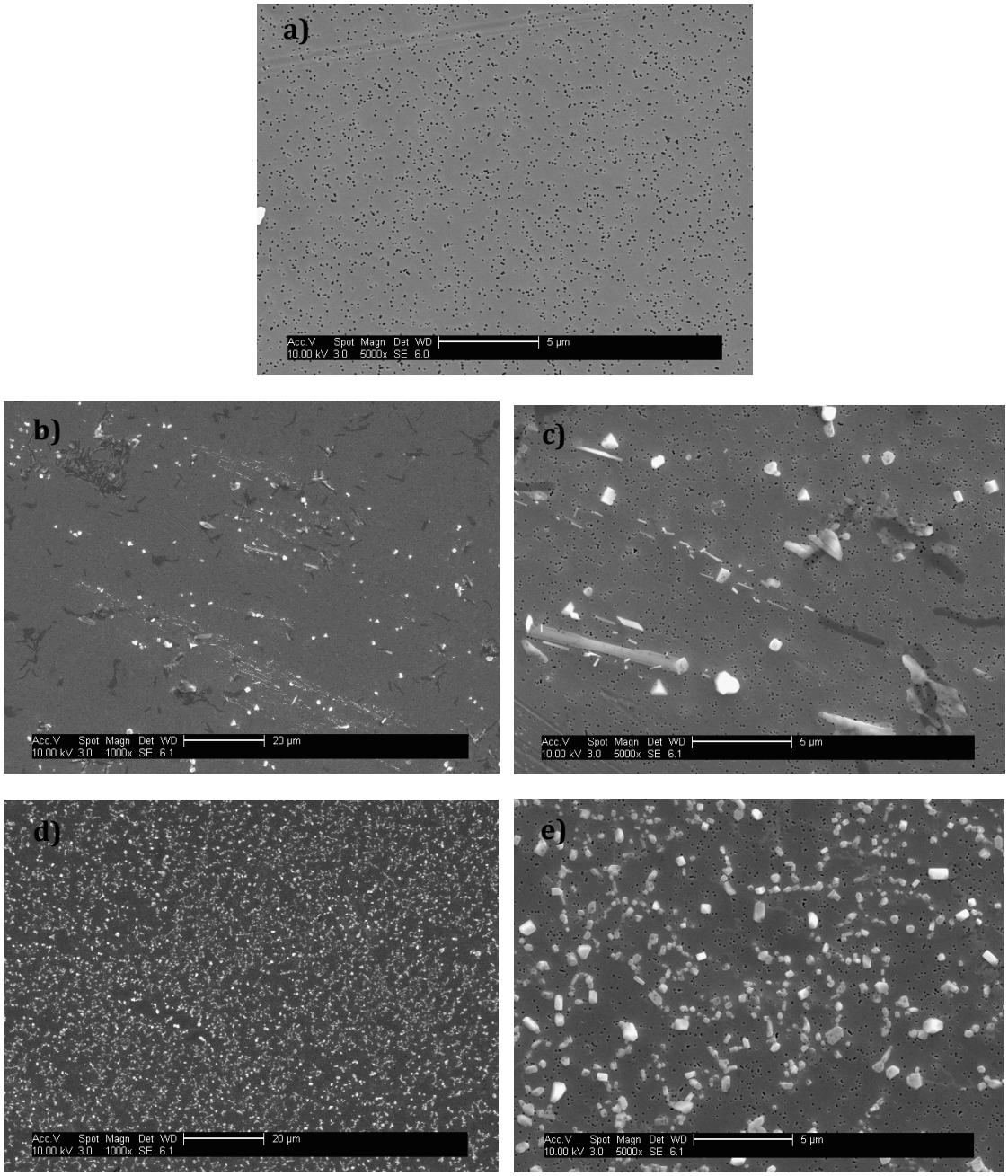

Figure 6.11. Electron microphotographs of the surface of the Pt working electrode from the developed AuPt sensing system (a) before the experiment, (b, c) after the analysis of undiluted sweat including rinsing steps and (d, e) without rinsing steps.

Figures a, b and d show 1,000x magnification images and figures c and e show a magnification of 5,000x.

Results showed the presence of sporadic material deposits on the surface of the rinsed electrode (Figure 6.11b,c), whose shape and relative size to the 0.1-μm pores of the electrode surface – a highly porous polycarbonate membrane sputter coated with Pt – can be better appreciated at a 5,000x magnification (Figure 6.11c). However, when the non-rinsed electrode was examined under the scanning electron microscope, a much higher surface coverage by these deposits was observed (Figure 6.11e,d). These results suggested that the prolonged exposure of the developed sensing system to undiluted sweat samples produces the diffusion of large amount of solutes through the enzyme laminate which could compromise the electrochemical properties of the electrode and hindering the oxidation of H_2O_2. Alternatively, rinsing the sensing system with PBS appears to facilitate the diffusion of part of these solutes out of the space between the electrode surface and the laminate.

The results presented in this section are preliminary and therefore, further investigations should be carried out in this area in order to investigate through ESEM whether components present in sweat cause the obstruction of the enzyme laminate pores on their way through, hindering the diffusion of lactate towards the active site of the enzyme and thus, contributing to the decrease of current response over time observed in previous experiments (Figures 6.8-6.10).

Further work should also focus on minimising electrode fouling produced by the adsorption of compounds from the biological sample. One approach to achieve this would be through reducing the pore-size of the membranes employed in the construction of the laminate in order to reduce the size exclusion limit of the solutes from the sample diffusing towards the electrode surface. Another approach that should be further studied is the coating of the electrode surface with a polymer to protect it and minimise blocking and fouling by irreversible adsorption of compounds present in complex biological samples. Previous authors have reported the anti-fouling properties provided by Nafion by coating the electrode surfaces with this polymer (Brett and Fungaro, 2000; Zhang *et al.*, 2013). As was

previously mentioned, next chapter will describe preliminary work performed on the study of Nafion as a potential polymer for the modification of AuPt electrode surface. Therefore, regardless of this polymer being studied in the present work for reducing interferences from oxidising species in the sample, further work should also focus on investigating the effect of the Nafion-modified AuPt electrodes described in this project for protecting the electrode surface and this way minimise those interferences produced by adsorption of compounds present in the sweat samples under analysis.

6.4 Conclusions

The objective behind the work presented in this chapter was to test the performance of the developed sensing design and show proof-of-principle operation for the monitoring of sweat lactate from both diluted and undiluted human samples.

Initial studies were performed on a synthetic sweat solution, prepared by dissolving the relevant compounds present in sweat in PBS pH 7.4, including ascorbic acid and uric acid, which as reported in the literature and according to our own studies can interfere with the current response signal. The sensing design showed a relatively high selectivity for lactate with an RSD of 5.3% between lactate solutions in PBS only and the synthetic sweat stock solution.

It was also shown that the sensor could detect lactate at physiologically relevant concentrations in the presence of reported interfering components, showing promise for the subsequent monitoring of lactate in human sweat samples.

The sensing system developed within this work was tested with 1/8 diluted human samples, which allowed for both assessing the performance of the sensor in a more complex solution as well as analysing the samples under study. The sensor exhibited consistency, and thus reliability, in the measurement of diluted sweat samples after its calibration. Differences in lactate concentrations were observed

between different body areas studied and also at different exercise times, which in both cases are in line with studies reported by the literature.

The capability of the sensing system for detecting lactate level fluctuations between different exercise times at different intensities in undiluted samples was also shown. However, the sensor's performance did diminish significantly with time of exposure to the undiluted sample.

Subsequent analyses performed in undiluted samples pointed to a progressive passivation of the electrode surface and/or fouling the laminate pores by substances present in the sample as the most likely cause/s of the decrease of response over time.

The surface of electrode systems after their exposure to undiluted sweat sample – with and without rinsing – was explored through SEM and compared. The exposure of the sensor to undiluted sweat sample appeared to produce the diffusion of some of its components through the enzyme laminate towards the electrode surface, potentially compromising its electrochemical properties. However, a rinsing step in PBS reduced the amount of these compounds, suggesting their diffusion back into the sample solution.

Further work will be required to investigate the possibility of components from sweat samples under analysis fouling the surface and pores of the enzyme laminate, thus contributing to a lower current response by hindering the flow of lactate towards the active site of the enzyme.

Further work will also be needed to minimise the fouling of the electrodes by the adsorption to their surface of those molecules diffusing through the enzyme laminate. This could be achieved by reducing the pores of the membranes employed in the construction of the enzyme laminate or by exploring the potential of electrode-surface modification with polymers such as Nafion.

CHAPTER 7

ELECTRODE-SURFACE MODIFICATION FOR IMPROVING THE SELECTIVITY OF THE SENSING SYSTEM

7 Electrode-surface modification for improving the selectivity of the sensing system

7.1 Introduction

This chapter describes and discusses the findings from a preliminary study investigating the feasibility of modifying the surface of the AuPt electrode system with Nafion, with the aim of evaluating the capability of the polymer to increase the sensor selectivity for lactate by reducing interferences produced by oxidising species present in sweat samples. The chapter will focus on the study of ascorbic acid and uric acid as interfering compounds.

7.1.1 Selectivity as a challenge in the development of diagnostic devices

In the development of diagnostic devices for clinical diagnosis, selectivity and sensitivity play critical roles. Biosensors, which are designed to meet these requirements, are generally highly selective due to the innate binding affinity of the immobilised recognition element for its substrate (Grieshaber *et al.*, 2008). Among these, electrochemical biosensors combine the high specificity provided by the biological recognition process with a well-known high sensitivity to the processes that take place on the surface of the electrodes (Ronkainen *et al.*, 2010; Rozlosnik, 2009). Chapter 5 described the steps followed to improve the sensitivity of the AuPt sensor, which was achieved by improving the stability of the enzyme in the cross-linking matrix and by increasing its concentration. Enzyme stability also plays an important role in the selectivity of the sensor. Nevertheless, enzyme-based electrochemical biosensors are widely known for their excellent selectivity due to the natural specificity of the enzyme for its substrate. However, when analysing biological samples, the presence of oxidisable species – such as ascorbic acid and uric acid – can affect the electrochemical signal and the selective

monitoring of the analyte, leading to the obtaining of false positives, which are especially undesirable in a clinical setting.

7.1.2 Ascorbic acid and uric acid as interfering compounds in sweat samples

For the development of the sensing system described in this thesis, one of the challenges is to assess the presence of interfering signals produced by the oxidation of compounds present in sweat samples (i.e. ascorbic acid and uric acid) and how to lower these interferences, in order to determine the value of lactate levels in real sweat samples from subjects, and potentially patients, under study.

Section 6.2 described and discussed preliminary studies performed to assess the presence of interference effects from uric acid and ascorbic acid on the electrochemical signal of the sensor when monitoring lactate. This study was performed using the median values of the interfering compounds, reported by a comprehensive review on the composition of human sweat (Stefaniak and Harvey, 2006). Results showed that no significant interferences from these compounds were found in the electrochemical response for lactate. However, concentrations of these compounds above their median value should also be considered and studied, as these could increase the background current response and affect the selectivity of the measurement. Table 7.1 summarises the median, minimum and maximum concentration of uric acid and ascorbic acid in human sweat reported by the literature.

Table 7.1. Composition of ascorbic acid and uric acid in human sweat (Harvey *et al.*, 2010)

Compound	Median concentration (M)	Minimum concentration (M)	Maximum concentration (M)
Uric acid	5.9×10^{-5}	4.2×10^{-6}	4.8×10^{-3}
Ascorbic acid	1.0×10^{-5}	1.1×10^{-7}	3.6×10^{-5}

It has to be noted that the values reported in the study mentioned above were obtained from non-exercise induced sweat secreted by healthy adult humans. However, it has been reported that patients developing bedsores can present increased levels of uric acid in sweat (Bader *et al.*, 2005; Bader and Oomens, 2006). Uric acid is the main by-product from the catabolism of purines and, together with other nitrogen metabolites (urea, creatinine) is excreted through the kidneys, this being one of the main functions of these organs(Huang *et al.*, 2002). Moreover, people suffering from high blood pressure, cardiovascular diseases or gout may present increased levels of uric acid, which is one of the biomarkers for their diagnosis (Alderman, 2002; Gagliardi *et al.*, 2009). Alternatively, it has been reported that patients suffering from hypoproteinemia (inadequate protein levels) exhibit lower resistance to pressure ulcer development (Maklebust and Sieggreen, 2001). This usually requires the administration of high protein supplements such as ascorbic acid in the form of vitamin C in order to increase the resistance of the patient to tissue damage (Sasöz *et al.*, 2002; Burns *et al.*, 2010). For all of the aforementioned conditions, levels of uric acid and ascorbic acid may be present in levels above their reported median value in hospitalised subjects, to which the sensor developed in this thesis would potentially be applied. Therefore, the present chapter considers concentrations of uric acid and ascorbic acid 34 and 30 times respectively, above their median reported value.

7.1.3 Ion-exchange polymers. Nafion.

It has been reported that by combining the bioselectivity and specificity of enzymes with the chemical and physical properties of numerous methods for the modification of the surface of the electrodes, it is possible to create a new generation of high-performance biosensing devices (Putzbach and Ronkainen 2013). Among these, the use of ion-exchange polymers has attracted a great deal of interest in many applications due to their semi-permeable characteristics, which allow the passage of the required analyte to the surface of the electrode while preventing that of other substances (due to their charge and/or size) that could

adsorb on to the surface, compromising its electrochemical properties, or undergo electrode reaction (Gouveia-Caridade and Brett, 2008). This use of ion-permselective layers, commonly between the sensing layer and the electrode surface, is a widely employed approach to lower interferences in peroxide-based electrochemical biosensors (Abdul-Aziz and Wong, 2011). Different kinds of materials have been employed and studied for this purpose. Among these, Nafion – an anionic membrane – has been widely used for minimising interferences in electrochemical sensors produced by the oxidation of uric acid and ascorbic acid (Rassaei *et al.*, 2014; Brown and Lowry, 2003). Other examples are cellulose acetate (Bindra *et al.*, 1991; Madaras *et al.*, 1996) and polysiloxane films (Jung and Wilson, 1996).

Nafion is a sulfonated fluoropoloymer with a hydrophobic backbone of polytetrafluoroethylene attached to hydrophilic side chains terminated with sulfonic end groups (Figure 7.1). This negatively charged polymer is commonly used because of its biocompatibility with enzymes due to its hydrophobic and hydrophilic properties. It is also chemically inert and exhibits relatively low adsorption levels of species from the sample solution (Ambrózy *et al.*, 2013).

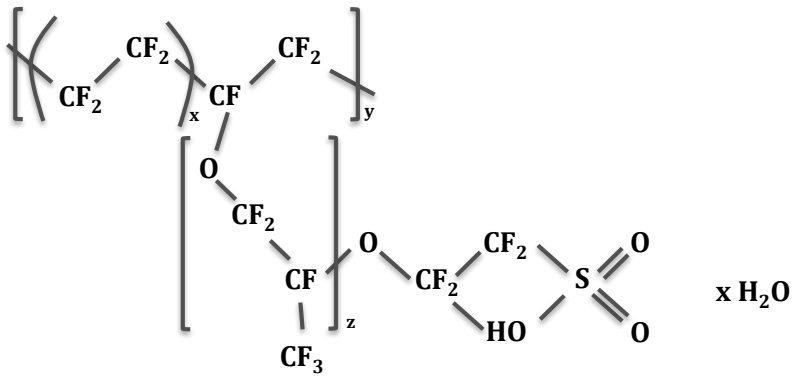

Figure 7.1. Molecular structure of Nafion.

7.1.4 Application of Nafion in the developed AuPt sensing system

In the work presented in this chapter, Nafion will be used in the developed AuPt system to modify the surface of the electrodes and be evaluated for its capability of reducing interferences from oxidative species – ascorbic acid and uric acid – and enhancing the selectivity of the lactate sensor.

Although the dip coating method is a fast and simple technique to cover the surface of electrodes with Nafion, the volume of sample applied and the thickness of the resulting layer, is unknown and therefore may vary between sensors, thus affecting the reproducibility of the response. Alternatively, the pipetting method is more reproducible since the volume of sample is known and can be controlled. The pipetting of Nafion on the surface of the electrode needs to be performed with a steady hand in order to avoid touching the electrode surface. Furthermore, the volume applied has to be considered since too much fluid could cause flooding from the sample out of the working electrode surface and into other components of the electrode system. The pipetting method was therefore chosen as the preferred procedure for coating the working electrode of the AuPt system with Nafion.

Since lactate, as uric acid and ascorbic acid, is an anion, it was considered that coating with Nafion any of the membranes, or both, would cause detrimental effects on lactate measurement, due to the close proximity and contact in some areas between the Nafion layer and the cross-linking mixture containing the LOD enzyme, potentially hindering the interaction between lactate and the active site of the enzyme. For this reason it was decided to prepare the AuPt sensors interrogated in the present chapter by applying Nafion to the surface of their Pt working electrodes. With this configuration (Figure 7.2a), the enzyme is separated from the Nafion film by the bottom membrane of the laminate, allowing for the lactate to access the enzyme layer and interact with the active site of the enzyme without coming into contact with the Nafion layer. The H_2O_2 produced from the enzyme reaction, along with other compounds present in the sample such as ascorbic acid and uric acid, would flow through the laminate towards the Nafion-

coated electrode surface. Here, H_2O_2 – of low molecular weight – would pass through the Nafion layer and be oxidised on the electrode surface, while the passage of both interfering compounds would be hindered due to their negative charge. In the present study, the Pt electrode surface of the AuPt sensing system was coated with 1 or 2 layers of Nafion. The resulting modified electrode surface was examined using a scanning electron microscope at 1,000x magnification and a homogeneously covered surface was observed with pore diameters between 1–5 μm in some areas, as shown in Figure 7.2b,c.

The protocol for the application of Nafion on the electrode surface is outlined in section 3.4.9. Sensors were prepared with 1 or 2 layers of 5% Nafion over the catalytic Pt layer of the electrode and the performance between these resulting systems was compared. The experiments conducted for this part of the project were performed on the AuPt electrode system, constructed as described in section 3.4.6.2.ii. Enzyme laminates were prepared, with and without LOD, following the protocol outlined in section 3.4.3 and using the optimised conditions for its preparation described in Chapter 5. The resulting systems were electrochemically interrogated following the chronoamperometry protocol described in section 3.4.2. A range of ascorbic acid concentrations, from 0.01 to 0.3 mM, and uric acid concentrations, from 0.059 to 2 mM, were analysed. Some of these solutions contained 1 mM lactate.

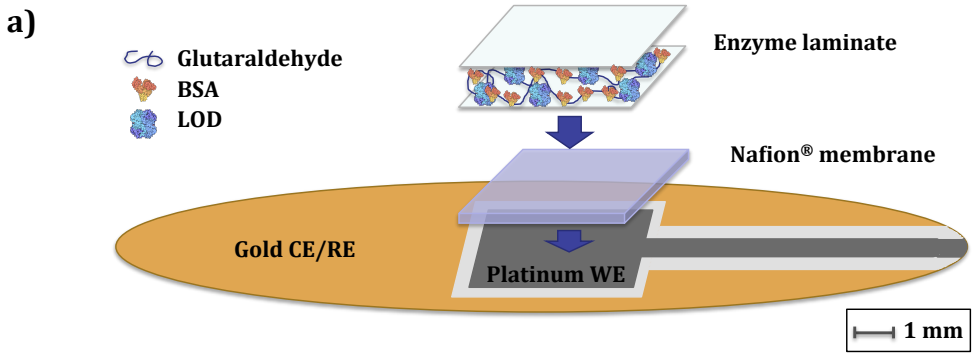

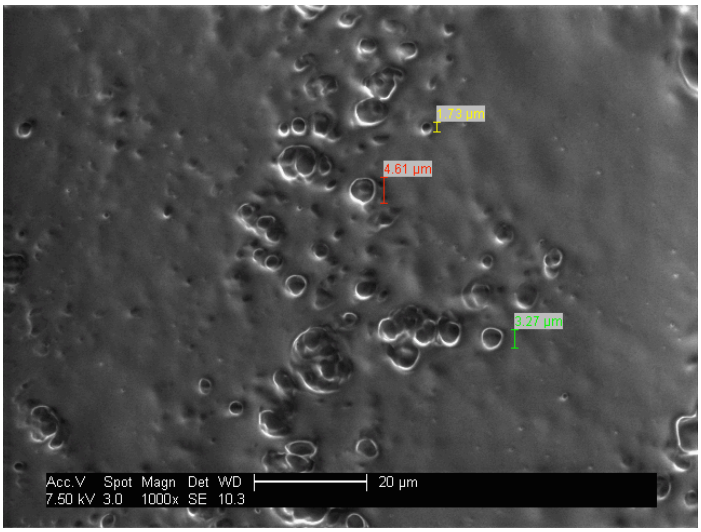

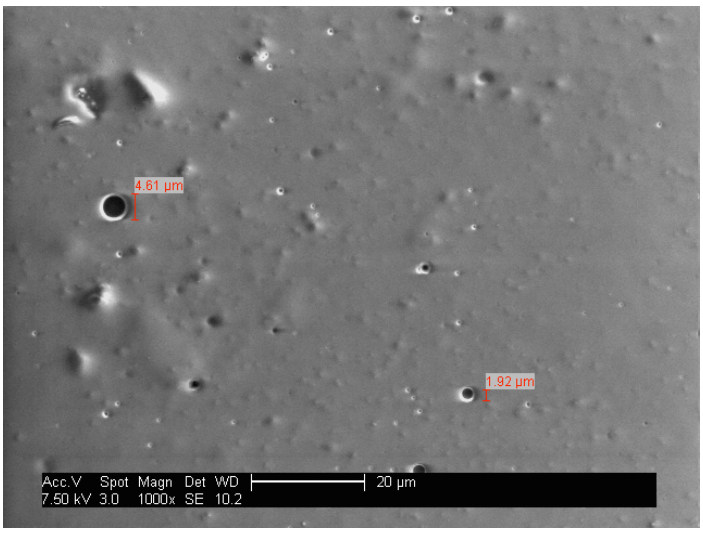

Figure 7.2. (a) Schematic view of the mechanical support of the AuPt system with the application of a Nafion layer on the surface of the Pt WE. (b,c) Electron microphotographs of the surface of a double Nafion layer covering the Pt WE.

7.2 Minimising interferences for ascorbic acid (AA)

The present section describes preliminary studies performed on the evaluation of Nafion as a means of minimising ascorbic acid interference during the monitoring of lactate by the developed AuPt system, with the aim to improve the selectivity of the sensor.

Two different sets of experiments were carried out for this study. The first one consisted of a peak test in which the AuPt sensing system was interrogated with different concentrations of ascorbic acid in 1 mM lactate. Such a low concentration of lactate was chosen, in the first place, so the oxidation of ascorbic acid was minimally masked by the oxidation of H_2O_2, as observed in preliminary studies performed with higher concentrations of lactate; and secondly so that any effect exerted by the Nafion layer(s) on the flow of lactate into the laminate and/or the passage of H_2O_2 towards the electrode surface could be better appreciated. The second set of experiments consisted of the consecutive addition of a stock solution of ascorbic acid in PBS, in order to study the sensor response for a range of concentrations of the metabolite. This second test provided a more accurate examination of small variations in current response for the range of ascorbic acid concentrations tested, with no possible interferences produced by the simultaneous oxidation of H_2O_2.

7.2.1 Peak test for ascorbic acid and lactate

For the study described in this section, AuPt laminate sensors were prepared and interrogated as described in section 7.1.4, without Nafion and with 1 and 2 coats of the polymer. The solutions employed for the interrogation of the sensors consisted of the preparation of 1 mM lactate in the presence of a range of ascorbic acid concentrations, from 0.01 to 0.3 mM, in PBS pH 7.4. The composition of each of these solutions are summarised in Table 7.2.

Table 7.2. Composition of the solutions tested for the analysis of ascorbic acid at different concentrations (0–0.3 mM) in 1 mM lactate.

Solution	[Lactate] (mM)	[Ascorbic acid] (mM)
1	1	0
2	1	0.01
3	1	0.036
4	1	0.1
5	1	0.3

The resulting AuPt sensing systems were placed in a 25-ml beaker with 15 ml of PBS and polarised at +650 mV until a baseline was reached. After this, 15 ml of each solution described in Table 7.2 were consecutively added to the beaker, where the sensor was placed, for their analysis. Prior to the addition of each sample, the sensor was exposed to PBS only, to rinse the membrane and repolarise the sensor. The 1 mM lactate solution in PBS was added first in order to obtain a control current response at 0 mM ascorbic acid, to which subsequent responses could be compared. The resulting current response of each solution analysed was recorded and normalised by subtracting the baseline current obtained with PBS only. The current response produced by each concentration of ascorbic acid was obtained by subtracting the normalised current response for 1 mM lactate in PBS (Table 7.2, Solution 1) and represented in a chart.

The first experiment performed was carried out using an AuPt sensing system constructed with no Nafion on the electrode surface in order to obtain a control current response for each ascorbic acid concentration (Figure 7.3a) to which corresponding current responses obtained by interrogating sensors with one and two layers of Nafion could be compared (Figure 7.3b).

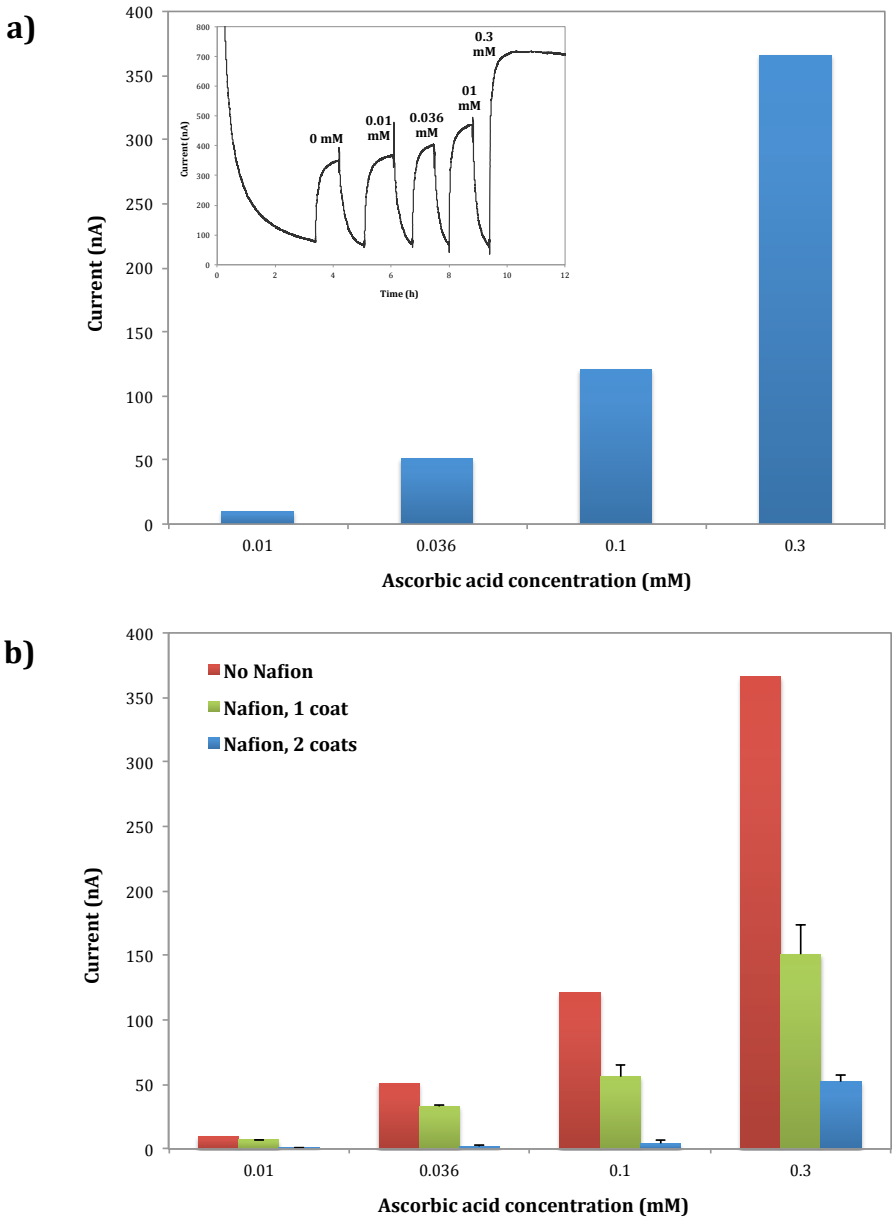

Figure 7.3. Bar diagrams obtained from the analysis of ascorbic acid (0.01–0.3 mM) with 1 mM lactate, representing (a) the control current obtained with no Nafion layer on the WE (inset with the chronoamperometric response of the AuPt sensor analysed) and (b) its comparison with the response obtained with the application of 1 and 2 coats of the polymer.

Results obtained from the analysis of the constructed AuPt sensing system with no Nafion on the electrode showed an increase from the control current response of 10 nA for 0.01 mM AA, 51 nA for 0.036 mM AA, 121 nA for 0.1 mM AA and 366 nA for 0.3 mM AA (Figure 7.3a). The current response obtained from the interrogation of the AuPt system with one layer of Nafion on the surface of the WE

showed a decrease in response of between 30-58% for the range of ascorbic acid concentrations analysed. Moreover, the application of 2 layers of Nafion on the electrode surface diminished this response for ascorbic acid in the range of 85.8–96.7% (Figure 7.3b). The decrease in response for each concentration of ascorbic acid with the application of 1 and 2 layers of Nafion on the electrode is summarised in Table 7.3.

No effect of the application of Nafion layers on the current response obtained for 1 mM lactate was observed. The current response did not exhibit a clear decrease with the application of 1 and 2 Nafion layers with respect to that obtained with the electrode system with no Nafion.

Table 7.3. Decrease in current response, with respect to the control, observed from the peak study performed for ascorbic acid at different concentrations (0.01–0.3 mM) with the application of 1 and 2 layers of Nafion on the WE.

[Ascorbic acid] (mM)	Nafion, 1 coat	Nafion, 2 coats
0.01	30.0%	90.0%
0.036	35.3%	96.1%
0.1	53.7%	96.7%
0.3	58.7%	85.8%

7.2.2 Successive additions of ascorbic acid

For the next study performed on ascorbic acid, AuPt laminate sensors were prepared and interrogated as described in section 7. This time, however, laminates were constructed without LOD enzyme since the solutions to be analysed did not contain lactate. As with the previous section, three sets of AuPt sensors were prepared: without Nafion and with 1 and 2 layers on the electrode surface. The resulting sensors were interrogated with successive additions of 0.03 mM ascorbic acid up to a concentration of 0.3 mM. This was achieved by polarising the AuPt sensing system at +650 mV in a 25-ml beaker with 15 ml of PBS and after a current baseline was reached, performing consecutive additions of 100 μl of a 4.5 mM

stock solution of ascorbic acid. The resulting current response with each addition of ascorbic acid was recorded and normalised by subtracting the baseline current obtained with PBS only and the values were represented in Figure 7.4.

As with the previous study, the first experiment performed was carried out using an AuPt sensing system constructed with no Nafion on the electrode surface in order to obtain a control current response for each ascorbic acid addition (Figure 7.4a) to which corresponding current responses obtained with one and two layers of Nafion could be compared (Figure 7.4b).

Results obtained from the interrogation of the AuPt sensing system with no Nafion showed an increase in current response for increasing concentrations of ascorbic acid. However, the current response recorded for these concentrations was significantly lower than the corresponding values obtained from the previous study (Figure 7.3). It was thought that this was due to the low concentrations of ascorbic acid employed in the study and a possible interference in the current response by the simultaneous oxidation of H_2O_2 taking place at the electrode. The application of the first layer of Nafion on the AuPt sensing system showed a decrease in current response of between 40.9-59% with respect to the control current response (AuPt with no Nafion layer) with the exception of 0.03 mM AA, for which the response decreased by 98.3%. Additionally, the application of a second Nafion layer on the electrode surface led to a decrease in response of 73.8-85.2% and 100% for 0.03 mM AA. The decay in response for each ascorbic acid concentration with the application of 1 and 2 layers of Nafion on the electrode is summarised in Table 7.4.

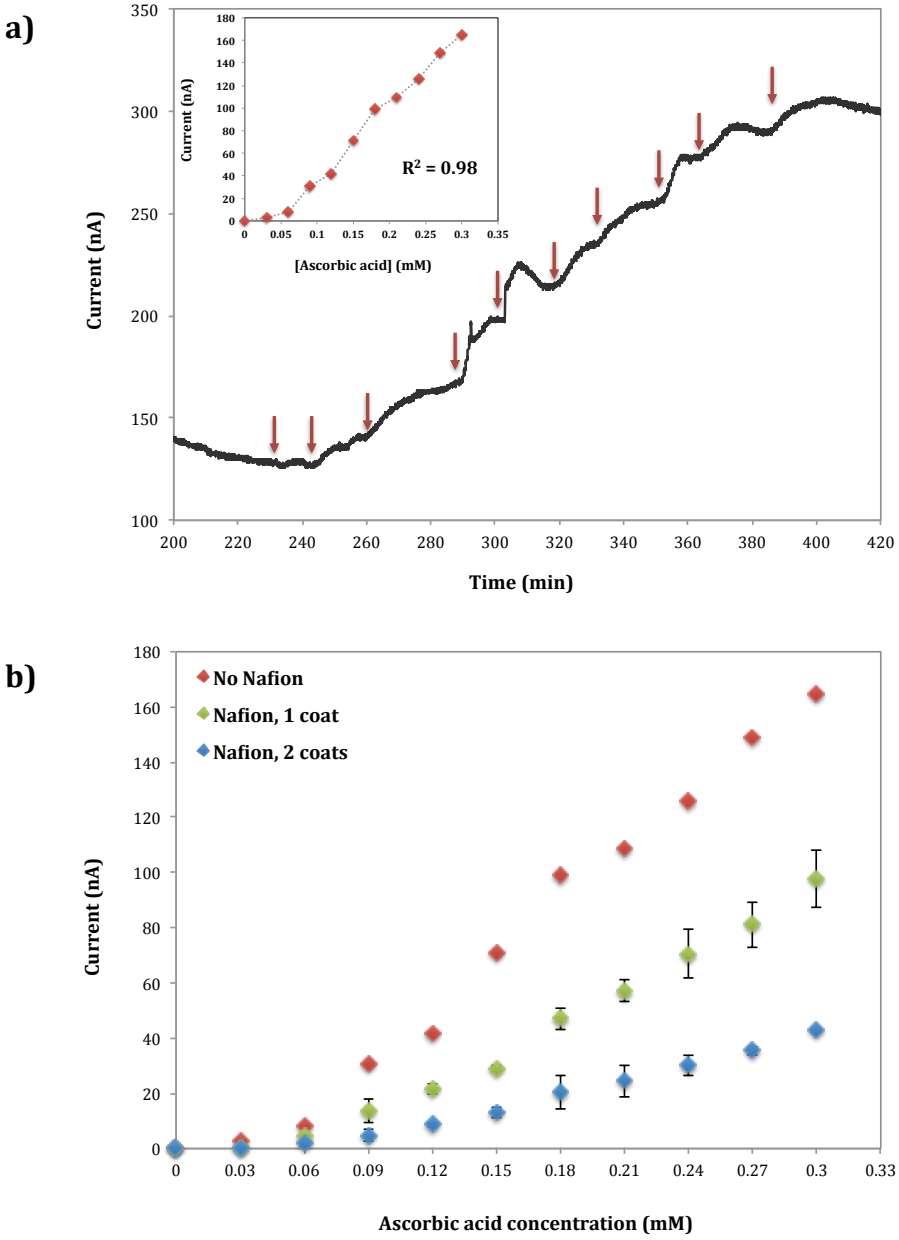

Figure 7.4. Analysis of ascorbic acid interferences in the electrochemical response by performing successive additions in the range 0–0.3 mM. (a) Chronoamperometric response and inset with calibration plot for AuPt with no Nafion layer and (b) comparison with the current response obtained with the addition of 1 and 2 layers of the polymer.

Table 7.4. Decrease in current response – with respect to the control – observed from the successive addition study performed for ascorbic acid at different concentrations (0.03–0.3 mM) with the application of 1 and 2 layers of Nafion on the WE.

[Ascorbic acid] (mM)	Nafion, 1 coat	Nafion, 2 coats
0.03	98.3%	100.0%
0.06	41.9%	73.8%
0.09	56.0%	85.2%
0.12	48.6%	79.4%
0.15	59.0%	81.7%
0.18	52.4%	79.5%
0.21	47.6%	77.6%
0.24	44.0%	76.2%
0.27	45.6%	76.2%
0.3	40.9%	74.0%

Results obtained from both sets of experiments described in the previous sections confirmed that ascorbic acid does interfere with the electrochemical response for lactate in the AuPt sensing system, as the literature suggested. However, this interference observed for the maximum concentration reported for a healthy subject (0.036 mM AA) had a maximum value of 51 nA and even for a concentration 10 times higher than this – and 30 times higher than the median value – (0.3 mM AA), the interference reached a maximum value of 366 nA when 1 mM lactate was present and 165 nA when only ascorbic acid was present in the solution. The interfering current response observed for ascorbic acid in the presence of lactate was approximately twice as high as when only ascorbic acid was present in the sample. It was considered that this was due to the oxidation of H_2O_2, interfering with the current signal for the oxidation of ascorbic acid. Moreover, the small intra-laminate sensor variability observed for the developed sensing system for lactate oxidation (section 5.7) could also be causing small alterations in the current response recorded for the interfering compound.

For the aforementioned reasons, it was considered that the presence of higher lactate levels would have masked the electrochemical signal produced by the oxidation of the same ascorbic acid levels considered in the present study due to higher amounts of H_2O_2 being produced and oxidised at the surface of the electrode, making the interference produced by ascorbic acid practically negligible.

Nevertheless, both studies performed showed that electrode-surface modification of the AuPt system with Nafion led to a notable decrease in interfering current response produced by ascorbic acid without it affecting the current response for lactate. Moreover, these studies indicated that the hindrance of the oxidation of ascorbic acid increased with the addition of a second layer of the polymer, leading to a decrease in interfering current response of up to 96.7% except for 0.03 mM AA, where no oxidation current was observed. To conclude, the obtained results showed the capability of Nafion for minimising interferences produced by the oxidation of ascorbic acid in the solution and that more layers of the polymer increased the charge-exclusion properties of the polymer film.

7.3 Minimising interferences for uric acid (UA)

This section describes preliminary studies performed on estimating the capability of Nafion to minimise electrochemical interferences produced by the oxidation of uric acid during the monitoring of lactate with the developed AuPt system in order to improve the selectivity of the sensor.

As with ascorbic acid, the evaluation of Nafion for reducing uric acid interferences was performed with the same two parallel sets of experiments as described in section 7.2. Experiments were performed on concentrations of uric acid of between 0.059–2 mM, all of which within the range of reported physiological concentrations in sweat from healthy volunteers.

7.3.1 Peak test for uric acid and lactate

For the study described in this section, AuPt laminate sensors were prepared and interrogated as described in section 7.1.4. Sensing systems without Nafion and with 1 and 2 coats of the polymer were constructed. The resulting sensors were interrogated with solutions containing 1 mM lactate in the presence of a range of

uric acid concentrations, from 0.059 to 2 mM, in PBS pH 7.4. The composition of each of these solutions are summarised in Table 7.5.

Table 7.5. Composition of the solutions tested for the analysis of uric acid at different concentrations (0–2 mM) in 1 mM lactate.

Solution	[Lactate] (mM)	[Uric acid] (mM)
1	1	0
2	1	0.059
3	1	0.5
4	1	2

As described in section 7.2.1, the constructed AuPt systems were introduced in a 25-ml beaker with 15 ml of PBS and polarised at +650 mV. When a baseline was reached, the sensor was interrogated with 15 ml of each solution described in Table 7.5, which were consecutively added to the beaker for analysis. Prior to the addition of each solution, the AuPt systems were exposed to PBS only in order to rinse the membranes and repolarise the sensor. The 1 mM lactate solution in PBS – added initially – provided a control current response with which to compare subsequent responses recorded with the additions of different concentrations of uric acid. The resulting current response recorded for each solution analysed was normalised by subtracting the baseline current obtained with PBS only. The current response produced by each concentration of uric acid was subsequently obtained by subtracting the normalised current response for 1 mM lactate in PBS (Table 7.5, Solution 1), and represented in Figure 7.5.

The first experiment performed was carried out using an AuPt sensing system constructed with no Nafion on the electrode surface in order to obtain a control current response for each uric acid concentration (Figure 7.5a) to which corresponding current responses obtained by interrogating sensors with one and two layers of Nafion could be compared (Figure 7.5b).

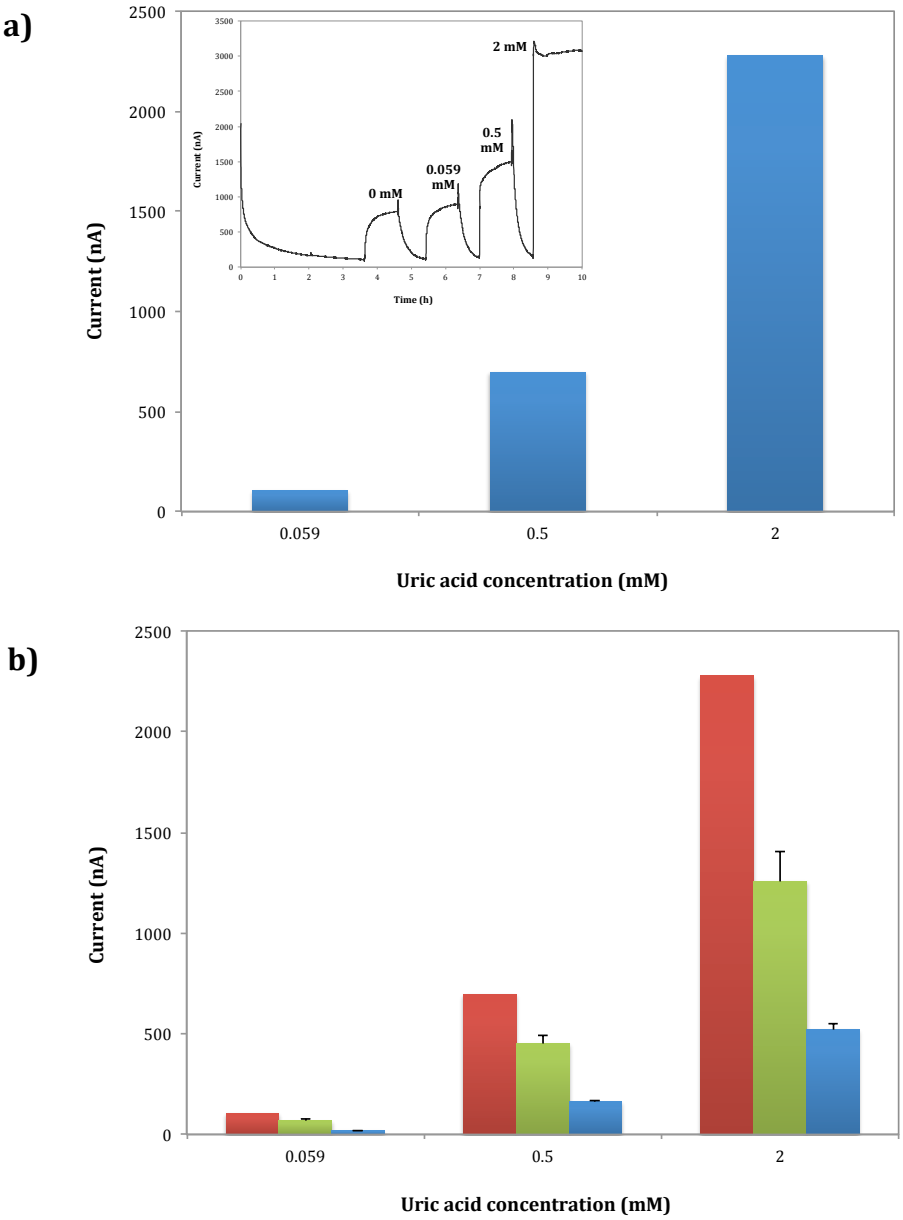

Figure 7.5. Bar diagrams obtained from the analysis of uric acid (0.059–2 mM) with 1 mM lactate, representing (a) the control current obtained with no Nafion layer on the WE (inset with the chronoamperometric response of the AuPt sensor analysed) and (b) its comparison with the response obtained with the application of 1 and 2 coats of the polymer.

Results obtained from the analysis of the constructed AuPt sensing system with no Nafion on the electrode showed an increase from the control current response of 104 nA for 0.059 mM UA, 697 nA for 0.5 mM UA and 2,277 nA for 2 mM UA (Figure 7.5a). The addition of one layer of Nafion on the WE of the AuPt electrode system led to a decrease in the current response of between 34.6-44.8%

and the addition of a second layer of the polymer further decreased the response to between 76.5-81.7% (Figure 7.5b). The decrease in response for each concentration of uric acid with the application of 1 and 2 layers of Nafion on the electrode surface is summarised in Table 7.6.

As with the analysis of ascorbic acid, no clear decrease in current response was observed for 1 mM lactate between that obtained with the AuPt system with no Nafion and those obtained with the application of 1 and 2 layers of the polymer.

Table 7.6. Decrease in current response – with respect to the control – observed from the peak study performed for uric acid at different concentrations (0.059–2 mM) with the application of 1 and 2 layers of Nafion on the WE.

[Uric acid] (mM)	Nafion, 1 coat	Nafion, 2 coats
0.059	34.6%	81.7%
0.5	35.2%	76.5%
2	44.8%	77.1%

7.3.2 Successive additions of uric acid

The second study performed on uric acid consisted of the evaluation of the interfering current response at different concentrations of the compound by performing successive additions of a concentrated solution of uric acid. For this study, three different sets of laminate sensors were constructed – without Nafion and with 1 and 2 layers of the polymer on the electrode surface – as outlined in section 7, however with the absence of LOD enzyme in the laminate preparation, as described in section 7.2.2 for ascorbic acid testing. The resulting sensors were interrogated for successive additions of 0.1 mM uric acid up to a concentration of 1 mM. This was achieved by polarising the AuPt sensing system at +650 mV in a 25–ml beaker with 15 ml of PBS and after a current baseline was reached, consecutive 100 μl additions of a 15.1 mM stock solution of uric acid were performed. The current response obtained from each addition of uric acid was recorded and

normalised by subtracting the baseline current at 0 mM uric acid (PBS only) and the values were represented in Figure 7.6.

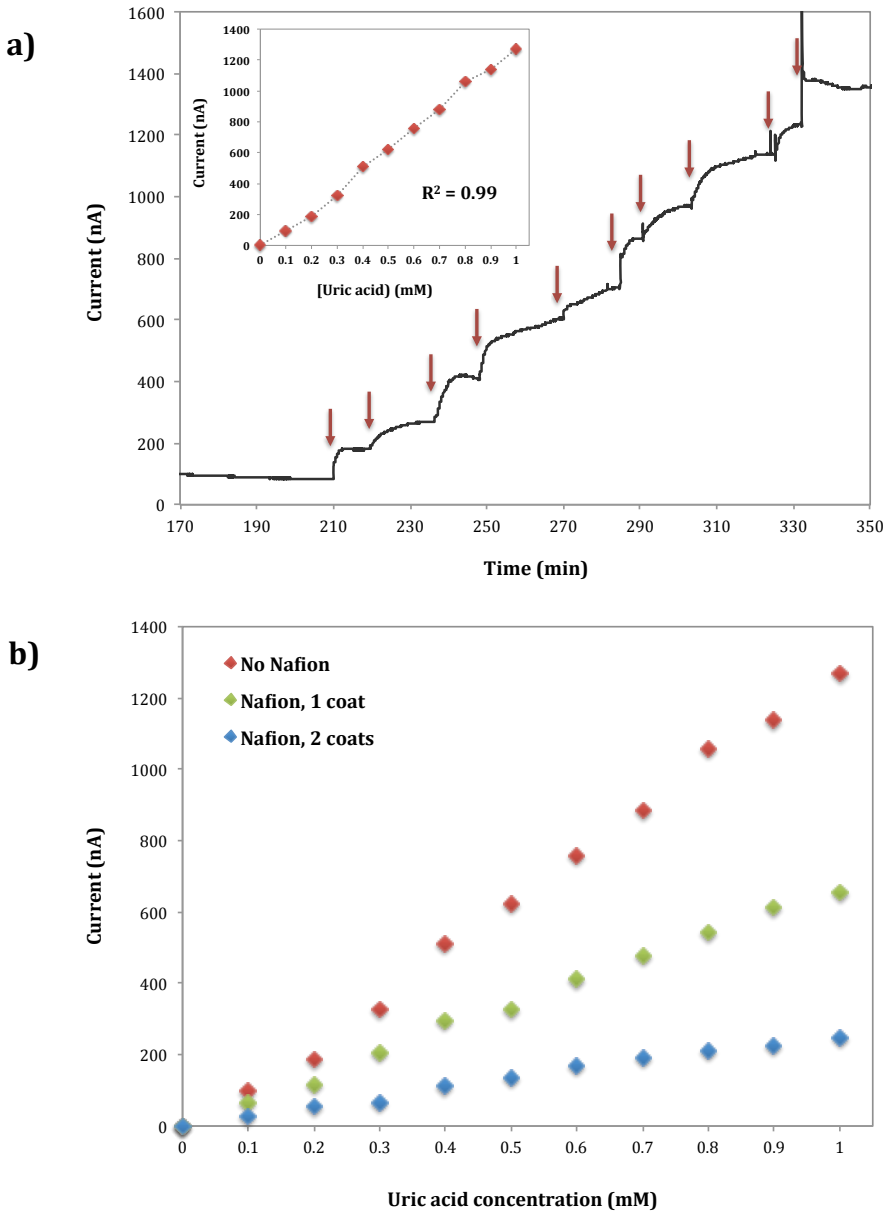

Figure 7.6. Analysis of uric acid interferences in the electrochemical response by performing successive additions in the range 0.1–1 mM. (a) Chronoamperometric response and inset with calibration plot for AuPt wit no Nafion layer and (b) comparison with the current response obtained with the addition of 1 and 2 layers of the polymer.

The first experiment performed was carried out using an AuPt sensing system constructed with no Nafion on the electrode surface in order to obtain a control current response for each uric acid concentration (Figure 7.6a) to which corresponding current responses obtained by interrogating sensors with one and two layers of Nafion could be compared (Figure 7.6b).

Results obtained from the interrogation of the AuPt sensing system without Nafion on the electrode surface showed an increase in current response for successive additions of uric acid. However, unlike that observed for ascorbic acid, the increase in current response for each uric acid concentration was very similar to the corresponding ones observed in the presence of 1 mM lactate (Figure 7.4). The application of one layer of Nafion on the surface of the WE led to a decrease in current response of between 32.8-48.5% with respect to the control (with no Nafion layer on the electrode surface). A further decrease of between 69.8-80.6% was observed with the addition of a second layer of Nafion. The decrease in response for each concentration of uric acid with the application of 1 and 2 layers of Nafion on the electrode is summarised in Table 7.7.

Table 7.7. Decrease in current response – with respect to the control – observed from the successive addition study performed for uric acid at different concentrations (0.1–1 mM) with the application of 1 and 2 layers of Nafion on the WE.

[Uric acid] (mM)	Nafion, 1 coat	Nafion, 2 coats
0.1	32.8%	69.8%
0.2	37.9%	71.0%
0.3	36.4%	79.8%
0.4	42.5%	78.3%
0.5	47.5%	78.2%
0.6	45.9%	78.0%
0.7	45.9%	78.5%
0.8	48.5%	80.1%
0.9	46.2%	80.2%
1	48.4%	80.6%

Results obtained from both sets of experiments described in the previous sections 7.3.1 and 7.3.2 confirmed that uric acid interferes with the current

response obtained with the AuPt sensing system, as suggested by the literature. The increase in current response for the reported median value of ascorbic acid (0.059 mM) was 104 nA over the control response for 1 mM lactate, which is relatively small. However, since the reported range of concentrations for the compound are of higher values than those for ascorbic acid, the interferences produced by the oxidation of uric acid at higher concentrations were of a greater magnitude (i.e. an increase in over 2.2 μA was observed for 2 mM UA), affecting the selectivity of the sensor more severely than with ascorbic acid.

Nevertheless, results showed the capability of Nafion to effectively minimise the interferences produced by the oxidation of uric acid on the surface of the electrode of up to 44.8% with the first layer and 81.7% with the second layer, without affecting the current response for 1 mM lactate. As an example for this, the interfering current response obtained from the presence of a concentration as high as 2 mM UA in a 1 mM lactate solution – hence doubling the concentration of lactate – was diminished from 2,277 to 520.5 nA (77.1%) after the application of 2 Nafion layers on the electrode surface. This again shows that applying a second Nafion layer increased the charge-exclusion properties of the polymer film.

Although a very significant decrease in interferences produced with high concentrations of uric acid was achieved with the application of two coats of Nafion, further investigations should be performed, studying the effect of adding more layers of Nafion to the surface of the electrode.

The aforementioned results from studies with ascorbic acid and uric acid show the capability of Nafion to reduce interferences produced from the presence of these compounds in the solution even at concentrations much higher than their reported median values in human sweat, which could potentially occur for hospitalised subjects suffering from medical conditions causing or caused by higher levels of these compounds.

Results also showed the compatibility of applying Nafion layers on the developed sensing system, even though the electrode surface is highly porous. Nevertheless, future work would also be needed to study whether the use of a non-porous surface in the construction of the electrode system onto which the Nafion layers are applied could improve the reproducibility of the sensing system and the lowering of interferences.

Since Nafion has also been applied to protect the electrode surface from the adsorption of molecules present in complex biological matrices, as previously mentioned, this polymer would be suitable for operating in physiological solutions due not only to the increased selectivity of the resulting system but also for the reduced passivation from protein adsorption. However, further work would need to be carried out analysing the ion and size-exclusive properties of Nafion with human sweat samples.

Further investigations should be carried out on modifying the AuPt electrode surface with other polymers in order to restrict the passage of ascorbic acid, uric acid and/or other molecules present in physiological solutions – due to their size or charge – such as cellulose acetate or polysiloxane films.

7.4 Conclusions

The proof-of-principle operation for the application of 1 and 2 Nafion films on the surface of the developed AuPt electrode system and the capability of the resulting sensors to detect lactate while minimising interferences produced from ascorbic acid and uric acid has been demonstrated.

Ascorbic acid and uric acid solutions at concentrations of up to approximately 30 times above their median values reported in human sweat were studied with the resulting sensing systems modified with Nafion. The current response produced from the oxidation of these compounds exhibited a decrease of up to 96.7% for ascorbic acid and 81.7% for uric acid with the application of two Nafion

layers on the electrode surface. No significant interferences caused by the layer(s) of Nafion on lactate sensing were observed.

Further work should be carried out on evaluating Nafion with human sweat samples in order to assess its capability for minimising interferences and hinder the passage of compounds present in the physiological sample and their adsorption to the surface of the electrode. Furthermore, other polymers should be studied as alternatives to Nafion for the modification of the electrode surface in the developed AuPt system.

CHAPTER 8

GENERAL CONCLUSIONS AND SUGGESTIONS FOR FURTHER WORK

8 General conclusions and suggestions for further work

8.1 General conclusions

The main purpose of this work was to demonstrate the proof of principle for the development of a novel flexible electrochemical enzymatic sensor, employing lactate oxidase for the continuous monitoring of sweat lactate *in vitro* and assess its potential for being applied as a body-worn device in order to provide real-time measurements for the early detection of hypoxic conditions, such as pressure ischemia.

Part of the work presented in this thesis was submitted to conferences and successfully invited for a poster (as shown in Appendix A) and an oral presentation under the following titles:

- "Development towards a novel flexible enzyme laminate-based sensor for analysis of lactate in undiluted sweat" (Poster presentation at the 3rd International Conference on Bio-Sensing Technology. Sitges, Spain 2013).
- "Novel flexible enzyme laminate-based sensor for analysis of lactate in undiluted sweat" (Oral presentation at Biosensors 2014. Melbourne, Australia 2014).

Part of the work within this thesis has also been submitted for publication to *Electrochemistry*. It is also intended to publish results obtained with the further analysis of clinical sweat samples with the developed sensing system in a separate original research paper.

The first experimental chapter (Chapter 4) described the steps followed towards the development of a novel flexible sensing platform for the monitoring of lactate *in vitro*. Different electrode-system designs were constructed and evaluated. Initial designs based on two separated gold-coated membranes as WE

and CE/RE were developed in many different configurations, but presented connection shorting, electrode blocking and/or other hindrance issues caused by the membranes of the system, which led to low current response for a range of concentrations of lactate.

A new design where both CE/RE and WE were sputter-coated on a single polycarbonate membrane with a constant separation between them by a non-coated region, based on the configuration of the Rank cell, was developed. It was shown that sputter-coating the WE with platinum instead of gold increased the current response and the current density of the electrode. The final design with a gold CE/RE and platinum-coated WE (AuPt) exhibited good inter and intra-sensor reproducibility, it is very thin (~30 μm) and therefore can be placed on a flexible support, where it showed mechanical stability over 24 bending-relaxation iterations.

The ability to improve the sensor's performance, in terms of reproducibility, working concentration range and current height (sensitivity) of the response, through the optimisation of parameters involved in the construction of the enzyme laminate in order to improve the activity and stability of lactate oxidase was investigated in Chapter 5. A decrease in the pore size of the bottom membrane of the laminate to 0.015 μm accompanied by an increase in the incubation time to 12 minutes and the use of fresh glutaraldehyde solutions at a higher concentration (10% v/v) improved the stability of the enzyme in the laminate and increased the working concentration range of the sensor.

Higher enzyme loading in the laminate (1,667 U ml^{-1}) and an improved preparation method of the enzyme in BSA increased notably the current height and the reproducibility of the electrochemical response. Higher concentrations of BSA (0.2 g ml^{-1}) appeared to increase the initial stability of the enzyme and the current response, however the latter exhibited a decrease over time and higher substrate concentrations, probably due to weak cross-linking between glutaraldehyde and the enzyme. The resulting optimised laminate exhibited good operational and mechanical stability over 27.4 hours and repeated bending-relaxation iterations,

showing the efficiency of the enzyme entrapment while preserving its activity and stability. These results suggested the potential of the developed sensing device for being applied as a body-worn device to provide continuous lactate monitoring over a significant period of time prior to its replacement.

The performance of the sensor and its capability to detect lactate in synthetic and human sweat solutions was assessed in Chapter 6. The sensor was shown to perform lactate measurements at physiologically relevant concentrations in synthetic sweat solutions containing some of the most significant components in sweat. These included two oxidisable species, ascorbic acid and uric acid. No significant interferences were found in the electrochemical response due to the presence of these compounds at their median concentration values.

Studies performed on the analysis of human sweat samples with the developed sensing system, although preliminary, showed the capability of the sensor to provide a reliable estimation of lactate levels in diluted sweat samples with prior calibration of the device. The capability to detect lactate level fluctuations in diluted samples from different body areas, between different subjects and at different levels of hypoxia (given by different times for intense-exercise performance) with the developed sensing system was shown. The capability of the sensor to detect lactate level fluctuations between different degrees of hypoxia was also shown for undiluted sweat samples.

The analysis of undiluted sweat samples remains a challenge, however, due to the amount of solutes present in the solution. It was hypothesised that these solutes could be causing the fouling of the enzyme laminate and/or the surface of the electrode, affecting significantly the electrochemical response over time.

The potential of modifying the electrode surface with a polymer such as Nafion for reducing possible interferences of oxidising compounds present in sweat, such as ascorbic acid and uric acid, at levels above their reported median values was investigated in Chapter 7. Studies showed that interferences produced by ascorbic acid at concentrations up to 30 times above the reported median, although these did not affect in great level to the selective electrochemical response of the sensor

for lactate, they could however be lowered by up to 96.7% with the application of two Nafion layers. On the contrary, interferences produced by uric acid at concentrations up to approximately 34 times above the reported median value were more significant than those for ascorbic acid. Nevertheless, interferences produced by the uric acid levels studied were lowered up to 81.7% with the application of two Nafion coats. The addition of Nafion layers to the electrode surface did not affect the selective electrochemical response of the sensor for lactate Results obtained with Nafion, although preliminary, show the compatibility of the polymer with the platinum electrode surface of the AuPt system and the capability of the resulting sensor to reduce significantly interferences produced by oxidising compounds present in sweat without interfering with the sensing of lactate. These results open the possibility of further research into the use of alternative polymers for the modification of the electrode surface in the AuPt system in order to improve its performance by reducing interferences and protecting the electrode from fouling by hindering the passage of solutes.

8.2 Suggestions for further work

This work provided a proof of principle for the development of a flexible enzyme laminate-based sensor containing lactate oxidase and for its capability of monitoring lactate in PBS, synthetic and human sweat solutions.

Significant improvements were made regarding the optimisation of the sensor's performance, in terms of reproducibility, working concentration range and height of current response (sensitivity). This was achieved through the study of the different parameters involved in the construction of the enzyme laminate in order to increase the stability of lactate oxidase in the immobilised matrix while preserving its activity. However, investigations on these and other parameters for improving the enzyme stability and the performance of the sensor should continue. In addition to this, it is believed that the reproducibility of the laminate system would be greatly improved through the automation of the laminate construction process, including the preparation of enzyme-BSA aliquots, mixing of the different

components for the crosslinking matrix and the pressure applied between membranes.

The capability of the sensor for detecting lactate in sweat samples was shown. Further investigations should however continue in this area, particularly in the study of the effect of undiluted sweat samples on the electrochemical response over time as well in ways to avoid laminate and/or electrode fouling, since this affected significantly the response of the sensor over time.

The capability of electrode-surface modification with Nafion for lowering interferences from oxidising species present in sweat was demonstrated. This opens a new area of research within the developed sensing system towards investigating the potential of other polymers, applied on the electrode surface and/or on the outer layer of the laminate. These could improve the performance of the sensor and the electrochemical response by protecting the electrode surface and/or the laminate from fouling and lower interferences from oxidisable species present in the sample. Moreover, given the compatibility of polymers with the platinum surface of the working electrode, the use of conductive-polymer layers on the electrode surface in order to increase the current response and thus sensitivity of the sensor should be investigated.

Finally, the sensing system developed in this work should be optimised for its use as a wearable device in order to provide *ex vivo* measurements and tested with sweat samples from hospitalised patients. It is believed that the ability to monitor lactate level fluctuations in real time along pressure ulceration and poor tissue perfusion (delivery of blood to a biological tissue) would not only provide invaluable information into the further understanding of biochemical processes involved in these, but also would make the developed sensor an essential tool for their early detection, improving notably the quality of life of the patient.

As a direct result from the work presented in this thesis, a preliminary study has already commenced at Gloucestershire Royal Hospital with the sponsors of this project on the collection of sweat from post-operative patients with low perfusion. The ethical approval for the collection of sweat samples from these

patients and the analysis with the sensing system developed in this work is at the time of writing in process.

References

Abdul-Aziz, A. and Wong, F. -. (2011), "Interference elimination of an amperometric glucose biosensor using poly(hydroxyethyl methacrylate) membrane", *Engineering in Life Sciences,* vol. 11, no. 1, pp. 20-25.

Alberts, B., Johnson, A., Lewis, J., Raff, M., Roberts, K. and Walter, P. (2002), *Molecular Biology of the Cell,* Fourth ed, Garland Science, New York.

Alderman, M. H. (2002), "Uric acid and cardiovascular risk", *Current Opinion in Pharmacology,* vol. 2, no. 2, pp. 126-130.

Ambrózy, A., Hlavatá, L. and Labuda, J. (2013), "Protective membranes at electrochemical biosensors", *Acta Chimica Slovaca,* vol. 6, no. 1, pp. 35-41.

Arthur, P. G., Giles, J. J. and Wakeford, C. M. (2000), "Protein synthesis during oxygen conformance and severe hypoxia in the mouse muscle cell line C2C12", *Biochimica et Biophysica Acta - General Subjects,* vol. 1475, no. 1, pp. 83-89.

Bader, D. and Oomens, C. (2006), "Recent advances in pressure ulcer research", in Romanelli, M., Clark, M., Cherry, G. W., et al (eds.) *Science and practice of pressure ulcer management,* Springer, London, pp. 11-26.

Bader, D., Wang, Y., Knight, S., Polliack, A., James, T. and Taylor, R. (2005), "Biochemical Status of Soft Tissues Subjected to Sustained Pressure", in Bader, D., Bouten, C., Colin, D., et al (eds.) *Pressure Ulcer Research. Current and Future Perspectives,* Springer, Heidelberg.

Bansal, C., Scott, R., Stewart, D. and Cockerell, C. J. (2005), "Decubitus ulcers: A review of the literature", *International journal of dermatology,* vol. 44, no. 10, pp. 805-810.

Barbosa, O., Torres, R., Ortiz, C., Berenguer-Murcia, A., Rodrigues, R. C. and Fernandez-Lafuente, R. (2013), "Heterofunctional supports in enzyme immobilization: From traditional immobilization protocols to opportunities in tuning enzyme properties", *Biomacromolecules,* vol. 14, no. 8, pp. 2433-2462.

Bard, A. J. and Faulkner, L. R. (2001), *Electrochemical Methods: Fundamentals and Applications,* Second ed, John Wiley & Sons, New York.

Bauer, J. D., Mancoll, J. S. and Phillips, L. G. (2006), "Pressure sores", in Thorne, C. H., Beasley, R. W., Aston, S. J., et al (eds.) *Grabb and Smith's Plastic Surgery,* Sixth ed, Lippincott Williams & Wilkins, Philadelphia, pp. 722-729.

Bellomo, R. and Kellum, J. A. (2008), "Acid-Base Balance and Kidney-Lung Interaction", in Papadakos, P. J. and Lachmann, B. (eds.) *Mechanical Ventilation: Clinical Applications and Pathophysiology,* Elsevier Health Sciences, Philadelphia.

Bellomo, R. (2002), "Bench-to-bedside review: Lactate and the kidney", *Critical Care,* vol. 6, no. 4, pp. 322-326.

Bennett, G., Dealey, C. and Posnett, J. (2004), "The cost of pressure ulcers in the UK", *Age and Ageing,* vol. 33, no. 3, pp. 230-235.

Berg, J. M., Tymoczko, J. L. and Stryer, L. (2006), *Biochemistry,* Sixth ed, W. H. Freeman, New York.

Biagi, S., Ghimenti, S., Onor, M. and Bramanti, E. (2012), "Simultaneous determination of lactate and pyruvate in human sweat using reversed-phase high-performance liquid chromatography: A noninvasive approach", *Biomedical Chromatography,* vol. 26, no. 11, pp. 1408-1415.

Bijman, J. and Quinton, P. M. (1987), "Lactate and bicarbonate uptake in the sweat duct of cystic fibrosis and normal subjects", *Pediatric research,* vol. 21, no. 1, pp. 79-82.

Bilitewski, U. and Turner, A. P. F. (2000), *Biosensors for environmental monitoring,* Harwood Academic Publishers, Amsterdam, the Netherlands.

Bindra, D. S., Zhang, Y., Wilson, G. S., Sternberg, R., Thévenot, D. R., Moatti, D. and Reach, G. (1991), "Design and in vitro studies of a needle-type glucose sensor for subcutaneous monitoring", *Analytical Chemistry,* vol. 63, no. 17, pp. 1692-1696.

Bours, G., Laat, E., Halfens, R. and Lubbers, M. (2001), "Prevalence, risk factors and prevention of pressure ulcers in Dutch intensive care units - Results of a cross-sectional survey", *Intensive care medicine,* vol. 27, no. 10, pp. 1599-1605.

Boutilier, R. G. (2001), "Mechanisms of cell survival in hypoxia and hypothermia", *Journal of Experimental Biology,* vol. 204, no. 18, pp. 3171-3181.

Brett, C. M. A. and Brett, A. M. O. (1998), *Electroanalysis,* Oxford Chemistry Primers, New York.

Brett, C. M. A. and Fungaro, D. A. (2000), "Modified Electrode Voltammetric Sensors for Trace Metals in Environmental Samples", *Journal of the Brazilian Chemical Society,* vol. 11, no. 3, pp. 298-303.

Bridel, J. (1993), "The epidemiology of pressure sores.", *Nursing standard (Royal College of Nursing (Great Britain) : 1987),* vol. 7, no. 42, pp. 25-30.

Bridge, K., Davis, F., Collyer, S. and Higson, S. ?. (2007), "Flexible Ultrathin PolyDVB/EVB Composite Membranes for the Optimization of a Lactate Sensor", *Electroanalysis,* vol. 19, no. 5, pp. 567-574.

Brown, F. O. and Lowry, J. P. (2003), "Microelectrochemical sensors for in vivo brain analysis: An investigation of procedures for modifying Pt electrodes using Nafion®", *Analyst,* vol. 128, no. 6, pp. 700-705.

Burns, T., Breathnach, S., Cox, N. and Griffiths, C. (2010), *Rook's Textbook of Dermatology,* 8th ed, Wiley-Blackwell, UK.

Bushman, J. B. (2002), *A brief explanation of the Nernst equation. Its importance in explaining anode and cathode polarization and potential changes*, available at: http://www.bushman.cc/pdf/nearnst_equation.pdf (accessed 24/10/2012).

Cai, X., Yan, J., Chu, H., Wu, M. and Tu, Y. (2010), "An exercise degree monitoring biosensor based on electrochemiluminescent detection of lactate in sweat", *Sensors and Actuators, B: Chemical,* vol. 143, no. 2, pp. 655-659.

Cao, L. (2006), "Introduction: Immobilized Enzymes: Past, Present and Prospects", in *Carrier-bound Immobilized Enzymes,* Wiley-VCH Verlag GmbH & Co. KGaA, , pp. 1-52.

Chaubey, A. and Malhotra, B. D. (2002), "Mediated biosensors", *Biosensors and Bioelectronics,* vol. 17, no. 6–7, pp. 441-456.

Chen, H., Zhang, Q., Dang, Y. and Shu, G. (2013), "The effect of glutaraldehyde cross-linking on the enzyme activity of immobilized ß-galactosidase on chitosan bead", *Advance Journal of Food Science and Technology,* vol. 5, no. 7, pp. 932-935.

Chen, Q., Kenausis, G. L. and Heller, A. (1998), "Stability of oxidases immobilized in silica gels", *Journal of the American Chemical Society,* vol. 120, no. 19, pp. 4582-4585.

Clark Jr., L. C. and Lyons, S. C. (1962), "Electrode systems for continuous monitoring in cardiovascular surgery.", *Annals of the New York Academy of Sciences,* vol. 102, pp. 29-45.

Collier, M. and Moore, Z. (2006), "Etiology and Risk Factors", in Romanelli, M., Clark, M., Cherry, G. W., et al (eds.) *Science and Practice of Pressure Ulcer Management,* Springer, USA.

Cosnier, S., Fontecave, M., Innocent, C. and Niviere, V. (1997), "An original electroenzymatic system: Flavin reductase-riboflavin for the improvement of dehydrogenase-based biosensors. Application to the amperometric detection of lactate", *Electroanalysis,* vol. 9, no. 9, pp. 685-688.

Coyle, S., Benito-Lopez, F., Byrne, R. and Diamond, D. (2010), "On-body chemical sensors for monitoring sweat", in Lay-Ekuakille, A. and Mukhopadhyay, S. C. (eds.) *Lecture Notes in Electrical Engineering,* Springer, Heidelberg, pp. 177-193.

Coyle, S., Wu, Y., Lau, K. -., Brady, S., Wallace, G. and Diamond, D. (2007), "Bio-sensing textiles - wearable chemical biosensors for health monitoring", *IFMBE Proceedings,* Vol. 13, pp. 35.

De Backer, D., Creteur, J., Zhang, H., Norrenberg, M. and Vincent, J. -. (1997), "Lactate production by the lungs in acute lung injury", *American Journal of Respiratory and Critical Care Medicine,* vol. 156, no. 4 I, pp. 1099-1104.

De Micheli, G., Ghoreishizadeh, S. S., Boero, C., Valgimigli, F. and Carrara, S. (2011), "An integrated platform for advanced diagnostics", *Proceedings -Design, Automation and Test in Europe, DATE,* pp. 1454.

Derbyshire, P. J. (2011), *Development towards a biosensor for the determination of lactate, uric acid and xanthine in sweat* Cranfield University, Cranfield Health, Cranfield, England.

Derbyshire, P. J., Barr, H., Davis, F. and Higson, S. P. J. (2012), "Lactate in human sweat: A critical review of research to the present day", *Journal of Physiological Sciences,* vol. 62, no. 6, pp. 429-440.

Edlich, R. F., Winters, K. L., Woodard, C. R., Buschbacher, R. M., Long, W. B., Gebhart, J. H. and Ma, E. K. (2004), "Pressure ulcer prevention", *Journal of long-term effects of medical implants,* vol. 14, no. 4, pp. 285-304.

Eggins, B. R. (2002), *Chemical Sensors and Biosensors,* John Wiley & Sons Ltd., England.

Faridnia, M. H., Palleschi, G., Lubrano, G. J. and Guilbault, G. G. (1993), "Amperometric biosensor for determination of lactate in sweat", *Analytica Chimica Acta,* vol. 278, no. 1, pp. 35-40.

Fellmann, N., Fabry, R. and Coudert, J. (1989), "Calf sweat lactate in peripheral arterial occlusive disease", *American Journal of Physiology - Heart and Circulatory Physiology,* vol. 257, no. 2.

Ferguson-Pell, M. and Hagisawa, S. (1988), "Biochemical changes in sweat following prolonged ischemia", *Journal of Rehabilitation Research and Development,* vol. 25, no. 3, pp. 57-62.

Fisher, A. C. (1996), *Electrode Dynamics,* Oxford Chemistry Primers, New York.

Fraden, J. (2004), *Handbook of Modern Sensors - Physics, Designs and Applications,* Third ed, Springer - Verlag, New York.

Gagliardi, A. C. M., Miname, M. H. and Santos, R. D. (2009), "Uric acid: A marker of increased cardiovascular risk", *Atherosclerosis,* vol. 202, no. 1, pp. 11-17.

Gallardo, E. and Queiroz, J. A. (2008), "The role of alternative specimens in toxicological analysis", *Biomedical Chromatography,* vol. 22, no. 8, pp. 795-821.

Gawlitta, D., Oomens, C. W. J., Bader, D. L., Baaijens, F. P. T. and Bouten, C. V. C. (2007), "Temporal differences in the influence of ischemic factors and deformation on the metabolism of engineered skeletal muscle", *Journal of applied physiology,* vol. 103, no. 2, pp. 464-473.

Göpel, W., Jones, T. A., Kleitz, M., Lundström, I. and Seiyama, T. (2008), *Sensors, Chemical and Biochemical Sensors Part II,* John Wiley & Sons, Germany.

Gorton, L. (2005), *Biosensors and modern biospecific analytical techniques,* Elsevier, Amsterdam; Boston.

Gouveia-Caridade, C. and Brett, C. M. A. (2008), "Strategies, development and applications of polymer-modified electrodes for stripping analysis", *Current Analytical Chemistry,* vol. 4, no. 3, pp. 206-214.

Great Britain. Department of Health (1995), *Pressure sores - a key quality indicator : a guide for NHS purchasers and providers*. Department of Health, Great Britain.

Green, J. M., Bishop, P. A., Muir, I. H. and Lomax, R. G. (2001), "Lactate-sweat relationships in younger and middle-aged men", *Journal of Aging and Physical Activity,* vol. 9, no. 1, pp. 67-77.

Grieshaber, D., MacKenzie, R., Vörös, J. and Reimhult, E. (2008), "Electrochemical biosensors - Sensor principles and architectures", *Sensors,* vol. 8, no. 3, pp. 1400-1458.

Hall, S. B., Khudaish, E. A. and Hart, A. L. (2000), "Electrochemical oxidation of hydrogen peroxide at platinum electrodes. Part V: inhibition by chloride", *Electrochimica Acta,* vol. 45, no. 21, pp. 3573-3579.

Hames, B. D. and Hooper, N. M. (2000), *Instant Notes in Biochemistry,* Second ed, Scientific Publishers Ltd., Oxford.

Harvey, C. J., LeBouf, R. F. and Stefaniak, A. B. (2010), "Formulation and stability of a novel artificial human sweat under conditions of storage and use", *Toxicology in Vitro,* vol. 24, no. 6, pp. 1790-1796.

House, J. L., Anderson, E. M. and Ward, W. K. (2007), "Immobilization techniques to avoid enzyme loss from oxidase-based biosensors: A one-year study", *Journal of Diabetes Science and Technology,* vol. 1, no. 1, pp. 18-27.

Huang, C. -., Chen, M. -., Huang, L. -. and Mao, I. -. (2002), "Uric acid and urea in human sweat", *Chinese Journal of Physiology,* vol. 45, no. 3, pp. 109-115.

Hulanicki, A., Glab, S. and Ingman, F. (1991), "Chemical sensors: definitions and classification", *Pure and Applied Chemistry,* vol. 63, no. 9, pp. 1247-1250.

Jia, W., Bandodkar, A. J., Valdés-Ramírez, G., Windmiller, J. R., Yang, Z., Ramírez, J., Chan, G. and Wang, J. (2013), "Electrochemical tattoo biosensors for real-time noninvasive lactate monitoring in human perspiration", *Analytical Chemistry,* vol. 85, no. 14, pp. 6553-6560.

Jung, S. -. and Wilson, G. S. (1996), "Polymeric mercaptosilane-modified platinum electrodes for elimination of interferants in glucose biosensors", *Analytical Chemistry,* vol. 68, no. 4, pp. 591-596.

Karlsson, J., Willerson, J. T., Leshin, S. J., Mullins, C. B. and Mitchell, J. H. (1975), "Skeletal muscle metabolites in patients with cardiogenic shock or severe congestive heart failure", *Scandinavian Journal of Clinical and Laboratory Investigation,* vol. 35, no. 1, pp. 73-79.

Khan, G. F., Ohwa, M. and Wemet, W. (1996), "Design of a Stable Charge Transfer Complex Electrode for a Third-Generation Amperometric Glucose Senor", *Analytical Chemistry,* vol. 68, no. 17, pp. 2939-2945.

Khodagholy, D., Curto, V. F., Fraser, K. J., Gurfinkel, M., Byrne, R., Diamond, D., Malliaras, G. G., Benito-Lopez, F. and Owens, R. M. (2012), "Organic electrochemical transistor incorporating an ionogel as a solid state electrolyte for lactate sensing", *Journal of Materials Chemistry,* vol. 22, no. 10, pp. 4440-4443.

Knight, S. L., Taylor, R. P., Polliack, A. A. and Bader, D. L. (2001), "Establishing predictive indicators for the status of loaded soft tissues", *Journal of applied physiology,* vol. 90, no. 6, pp. 2231-2237.

Korotcenkov, G. (2010), *Chemical Sensors: Volume 1 General Approaches,* Momentum Press, New York.

Korotcenkov, G., Han, S. D. and Stetter, J. R. (2009), "Review of electrochemical hydrogen sensors", *Chemical reviews,* vol. 109, no. 3, pp. 1402-1433.

Koschwanez, H. E. and Reichert, W. M. (2007), "In vitro, in vivo and post explantation testing of glucose-detecting biosensors: Current methods and recommendations", *Biomaterials,* vol. 28, no. 25, pp. 3687-3703.

Kreyden, O. P. and Scheidegger, E. P. (2004), "Anatomy of the sweat glands, pharmacology of botulinum toxin, and distinctive syndromes associated with hyperhidrosis", *Clinics in dermatology,* vol. 22, no. 1, pp. 40-44.

Kruse, J. A., Zaidi, S. A. and Carlson, R. W. (1987), "Significance of blood lactate levels in critically ill patients with liver disease", *American Journal of Medicine,* vol. 83, no. 1, pp. 77-82.

Kukumberg, P., Valkovic, P., Blazicek, P., Guth, A., Martinkova, J., Provaznik, V. and Jagla, F. (2009), "Sweat: A potential marker of clinical activity in panic disorder", *Neuroendocrinology letters,* vol. 30, no. 3, pp. 400-402.

Kuno, Y. (1934), *The physiology of human perspiration,* J. & A. Churchill.

Laccourreye, O., Bernard, D., De Lacharriere, O., Bazin, R. and Brasnu, D. (1993), "Frey's syndrome analysis with biosensor: A preliminary study", *Archives of Otolaryngology - Head and Neck Surgery,* vol. 119, no. 9, pp. 940-944.

Lahmarm, N. A., Halfens, R. J. G. and Dassen, T. (2005), "Prevalence of pressure ulcers in Germany", *Journal of Clinical Nursing,* vol. 14, no. 2, pp. 165-172.

Lamas-Ardisana, P. J., Loaiza, O. A., Añorga, L., Jubete, E., Borghei, M., Ruiz, V., Ochoteco, E., Cabañero, G. and Grande, H. J. (2014), "Disposable amperometric biosensor based on lactate oxidase immobilised on platinum nanoparticle-decorated carbon nanofiber and poly(diallyldimethylammonium chloride) films", *Biosensors and Bioelectronics,* vol. 56, pp. 345-351.

Leonida, M. D., Starczynowski, D. T., Waldman, R. and Aurian-Blajeni, B. (2003), "Polymeric FAD used as enzyme-friendly mediator in lactate detection", *Analytical and Bioanalytical Chemistry,* vol. 376, no. 6, pp. 832-837.

Lillis, B., Grogan, C., Berney, H. and Lane, W. A. (2000), "Investigation into immobilisation of lactate oxidase to improve stability", *Sensors and Actuators B: Chemical,* vol. 68, no. 1–3, pp. 109-114.

Liu, J. and Wang, J. (2001), "A Novel Improved Design for the First-generation Glucose Biosensor", *Food Technology and Biotechnology,* vol. 39, no. 1, pp. 55-58.

Lobo-Castañón, M. J., Miranda-Ordieres, A. J. and Tuñón-Blanco, P. (1997), "A bienzyme-poly-(o-phenylenediamine)-modified carbon paste electrode for the amperometric detection of l-lactate", *Analytica Chimica Acta,* vol. 346, no. 2, pp. 165-174.

Lyder, C. H. and Ayello, E. A. (2008), "Pressure ulcers: a patient safety issue.", in Hughes, R. G. (ed.) *Patient safety and quality. An evidence-based handbook for nurses*. AHRQ, U.S.

MacLean, D. A., Bangsbo, J. and Saltin, B. (1999), "Muscle interstitial glucose and lactate levels during dynamic exercise in humans determined by microdialysis", *Journal of applied physiology,* vol. 87, no. 4, pp. 1483-1490.

Madaras, M. B., Popescu, I. C., Ufer, S. and Buck, R. P. (1996), "Microfabricated amperometric creatine and creatinine biosensors", *Analytica Chimica Acta,* vol. 319, no. 3, pp. 335-345.

Majumder, A. B., Mondal, K., Singh, T. P. and Gupta, M. N. (2008), "Designing cross-linked lipase aggregates for optimum performance as biocatalysts", *Biocatalysis and Biotransformation,* vol. 26, no. 3, pp. 235-242.

Maklebust, J. and Sieggreen, M. (2001), *Pressure Ulcers: Guidelines for Prevention and Management,* Third ed, Springhouse Publishing Co, U. S.

Mallik, A. and Ray, B. C. (2011), "Evolution of Principle and Practice of Electrodeposited Thin Film: A Review on Effect of Temperature and Sonication", *International Journal of Electrochemistry,* vol. 2011.

Marek, E. M., Volke, J., Hawener, I., Platen, P., Mückenhoff, K. and Marek, W. (2010), "Measurements of lactate in exhaled breath condensate at rest and after maximal exercise in young and healthy subjects", *Journal of Breath Research,* vol. 4, no. 1.

Maslauskas, K., Samsanavičius, D., Rimdeika, R. and Kaikaris, V. (2009), "Surgical treatment of pressure ulcers: An 11-year experience at the Department of Plastic and Reconstructive Surgery of Hospital of Kaunas University of Medicine", *Medicina,* vol. 45, no. 4, pp. 269-275.

Massie, J., Gaskin, K., Van Asperen, P. and Wilcken, B. (2000), "Sweat testing following newborn screening for cystic fibrosis", *Pediatric pulmonology,* vol. 29, no. 6, pp. 452-456.

Matijošytė, I., Arends, I. W. C. E., de Vries, S. and Sheldon, R. A. (2010), "Preparation and use of cross-linked enzyme aggregates (CLEAs) of laccases", *Journal of Molecular Catalysis B: Enzymatic,* vol. 62, no. 2, pp. 142-148.

Matsen, F. A.,3rd, Wyss, C. R., King, R. V., Barnes, D. and Simmons, C. W. (1981), "Factors affecting the tolerance of muscle circulation and function for increased tissue pressure", *Clinical orthopaedics and related research,* vol. (155), no. 155, pp. 224-230.

Mayo Foundation for Medical Education and Research , *Diseases and Conditions - Sweat Glands*, available at: http://www.mayoclinic.org/diseases-conditions/hyperhidrosis/multimedia/sweat-glands/img-20007980 (accessed 09/10).

Mena-Bravo, A. and Luque de Castro, M. D. (2014), "Sweat: A sample with limited present applications and promising future in metabolomics", *Journal of pharmaceutical and biomedical analysis,* vol. 90, pp. 139-147.

Migneault, I., Dartiguenave, C., Bertrand, M. J. and Waldron, K. C. (2004), "Glutaraldehyde: Behavior in aqueous solution, reaction with proteins, and application to enzyme crosslinking", *BioTechniques,* vol. 37, no. 5, pp. 790-802.

Minagawa, H., Nakayama, N., Matsumoto, T. and Ito, N. (1998), "Development of long life lactate sensor using thermostable mutant lactate oxidase", *Biosensors and Bioelectronics,* vol. 13, no. 3–4, pp. 313-318.

Mindt, W., Racine, P. and Schläpfer, P. (1973), "Sensoren für Lactat und Glucose", *Berichte der Bunsengesellschaft für physikalische Chemie,* vol. 77, no. 10-11, pp. 804-808.

Mitsubayashi, K., Suzuki, M., Tamiya, E. and Karube, I. (1994), "Analysis of metabolites in sweat as a measure of physical condition", *Analytica Chimica Acta,* vol. 289, no. 1, pp. 27-34.

Morris, D., Coyle, S., Wu, Y., Lau, K. T., Wallace, G. and Diamond, D. (2009), "Bio-sensing textile based patch with integrated optical detection system for sweat monitoring", *Sensors and Actuators, B: Chemical,* vol. 139, no. 1, pp. 231-236.

Moyer, J., Wilson, D., Finkelshtein, I., Wong, B. and Potts, R. (2012), "Correlation between sweat glucose and blood glucose in subjects with diabetes", *Diabetes Technology and Therapeutics,* vol. 14, no. 5, pp. 398-402.

National Pressure Ulcer Advisory Panel (2007), *Pressure Ulcer Category/Staging Illustrations*, available at: http://www.npuap.org/resources/educational-and-clinical-resources/pressure-ulcer-categorystaging-illustrations/ (accessed 03/10).

National Pressure Ulcer Advisory Panel & European Pressure Ulcer Advisory Panel (2009), "Pressure Ulcer Prevention - Quick Reference Guide", [Online], , pp. 03/10 available at: http://www.npuap.org/wp-content/uploads/2012/02/Final_Quick_Prevention_for_web_2010.pdf.

NHS Choices (2014), *Pressure ulcers - Causes*, available at: http://www.nhs.uk/Conditions/Pressure-ulcers/Pages/Causes.aspx (accessed 03/10).

Nikolaus, N. and Strehlitz, B. (2008), "Amperometric lactate biosensors and their application in (sports) medicine, for life quality and wellbeing", *Microchimica Acta,* vol. 160, no. 1-2, pp. 15-55.

Nunes, L. A. S. and Macedo, D. V. D. (2013), "Saliva as a diagnostic fluid in sports medicine: Potential and limitations", *Jornal Brasileiro de Patologia e Medicina Laboratorial,* vol. 49, no. 4, pp. 247-255.

Nyamsi Hendji, A., Bataillard, P. and Jaffrezic-Renault, N. (1993), "Covalent immobilization of glucose oxidase on silanized platinum microelectrode for the monitoring of glucose", *Sensors and Actuators B: Chemical,* vol. 15, no. 1–3, pp. 127-134.

Okorie, O. D. and Dellinger, P. (2011), "Lactate: Biomarker and Potential Therapeutic Target", in Levy, M. M. (ed.) *Biomarkers in the Critically Ill Patient, an Issue of Critical Care Clinics,* W. B. Saunders, Philadelphia.

Okuda, K., Urabe, I., Yamada, Y. and Okada, H. (1991), "Reaction of glutaraldehyde with amino and thiol compounds", *Journal of Fermentation and Bioengineering,* vol. 71, no. 2, pp. 100-105.

P.J. Higson, S., Desai, M., Koochaki, Z. and Vadgama, P. M. (1993), "Glucose oxidase enzyme electrode: relation between inner membrane permeability and substrate response", *Analytica Chimica Acta,* vol. 276, no. 2, pp. 335-340.

Papanas, N., Boulton, A. J. M., Malik, R. A., Manes, C., Schnell, O., Spallone, V., Tentolouris, N., Tesfaye, S., Valensi, P., Ziegler, D. and Kempler, P. (2013), "A simple new non-invasive sweat indicator test for the diagnosis of diabetic neuropathy", *Diabetic Medicine,* vol. 30, no. 5, pp. 525-534.

Patterson, M. J., Galloway, S. D. R. and Nimmo, M. A. (2000), "Variations in regional sweat composition in normal human males", *Experimental physiology,* vol. 85, no. 6, pp. 869-875.

Phillips, L. and Buttery, J. (2009), "Exploring pressure ulcer prevalence and preventative care", *Nursing times,* vol. 105, no. 16, pp. 34-36.

Pilardeau, P., Vaysse, J., Garnier, M., Joublin, M. and Valeri, L. (1979), "Secretion of eccrine sweat glands during exercise.", *British journal of sports medicine,* vol. 13, no. 3, pp. 118-121.

Pilardeau, P. A., Lavie, F., Vaysse, J., Garnier, M., Harichaux, P., Margo, J. N. and Chalumeau, M. T. (1988), "Effect of different work-loads on sweat production and composition in man", *Journal of Sports Medicine and Physical Fitness,* vol. 28, no. 3, pp. 247-252.

Pletcher, D., Greff, R., Peat, R. and Peter, L. M. (2001), *Instrumental Methods in Electrochemistry,* Woodhead Publishing, Chichester, England.

Polliack, A., Taylor, R. and Bader, D. (1993), "Analysis of sweat during soft tissue breakdown following pressure ischemia", *Journal of Rehabilitation Research and Development,* vol. 30, no. 2, pp. 250-259.

Polliack, A., Taylor, R. and Bader, D. (1997), "Sweat analysis following pressure ischaemia in a group of debilitated subjects", *Journal of Rehabilitation Research and Development,* vol. 34, no. 3, pp. 303-308.

Pribil, M. M., Laptev, G. U., Karyakina, E. E. and Karyakin, A. A. (2014), "Noninvasive hypoxia monitor based on gene-free engineering of lactate oxidase for analysis of undiluted sweat", *Analytical Chemistry,* vol. 86, no. 11, pp. 5215-5219.

Qi, Z. (2008), "Electrochemical Methods for Catalyst Activity Evaluation", in Zhang, J. (ed.) *PEM Fuel Cell Electrocatalysts and Catalyst Layers: Fundamentals and Applications,* Springer, London.

Rassaei, L., Olthuis, W., Tsujimura, S., Sudhölter, E. J. R. and Van Den Berg, A. (2014), "Lactate biosensors: Current status and outlook", *Analytical and Bioanalytical Chemistry,* vol. 406, no. 1, pp. 123-137.

Reshmi, R. and Sugunan, S. (2013), "Improved biochemical characteristics of crosslinked β-glucosidase on nanoporous silica foams", *Journal of Molecular Catalysis B: Enzymatic,* vol. 85–86, no. 0, pp. 111-118.

Rimachi, R., Bruzzi De Carvahlo, F., Orellano-Jimenez, C., Cotton, F., Vincent, J. L. and De Backer, D. (2012), "Lactate/pyruvate ratio as a marker of tissue hypoxia in circulatory and septic shock", *Anaesthesia and Intensive Care,* vol. 40, no. 3, pp. 427-432.

Ronkainen, N. J., Halsall, H. B. and Heineman, W. R. (2010), "Electrochemical biosensors", *Chemical Society Reviews,* vol. 39, no. 5, pp. 1747-1763.

Rozlosnik, N. (2009), "New directions in medical biosensors employing poly(3,4-ethylenedioxy thiophene) derivative-based electrodes", *Analytical and Bioanalytical Chemistry,* vol. 395, no. 3, pp. 637-645.

Sakharov, D. A., Shkurnikov, M. U., Vagin, M. Y., Yashina, E. I., Karyakin, A. A. and Tonevitsky, A. G. (2010), "Relationship between lactate concentrations in active muscle sweat and whole blood", *Bulletin of experimental biology and medicine,* vol. 150, no. 1, pp. 83-85.

Sánchez, P. D., Blanco, P. T., Alvarez, J. M. F., Smyth, M. R. and O'Kennedy, R. (1990), "Flow-injection analysis of hydrogen peroxide using a horseradish peroxidase-modified electrode detection system", *Electroanalysis,* vol. 2, no. 4, pp. 303-308.

Sasöz, N., Kisa, Ü and Apan, A. (2002), "Ischaemia-reperfusion injury of rat ovary and the effects of vitamin C, mannitol and verapamil", *Human Reproduction,* vol. 17, no. 11, pp. 2972-2976.

Sato, K. and Dobson, R. L. (1973), "Glucose metabolism of the isolated eccrine sweat gland. II. The relation between glucose metabolism and sodium transport", *Journal of Clinical Investigation,* vol. 52, no. 9, pp. 2166-2174.

Sato, K., Kang, W. H., Saga, K. and Sato, K. T. (1989), "Biology of sweat glands and their disorders. I. Normal sweat gland function", *Journal of the American Academy of Dermatology,* vol. 20, no. 4, pp. 537-563.

Sayeed, M. M. and Murthy, P. N. A. (1981), "Adenine nucleotide and lactate metabolism in the lung in endotoxin shock", *Circulatory shock,* vol. 8, no. 6, pp. 657-666.

Sears, M. E., Kerr, K. J. and Bray, R. I. (2012), "Arsenic, cadmium, lead, and mercury in sweat: A systematic review", *Journal of Environmental and Public Health,* vol. 2012.

Sheldon, R. A. (2007), "Cross-linked enzyme aggregates (CLEA®s): Stable and recyclable biocatalysts", *Biochemical Society transactions,* vol. 35, no. 6, pp. 1583-1587.

Sheldon, R. A. (2011), "Characteristic features and biotechnological applications of cross-linked enzyme aggregates (CLEAs)", *Applied Microbiology and Biotechnology,* vol. 92, no. 3, pp. 467-477.

Smith, I., Kumar, P., Molloy, S., Rhodes, A., Newman, P. J., Grounds, R. M. and Bennett, E. D. (2001), "Base excess and lactate as prognostic indicators for patients admitted to intensive care", *Intensive care medicine,* vol. 27, no. 1, pp. 74-83.

Spehar-Deleze, A., Anastasova, S., Popplewell, J. and Vadgama, P. (2012), "Extreme Physiological State: Development of Tissue Lactate Sensor", *Wearable and Implantable Body Sensor Networks (BSN), 2012 Ninth International Conference on,* pp. 17.

Stefaniak, A. B. and Harvey, C. J. (2006), "Dissolution of materials in artificial skin surface film liquids", *Toxicology in Vitro,* vol. 20, no. 8, pp. 1265-1283.

Stekelenburg, A., Oomens, C. W. J., Strijkers, G. J., Nicolay, K. and Bader, D. L. (2006), "Compression-induced deep tissue injury examined with magnetic resonance imaging and histology", *Journal of applied physiology,* vol. 100, no. 6, pp. 1946-1954.

Stekelenburg, A., Strijkers, G. J., Parusel, H., Bader, D. L., Nicolay, K. and Oomens, C. W. (2007), "Role of ischemia and deformation in the onset of compression-induced deep tissue injury: MRI-based studies in a rat model", *Journal of applied physiology,* vol. 102, no. 5, pp. 2002-2011.

Stekelenburg, A., Gawlitta, D., Bader, D. L. and Oomens, C. W. (2008), "Deep Tissue Injury: How Deep is Our Understanding?", *Archives of Physical Medicine and Rehabilitation,* vol. 89, no. 7, pp. 1410-1413.

Stojek, Z. (2002), "The electrical double layer and its structure", in Scholz, F. (ed.) *Electroanalytical Methods: Guide to Experiments and Applications,* Springer-Verlag Berlin Heidelberg, Germany.

Sung, W. J. and Bae, Y. H. (2006), "Glucose oxidase, lactate oxidase, and galactose oxidase enzyme electrode based on polypyrrole with polyanion/PEG/enzyme conjugate dopant", *Sensors and Actuators B: Chemical,* vol. 114, no. 1, pp. 164-169.

Thevenot, D. R., Toth, K., Durst, R. A. and Wilson, G. S. (2001), "Electrochemical biosensors: recommended definitions and classification", *Biosensors & bioelectronics,* vol. 16, no. 1-2, pp. 121-131.

Thompson, D. (2005), "A critical review of the literature on pressure ulcer aetiology.", *Journal of wound care,* vol. 14, no. 2, pp. 87-90.

Turner, A. P. F., Chen, B. and Piletsky, S. A. (1999), "In vitro diagnostics in diabetes: Meeting the challenge", *Clinical chemistry,* vol. 45, no. 9, pp. 1596-1601.

Urban, P. and Lederer, F. (1988), "Inactivation of flavocytochrome b2 with fluoropyruvate. Reaction at the active-site histidine.", *European Journal of Biochemistry,* vol. 173, no. 1, pp. 155-162.

Van Heyningen, R. and Weiner, J. S. (1952), "The effect of arterial occlusion on sweat composition.", *The Journal of physiology,* vol. 116, no. 4, pp. 404-413.

Van Loon, L. J. C., Greenhaff, P. L., Constantin-Teodosiu, D., Saris, W. H. M. and Wagenmakers, A. J. M. (2001), "The effects of increasing exercise intensity on muscle fuel utilisation in humans", *Journal of Physiology,* vol. 536, no. 1, pp. 295-304.

Wang, J. (2006), *Analytical electrochemistry,* Third ed, John Wiley and Sons, Hoboken, New Jersey.

Wang, J. (2008), "Electrochemical glucose biosensors", *Chemical reviews,* vol. 108, no. 2, pp. 814-825.

Weber, J., Kumar, A., Kumar, A. and Bhansali, S. (2006), "Novel lactate and pH biosensor for skin and sweat analysis based on single walled carbon nanotubes", *Sensors and Actuators, B: Chemical,* vol. 117, no. 1, pp. 308-313.

Wei, X., Zhang, M. and Gorski, W. (2003), "Coupling the lactate oxidase to electrodes by ionotropic gelation of biopolymer", *Analytical Chemistry,* vol. 75, no. 9, pp. 2060-2064.

Weng, M. -. (2008), "The effect of protective treatment in reducing pressure ulcers for non-invasive ventilation patients", *Intensive and Critical Care Nursing,* vol. 24, no. 5, pp. 295-299.

Williams, D. L., Doig Jr., A. R. and Korosi, A. (1970), "Electrochemical-enzymatic analysis of blood glucose and lactate.", *Analytical Chemistry,* vol. 42, no. 1, pp. 118-121.

Yoo, E. -. and Lee, S. -. (2010), "Glucose biosensors: An overview of use in clinical practice", *Sensors,* vol. 10, no. 5, pp. 4558-4576.

Zaydan, R., Dion, M. and Boujtita, M. (2004), "Development of a New Method, Based on a Bioreactor Coupled with an L-Lactate Biosensor, toward the Determination of a Nonspecific Inhibition of L-Lactic Acid Production during Milk Fermentation", *Journal of Agricultural and Food Chemistry,* vol. 52, no. 1, pp. 8-14.

Zhang, W. and Li, G. (2004), "Third-Generation Biosensors Based on the Direct Electron Transfer of Proteins", *Analytical Sciences,* vol. 20, no. 4, pp. 603-609.

Zhang, Z., Zheng, J., Zhang, Y., Zhang, W., Li, L., Cao, Z., Wang, H., Li, C., Gao, Y. and Liu, J. (2013), "Anti-fouling in situ deposited antimony/nafion film electrode for electrochemical stripping analysis", *International Journal of Electrochemical Science,* vol. 8, no. 3, pp. 4183-4193.

Appendix B. Ethics approval for *in vitro* human sweat trials.

25rd July 2012

Dear Seamus

Project Reference No 16/12: Measuring the lactate content in human sweat samples using a novel biosensor

Thank you for undertaking the required amendments and submitting the revised approval form. I can confirm that your study now has ethical approval from the CUHREC Committee.

Subsequent to approval being given by the committee, applicants are responsible for:

- reporting of any adverse incidents occurring during the course of the study to the committee, even if the incident is not directly related to the study (e.g. a complaint by a participant);
- notifying the committee of any major changes to the protocol and obtaining further ethical approval as appropriate;
- notifying the committee when the study has ended.

The committee may revoke approval for a submission if they become aware of any unethical or other improper practices during the execution of the research.

Yours sincerely

Professor Paul Harrison
Chairman
Cranfield University Health Ethics Committee